SCATTERING OF ELASTIC WAVES FROM A CORRUGATED INTERFACE

A THESIS SUBMITTED IN PARTIAL FULFILMENT OF THE REQUIREMENTS FOR THE DEGREE OF DOCTOR OF PHILOSOPHY

J. LALVOHBIKA

Ph.D. REGN. No.: MZU/Ph.D./687 of 16.05.2014

MZU REGN. No.: 5668 of 2013

DEPARTMENT OF MATHEMATICS AND COMPUTER SCIENCE

SCHOOL OF PHYSICAL SCIENCES

MIZORAM UNIVERSITY

JULY, 2020

SCATTERING OF ELASTIC WAVES FROM A CORRUGATED INTERFACE

By

J. Lalvohbika

Department of Mathematics and Computer Science

Supervisor : Dr. S. Sarat Singh

Submitted

In partial fulfilment of the requirement of the Degree of Doctor of

Philosophy in Mathematics of Mizoram University, Aizawl

DEPARTMENT OF MATHEMATICS & COMPUTER SCIENCE
MIZORAM UNIVERSITY

Aizawl – 796 004, Mizoram: INDIA
Fax: 0389 - 2330644
Phone: +919862626776(m)
+919863264645(m)
e-mail: saratcha32@yahoo.co.uk

Dr. S. Sarat Singh
Associate Professor

CERTIFICATE

This is to certify that the thesis entitled "Scattering of elastic waves from a corrugated interface" submitted by Mr. J. Lalvohbika for the award of the degree of Doctor of Philosophy (Ph. D.) in Mathematics, is a bonafide record of the original research carried out by him under my supervision. He has been duly registered and the thesis is worthy of being considered for the award of the Ph. D. degree.

I, the undersigned has declared that this research work has been done under my supervision and has not been submitted for any degree in any other University/Institute.

Dr. S. Sarat Singh

(Supervisor)

SCHOLAR'S DECLARATION

I, Mr. J. Lalvohbika, hereby declare that the subject matter of this thesis entitled "Scattering of elastic waves from a corrugated interface" is the record of work done by me, that the contents of this thesis do not form basis of the award of any previous degree to me or to the best of my knowledge to anybody else, and that the thesis has not been submitted by me for any research degree in other University/Institute.

This is being submitted to the Mizoram University for the partial fulfilment of the degree of Doctor of Philosophy (Ph. D.) in Mathematics.

<div align="right">

J. Lalvohbika

(MZU/Ph.D./687 of 16.05.2014)

Extension Letter: No. 16-2/MZU(Acad)/19/29-31

Dated 18th June 2019 upto 15.5.2021

(Candidate)

</div>

Dr. S. Sarat Singh   Dr. Jay Prakash Singh

(Supervisor)   (Head of Department)

Dept. Maths. & Comp. Sc.   Dept. Maths. & Comp. Sc.

Mizoram University   Mizoram University

ACKNOWLEDGEMENT

able advice, good co-operation and full support during my research work.

I express my deepest thanks to my wife, Mrs. Malsawmtluangi and my beloved family members for their continuous support and encouragement throughout my research work.

Lastly, a heartiest gratitude should be conveyed to the Lord Almighty for blessing me with health, strength and guidance in order to complete my research work.

Dated: ....

Place: Aizawl   J. Lalvohbika

PREFACE

The present thesis entitled "**Scattering of elastic waves from a corrugated interface**" is an outcome of the research carried out by me under the supervision of Dr. S. Sarat Singh, Department of Mathematics & Computer Science, Mizoram University, Aizawl - 796 004, Mizoram, INDIA.

This thesis studies the reflection and transmission of elastic waves from a corrugated interface using Rayleigh's technique. The existence of regular and irregular waves have been observed in our analysis. We have obtained the amplitude and energy ratios of the regularly and irregularly reflected and transmitted waves. These ratios have been analyzed for a particular type of interface, $z = d\cos px$ and they are computed numerically.

It consists of six chapters. The first chapter is the general introduction. It contains basic definitions, different types of anisotropic symmetry, stress-strain relationship with generalized Hooke's law, conservation of linear momentum, Spectrum theorem, Rayleigh's method of approximation, importance of wave propagation and review of literature.

In the second chapter, the problem of reflection and transmission of qSV/qP-wave due to incident plane qSV-wave at a corrugated interface between two dissimilar monoclinic elastic half-spaces has been investigated. The reflection and transmission coefficients of the reflected and transmitted waves are obtained using Rayleigh's method of approximation. These coefficients are computed numerically for a particular type of model, $z = d\cos py$ and results are represented graphically.

The third chapter deals with the problems of reflection and transmission of elastic waves at a corrugated interface between two dissimilar nematic elastomer half-spaces, separately for the incident qP and qSV-waves. We find the amplitude and energy ratios of the reflected and transmitted waves using suitable boundary conditions. In the fourth chapter, we have discussed the phenomena of reflection and transmission of qSH-wave at a corrugated interface between two different nematic elastomer

half-spaces. Here also we have analyzed the effects of corrugation and frequency parameters on the amplitude and energy ratios. We come across that these ratios are functions of the angle of incidence, elastic constants, coupling constants, the characteristic time of rubber relaxation, the director rotation-times, frequency and corrugation parameters.

In the fifth chapter, the problem of elastic waves at a corrugated interface between two different incompressible transversely isotropic fibre-reinforced half-spaces has been investigated. There exist two reflected and transmitted quasi shear waves in certain angular range of propagation, in which the outer slowness is re-entrant. We have found the amplitude and energy ratios using Rayleigh's technique.

Chapter six is summary and conclusions. A list of references has been given at the end of the thesis.

Contents

LIST OF FIGURES

Chapter 1

General Introduction

1.1   Basic definition

The theory of elastodynamic wave scattering is based on two foundations - continuum mechanics of elastic media and the general principles of scattering theory. *Continuum Mechanics* is a branch of mechanics that deals with kinematics and mechanical behavior of materials modeled as continuous mass rather than discrete particles. If a body contains a sufficiently large number of molecules, so that the distances between two neighboring molecules are negligible in comparison with the dimensions of the body, then the body is said to be a continuous body and it behaves in accordance with the laws of mechanics. The study of deformation behavior of matter can be approached fundamentally by considering the bulk material as continuous medium. In such a study, we assume that the matter in the body is continuously distributed and fills the entire region of the space it occupies, without gaps or empty spaces. Continuum mechanics also deals with the deformation of matter under the action of forces and thermal effects. The treatment is given for all the forms of matter, i.e., solids, liquids and gasses in a unified framework. The framework of continuum mechanics is developed by assuming fundamental laws of mechanics and thermodynamics as axioms. The theory is based upon the basic concept of stress, motion and deformation, upon the laws of conservation of mass, linear momentum,

moment of momentum and energy, and on the constitutive relations. The *constitutive relations* characterize the mechanical and thermal response of a materials, while the basic *conservation laws* abstract the common features of all mechanical phenomena irrespective of constitutive relations. From the view of continuum mechanics the body is idealized as a continuous medium and the physical phenomena are described in mathematical terms by introducing appropriate mathematical abstractions, which leads to a system of partial differential equations with boundary and initial conditions. The system of differential equations will be solved by employing the techniques of applied mathematics to obtain analytical expression for some of the field variables in terms of position and time as well as in terms of the geometrical and material parameters.

An elastic body is a continuum solid when subjected to external loads get deformed and return to its original shape and size after the removal of external forces. If the external forces are applied on the continuous body, the relative positions of its constituent particles get altered, then the continuous body is said to be *strained body* and the change in the relative positions of the particles is known as *deformation*. At this stage, the particles resist to change their positions but the external force makes them to change their positions up to some extent and when the external forces are withdrawn, these particles at once regain their original shape and size. The elastic property of a continuum body depends on the strength of resistance, so greater the resistance of a body to deform the more is the elasticity. The measure of intensity of internal forces generated in a body is called *stress*, and the deformation of the body due to application of stress is called *strain*, so the strain indicates local deformation in a body. Stress and strain are simultaneously occurring, the strain set up in a body in such a way that there is a change in volume but no change in shape, is called *dilatation*. There are two kinds of dilatation, 'compression' and 'rarefaction', in which volume is reduced and increased respectively. Another elastic deformation is called *shear* if there is a change in shape and size but not in a volume (Love, 1892).

If the elastic constants are same for all points of the medium, then the body is called *elastically homogeneous*, but if they are functions of the position, then the body is said to be *elastically inhomogeneous*. The material is *elastically isotropic* if there are no preferred directions in the material and the elastic constants must be the same whatever the orientation of the cartesian coordinate system in which the components of stress (τ_{ij}) and strain (e_{ij}) are evaluated. The isotropic material has infinite number of axis of symmetry, that means the isotropic materials have identical values of physical properties in all direction. In other words, a material is said to be isotropic if the rotation of particle in the un-deformed state, has no influence on the stress tensor. There are materials in which certain physical properties vary with direction from which they are measured. For instance, the refractive index or density of a material is different when measured along certain different axes, such materials are said to be *anisotropic materials*. The general elastic constitutive model formulated to describe the mechanical behavior of material is anisotropic model. This kind of materials has no material symmetry. *Orthotropic* materials are the subclass of anisotropic materials, which has material properties that differ along three mutually-orthogonal axes of rotational symmetry. Glass and metals are examples of isotropic materials while wood and composites are the common examples of anisotropic materials. In wood, we can define three mutually perpendicular directions at each point in which the properties along axial direction, radial direction and circumferential direction are different.

A wave can be described as a disturbance or variation that transfers energy progressively from point to point in a medium and that may take the form of an elastic deformation or of a variation of pressure, electric or magnetic intensity, electric potential, or temperature. The medium through which the wave travels may experience some local oscillations as the wave passes, but the particles in the medium do not necessarily travel with the wave. The disturbance may take any of a number of shapes, from a finite width pulse to an infinitely long sine wave. Mainly there are

two types of waves -Mechanical and Electromagnetic waves. *Mechanical waves* propagates through medium, deforming the substance of the medium and are characterized by the transport of energy through motions of particles about an equilibrium position. Deformability and inertia are essential properties of a medium for the transmission of mechanical wave motions. All real materials are of course deformable and possess mass and thus all real materials transmit mechanical waves. While *electromagnetic waves* do not require a medium to propagate and can travel through vacuum, such as light waves traveling from sun to the earth. A wave propagated by a medium having inertia and elasticity, in which displaced particles transfer momentum to adjoining particles, and are themselves restored to their original position is known as *elastic wave.*

When elastic waves propagate, the energy of elastic deformation is transferred in the absence of a flow of matter, which occurs only in special cases, such as during an acoustic wind. A special feature of elastic wave is that their phase and group velocities are independent of the wave amplitude and the wave geometry. An elastic wave may be a plane, spherical or cylindrical wave. They are longitudinal and shear waves. Only longitudinal/compressional waves can propagate in liquids and gases, which are elastic with respect to volume but not with respect to shape. The phase velocity of waves in fluids and gases is given by $c = \sqrt{K/\rho}$, where K is the bulk modulus and ρ is the density of the medium. In longitudinal waves, the particle motion is parallel to the direction of wave propagation, and the deformation is a combination of uniform compression or extension and pure shear. In shear waves, the particle motion is perpendicular to the direction of wave propagation and the deformation is pure shear. For isotropic solids in bulk form, the phase velocity of longitudinal and shear waves in isotropic medium are respectively given by $\sqrt{(K + 4/3G)/\rho}$ and $\sqrt{G/\rho}$, where G is the modulus of elasticity.

Seismic waves, sound waves and ultrasonic waves in liquids and gases are good examples of elastic waves. Seismic waves are of two types - Body waves and Surface

waves. *Body waves* travel through the interior of the medium and these waves are known as Primary waves (P-waves) and Secondary waves (S-waves). The P-waves are compressional waves and longitudinal in nature, and S-waves are shear waves and transverse in nature which can be polarized into vertical (SV-waves) and horizontal (SH-waves) directions. *Surface waves* travel along the surface of the medium, the amplitude or strength of these waves fades exponentially from the boundary surface of the medium. Rayleigh waves, Love waves, Stoneley waves, Lamb waves etc. are examples of surface waves. *Rayleigh waves* can propagate at the boundary between a solid half space and a vacuum, liquid or gas and such waves are taken as a combination of non-uniform longitudinal and shear waves whose amplitudes decrease exponentially with distance from the free boundary surface. Propagating disturbances confined to the neighborhood of a surface occur not only in the vicinity of a free surface but also at the interface of two half-spaces filled with different materials. Thus, there can be surface waves at the interface of a solid and a fluid and also at the interface of two solids. Such waves are called *Stoneley waves*. *Love waves* are horizontally polarized surface waves and it is a result of the interference of many shear waves (S-waves) guided by an elastic layer, which is welded to an elastic half-space on one side while bordering a vacuum on the other side. Love and Rayleigh waves are guided by the free surface of the Earth. They follow along after the P and S-waves have passed through the body of the medium. Both Love and Rayleigh waves involve horizontal particle motion, but only the latter type has vertical ground displacements. As Love and Rayleigh waves travel, they disperse into long wave trains and cause much of the shaking felt during earthquakes at substantial distances from the source. *Lamb waves* are a specific case of surface-guided waves that propagate in solid plates or spheres and their particle motion lies in the plane that contains the direction of wave propagation and the plane normal. An infinite medium supports just two wave modes traveling at unique velocities, but plates support two infinite sets of Lamb wave modes, whose velocities depend on the relationship between wavelength and plate thickness.

1.2 Stress and Strain

Let us consider, in a continuous medium, a region of volume V surrounded by a closed surface ΔS, in such away that there is matter on both sides of the surface with unit normal vector, $\widehat{\mathbf{n}}$. The force acting on this surface per unit surface area is called the *traction* and is given by (Pike and Sabatier, 2002)

$$\mathbf{T} = \boldsymbol{\tau} \cdot \widehat{\mathbf{n}}, \tag{1.1}$$

where $\boldsymbol{\tau}$ is the stress.
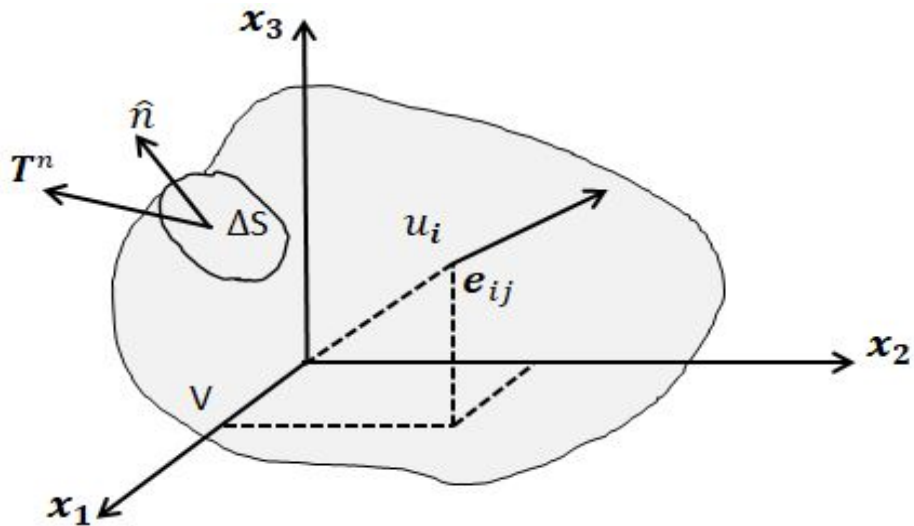
Figure 1.1: The stress, strain and displacement in an elastic medium

For each point inside V, we define elastic stresses, strains and displacements as a continuous functions of the spacial coordinates and time (Fig. 1.1). Stresses at a point inside V are the limits of the quotients of the forces that act at this point per unit surface through a plane with a certain orientation. The stress through a plane with unit normal $\widehat{\mathbf{n}}$ represented by a vector $\mathbf{T}^n$ is given by

$$\mathbf{T}^n(x_i, n) = \lim_{\Delta S \to 0} \frac{\mathbf{F}}{\Delta S}, \tag{1.2}$$

where $\mathbf{F}$ is the force acting on ΔS.

Stress is represented by a second order tensor $\boldsymbol{\tau}$ with nine quantities, τ_{ij} (Sokolnikoff, 1956; Udias, 2000) which are the stresses through three orthogonal planes. In Cartesian co-ordinates system, the stress vectors ($\mathbf{T^n}$), unit normal ($\hat{\mathbf{n}}$) and stress tensors (τ_{ij}) are shown in Figs. 1.2 and 1.3.
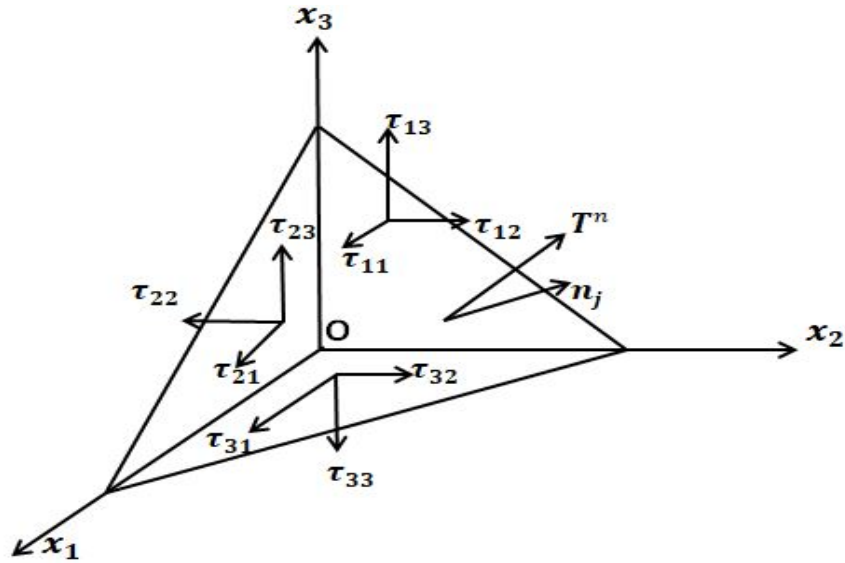
Figure 1.2: The stress tensors, τ_{ij} and stress vector, T^n in a tetrahedron.
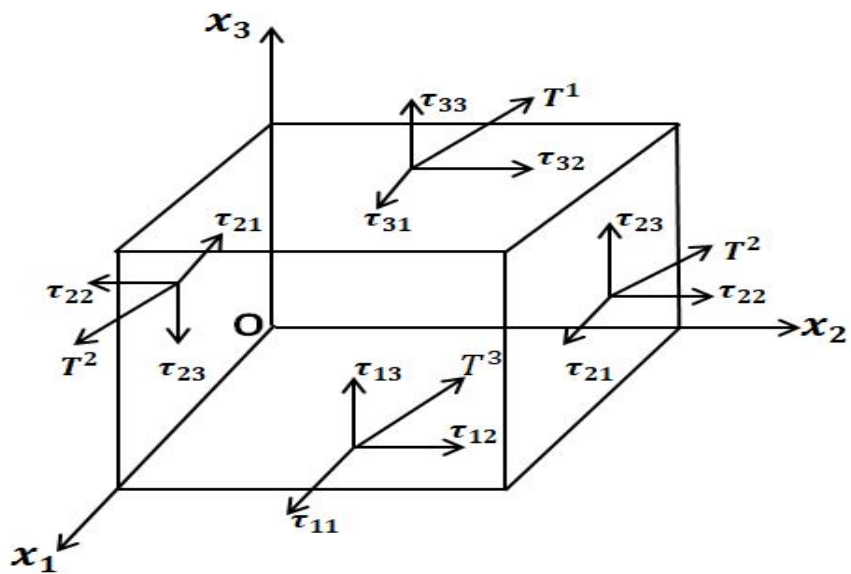
Figure 1.3: The stress tensors, τ_{ij} and the stress vector, T^n in a rectangular parallelepiped.

The state of stress at any point of a medium is completely characterized by these nine quantities. If $\mathbf{T^n}$ be the stress vector acting at a point of a surface to which $\widehat{\mathbf{n}}$ is normal, then the stress tensor is represented by

$$\mathbf{T^n} = \tau_{ij} n_j, \qquad (i,\ j = 1,\ 2,\ 3) \qquad (1.3)$$

where τ_{ij} is the jth components of stress vector acting on a surface element to which x_i-axis is normal.

The strain tensor, e_{ij} in terms of the components of displacement vector, $\mathbf{u} = (u_1, u_2, u_3)$ is given by (Sokolnikoff, 1956)

$$e_{ij} = \frac{1}{2}(u_{i,j} + u_{j,i}), \qquad (i,\ j = 1,\ 2,\ 3) \qquad (1.4)$$

The relationship between the stress tensor (τ_{ij}) and the strain components (e_{ij}) for an elastic continuum is given by generalized *Hooke's Law* which states that for sufficiently small strain, each component of stress tensor is a linear combination of the components of strain tensor as

$$\tau_{ij} = C_{ijkl} e_{kl}, \qquad (i,\ j,\ k,\ l = 1,\ 2,\ 3) \qquad (1.5)$$

In matrix notation, it may be represented by

$$
\begin{pmatrix} \tau_{11} \\ \tau_{12} \\ \tau_{13} \\ \tau_{21} \\ \tau_{22} \\ \tau_{23} \\ \tau_{31} \\ \tau_{32} \\ \tau_{33} \end{pmatrix}
=
\begin{pmatrix}
C_{1111} & C_{1112} & C_{1113} & C_{1121} & C_{1122} & C_{1123} & C_{1131} & C_{1132} & C_{1133} \\
C_{1211} & C_{1212} & C_{1213} & C_{1221} & C_{1222} & C_{1223} & C_{1231} & C_{1232} & C_{1233} \\
C_{1311} & C_{1312} & C_{1313} & C_{1321} & C_{1322} & C_{1323} & C_{1331} & C_{1332} & C_{1333} \\
C_{2111} & C_{2112} & C_{2113} & C_{2121} & C_{2122} & C_{2123} & C_{2131} & C_{2132} & C_{2133} \\
C_{2211} & C_{2212} & C_{2213} & C_{2221} & C_{2222} & C_{2223} & C_{2231} & C_{2232} & C_{2233} \\
C_{2311} & C_{2312} & C_{2313} & C_{2321} & C_{2322} & C_{2323} & C_{2331} & C_{2332} & C_{2333} \\
C_{3111} & C_{3112} & C_{3113} & C_{3121} & C_{3122} & C_{3123} & C_{3131} & C_{3132} & C_{3133} \\
C_{3211} & C_{3212} & C_{3213} & C_{3221} & C_{3222} & C_{3223} & C_{3231} & C_{3232} & C_{3233} \\
C_{3311} & C_{3312} & C_{3313} & C_{3321} & C_{3322} & C_{3323} & C_{3331} & C_{3332} & C_{3333}
\end{pmatrix}
\begin{pmatrix} e_{11} \\ e_{12} \\ e_{13} \\ e_{21} \\ e_{22} \\ e_{23} \\ e_{31} \\ e_{32} \\ e_{33} \end{pmatrix}
$$

where C_{ijkl} are the elastic coefficients. We know that C_{ijkl} is a fourth order tensor

and they are 81 in total. These coefficients are independent of e_{ij} but may vary from point to point of the body. The number of these constants may be reduced due to the symmetry and nature of the material body, i.e., general anisotropy, monoclinic, orthotropic, transversely isotropic, cubic and isotropic materials.

(i) **Stress symmetry**

Since the stress tensors are symmetric, $\tau_{ij} = \tau_{ji}$ and we have six independent stress tensors, viz. $\tau_{11}, \tau_{22}, \tau_{33}, \tau_{12}, \tau_{13}$ and τ_{23}.

We have

$$\tau_{ij} = C_{ijkl}e_{kl}, \qquad \text{and} \qquad \tau_{ji} = C_{jikl}e_{kl}. \tag{1.6}$$

On subtracting these two equations, we get $C_{ijkl} = C_{jikl}$.

Now there are six independent choices to express i and j together and still nine independent ways to express k and l taken together. Thus with this symmetry, the number of independent elastic constants reduce to $6 \times 9 = 54$.

(ii) **Strain symmetry**

There are six independent strain components, i.e., $e_{11}, e_{22}, e_{33}, e_{12}, e_{13}$ and e_{23} due to $e_{ij} = e_{ji}$.

From Eq. (1.5), we have

$$\tau_{ij} = C_{ijkl}e_{kl} \qquad \text{and} \qquad \tau_{ij} = C_{ijlk}e_{lk}, \tag{1.7}$$

which give $C_{ijkl} = C_{ijlk}$. With this symmetry, there are six independent choices to express both i and j as well as k and l taken together. Thus, the number of independent elastic coefficients reduce to $6 \times 6 = 36$. Thus, the Hooke's law takes the form

$$\tau_{ij} = C_{ijkl}e_{kl}, \quad (i, j, k, l = 1, 2, 3) \tag{1.8}$$

where $C_{ijkl} = C_{jikl} = C_{jilk} = C_{ijlk}$.

This Hooke's law may also be expressed in a compact form of equation as

$$\tau_i = C_{ij}e_j, \quad i, j = 1, 2, 3, 4, 5, 6. \tag{1.9}$$

(iii) **Strain energy function**

The strain energy density function (W) is a quadratic function of strain given as

$$W = \frac{1}{2}C_{ij}e_i e_j, \tag{1.10}$$

with the property

$$\frac{\partial W}{\partial e_i} = \tau_i, \quad i = 1, 2, 3, 4, 5, 6. \tag{1.11}$$

On differentiating Eq. (1.10) with respect to e_k, we get

$$\frac{\partial W}{\partial e_k} = \frac{1}{2}C_{ik}e_i + \frac{1}{2}C_{kj}e_j. \tag{1.12}$$

Since i and j are the dummy suffixes, the above equations give

$$\tau_k = \frac{1}{2}(C_{ik} + C_{ki})e_i, \tag{1.13}$$

and resulting $C_{ij} = C_{ji} \quad \forall\, i, j$.

Thus, the number of elastic coefficients reduce to 21. These 21 independent constants represent the characteristics for a general *anisotropic* or *aelotropic material*.

(iv) **Symmetry with respect to a plane**

Consider an elastic solid having symmetry with x_1x_2-plane. We have transformed the axis of the Cartesian co-ordinate as $x_1 \to x_1'$, $x_2 \to x_2'$, $x_3 \to -x_3'$ and C_{ij}'s are invariant under this transformation. The direction cosines for this transformation is

	x_1	x_2	x_3
x_1'	1	0	0
x_2'	0	1	0
x_3'	0	0	-1

Table 1.1: Direction cosines

We know that

$$\tau_{\alpha\beta}' = l_{\alpha i}l_{\beta j}\tau_{ij}, \quad \text{and} \quad e_{\alpha\beta}' = l_{\alpha i}l_{\beta j}e_{ij}, \tag{1.14}$$

where l_{ij} is the direction cosine.

We have

$$\tau_1' = \tau_1, \tau_2' = \tau_2, \tau_3' = \tau_3, \tau_4' = -\tau_4, \tau_5' = -\tau_5, \tau_6' = \tau_6$$

$$\text{and } e_1' = e_1, e_2' = e_2, e_3' = e_3, e_4' = -e_4, e_5' = -e_5, e_6 = e_6. \tag{1.15}$$

Hence, we have

$$\tau_1 = C_{11}e_1 + C_{12}e_2 + C_{13}e_3 - C_{14}e_4 - C_{15}e_5 + C_{16}e_6. \tag{1.16}$$

Using Eqs.(1.15) and (1.16), we get $C_{14} = C_{15} = 0$.

Similarly, we get

$$C_{24} = C_{25} = C_{34} = C_{35} = C_{64} = C_{65} = C_{41} = C_{42}$$

$$= C_{43} = C_{46} = C_{51} = C_{52} = C_{53} = C_{56} = 0.$$

Thus, the number of elastic constants reduce to 13 and such anisotropic materials are known as *monoclinic medium.* Lithium tantalate, Lithium neobate, Beta-sulfur, gypsum, borax, orthoclase, kaolin, muscovite, clinoamphibole, clinopyroxene, jadeite, azurite, and spodumene crystallize show the monoclinic symmetry.

Similarly by considering the symmetry with respect to x_2x_3-plane, we can get

$$C_{16} = C_{26} = C_{36} = C_{45} = C_{54} = C_{61} = C_{62} = C_{63} = 0.$$

In this case, the number of independent elastic coefficients reduce to 9 and such anisotropic materials are known as *orthotropic elastics.* Unidirectional fibrous composites and woods are an example of orthotropic materials. We may note that if we consider elastic symmetry with respect to x_1x_3-plane, there is no further reduction in the number of elastic coefficients. Thus, if there are two orthogonal planes of elastic symmetry, then the third orthogonal plane is automatically a plane of elastic symmetry.

(v) **Symmetry with respect to axis**

We transform the Cartesian co-ordinates by rotating x_1, x_2 and x_3-axes through a right angle about x_1-axis. The table of direction cosines for this transformation is

	x_1	x_2	x_3
x_1'	1	0	0
x_2'	0	0	1
x_3'	0	-1	0

Table 1.2: Direction cosines

Using these direction cosines into Eq. (1.14), we obtain

$$C_{12} = C_{13}, \quad C_{33} = C_{22}, \quad C_{55} = C_{66}.$$

Thus, the number of elastic coefficients reduce to 6.

Next, we consider the rotation of axes through a right angle about x_3-axis and we obtain

$$C_{13} = C_{23}, \quad C_{11} = C_{22}, \quad C_{44} = C_{55}.$$

In this symmetry, the number of elastic coefficients reduce to 3 and such anisotropic materials are said to be *cubic symmetry*.

If we transform the Cartesian co-ordinates by rotating x_1, x_2 and x_3-axes through an angle θ about x_3-axis. The direction cosines for this transformation is

	x_1	x_2	x_3
x_1'	$\cos\theta$	$\sin\theta$	0
x_2'	$-\sin\theta$	$\cos\theta$	0
x_3'	0	0	1

Table 1.3: Direction cosines

Using these direction cosines into Eq. (1.14), one may obtain

$$C_{44} = \frac{1}{2}(C_{11} - C_{12}) = \mu \ \text{ and } \ C_{12} = \lambda$$

as the only two elastic constants. Such materials are said to be *isotropic elastic body*

and Hooke's law, in this case, is given by

$$\tau_{ij} = \lambda\delta_{ij}\Theta + 2\mu e_{ij}, \quad i,j = 1,2,3 \tag{1.17}$$

where $\Theta = e_{ii}, i = 1,2,3$. The strain components (e_{ij}) may be represented as

$$e_{ij} = \frac{-\lambda\delta_{ij}}{2\mu(3\lambda + 2\mu)}\nu + \frac{1}{2\mu}\tau_{ij}, \tag{1.18}$$

where $\nu = (3\lambda + 2\mu)\Theta$ with λ and μ as Lamé parameters.

1.3 Linear momentum and the stress tensor

Consider a continuum body with volume V and boundary S. This boundary surface is subjected to the distribution of surface traction $\mathbf{T}(\mathbf{x}, \mathbf{t})$ per unit area acting on every point and each mass element of the body may be acted with a body force, $\mathbf{F}(\mathbf{x}, \mathbf{t})$ per unit volume. The principle of balance of linear momentum states that the instantaneous rate of change of the linear momentum of a body is equal to the resultant external force acting on the body at the particular instant of time which may be written as

$$\int_S \mathbf{T}(\mathbf{x},\mathbf{t})ds + \int_V \rho\mathbf{F}(\mathbf{x},\mathbf{t})dv = \int_V \rho\ddot{\mathbf{u}}dv. \tag{1.19}$$

Inserting Eq. (1.3) into Eq. (1.19), we have

$$\int_S \tau_{ij}n_j ds + \int_V \rho F_i dv = \int_V \rho\ddot{u}_i dv. \tag{1.20}$$

Using Gauss's divergence theorem, the surface integral can be transformed into a volume integral as

$$\int_S \tau_{ij}n_j ds = \int_V \tau_{ij,j}dv. \tag{1.21}$$

Using Eqs. (1.21) and (1.20), we get

$$\int_V (\tau_{ij,j} + \rho F_i - \rho\ddot{u}_i)dv = 0. \tag{1.22}$$

Since the integrand is continuous and V is arbitrary, we can take

$$\tau_{ij,j} + \rho F_i = \rho \ddot{u}_i, \qquad (i, j = 1, 2, 3). \tag{1.23}$$

This equation is also known as Cauchy's first equation of motion.

1.4 Spectrum theorem

Let **AB** and **CD** be two incident plane waves with wave front BF on a periodic surface whose wavelength BD is $2\pi/np$. Suppose **BF** and **DG** are the reflected waves. The incident and reflected waves make angles α and α_n respectively with the vertical on the periodic surface as shown in Figure 1.4.
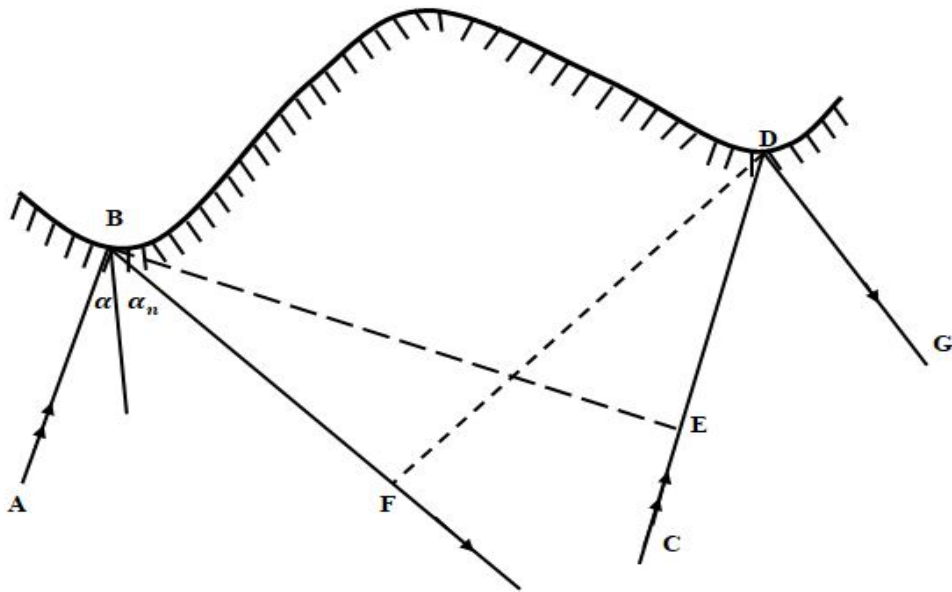
Figure 1.4: Incident and reflected plane waves.

The wave front meets the surface at B and that point starts radiating reflected waves before the wave front of the incident wave arrives at the point D of the surface. Hence, there is a difference between the length of the paths of two reflected waves. Let BE and DF be normal to **CD** and **BF** respectively. The wave emerging from B

covers a distance which exceeds that covered by the wave emerging from D by

$$|BF| - |DE| = \frac{2\pi}{np}(\sin \alpha_n - \sin \alpha)$$

Thus, the phase difference between the two waves is $\frac{2\pi k}{np}(\sin \alpha_n - \sin \alpha)$, where k is wavenumber. For the constructive interference, the phase difference between these waves must be a multiple of 2π. Hence, we have

$$\sin \alpha_n - \sin \alpha = \pm \frac{|np|}{k}. \tag{1.24}$$

This equation may be written as

$$\sin \alpha_n^+ = \sin \alpha + \frac{|np|}{k}, \qquad \sin \alpha_n^- = \sin \alpha - \frac{|np|}{k}, \tag{1.25}$$

where α_n^+ and α_n^- are respectively angles of the scattered waves to the right and left sides of the plane wave as shown in Figure 1.5.
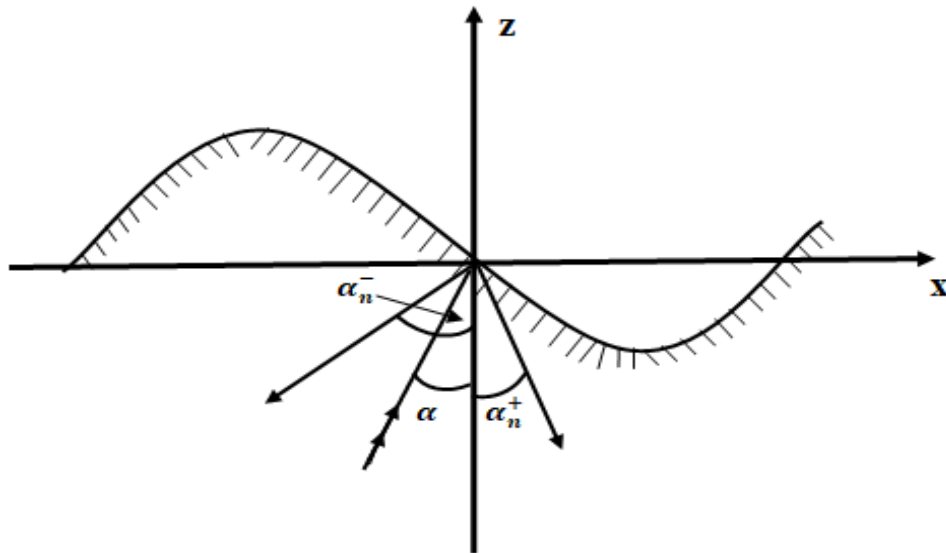
Figure 1.5: The angles of reflected waves α_n^+ and α_n^- with incident angle, α.

1.5 Rayleigh's method of approximation

Rayleigh (1907) was the first who had studied the problem on the scattering of light or sound waves. In his method, the function defining the corrugated interface in the boundary condition is expanded in Fourier series and the unknown coefficients in the solutions are determined in terms of small parameter up to any given order of approximation, which is the characteristics of the corrugated interface.

In order to explain this method, let us take a corrugated interface given by $z = \zeta(x)$ separating two media. This function is periodic in x and independent of y whose mean value is zero. The Fourier series expansion of $\zeta(x)$ is

$$\zeta(x) = \sum_{n=1}^{\infty} (\zeta_{+n} e^{\imath npx} + \zeta_{-n} e^{-\imath npx}) \tag{1.26}$$

$$= c_1 \cos px + c_2 \cos 2px + s_2 \sin 2px + ... + c_n \cos npx + s_n \sin npx + ...,$$

where $\zeta_{+1} = \zeta_{-1} = c_1/2, \ \zeta_{\pm n} = (c_n \mp \imath s_n)/2$.

The direction cosines of the normal, $\boldsymbol{\nu}$ to $z = \zeta(x)$ are $< 1/\sqrt{1+\zeta'^2}, 0, \zeta'^2/\sqrt{1+\zeta'^2} >$ and those of tangent, $\mathbf{t}$ are $< -\zeta'^2/\sqrt{1+\zeta'^2}, 0, 1/\sqrt{1+\zeta'^2} >$, where $\zeta' = d\zeta/dx$. The normal (N_ν) and tangential stresses (T_ν, Y_ν) in the νyt-system are connected to those X_x, Z_x, Z_z in the xyz-system by the following relation as

$$N_\nu = [(Z_z - X_x)\zeta' + Z_x(1 - \zeta'^2)]/(1 + \zeta'^2),$$

$$T_\nu = [Z_z + \zeta'^2 X_x - 2\zeta' Z_x]/(1 + \zeta'^2), \quad Y_\nu = [Y_z - \zeta' Y_x]/\sqrt{(1 + \zeta'^2)}. \tag{1.27}$$

The total displacements for SH-waves in the two half-spaces after dropping the common factor $(e^{i\omega t})$ are given by (Assano, 1960)

$$v = e^{i\sqrt{\sigma_1}h_1 x \sin\alpha} [A_0 e^{i\sqrt{\sigma_1}h_1 z \cos\alpha} + A_1 e^{-i\sqrt{\sigma_1}h_1 z \cos\alpha} + \sum_{n=1}^{\infty} A_n^{\pm} e^{i(\pm npx - \sqrt{\sigma_1}h_1 z \cos\alpha_n^{\pm})}],$$

$$v' = e^{i\sqrt{\sigma_1}h_1 x \sin\alpha} [B_1 e^{i\sqrt{\sigma_2}h_2 z \cos\beta} + \sum_{n=1}^{\infty} B_n^{\pm} e^{i(\pm npx + \sqrt{\sigma_2}h_2 z \cos\beta_n^{\pm})}], \tag{1.28}$$

where A_i and B_i are amplitude constants, $h_i^2 = \rho_i \omega^2/(\lambda_i + 2\mu_i)$, ω is the angular frequency, ρ_i is the density and $\sigma_i = (\lambda_i + 2\mu_i)/\mu_i$.

There are continuity of displacements and tangential stress at $z = \zeta(x)$. These conditions are given by

$$A_0 e^{i\sqrt{\sigma_1}h_1\zeta\cos\alpha} + A_1 e^{-i\sqrt{\sigma_1}h_1\zeta\cos\alpha} + \sum_{n=1}^{\infty} A_n^{\pm} e^{i(\pm npx - \sqrt{\sigma_1}h_1\zeta\cos\alpha_n^{\pm})}$$

$$= B_1 e^{i\sqrt{\sigma_2}h_2\zeta\cos\beta} + \sum_{n=1}^{\infty} B_n^{\pm} e^{i(\pm npx + \sqrt{\sigma_2}h_2\zeta\cos\beta_n^{\pm})}, \qquad (1.29)$$

$$\mu[A_0\sqrt{\sigma_1}h_1(\cos\alpha - \zeta'\sin\alpha)e^{i\sqrt{\sigma_1}h_1\zeta\cos\alpha} - A_1\sqrt{\sigma_1}h_1(\cos\alpha + \zeta'\sin\alpha)e^{-i\sqrt{\sigma_1}h_1\zeta\cos\alpha}$$

$$- \sum_{n=1}^{\infty} A_n^{\pm} e^{\pm inpx}\{\sqrt{\sigma_1}h_1\cos\alpha_n^{\pm} + (\sqrt{\sigma_1}h_1\sin\alpha \pm np)\zeta'\}e^{-i\sqrt{\sigma_1}h_1\zeta\cos\alpha_n^{\pm}}]$$

$$= \mu'[B_1(\sqrt{\sigma_2}h_2\cos\beta - \sqrt{\sigma_1}h_1\zeta'\sin\alpha)e^{i\sqrt{\sigma_2}h_2\zeta\cos\beta}$$

$$+ \sum_{n=1}^{\infty} B_n^{\pm} e^{\pm inpx}\{\sqrt{\sigma_2}h_2\cos\beta_n^{\pm} - (\sqrt{\sigma_1}h_1\sin\alpha \pm np)\zeta'\}e^{i\sqrt{\sigma_2}h_2\zeta\cos\beta_n^{\pm}}]. \qquad (1.30)$$

Note that slope and amplitude of the corrugated interface are small enough so that

$$e^{\pm i\sqrt{\sigma_1}h_1\zeta\cos\alpha} = 1 \pm i\sqrt{\sigma_1}h_1\zeta\cos\alpha - \sigma_1 h_1^2\zeta^2\cos^2\alpha \pm \text{...... etc.} \qquad (1.31)$$

Using Eq.(1.31) into Eqs.(1.29) and (1.30), we may find the amplitude ratios corresponding to regular and irregular waves of any order (n) of approximations. Homma (1940) used this method for the first time in the Seismic waves. Sato (1955) solved the problem of the reflected waves at a corrugated free surface by Rayleigh's technique.

1.6 Importance of wave propagation

Wave propagation and their phenomena of reflection and transmission from a boundary surface is an elegant and fascinating subject that deals with numerous problems in various fields, i.e., Seismology, geophysics, Earthquake engineering, tele-communication, medicines (echography), metallurgy (non-destructive testing) and signal processing. These waves are useful in detection of notches and faults in different types of materials such as in railway tracks, buried land-mines, etc. Seismic waves

are useful tool for investigating the internal structure of the earth and also used for exploration of valuable materials such as minerals, crystals, fluids (oils, water) etc. beneath the earth surface.

The nature of the composition of matters in the Earth's crust plays an important role in changing the characteristics of the seismic signals recorded on the surface of the Earth. These seismic signals carry a lot of information with them about the internal structures of the Earth's interior and their dynamic characteristics can be carried out up to a large extent. The surface waves are very helpful for the study of crustal and upper mantle structures. The knowledge about the upper structure of the Earth helps the seismologists in studying the nature of the possible sources of Earthquakes and which, in turn, further help in the prediction.

The Earth is approximated by various models in the study of Seismic waves. These models are mathematical frameworks within which observed seismograms are related to the Earth's interior via model parameters. To achieve a better study of Earth's structures, especially for deep interior, the studies of wave propagation in Earth's models become more important. It is proved that S-waves can not travel through the interior of the core. This leads to the conclusion that the Earth core is composed of material which is non-viscous liquid like and is believed to be in liquid form at high temperature and harder than the solid. Earth's strata has different layers and there are many experimental evidences that the discontinuities/interfaces between these layers are not perfectly plane, but they are of corrugated and hence irregular in nature. These irregular natures of the interfaces affect in the reflection and transmission phenomena of the elastic waves. Thus, it is important to take into account the problems related with the effects of irregular interfaces. If the structure of the earth were simple enough like uniform and homogeneous, it would be easy to grasp the nature of the Earthquake motion. The geophysical exploration methods such as seismic, gravity and other prospecting and also geodesic measurement have revealed the existence of roughness/corrugation in many parts of the world. Thus,

it is necessary to study the effect of the undulation of the boundary surface on the propagation of elastic waves.

1.7   Review of literatures

The theory of wave propagation is an interesting area of research since long. Lamb (1881) examined into the nature of the fundamental modes of vibration of an elastic sphere and discussed the vibrations of an elastic solid having finite dimensions. Rayleigh (1885) investigated the behavior of waves on the plane free surface of an infinite homogeneous isotropic elastic solid, their character are such that the disturbance confined to a superficial region of thickness comparable with the wave-length. Love (1892) discussed the general Mathematical theory of the elastic properties of the first class of bodies. Cosserat and Cosserat (1909) explained the statics and dynamics of deformable media. Aki and Richards (1930) explored the propagation of seismic waves in realistic Earth models including the theories of fracture and rupture propagation. Christie (1955) showed that an incident dilatation wave on a free surface produces reflected dilatation and distortion waves. Brekhoviskikh (1960) presented a systematic exposition on the theory of propagation of elastic and electromagnetic waves in layered media. Mindlin (1964) formulated a linear theory of a three-dimensional elastic continuum which has some of the properties of a crystal lattice. Fedorov (1968) adopted the theory of elastic waves in crystals.

Gurtin (1981) introduced the linear and nonlinear theories of elasticity in the continuum mechanics for an ideal compressible viscous fluids. Spencer (1984) studied numerous problems related with deformation and stress of fibre-reinforced composite anisotropic materials. Chadwick (1985) investigated the basic characteristics of surface waves in an anisotropic elastic body which depend crucially on the transonic states defined by the sets of parallel tangents to a centered section of the slowness surface. Kielczynski and Pajewski (1987) analyzed the validity of an approximate reflection coefficient for an obliquely incident SH-wave at a plane interface between

an elastic solid and a viscoelastic liquid. Doyle (1989, 1997) discussed the subject of wave propagation in structures using the fast Fourier transform (FFT) and discrete Fourier transform (DFT) based spectral analysis methodology. Golubovic and Lubensky (1989) analyzed the structural phase transitions in amorphous solids associated with vanishing bulk and shear modulus. Dowaikh and Ogden (1990) investigated the propagation of surface waves on the half-space of incompressible isotropic elastic material. Hosten (1991) discussed a method of characterizing orthotropic and viscoelastic behavior of some composite materials. Chattopadhyay and Choudhury (1995b) studied the problem of reflection/transmission of magneto-elastic shear waves in two infinite self-reinforced elastic half-spaces. Ogden and Sotiropoulos (1997) illustrated the influence of pre-stress and finite strain on the reflection of plane waves from the surface free boundary of an incompressible isotropic elastic solid. Anderson *et al.* (1999) developed a continuum theory for the mechanical behavior of rubber-like solids that are formed by the cross-linking of polymeric fluids containing nematic molecules as elements of their main-chains or as pendant side-groups. Gebretsadkan and Karla (2002) investigated the propagation of linear waves in relativistic anisotropic magneto-hydrodynamics and plotted the Fresnal ray surface. Singh and Singh (2004) studied the problem of plane waves in fibre-reinforced elastic media and showed that the phase velocities of quasi P and SV-waves depend on the angle of propagation.

Zhu and Tsvankin (2006) developed a consistent analytic treatment of plane wave for transversely isotropic media. Chattopadhyay and Venkateswarlu (2007) obtained the phase velocities of quasi P and quasi SV-waves in terms of propagation vector of plane waves in the fibre reinforced medium. Ota (2009) examined the singularities of the scattering kernel for incident transverse wave. Vinh and Giang (2011) derived the velocity of Stoneley waves propagating along the loosely bonded interface of two isotropic elastic half-spaces using the complex function method. Singh (2011a) studied the effect of initial stresses on incident qSV-waves at a plane interface of two

dissimilar pre-stressed elastic half-spaces and derived the reflection and refraction coefficients. Singh (2017) investigated the problem of plane waves propagation in anisotropic nematic elastomers and obtained the phase velocity and attenuation co-efficients for the plane harmonic waves. The problems based on waves and vibrations have been analyzed by many researchers with different elastic models and they are in several books and research papers such as Lamb (1917a, 1917b), Love (1911), Carlson and Heins (1946), Sokolnikof (1956), Ewing *et al.* (1957), Toupin, (1962), Scott (1975), Achenbach (1976), Ben-Menahem and Singh (1981), Sobczyk (1985), Bullen and Bolt (1985), Abeyaratne (1988), Bowen (1989), Graff (1991), Lai *et al.* (1993), Sheriff and Geldart (1995), Chattopadhyay *et al.* (1997), Xia *et al.* (1999), Udias (1999), Singh (1999), Singh and Khurana (2002), Pujol (2003), Zarutskii and Podilchuk (2006), Muller (2007), Reddy (2008), Nair (2009), Shearer (2009), Wilman-ski (2010), Blum *et al.* (2011), Clive and Irving (2013), Rose (2014), Zhang *et al.* (2019), Malla *et al.* (2019), Saed and Terentjev (2020) and Ohzono *et al.* (2019, 2020).

Chattopadhyay and Choudhury (1995a) discussed the reflection of P-waves at the free and rigid boundaries in a medium of monoclinic type and obtained phase velocity of Rayleigh wave and reflection coefficients of the reflected waves. Chattopadhyay and Saha (1996) investigated the phenomena of reflection and refraction of incident P-waves at a plane interface between two monoclinic half-spaces. Chattopadhyay *et al.* (1996) discussed the problem of incident SV-wave in the monoclinic elastic half-space and derived the reflection coefficients for P and SV-waves. Chattopadhyay and Saha (1999) investigated the problem of reflection/refraction of incident quasi SV-wave at a plane interface of two monoclinic half-spaces. Sotiropoulos and Nair (1999) examined the reflection of plane elastic waves from a free surface of mono-clinic incompressible materials under plane strain conditions. Singh and Khurana (2001, 2002) studied the problems of reflected and transmitted P and SV-waves at an interface of two monoclinic elastic half-spaces and obtained the reflection and

transmission coefficients using suitable boundary conditions. Singh *et al.* (2003) obtained the closed form analytical expression for the horizontal displacement due to a long inclined strike-slip fault situated in a monoclinic elastic half-space. Chattopadhyay and Rajneesh (2006) derived the reflection and refraction coefficients of the plane waves at an interface between isotropic and anisotropic triclinic crystalline half-spaces. Singh (2010) discussed the reflected waves from a thermally insulated stress free thermoelastic solid of monoclinic type and observed the effects of anisotropy and thermal relaxation times. Chattopadhyay *et al.* (2013) obtained the closed form expressions for the amplitude ratios of qP, qSV and qSH-waves from the interface between two distinct generally anisotropic half-spaces. Kumari *et al.* (2014) studied the phenomena of reflection and refraction of incident quasi (P/SV)-waves in dissimilar monoclinic media separated by an isotropic layer of finite thickness.

Liquid-crystalline elastomers (LCEs) represent a novel and exciting physical system that combines the local orientational symmetry breaking and the entropic rubber elasticity. Nematic elastomers (NEs) are soft materials, rubbery solids made up of cross-linking of nematic crystalline molecules called mesogens either incorporated into the main chain or pendant from them (Finkelmann *et al.*, 1981). The mesogens are rigid rod-like molecules attached to the polymeric backbone. They are randomly oriented at high temperature but upon cooling through the isotropic-nematic transition temperature, they align along a common direction described by the nematic director (Warner and Terentjev, 1996). One of the characteristic property of NEs is the presence of long macromolecules with rare intermolecular transversal bonds. There is an interplay between elastic and orientational order which is responsible for many fascinating properties that are different from elastic solids and liquid crystals (de Gennes and Prost, 1993). It's soft matter properties lead to growing interest in the field of microelectronics, biomechanics, nanomechanics and device applicable in mechanical damping, optics or acoustics, where there are possibility of accoustic polarization. These materials also display many unusual mechanical properties in-

cluding the formation of fine-scale microstructures and fine-scale wrinkles (Xie and Zhang, 2005; Ohm *et al.*, 2012).

Mitchell *et al.* (1987) described the preparation of a range of acrylate-based side-chain liquid crystal elastomers and showed that materials containing upto 13 mol percent of cross-linking units exhibit a nematic-isotropic transition. Semenov and Kokhlov (1988) studied the conditions for phase equilibrium of liquid-crystalline polymers. Kupfer and Finkelmann (1991) introduced an approach for alignment of elastomers and liquid crystal polymers with more permanent and macroscopically uniform. Kupfer *et al.* (1993) synthesized a series of liquid single-crystal elastomers with different cross-linking densities. Terentjev (1993) derived the general phenomenological free energy for a liquid crystalline elastomer under arbitrary strain and orientational distortions. Using the group representations method, he obtained all invariants describing the coupling of translational and orientational deformations and/or external electric field. Bladon *et al.* (1994) showed that monodomain nematic networks formed by cross-linking polymer liquid crystals in ordered states retain a memory of their anisotropic cross-linking conditions. Kundler and Finkelmann (1995) investigated the strain-induced director reorientation process in nematic liquid single crystal elastomers for the case of an arbitrary angle between the original director and the external stress axis. Verwey *et al.* (1996) studied the elastic and orientational response of a uniform nematic elastomer subjected to an extension perpendicular to its director. Finkelmann *et al.* (1997) presented an experimental and theoretical investigation of the critical formation of stripe domains in monodomain nematic elastomers. Clarke and Terentjev (1998) discussed the dynamics of stress relaxation before, during and after the polydomain-monodomain transition. Teixeira and Warner (1999) studied analytically and numerically the dynamics of 'how does an anisotropic nematic elastomer respond elastically and orientationally to an imposed strain?'. Terentjev (1999) examined the unusual mechanical properties of nematic and smectic rubbers, their randomly disordered equilibrium textures, some aspects of dynamics and me-

chanical relaxation.

Uchida (2000) investigated the properties of disordered nematic elastomers and gels emphasizing on the roles of nonlocal elastic interactions and cross-linking conditions. Long and Morse (2000) described the linear viscoelastic response of monodomains of unentangled nematic liquid crystalline polymers using a generalized Rouse model. Clarke *et al.* (2001) presented a combine theoretical and experimental study of linear viscoelastic response in oriented monodomain nematic elastomers. Selinger *et al.* (2002a) showed that the molecules in a nematic liquid-crystal cell can be realigned by an ultrasonic wave leading to the change in the optical transmission through a cell. Fradkin *et al.* (2003) investigated the problem of viscoelastic theory of nematic elastomers in the low-frequency limit and discussed the spectral and polarization properties of acoustic waves. Cermelli *et al.* (2004) derived a supplemental evolution equation for an interface between the nematic and isotropic phases of a liquid crystal neglecting the liquid flow. Brand *et al.* (2006) analyzed the selected macroscopic properties of side chain liquid crystalline elastomers focusing on the influence of relative rotations between the director and the strain field. DeSimone and Teresi (2009) discussed several elastic energies for nematic elastomers with small strain expansions both for the cases of large director rotations and small director changes. Ericksen (1960), Leslie (1966), Mitchell *et al.* (1993), Bladon *et al.* (1993), Brand and Plenier (1994), Alexe-Ionescu *et al.* (1994), Verwey *et al.* (1996), Anderson *et al.* (1999), Everaers (1999), DeSimone and Dolzmann (2000), Schmidtke *et al.* (2000), Schonstein *et al.* (2001), Finkelmann *et al.* (2001), Terentjev and Warner, (2001), Fried and Todres (2002), Conti *et al.* (2002), Selinger *et al.* (2002b), Warner and Terentjev, (2003), Ohm *et al.* (2011), Wim (2012), Guin *et al.* (2018), Gattinger *et al.* (2019) and Ditter *et al.* (2020) also discussed different problems related with nematic elastomers.

Othman and Song (2008) established the equations of motion for the generalized magneto-thermoelastic materials with two relaxation times and discussed the effects

of reference temperature, the applied magnetic field and thermal coupling on the reflection coefficient of the reflected waves. Zakharov (2011) investigated the localized waves near the stress-free surface or the free edge of a solid with a thin nematic coating. Matteis (2012) introduced and analyzed a variational theory proposed on the interaction of acoustic fields and the nematic texture of a liquid crystal. Yang *et al.* (2014) studied the characteristic equations for Rayleigh wave propagation in NEs based on viscoelastic theory at low frequency limit and obtained the dispersion equation. Plucinsky and Bhattacharya (2017) showed analytically and numerically that nematic elastomer sheets can suppress wrinkling by modifying the expected state of stress through the formation of microstructures. Urbanski *et al.* (2017) investigated the liquid crystals in micron-scale droplets and documented their extraordinary responsiveness and large diversity of self-assembled structures of liquid crystals. Zhao and Liu (2018) studied the problem of transverse wave dispersion in an NE beam by considering anisotropy and viscoelasticity in the low frequency limit.

Green (1982) obtained the phase velocity of flexural waves (Lamb waves) in a plate of transversely isotropic material with the axis of transverse isotropy lying in the plane of the plate. Belfield *et al.* (1983) revealed about the anisotropic behavior of fibre-reinforced elastic plates in such away that the reinforcement are continuously distributed in concentric circles. Baylis and Green (1986) used a continuum model to explain the mechanical properties of flexural waves in fibre-reinforced laminated plates. Rogerson (1991) investigated various dynamic properties of transversely isotropic incompressible elastic medium and obtained the wave speeds in explicit form. Dowaik and Ogden (1991) examined the propagation of an interfacial (Stoneley) waves along the boundary between two half-spaces of pre-stressed incompressible isotropic elastic materials. Payton (1992) developed a model on a transversely isotropic elastic solid whose slowness surface has two conical points on the symmetry axis. Rogerson (1992) examined the dynamic response of a six-ply fibre-reinforced laminated plate to an impulsive line load acting on the upper sur-

face. Chadwick (1993) concluded that exceptional transonic states arise only when the direction of transverse isotropy is either in the reference plane or at right angles to the reference vector. Nair and Sotiropoulos (1997) examined the propagation of elastic plane waves in orthotropic incompressible materials under plane strain conditions. Rogerson and Sandiford (2000) derived the dispersion relation associated with small amplitude waves propagating along a common principal direction in a two layer perfectly bonded elastic structure. Destrade (2001) obtained the secular equation for surface acoustic waves traveling in an orthotropic incompressible half-space using the first integral method. Chattopadhyay and Rogerson (2001) studied the problem of reflection of plane waves from a traction-free boundary of incompressible elastic material. Itskov and Aksel (2002) studied elastic constants and their admissible values for incompressible and slightly compressible anisotropic materials.

Kossovich *et al.* (2002) derived the dispersion relation associated with harmonic waves in an incompressible transversely isotropic elastic plate. Ogden and Vinh (2004) obtained the characteristic equation for the Rayleigh wave in an incompressible orthotropic material. Prikazchikov and Rogerson (2004) investigated the problem of surface wave propagation in the transversely isotropic incompressible pre-stressed half-space. Spencer and Soldatos (2007) showed that the stress and couple stress are direct and successive functions of first and second dimensional differentials of the displacement. Singh (2007b) assumed a suitable boundary conditions to obtain the amplitude ratios at free surface of transversely isotropic incompressible elastic half-space. There are many other papers on fibre-reinforced and transversely isotropic materials such as Pipkin (1979), Payton (1983), Lauke and Schultrich (1983), Chadwick (1989a,1989b), Chattopadhyay and Choudhury (1990), Tomar *et al.* (2002), Rouison *et al.* (2004), Kumar and Hundal (2007), Munch *et al.* (2011), Chen *et al.* (2011), Komijani *et al.* (2013), Chabaud *et al.* (2013), Mohammed *et al.* (2015), Koniuszewska and Kaczmar (2016), Abhemanyu *et al.* (2019), Sanjay *et al.* (2019) and Mahanty *et al.* (2020).

Ogden and Singh (2011) derived the general constitutive equation for a transversely isotropic hyper-elastic solid in the presence of initial stress based on the theory of invariants. Abd-Alla *et al.* (2013) investigated the propagation of surface waves in fibre-reinforced anisotropic elastic medium subjected to gravity field. They derived the frequency equations of Stoneley waves, Rayleigh waves and Love waves. Singh *et al.* (2014) analyzed reflection and refraction patterns of elastic waves due to incident plane wave at an interface of two dissimilar incompressible transversely isotropic fibre-reinforced elastic half-spaces. Chatterjee and Chattopadhyay (2015) investigated the propagation of SH-waves in slightly compressible finitely deformed elastic half-spaces. Zak and Krawczuk (2018) analyzed certain aspects related to the dynamic behavior of isotropic shell-like structures by using an approach known as the time-domain spectral finite element method ($TD - SFEM$). Kumari *et al.* (2019) investigated SH-wave propagating in a visco-elastic fibre-reinforced layer resting over a porous half-space and obtained the displacement components using method of separation of variable. Verma *et al.* (2019) examined the issue of versatile plastic change in transversely isotropic spherical shell with the condition of uniform internal pressure.

The study of scattering waves from a rough or corrugated surface is interesting and useful in a number of fields. Blake (1950) applied probability theory to study the reflected radio waves from a rough sea. Rice (1951) dealt with the reflection of plane electromagnetic waves from a surface $z = f(x, y)$ using the perturbation method. Miles (1954) examined the reflection of a plane wave at a rough interface separating two fluid media. Kuo and Nafe (1962) investigated the problem of Rayleigh wave propagation in a solid layer overlying a solid half-space separated by a sinusoidal interface. Abubakar (1962a) obtained an approximate solution of the two-dimensional problem of reflection of plane harmonic P and SV-waves at an irregular boundary by using modified Rice's perturbation method. Dunkin and Eringen (1963) showed that

the magnetic field has been much more effective than the electric field in the couplings between the elastic and electromagnetic waves. Levy and Deresiewicz (1967) studied the behavior of the reflected and transmitted waves from a layered medium whose internal interfaces are irregular. Kennet (1972) discussed the scattering of seismic waves using the first-order perturbation theory. Gupta (1978) studied the two dimensional model of reflection and refraction phenomena of waves from the curved surface. Gupta (1987) studied reflection and transmission coefficients of plane SH-waves at a corrugated interface between two laterally and vertically heterogeneous media by using Rayleighs method of approximation. Paul and Campillo (1988) analyzed the problem of the effect of small scale irregularities on the reflected elastic waves using a discretized form of boundary integral equations.

Nayfeh (1991) derived analytical expressions for the reflection and transmission coefficients of the elastic waves from the interface of liquid/anisotropic half-spaces. Korneev and Johnson (1993) described the complete and exact solution for the problem of an incident P-wave scattered by an elastic spherical inclusion. Zhang and Shinozuka (1996) investigated the effects of irregular boundaries on the propagation of seismic waves in a layered half-space. Kumar *et al.* (2003) investigated the problem of reflection and transmission of SH-waves at a corrugated interface between two different transversely isotropic and vertically heterogeneous elastic solid half-spaces. Kaur and Tomar (2004) investigated the problem of reflection and transmission of shear wave incident upon a corrugated interface between two monoclinic elastic half-spaces using Rayleigh's technique. Kaur *et al.* (2005) obtained the reflection and transmission coefficients due to incident plane SH-waves at a corrugated interface between two isotropic, laterally and vertically heterogeneous viscoelastic solid half-spaces. Tomar and Singh (2006) derived the expressions of reflection and refraction coefficients for first and second order approximation of the corrugation due to incident plane harmonic SH-wave at a corrugated interface between two different perfectly conducting self-reinforced elastic half-spaces. Dravinsky (2007) analyzed anti-plane strain and

plane strain models for scattering of harmonic waves by a sedimentary basin with corrugated interface using an indirect boundary integral equation method. Singh and Tomar (2007a, 2008a) investigated the problem of qP-waves at a corrugated interface between two dissimilar monoclinic elastic half-spaces and obtained the reflection and transmission coefficients of the irregular waves. Tomar and Kaur (2007b) obtained the reflection and transmission coefficients due to incident plane SH-wave at a corrugated interface between a laterally and vertically inhomogeneous anisotropic and isotropic viscoelastic solid half-space. Singh and Tomar (2008b) studied a plane qP-wave incident at a corrugated interface between two dissimilar pre-stressed elastic solid half-spaces and obtained the reflection and transmission coefficients corresponding to regular and irregular waves.

Yu and Dravinsky (2009) investigated the scattering of plane harmonic P, SV or Rayleigh waves from corrugated cavity completely embedded in an isotropic half-space or full-space by using a direct method of boundary integral equation. Chattopadhyay $et\ al.$ (2009) investigated the problem of reflection and transmission of plane quasi P-waves at a corrugated interface between distinct triclinic elastic half-spaces. They obtained the closed form expressions for reflection and transmission coefficients using Rayleigh's method of approximation. Singh and Singh (2013) explained the effect of corrugation for incident qSV-wave in pre-stressed elastic half-spaces with the help of Rayleigh's method and obtained the reflection and transmission coefficients of the regularly and irregularly reflected and transmitted waves. Singh $et\ al.$ (2016) investigated the effect of sandiness, heterogeneity and gravity on phase velocity and attenuation of SH-waves propagating in a corrugated interface of heterogeneous elastic and viscoelastic half-spaces. Kumhar $et\ al.$ (2019) investigated the traversal of torsional wave at a corrugated interface between viscoelastic sandy medium and inhomogeneous half-space. They employed the variable separation method to obtain analytical solution of displacement components. The scattering of acoustic and electromagnetic waves from irregular surface has been dealt by several

investigators, notably Rayleigh (1877, 1893), Feinberg (1944), Brekhovskikh (1952), Elliott (1954), Asano (1960, 1961, 1966), Dunkin and Eringen (1962), Abubakar (1962b, 1962c), Deresiewicz and Wolf (1964), Gupta (1987), Lakhtakia *et al.* (1993), Voronovich (1994), Tomar and Saini (1997), Tomar and Kaur (2003, 2007a), Benerjee and Kundu (2006), Singh and Tomar (2007b, 2007c), Tong and Chew (2009), Singh (2011b, 2013), Singh *et al.* (2015), Kumar *et al.* (2016).

Chapter 2

Response of corrugated interface on incident qSV-wave in monoclinic elastic half-spaces[1]

2.1   Introduction

The propagation of elastic waves and their reflection and transmission from discontinuities and interfaces are great concerned of many researchers. Chattopadhyay and Saha (1996, 1999) obtained the reflection and transmission coefficients of P and qSV-waves at a plane interface between two different monoclinic media. Singh and Khurana (2001) also investigated the reflection and transmission of P and SV-waves at the interface between two monoclinic elastic half-spaces. Singh (2013) studied the problem on reflection and transmission of plane waves at an imperfect interface between two dissimilar monoclinic elastic half-spaces.

This chapter is concerned with the problem of reflection and transmission of elastic qSV and qP-waves due to incident plane qSV-wave at a corrugated interface between two dissimilar monoclinic elastic half-spaces. There exist regularly and irregularly reflected and transmitted elastic waves due to corrugated interface. Using Rayleigh's method of approximation, the expressions of the reflection and transmission coefficients of regular and irregular waves are obtained for the first order of approximation.

These coefficients are derived and computed numerically for a special type of interface, $z = d \cos py$ and discussed the effects of corrugation and frequency parameter. We come to know that these coefficients are functions of elastic constants, angle of propagation, frequency and corrugation parameters.

2.2 Basic equations

The constitutive relation in a homogeneous monoclinic elastic material with yz-plane as the plane of symmetry are given by Singh and Khurana (2001)

$$\tau_{11} = c_{11}e_{11} + c_{12}e_{22} + c_{13}e_{33} + 2c_{14}e_{23}, \tau_{22} = c_{12}e_{11} + c_{22}e_{22} + c_{23}e_{33} + 2c_{24}e_{23},$$

$$\tau_{23} = c_{14}e_{11} + c_{24}e_{22} + c_{34}e_{33} + 2c_{44}e_{23}, \tau_{33} = c_{13}e_{11} + c_{23}e_{22} + c_{33}e_{33} + 2c_{34}e_{23},$$

$$\tau_{12} = 2(c_{55}e_{13} + c_{56}e_{12}), \tau_{13} = 2(c_{56}e_{13} + c_{66}e_{12}), \quad (2.1)$$

where $\mathbf{u} = (u_1, u_2, u_3)$ are components of displacement, τ_{ij} are stress tensor, c_{ij} $(i, j = 1, 2, 3, ..., 6)$ are elastic constants and e_{ij} is the strain tensor given by

$$e_{ij} = \frac{1}{2}\left(\frac{\partial u_i}{\partial x_j} + \frac{\partial u_j}{\partial x_i}\right).$$

The equations of motion in such anisotropic materials without body forces are given by

$$\frac{\partial \tau_{ij}}{\partial x_j} = \rho \frac{\partial^2 u_i}{\partial t^2}, \quad (i, j = 1, 2, 3) \quad (2.2)$$

where ρ is density of the medium.

Let us consider two-dimensional wave propagation in yz-plane so that

$$u_1 = 0, \quad \frac{\partial}{\partial x_1} \equiv \frac{\partial}{\partial x} \equiv 0, \quad \frac{\partial}{\partial x_2} \equiv \frac{\partial}{\partial y} \text{ and } \frac{\partial}{\partial x_3} \equiv \frac{\partial}{\partial z}.$$

The equations of motion in terms of displacements components can be written as

$$c_{22}\frac{\partial^2 u_2}{\partial y^2} + c_{44}\frac{\partial^2 u_2}{\partial z^2} + c_{24}\frac{\partial^2 u_3}{\partial y^2} + c_{34}\frac{\partial^2 u_3}{\partial z^2} + 2c_{24}\frac{\partial^2 u_2}{\partial y \partial z} + (c_{23} + c_{44})\frac{\partial^2 u_3}{\partial y \partial z} = \rho\frac{\partial^2 u_2}{\partial t^2}, \quad (2.3)$$

$$c_{24}\frac{\partial^2 u_2}{\partial y^2} + c_{34}\frac{\partial^2 u_2}{\partial z^2} + c_{44}\frac{\partial^2 u_3}{\partial y^2} + c_{33}\frac{\partial^2 u_3}{\partial z^2} + 2c_{34}\frac{\partial^2 u_3}{\partial y \partial z} + (c_{23} + c_{44})\frac{\partial^2 u_2}{\partial y \partial z} = \rho\frac{\partial^2 u_3}{\partial t^2}. \quad (2.4)$$

It may be noted that Eqs. (2.3) and (2.4) are the equations of motion for the coupled qSV and qP-waves. The solution of these equations may be taken in the form

$$< u_2, u_3 >= A(d_2, d_3) \exp\{ik(ct - p_2 y - p_3 z)\}, \tag{2.5}$$

where c is the phase velocity, k the wavenumber, $\mathbf{p} = (0, p_2, p_3)$ is the unit propagation vector, $\mathbf{d} = (0, d_2, d_3)$ is the unit displacement vector.

Using these expressions of u_2 and u_3 into Eqs. (2.3) and (2.4), we have

$$(X - \rho c^2)d_2 + Y d_3 = 0, \quad Y d_2 + (W - \rho c^2)d_3 = 0, \tag{2.6}$$

where

$$X = c_{22}p_2^2 + c_{44}p_3^2 + 2c_{24}p_2 p_3, \quad Y = c_{24}p_2^2 + c_{34}p_3^2 + (c_{23} + c_{44})p_2 p_3,$$

$$W = c_{44}p_2^2 + c_{33}p_3^2 + 2c_{34}p_2 p_3. \tag{2.7}$$

Using Eq. (2.6), we get

$$2\rho c_{2,1}^2 = X + W \mp \sqrt{(X - W)^2 + 4Y^2}, \tag{2.8}$$

where $(-ve)$ sign represents for the phase velocity of qSV-waves (c_2) and $(+ve)$ sign represents for that of qP-waves (c_1).

2.3 Problem formulation

Consider the cartesian coordinates with x and y-axis lying horizontal and z-axis as vertical with positive direction pointing downward. Suppose two dissimilar homogeneous monoclinic half-spaces, given by $M = \{(y, z) : y \in \mathbb{R}, z \in [\zeta, \infty)\}$ and $M' = \{(y, z) : y \in \mathbb{R}, z \in (-\infty, \zeta)\}$ are separated by $z = \zeta(y)$, which is a periodic function of y independent of x whose mean value is zero. We will denote all elastic constants, stress tensors and displacement components in medium, M without prime and those of M' with primes. The complete geometry of the problem is given in Figure 2.1.
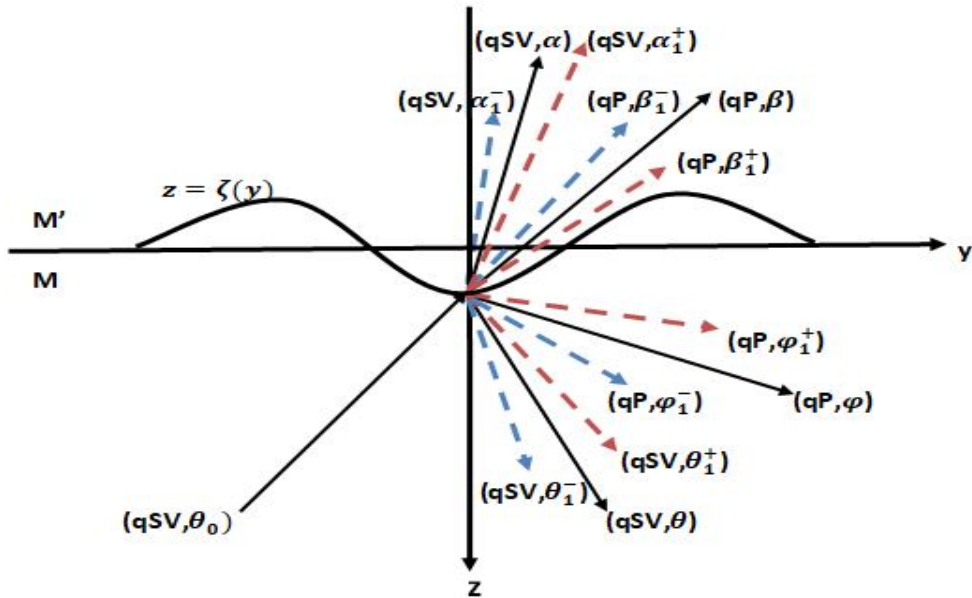
Figure 2.1: Geometry of the problem.

The Fourier series expansion of $\zeta(y)$ is given as

$$\zeta(y) = \sum_{n=1}^{\infty}(\zeta_{+n}e^{\imath npy} + \zeta_{-n}e^{-\imath npy}), \qquad (2.9)$$

where ζ_{+n} and ζ_{-n} are the coefficients of series expansion of order n, p is the wavenumber and $\imath = \sqrt{-1}$.

Introduce constants $d, c_n,$ and s_n as

$$\zeta_{\pm 1} = \frac{d}{2}, \quad \zeta_{\pm n} = \frac{c_n \mp \imath s_n}{2}, \quad (n = 2, 3, 4, ...)$$

so that

$$\zeta(y) = d\cos(py) + \sum_{n=2}^{\infty}[c_n\cos(npy) + s_n\sin(npy)]. \qquad (2.10)$$

If the interface is represented by only one cosine term, i.e. $\zeta(y) = d\cos(py)$, then the wavelength of corrugation is $2\pi/p$ and d is the amplitude of corrugation.

We shall now discuss the reflection and transmission of elastic waves due to incident plane qSV-wave at the corrugated interface, $z = \zeta(y)$. Suppose a plane qSV-wave propagating in the half-space, M with an angle θ_0 and amplitude constant A_0

be incident at the corrugated interface. This incident wave give rises regularly and irregularly reflected and transmitted qSV and qP-waves (Asano, 1961).

The full structures of reflected and transmitted waves are given by:

(for the half-space, M)

$$u_2 = A_0 e^{P_0'} + A e^P + B e^Q + \sum_{n=1}^{\infty}\{A_n^{\pm} e^{P_n^{\pm}} + B_n^{\pm} e^{Q_n^{\pm}}\}, \qquad (2.11)$$

$$u_3 = D_0 e^{P_0'} + D e^P + E e^Q + \sum_{n=1}^{\infty}\{D_n^{\pm} e^{P_n^{\pm}} + E_n^{\pm} e^{Q_n^{\pm}}\}, \qquad (2.12)$$

where $(A,\ D)$ are amplitude constants of the regularly reflected qSV-wave at angle θ, $(A_n^{\pm}, D_n^{\pm})$ are amplitude constants of the irregularly reflected qSV-waves at angles $\theta_n^{\pm}$, $(B,\ E)$ are amplitude constants of the regularly reflected qP-wave at angle ϕ, $(B_n^{\pm}, E_n^{\pm})$ are amplitude constants of the irregularly reflected qP-waves at angles $\phi_n^{\pm}$ and the expressions of $P_0', P, P_n^{\pm}, Q, Q_n^{\pm}$ are given by $P_0' = \imath\omega\{t - \frac{y\sin\theta_0 - z\cos\theta_0}{c_0}\}$, $P = \imath\omega\{t - \frac{y\sin\theta + z\cos\theta}{c_2}\}$, $P_n^{\pm} = \imath\omega\{t - \frac{y\sin\theta_n^{\pm} + z\cos\theta_n^{\pm}}{c_2}\}$, $Q = \imath\omega\{t - \frac{y\sin\phi + z\cos\phi}{c_1}\}$ and $Q_n^{\pm} = \imath\omega\{t - \frac{y\sin\phi_n^{\pm} + z\cos\phi_n^{\pm}}{c_1}\}$.

These amplitude constants satisfy the following relations (Singh and Khurana, 2001)

$$A_0 = F_0 D_0, \quad A = FD, \quad B = F_{10}E, \quad A_n^{\pm} = F_n^{\pm} D_n^{\pm}, \quad B_n^{\pm} = F_{1n}^{\pm} E_n^{\pm}, \qquad (2.13)$$

where

$$F_0 = \frac{Y_0}{\rho c_0^2 - X_0}, \quad F = \frac{Y_{10}}{\rho c_2^2 - X_{10}}, \quad F_{10} = \frac{Y_{20}}{\rho c_1^2 - X_{20}}, \quad F_n^{\pm} = \frac{Y_{1n}^{\pm}}{\rho c_2^2 - X_{1n}^{\pm}},$$

$$F_{1n}^{\pm} = \frac{Y_{2n}^{\pm}}{\rho c_1^2 - X_{2n}^{\pm}}, \quad 2\rho c_0^2 = X_0 + W_0 - \sqrt{(X_0 - W_0)^2 + 4Y_0^2},$$

$$2\rho c_2^2 = X_{10} + W_{10} - \sqrt{(X_{10} - W_{10})^2 + 4Y_{10}^2},$$

$$2\rho c_1^2 = X_{20} + W_{20} + \sqrt{(X_{20} - W_{20})^2 + 4Y_{20}^2}.$$

(for the half-space, M')

$$u_2' = Ge^R + He^S + \sum_{n=1}^{\infty}\{G_n^{\pm}e^{R_n^{\pm}} + H_n^{\pm}e^{S_n^{\pm}}\}, \tag{2.14}$$

$$u_3' = Ie^R + Je^S + \sum_{n=1}^{\infty}\{I_n^{\pm}e^{R_n^{\pm}} + J_n^{\pm}e^{S_n^{\pm}}\}, \tag{2.15}$$

where $(G,\ I)$ are amplitude constants of the regularly transmitted qSV-wave at angle α, $(G_n^{\pm}, I_n^{\pm})$ are amplitude constants of the irregularly transmitted qSV-waves at angles $\alpha_n^{\pm}$, (H, J) are amplitude constants of the regularly transmitted qP-wave at angle β, $(H_n^{\pm}, J_n^{\pm})$ are amplitude constants of the irregularly transmitted qP-waves at angles $\beta_n^{\pm}$ and the expressions of $R, R_n^{\pm}, S, S_n^{\pm}$ are given by

$$R = \imath\omega\{t - \frac{y\sin\alpha - z\cos\alpha}{c_2'}\}, \quad R_n^{\pm} = \imath\omega\{t - \frac{y\sin\alpha_n^{\pm} - z\cos\alpha_n^{\pm}}{c_2'}\},$$

$$S = \imath\omega\{t - \frac{y\sin\beta - z\cos\beta}{c_1'}\} \quad \text{and} \quad S_n^{\pm} = \imath\omega\{t - \frac{y\sin\beta_n^{\pm} - z\cos\beta_n^{\pm}}{c_1'}\}.$$

These amplitude constants also satisfy the following relations

$$G = F_{20}I, \quad H = F_{30}J, \quad G_n^{\pm} = F_{2n}^{\pm}I_n^{+}, \quad H_n^{\pm} = F_{3n}^{\pm}J_n^{\pm}, \tag{2.16}$$

where

$$F_{20} = \frac{Y_{30}}{\rho'c_2'^2 - X_{30}}, \quad F_{30} = \frac{Y_{40}}{\rho'c_1'^2 - X_{40}}, \quad F_{2n}^{\pm} = \frac{Y_{3n}^{\pm}}{\rho'c_2'^2 - X_{3n}^{\pm}}, \quad F_{3n}^{\pm} = \frac{Y_{4n}^{\pm}}{\rho'c_1'^2 - X_{4n}^{\pm}},$$

$$2\rho'c_2'^2 = X_{30} + W_{30} - \sqrt{(X_{30} - W_{30})^2 + 4Y_{30}^2},$$

$$2\rho'c_1'^2 = X_{40} + W_{40} + \sqrt{(X_{40} - W_{40})^2 + 4Y_{40}^2}.$$

The expressions of X, Y and W with corresponding suffixes are obtained from Eq.(2.7) by inserting (p_2, p_3); for incident qSV-wave : $(\sin\theta_0, -\cos\theta_0)$, for regularly reflected qSV-wave : $(\sin\theta, \cos\theta)$, for irregularly reflected qSV-wave : $(\sin\theta_n^{\pm}, \cos\theta_n^{\pm})$, for regularly reflected qP-wave : $(\sin\phi, \cos\phi)$, for irregularly reflected qP-wave : $(\sin\phi_n^{\pm}, \cos\phi_n^{\pm})$, for regular transmitted qSV-wave : $(\sin\alpha, -\cos\alpha)$, for irregularly transmitted qSV-wave : $(\sin\alpha_n^{\pm}, -\cos\alpha_n^{\pm})$, for regularly transmitted qP-wave : $(\sin\beta, -\cos\beta)$, for irregularly transmitted qP-wave : $(\sin\beta_n^{\pm}, -\cos\beta_n^{\pm})$.

The Snell's law of this problem is given by Asano (1960)

$$\frac{\sin\theta_0}{c_0(\theta_0)} = \frac{\sin\theta}{c_2(\theta)} = \frac{\sin\phi}{c_1(\phi)} = \frac{\sin\alpha}{c_2'(\alpha)} = \frac{\sin\beta}{c_1'(\beta)} = \frac{1}{c_a},$$

(2.17)

where c_a is apparent velocity.

Moreover, Spectrum theorem gives the relations between the angle of regular wave and those of irregular waves (Abubakar, 1962a)

$$\sin\left\{\begin{array}{c}\theta_n^{\pm}\\\phi_n^{\pm}\\\alpha_n^{\pm}\\\beta_n^{\pm}\end{array}\right\} - \sin\left\{\begin{array}{c}\theta\\\phi\\\alpha\\\beta\end{array}\right\} = \pm\frac{np}{\omega}\left\{\begin{array}{c}c_2\\c_1\\c_2'\\c_1'\end{array}\right\}, \quad n = 1, 2, ...$$

(2.18)

where $(+ve)$ signs of the right hand side correspond to $(+ve)$ signs of the left hand side, while $(-ve)$ signs of the right hand side correspond to $(-ve)$ signs of the left hand side of the equation.

2.4   Boundary conditions

The component of displacements and tractions (normal and shear) are continuous at the corrugated interface. Mathematically, these conditions at $z = \zeta(y)$ can be written as

$$u_2 = u_2', \qquad u_3 = u_3',$$

(2.19)

$$\tau_{32} + (\tau_{33} - \tau_{22})\zeta' - \tau_{23}\zeta'^2 = \tau_{32}' + (\tau_{33}' - \tau_{22}')\zeta' - \tau_{23}'\zeta'^2,$$

(2.20)

$$\tau_{33} - 2\tau_{23}\zeta' + \tau_{22}\zeta'^2 = \tau_{33}' - 2\tau_{23}'\zeta' + \tau_{22}'\zeta'^2,$$

(2.21)

where ζ' is the derivative of ζ with respect to y.

Inserting Eq. (2.1) into (2.20) and (2.21), we get

$$\{(c_{23} - c_{22})\zeta' + c_{24}(1 - \zeta'^2)\}\frac{\partial u_2}{\partial y} + \{(c_{33} - c_{23})\zeta' + c_{34}(1 - \zeta'^2)\}\frac{\partial u_3}{\partial z} + \{(c_{34} - c_{24}\zeta'$$

$$+ c_{44}(1 - \zeta'^2)\}(\frac{\partial u_2}{\partial z} + \frac{\partial u_3}{\partial y}) = \{(c'_{23} - c'_{22})\zeta' + c'_{24}(1 - \zeta'^2)\}\frac{\partial u'_2}{\partial y} + \{(c'_{33} - c'_{23})\zeta'$$

$$+ c'_{34}(1 - \zeta'^2)\}\frac{\partial u'_3}{\partial z} + \{(c'_{34} - c'_{24}\zeta' + c'_{44}(1 - \zeta'^2)\}(\frac{\partial u'_2}{\partial z} + \frac{\partial u'_3}{\partial y}), \quad (2.22)$$

$$\{c_{23} + c_{22}\zeta'^2 - 2c_{24}\zeta'\}\frac{\partial u_2}{\partial y} + \{c_{33} + c_{23}\zeta'^2 - 2c_{34}\zeta'\}\frac{\partial u_3}{\partial z} + \{c_{34} + c_{24}\zeta'^2 - 2c_{44}\zeta'\}$$

$$\times (\frac{\partial u_2}{\partial z} + \frac{\partial u_3}{\partial y}) = \{c'_{23} + c'_{22}\zeta'^2 - 2c'_{24}\zeta'\}\frac{\partial u'_2}{\partial y} + \{c'_{33} + c'_{23}\zeta'^2 - 2c'_{34}\zeta'\}\frac{\partial u'_3}{\partial z}$$

$$+ \{c'_{34} + c'_{24}\zeta'^2 - 2c'_{44}\zeta'\}(\frac{\partial u'_2}{\partial z} + \frac{\partial u'_3}{\partial y}). \quad (2.23)$$

Using Eqs.(2.11), (2.12), (2.14), (2.15), (2.17) and (2.18) into Eqs.(2.19), (2.22) and (2.23), we get

$$D_0 e^{\imath\zeta K_0} + D e^{-\imath\zeta K} + E e^{-\imath\zeta L} + \sum_{n=1}^{\infty}\{D_n^{\pm} e^{\mp \imath npy - \imath\zeta K_n^{\pm}} + E_n^{\pm} e^{\mp \imath npy - \imath\zeta L_n^{\pm}}\}$$

$$= I e^{\imath\zeta M} + J e^{\imath\zeta N} + \sum_{n=1}^{\infty}\{I_n^{\pm} e^{\mp \imath npy + \imath\zeta M_n^{\pm}} + J_n^{\pm} e^{\mp \imath npy + \imath\zeta N_n^{\pm}}\}, \quad (2.24)$$

$$A_0 e^{\imath\zeta K_0} + A e^{-\imath\zeta K} + B e^{-\imath\zeta L} + \sum_{n=1}^{\infty}\{A_n^{\pm} e^{\mp \imath npy - \imath\zeta K_n^{\pm}} + B_n^{\pm} e^{\mp \imath npy - \imath\zeta L_n^{\pm}}\}$$

$$= G e^{\imath\zeta M} + H e^{\imath\zeta N} + \sum_{n=1}^{\infty}\{G_n^{\pm} e^{\mp \imath npy + \imath\zeta M_n^{\pm}} + H_n^{\pm} e^{\mp \imath npy + \imath\zeta N_n^{\pm}}\}, \quad (2.25)$$

$$[(c_{23} - c_{22})\zeta' + c_{24}(1 - \zeta'^2)][P_0 A_0 e^{\imath\zeta K_0} + P_0 A e^{-\imath\zeta K} + P_0 B e^{-\imath\zeta L} + \sum_{n=1}^{\infty}\{(P_0 \pm np)A_n^{\pm}$$

$$\times e^{\mp \imath npy - \imath\zeta K_n^{\pm}} + (P_0 \pm np)B_n^{\pm} e^{\mp \imath npy - \imath\zeta L_n^{\pm}}\}] + [(c_{33} - c_{23})\zeta' + c_{34}(1 - \zeta'^2)][-K_0 D_0$$

$$\times e^{\imath\zeta K_0} + K D e^{-\imath\zeta K} + L E e^{-\imath\zeta L} + \sum_{n=1}^{\infty}\{K_n^{\pm} D_n^{\pm} e^{\mp \imath npy - \imath\zeta K_n^{\pm}} + L_n^{\pm} E_n^{\pm} e^{\mp \imath npy - \imath\zeta L_n^{\pm}}\}]$$

$$+ [(c_{34} - c_{24})\zeta' + c_{44}(1 - \zeta'^2)][-K_0 A_0 e^{\imath\zeta K_0} + K A e^{-\imath\zeta K} + L B e^{-\imath\zeta L} + P_0 D_0 e^{\imath\zeta K_0}$$

$$+ P_0 D e^{-\imath\zeta K} + P_0 E e^{-\imath\zeta L} + \sum_{n=1}^{\infty}\{K_n^{\pm} A_n^{\pm} e^{\mp \imath npy - \imath\zeta K_n^{\pm}} + L_n^{\pm} B_n^{\pm} e^{\mp \imath npy - \imath\zeta L_n^{\pm}} + (P_0 \pm np)$$

$$\times D_n^{\pm} e^{\mp \imath npy - \imath\zeta K_n^{\pm}} + (P_0 \pm np)E_n^{\pm} e^{\mp \imath npy - \imath\zeta L_n^{\pm}}\}] = [(c'_{23} - c'_{22})\zeta' + c'_{24}(1 - \zeta'^2)][P_0 G$$

$$\times e^{\iota \zeta M} + P_0 H e^{\iota \zeta N} + \sum_{n=1}^{\infty} \{ (P_0 \pm np) G_n^{\pm} e^{\mp \iota npy + \iota \zeta M_n^{\pm}} + (P_0 \pm np) H_n^{\pm} e^{\mp \iota npy + \iota \zeta N_n^{\pm}} \}]$$

$$- [(c'_{33} - c'_{23})\zeta' + c'_{34}(1 - \zeta'^2)][MIe^{\iota \zeta M} + NJe^{\iota \zeta N} + \sum_{n=1}^{\infty} \{ M_n^{\pm} I_n^{\pm} e^{\mp \iota npy + \iota \zeta M_n^{\pm}}$$

$$+ N_n^{\pm} J_n^{\pm} e^{\mp \iota npy + \iota \zeta N_n^{\pm}} \}] - [(c'_{34} - c'_{24})\zeta' + c'_{44}(1 - \zeta'^2)][MGe^{\iota \zeta M} + NHe^{\iota \zeta N}$$

$$- P_0 I e^{\iota \zeta M} - P_0 J e^{\iota \zeta N} + \sum_{n=1}^{\infty} \{ M_n^{\pm} G_n^{\pm} e^{-\iota npy + \iota \zeta M_n^{\pm}} + N_n^{\pm} H_n^{\pm} e^{\mp \iota npy + \iota \zeta N_n^{\pm}}$$

$$- (P_0 \pm np) I_n^{\pm} e^{\mp \iota npy + \iota \zeta M_n^{\pm}} - (P_0 \pm np) J_n^{\pm} e^{\mp \iota npy + \iota \zeta N_n^{\pm}} \}], \qquad (2.26)$$

$$[c_{23} + c_{22}\zeta'^2 - 2c_{24}\zeta'][P_0 A_0 e^{\iota \zeta K_0} + P_0 A e^{-\iota \zeta K} + P_0 B e^{-\iota \zeta L} + \sum_{n=1}^{\infty} \{ (P_0 \pm np) A_n^{\pm}$$

$$e^{\mp \iota npy - \iota \zeta K_n^{\pm}} + (P_0 \pm np) B_n^{\pm} e^{\mp \iota npy - \iota \zeta L_n^{\pm}} \}] + [c_{33} + c_{23}\zeta'^2 - 2c_{34}\zeta'][-K_0 D_0 e^{\iota \zeta K_0}$$

$$+ KD e^{-\iota \zeta K} + LE e^{-\iota \zeta L} + \sum_{n=1}^{\infty} \{ K_n^{\pm} D_n^{\pm} e^{\mp \iota npy - \iota \zeta K_n^{\pm}} + L_n^{\pm} E_n^{\pm} e^{\mp \iota npy - \iota \zeta L_n^{\pm}} \}]$$

$$+ [c_{34} + c_{24}\zeta'^2 - 2c_{44}\zeta'][-K_0 A_0 e^{\iota \zeta K_0} + KA e^{-\iota \zeta K} + LB e^{-\iota \zeta L} + P_0 D_0 e^{\iota \zeta K_0}$$

$$+ P_0 D e^{-\iota \zeta K} + P_0 E e^{-\iota \zeta L} + \sum_{n=1}^{\infty} \{ K_n^{\pm} A_n^{\pm} e^{\mp \iota npy - \iota \zeta K_n^{\pm}} + L_n^{\pm} B_n^{\pm} e^{\mp \iota npy - \iota \zeta L_n^{\pm}}$$

$$+ (P_0 \pm np) D_n^{\pm} e^{\mp \iota npy - \iota \zeta K_n^{\pm}} + (P_0 \pm np) E_n^{\pm} e^{\mp \iota npy - \iota \zeta L_n^{\pm}} \}] = [c'_{23} + c'_{22}\zeta'^2 - 2c'_{24}\zeta']$$

$$[P_0 G e^{\iota \zeta M} + P_0 H e^{\iota \zeta N} + \sum_{n=1}^{\infty} \{ (P_0 \pm np) G_n^{\pm} e^{\mp \iota npy + \iota \zeta M_n^{\pm}} + (P_0 \pm np) H_n^{\pm} e^{\mp \iota npy + \iota \zeta N_n^{\pm}} \}]$$

$$- [c'_{33} + c'_{23}\zeta'^2 - 2c'_{34}\zeta'][MIe^{\iota \zeta M} + NJe^{\iota \zeta N} + \sum_{n=1}^{\infty} \{ M_n^{\pm} I_n^{\pm} e^{\mp \iota npy + \iota \zeta M_n^{\pm}} + N_n^{\pm} J_n^{\pm}$$

$$\times e^{\mp \iota npy + \iota \zeta N_n^{\pm}} \}] - [c'_{34} + c'_{24}\zeta'^2 - 2c'_{44}\zeta'][MGe^{\iota \zeta M} + NHe^{\iota \zeta N} - P_0 I e^{\iota \zeta M} - P_0 J e^{\iota \zeta N}$$

$$+ \sum_{n=1}^{\infty} \{ M_n^{\pm} G_n^{\pm} e^{\mp \iota npy + \iota \zeta M_n^{\pm}} + N_n^{\pm} H_n^{\pm} e^{\mp \iota npy + \iota \zeta N_n^{\pm}} - (P_0 \pm np) I_n^{\pm} e^{\mp \iota npy + \iota \zeta M_n^{\pm}}$$

$$- (P_0 \pm np) J_n^{\pm} e^{\mp \iota npy + \iota \zeta N_n^{\pm}} \}], \qquad (2.27)$$

where

$$P_0 = \frac{\omega \sin \theta_0}{c_0}, \quad K_0 = \frac{\omega \cos \theta_0}{c_0}, \quad K = \frac{\omega \cos \theta}{c_2}, \quad K_n^{\pm} = \frac{\omega \cos \theta_n^{\pm}}{c_2}, \quad L = \frac{\omega \cos \phi}{c_1},$$

$$L_n^{\pm} = \frac{\omega \cos \phi_n^{\pm}}{c_1}, \quad M = \frac{\omega \cos \alpha}{c'_2}, \quad M_n^{\pm} = \frac{\omega \cos \alpha_n^{\pm}}{c'_2}, \quad N = \frac{\omega \cos \beta}{c'_1}, \quad N_n^{\pm} = \frac{\omega \cos \beta_n^{\pm}}{c'_1}.$$

2.5   Solution of first order approximation

We assume that the amplitude of the corrugated interface is very small so that higher powers of ζ are neglected such that

$$e^{\pm\imath\zeta K_0} = 1 \pm \imath\zeta K_0 - 0(\zeta^2), \quad e^{\pm\imath\zeta K} = 1 \pm \imath\zeta K - 0(\zeta^2). \tag{2.28}$$

Using Eqs. (2.9), (2.13), (2.16) and (2.28) into Eqs.(2.24)-(2.27) and collecting terms independent of ζ and y, we obtain a set of equations

$$RS = T, \tag{2.29}$$

where

$$R = \begin{bmatrix} 1 & 1 & -1 & -1 \\ F & F_{10} & -F_{20} & -F_{30} \\ l_1 & l_2 & -l_3 & -l_4 \\ m_1 & m_2 & -m_3 & -m_4 \end{bmatrix}, \quad S = \begin{bmatrix} D/D_0 \\ E/D_0 \\ I/D_0 \\ J/D_0 \end{bmatrix}, \quad T = \begin{bmatrix} -1 \\ -F_0 \\ -l_0 \\ -m_0 \end{bmatrix}$$

,

$l_0 = (F_0 c_{24} + c_{44})P_0 - (F_0 c_{44} + c_{34})K_0, \quad l_1 = (Fc_{24} + c_{44})P_0 + (Fc_{44} + c_{34})K,$

$l_2 = (F_{10}c_{24} + c_{44})P_0 + (F_{10}c_{44} + c_{34})L, \quad l_3 = (F_{20}c'_{24} + c'_{44})P_0 - (F_{20}c'_{44} + c'_{34})M,$

$l_4 = (F_{30}c'_{24} + c'_{44})P_0 - (F_{30}c'_{44} + c'_{34})N, \quad m_0 = (F_0 c_{23} + c_{34})P_0 - (F_0 c_{34} + c_{33})K_0,$

$m_1 = (Fc_{23} + c_{34})P_0 + (Fc_{34} + c_{33})K, \quad m_2 = (F_{10}c_{23} + c_{34})P_0 + (F_{10}c_{34} + c_{33})L,$

$m_3 = (F_{20}c'_{23} + c'_{34})P_0 - (F_{20}c'_{34} + c'_{33})M, \quad m_4 = (F_{30}c'_{23} + c'_{34})P_0 - (F_{30}c'_{34} + c'_{33})N.$

On solving Eq.(2.29), we get

$$\frac{D}{D_0} = \frac{\Delta_D}{\Delta}, \quad \frac{E}{D_0} = \frac{\Delta_E}{\Delta}, \quad \frac{I}{D_0} = \frac{\Delta_I}{\Delta}, \quad \frac{J}{D_0} = \frac{\Delta_J}{\Delta}, \tag{2.30}$$

where

$$\Delta = \begin{vmatrix} 1 & 1 & -1 & -1 \\ F & F_{10} & -F_{20} & -F_{30} \\ l_1 & l_2 & -l_3 & -l_4 \\ m_1 & m_2 & -m_3 & -m_4 \end{vmatrix}$$

and the values of Δ_D, Δ_E, Δ_I and Δ_J are obtained by replacing first, second, third and fourth column of Δ with column matrix, T respectively. This equation gives the ratios of the amplitude constants corresponding to the vertical components of the displacement.

The ratios of the amplitude constants corresponding to horizontal components of displacement is obtained with the help of Eqs. (2.13), (2.16) and (2.30) as

$$\frac{A}{A_0} = \frac{F}{F_0}\frac{\Delta_D}{\Delta}, \quad \frac{B}{A_0} = \frac{F_{10}}{F_0}\frac{\Delta_E}{\Delta}, \quad \frac{G}{A_0} = \frac{F_{20}}{F_0}\frac{\Delta_I}{\Delta}, \quad \frac{H}{A_0} = \frac{F_{30}}{F_0}\frac{\Delta_J}{\Delta}. \tag{2.31}$$

Now, the amplitude of incident qSV-wave is given by $\sqrt{A_0^2 + D_0^2} = \sqrt{1 + F_0^2}\,D_0$. Similarly, we find the amplitudes of reflected and transmitted qSV and qP-waves. Thus, the reflection and transmission coefficients of reflected and transmitted qSV and qP-waves for the incident qSV-wave are given by

$$r_{sv} = \sqrt{\frac{1 + F^2}{1 + F_0^2}}\frac{\Delta_D}{\Delta}, \qquad r_p = \sqrt{\frac{1 + F_{10}^2}{1 + F_0^2}}\frac{\Delta_E}{\Delta}. \tag{2.32}$$

$$t_{sv} = \sqrt{\frac{1 + F_{20}^2}{1 + F_0^2}}\frac{\Delta_I}{\Delta}, \qquad t_p = \sqrt{\frac{1 + F_{30}^2}{1 + F_0^2}}\frac{\Delta_J}{\Delta}. \tag{2.33}$$

We come to know that these coefficients depend on elastic constants and angle of incidence.

Next, comparing coefficients of $e^{\mp i n p y}$ on both the sides of those equations, we get

$$R^{\mp}S^{\mp} = T^{\mp}, \tag{2.34}$$

where

$$
R^{\mp} = \begin{bmatrix} 1 & 1 & -1 & -1 \\ F_n^{\pm} & F_{1n}^{\pm} & -F_{2n}^{\pm} & -F_{3n}^{\pm} \\ g_5^{\mp} & g_6^{\mp} & -g_7^{\mp} & -g_8^{\mp} \\ h_5^{\mp} & h_6^{\mp} & -h_7^{\mp} & -h_8^{\mp} \end{bmatrix}, \quad S^{\mp} = \begin{bmatrix} D_n^{\pm}/D_0 \\ E_n^{\pm}/D_0 \\ I_n^{\pm}/D_0 \\ J_n^{\pm}/D_0 \end{bmatrix}, \quad T^{\mp} = \begin{bmatrix} f_1^{\mp} \\ f_2^{\mp} \\ f_3^{\mp} \\ f_4^{\mp} \end{bmatrix},
$$

$$
f_1^{\mp} = \imath\zeta_{\mp n}[-K_0 + K\frac{D}{D_0} + L\frac{E}{D_0} + M\frac{I}{D_0} + N\frac{J}{D_0}],
$$

$$
f_2^{\mp} = \imath\zeta_{\mp n}[-F_0 K_0 + FK\frac{D}{D_0} + F_{10}L\frac{E}{D_0} + F_{20}M\frac{I}{D_0} + F_{30}N\frac{J}{D_0}],
$$

$$
f_3^{\mp} = \imath[g_0^{\mp} + g_1^{\mp}\frac{D}{D_0} + g_2^{\mp}\frac{E}{D_0} - g_3^{\mp}\frac{I}{D_0} - g_4^{\mp}\frac{J}{D_0}],
$$

$$
f_4^{\mp} = \imath[h_0^{\mp} + h_1^{\mp}\frac{D}{D_0} + h_2^{\mp}\frac{E}{D_0} - h_3^{\mp}\frac{I}{D_0} - h_4^{\mp}\frac{J}{D_0}],
$$

$$
g_0^{\mp} = [\{\mp(c_{23} - c_{22})npP_0 + c_{24}P_0K_0 \pm (c_{34} - c_{24})npK_0 - c_{44}K_0^2\}F_0 \pm (c_{33} - c_{23})npK_0
$$
$$
- c_{34}K_0^2 \mp (c_{34} - c_{24})npP_0 + c_{44}P_0K_0]\zeta_{\mp n},
$$

$$
g_1^{\mp} = [\{\mp(c_{23} - c_{22})npP_0 - c_{24}P_0K \mp (c_{34} - c_{24})npK - c_{44}K^2\}F \mp (c_{33} - c_{23})npK
$$
$$
- c_{34}K^2 \mp (c_{34} - c_{24})npP_0 - c_{44}P_0K]\zeta_{\mp n},
$$

$$
g_2^{\mp} = [\{\mp(c_{23} - c_{22})npP_0 - c_{24}P_0L \mp (c_{34} - c_{24})npL - c_{44}L^2\}F_{10} \mp (c_{33} - c_{23})npL
$$
$$
- c_{34}L^2 \mp (c_{34} - c_{24})npP_0 - c_{44}P_0L]\zeta_{\mp n},
$$

$$
g_3^{\mp} = [\{\mp(c_{23}' - c_{22}')npP_0 + c_{24}'P_0M \pm (c_{34}' - c_{24}')npM - c_{44}'M^2\}F_{20} \pm (c_{33}' - c_{23}')npM
$$
$$
- c_{34}'M^2 \mp (c_{34}' - c_{24}')npP_0 + c_{44}'P_0M]\zeta_{\mp n},
$$

$$
g_4^{\mp} = [\{\mp(c_{23}' - c_{22}')npP_0 + c_{24}'P_0N \pm (c_{34}'c_{24}')npN - c_{44}'N^2\}F_{30} \pm (c_{33}' - c_{23}')npN
$$
$$
- c_{34}'N^2 mp(c_{34}' - c_{24}')npP_0 + c_{44}'P_0N]\zeta_{\mp n},
$$

$$
g_5^{\mp} = -[\{c_{44}K_n^{\pm} + c_{24}(P_0 \pm np)\}F_n^{\pm} + c_{34}K_n^{\pm} + c_{44}(P_0 \pm np)],
$$

$$
g_6^{\mp} = -[\{c_{44}L_n^{\pm} + c_{24}(P_0 \pm np)\}F_{1n}^{\pm} + c_{34}L_n^{\pm} + c_{44}(P_0 \pm np)],
$$

$$
g_7^{\mp} = \{c_{44}'M_n^{\pm} - c_{24}'(P_0 \pm np)\}F_{2n}^{\pm} + c_{34}'M_n^{\pm} - c_{44}'(P_0 \pm np),
$$

$$
g_8^{\mp} = \{c_{44}'N_n^{\pm} - c_{24}'(P_0 \pm np)\}F_{3n}^{\pm} + c_{34}'N_n^{\pm} - c_{44}'(P_0 \pm np),
$$

$$h_0^{\mp} = \{(c_{23}P_0K_0 \pm 2c_{24}npP_0 - c_{34}K_0^2 - 2c_{44}npK_0)F_0 - c_{33}K_0^2 \mp 2c_{34}npK_0$$

$$+ c_{34}P_0K_0 \pm 2c_{44}npP_0\}\zeta_{\mp n},$$

$$h_1^{\mp} = \{(-c_{23}P_0K \pm 2c_{24}npP_0 - c_{34}K^2 \pm 2c_{44}npK)F - c_{33}K^2 \pm 2c_{34}npK$$

$$- c_{34}P_0K \pm 2c_{44}npP_0\}\zeta_{\mp n},$$

$$h_2^{\mp} = [\{-c_{23}P_0L \pm 2c_{24}npP_0 - c_{34}L^2 \pm 2c_{44}npL\}F_{10} - c_{33}L^2 \pm 2c_{34}npL$$

$$- c_{34}P_0L \pm 2c_{44}npP_0]\zeta_{\mp n},$$

$$h_3^{\mp} = [\{c_{23}'P_0M \pm 2c_{24}'npP_0 - c_{34}'M^2 \mp 2c_{44}'npM\}F_{20} - c_{33}'M^2 \mp 2c_{34}'npM$$

$$+ c_{34}'P_0M \pm 2c_{44}'npP_0]\zeta_{\mp n},$$

$$h_4^{\mp} = [\{c_{23}'P_0N \pm 2c_{24}'npP_0 - c_{34}'N^2 \mp 2c_{44}'npN\}F_{30} - c_{33}'N^2 \mp 2c_{34}'npN$$

$$+ c_{34}'P_0N \pm 2c_{44}'npP_0]\zeta_{\mp n},$$

$$h_5^{\mp} = -[\{c_{23}(P_0 \pm np) + c_{34}K_n^{\pm}\}F_n^{\pm} + c_{33}K_n^{\pm} + c_{34}(P_0 \pm np)],$$

$$h_6^{\mp} = -[\{c_{23}(P_0 \pm np) + c_{34}L_n^{\pm}\}F_{1n}^{\pm} + c_{33}L_n^{\pm} + c_{34}(P_0 \pm np)],$$

$$h_7^{\mp} = \{-c_{23}'(P_0 \pm np) + c_{34}'M_n^{\pm}\}F_{2n}^{\pm} + c_{33}'M_n^{\pm} - c_{34}'(P_0 \pm np),$$

$$h_8^{\mp} = \{-c_{23}'(P_0 \pm np) + c_{34}'N_n^{\pm}\}F_{3n}^{\pm} + c_{33}'N_n^{\pm} - c_{34}'(P_0 \pm np).$$

Solving Eq. (2.34), we get

$$\frac{D_n^{\pm}}{D_0} = \frac{\Delta_{D_n^{\pm}}}{\Delta^{\pm}}, \quad \frac{E_n^{\pm}}{D_0} = \frac{\Delta_{E_n^{\pm}}}{\Delta^{\pm}}, \quad \frac{I_n^{\pm}}{D_0} = \frac{\Delta_{I_n^{\pm}}}{\Delta^{\pm}}, \quad \frac{J_n^{\pm}}{D_0} = \frac{\Delta_{J_n^{\pm}}}{\Delta^{\pm}}, \qquad (2.35)$$

where

$$\Delta^{\pm} = \begin{vmatrix} 1 & 1 & -1 & -1 \\ F_n^{\pm} & F_{1n}^{\pm} & -F_{2n}^{\pm} & -F_{3n}^{\pm} \\ g_5^{\mp} & g_6^{\mp} & -g_7^{\mp} & -g_8^{\mp} \\ h_5^{\mp} & h_6^{\mp} & -h_7^{\mp} & -h_8^{\mp} \end{vmatrix}$$

and the values of $\Delta_{D_n^{\pm}}$, $\Delta_{E_n^{\pm}}$, $\Delta_{I_n^{\pm}}$ and $\Delta_{J_n^{\pm}}$ are obtained by replacing first, second, third and fourth column of $\Delta^{\pm}$ with column matrix, $T^{\mp}$ respectively. This equation gives the ratios of the amplitude constants of irregular waves corresponding to the vertical components of the displacement.

The ratios of the amplitude constants of irregular waves corresponding to horizontal components of displacement are obtained with the help of Eqs. (2.13), (2.16) and (2.35) as

$$\frac{A_n^\pm}{A_0} = \frac{F_n^\pm}{F_0}\frac{\Delta_{D_n^\pm}}{\Delta^\pm}, \quad \frac{B_n^\pm}{A_0} = \frac{F_{1n}^\pm}{F_0}\frac{\Delta_{E_n^\pm}}{\Delta^\pm}, \quad \frac{G_n^\pm}{A_0} = \frac{F_{2n}^\pm}{F_0}\frac{\Delta_{I_n^\pm}}{\Delta^\pm}, \quad \frac{H_n^\pm}{A_0} = \frac{F_{3n}^\pm}{F_0}\frac{\Delta_{J_n^\pm}}{\Delta^\pm}. \quad (2.36)$$

The reflection and transmission coefficients of the first order of approximation for irregularly reflected and transmitted qSV and qP-waves are

$$r_{sv\pm}^n = \sqrt{\frac{1+F_n^{\pm2}}{1+F_0^2}}\frac{\Delta_{D_n^\pm}}{\Delta^\pm}, \qquad r_{p\pm}^n = \sqrt{\frac{1+F_{1n}^{\pm2}}{1+F_0^2}}\frac{\Delta_{E_n^\pm}}{\Delta^\pm},$$

$$t_{sv\pm}^n = \sqrt{\frac{1+F_{2n}^{\pm2}}{1+F_0^2}}\frac{\Delta_{I_n^\pm}}{\Delta^\pm}, \qquad t_{p\pm}^n = \sqrt{\frac{1+F_{3n}^{\pm2}}{1+F_0^2}}\frac{\Delta_{J_n^\pm}}{\Delta^\pm}. \quad (2.37)$$

We come to know from Equation (2.37) that the coefficients corresponding to the irregularly reflected and transmitted qSV and qP-waves are functions of the elastic constants, angle of incidence, corrugation and frequency parameters.

2.6 Special case: An interface of $z = d\cos py$

When the interface is represented by only one cosine term, $z = d\cos py$, with d as the amplitude of corrugation. In this case

$$\zeta_{-n} = \zeta_{+n} = \begin{cases} 0 & \text{if } n \neq 1, \\ \dfrac{d}{2} & \text{if } n = 1. \end{cases} \quad (2.38)$$

Thus, using these values, the reflection and transmission coefficients for the first order approximation of the corrugation are given by

$$r_{sv\pm}^1 = \sqrt{\frac{1+F_1^{\pm2}}{1+F_0^2}}\frac{\Delta_{D_1^\pm}}{\Delta^\pm}, \qquad r_{p\pm}^1 = \sqrt{\frac{1+F_{11}^{\pm2}}{1+F_0^2}}\frac{\Delta_{E_1^\pm}}{\Delta^\pm},$$

$$t_{sv\pm}^1 = \sqrt{\frac{1+F_{21}^{\pm2}}{1+F_0^2}}\frac{\Delta_{I_1^\pm}}{\Delta^\pm}, \qquad t_{p\pm}^1 = \sqrt{\frac{1+F_{31}^{\pm2}}{1+F_0^2}}\frac{\Delta_{J_1^\pm}}{\Delta^\pm}, \quad (2.39)$$

where values of $F_1^\pm$, $F_{11}^\pm$, $F_{21}^\pm$, $F_{31}^\pm$, $\Delta^\pm$, $\Delta_{D_1^\pm}$, $\Delta_{E_1^\pm}$, $\Delta_{I_1^\pm}$ and $\Delta_{J_1^\pm}$ are obtained from Eq.(2.37) by using Eq.(2.38). We will compute these coefficients for a particular model.

2.7 Particular case

(a) When the two monoclinic half-spaces, M and M' reduce to transversely isotropic half-spaces with the axis of symmetry coinciding with the x-axis, we have

$$c_{12} = c_{13}, \quad c_{22} = c_{33}, \quad c_{55} = c_{66}, \quad c_{23} = c_{22} - 2c_{44}, \quad c_{14} = c_{24} = c_{34} = c_{56} = 0,$$

$$c_{12}' = c_{13}', \quad c_{22}' = c_{33}', \quad c_{55}' = c_{66}', \quad c_{23}' = c_{22}' - 2c_{44}', \quad c_{14}' = c_{24}' = c_{34}' = c_{56}' = 0.$$

Using these values in Eqs.(2.32), (2.33) and (2.37), we may obtain the reflection and transmission coefficients corresponding to the regular and irregular waves.

(b) If the corrugation of the interface is neglected, i.e., $d = 0$, the problem reduces to the reflection and transmission of elastic waves at a plane interface between two monoclinic elastic half-space. The reflection and transmission coefficients of the reflected and transmitted qSV and qP-waves are given by Eqs.(2.32) and (2.33). These results exactly match with those of Singh and Khurana (2001).

(c) If the half-space, M' is absent, then the problem reduces to the reflection of qSV and qP-waves for the incident qSV-wave. The reflection coefficients are given by Eq.(2.32) with the following modified values

$$\Delta = l_1 m_2 - l_2 m_1, \quad \Delta_D = m_0 l_2 - l_0 m_2, \quad \Delta_E = m_1 l_0 - m_0 l_1.$$

These results exactly match with those of Singh and Khurana (2002).

2.8 Numerical results and discussion

We will compute the angles of reflected and transmitted waves through Snell's law given by Eq.(2.17) in which the apparent velocity c_a is related with dimensionless

velocity by $\bar{c} = \frac{c_a}{\lambda}$. Let us find out the angles of reflected qSV and qP-waves in the half-space, M. Eq.(2.8) can be written as

$$\bar{c}^4 - (\bar{W} + \bar{X})\bar{c}^2 + (\bar{W}\bar{X} - \bar{Y}^2) = 0, \tag{2.40}$$

where $\bar{X} = \frac{X}{p_2^2 c_{44}}, \quad \bar{Y} = \frac{Y}{p_2^2 c_{44}}, \quad \bar{W} = \frac{W}{p_2^2 c_{44}}, \quad \lambda = \sqrt{\frac{c_{44}}{\rho}}, \quad \bar{c}_{ij} = \frac{c_{ij}}{c_{44}}$.

There are two roots of $\bar{c}^2$ corresponding to qSV and qP-waves for a given $p = \dfrac{p_3}{p_2}$, and for a given value of $\bar{c}$, there are two roots of p corresponding to the angles of reflected qSV and qP-waves (Singh and Tomar, 2007a). Substituting the values of $\bar{X}, \bar{Y}$, and $\bar{W}$ into Eq.(2.40), we get

$$d_0 p^4 + d_1 p^3 + d_2 p^2 + d_3 p + d_4 = 0 \tag{2.41}$$

where

$d_0 = \bar{c}_{33} - \bar{c}_{34}^2, \quad d_1 = 2(\bar{c}_{24}\bar{c}_{33} - \bar{c}_{23}\bar{c}_{34}), \quad d_2 = 1 + \bar{c}_{22}\bar{c}_{33} + 2\bar{c}_{24}\bar{c}_{34} - (1 + \bar{c}_{23})^2 - (1 + \bar{c}_{33})\bar{c}^2,$

$d_3 = 2\left\{ \bar{c}_{22}\bar{c}_{34} - \bar{c}_{23}\bar{c}_{24} - (\bar{c}_{24} + \bar{c}_{34})\bar{c}^2 \right\}, \quad d_4 = \bar{c}^4 - (1 + \bar{c}_{22})\bar{c}^2 + \bar{c}_{22} - \bar{c}_{24}^2.$

We transform this equation with $q = \dfrac{1}{p} = \dfrac{p_2}{p_3}$ so that

$$d_4 q^4 + d_3 q^3 + d_2 q^2 + d_1 q + d_0 = 0. \tag{2.42}$$

This equation has two positive roots, i.e., the smaller positive root (q_1) and the larger positive root (q_2) which represent the directions of reflected qSV and qP-waves respectively. Thus, $\theta = \tan^{-1}(q_1)$ and $\phi = \tan^{-1}(q_2)$. Similarly, in the half-space M', the angles of transmitted qSV and qP-waves are obtained as $\alpha = \tan^{-1}(q_1')$ and $\beta = \tan^{-1}(q_2')$.

For the numerical computation, the following relevant values of elastic constants are taken (Singh and Tomar, 2008):

(for half-space, M-Lithium tantalate)

$c_{24} = 0.11 \times 10^{11} N/m^2, \; c_{23} = 0.80 \times 10^{11} N/m^2, \; c_{34} = 0, \; c_{44} = 0.94 \times 10^{11} N/m^2,$

$c_{33} = 2.75 \times 10^{11} N/m^2, \; c_{22} = 2.33 \times 10^{11} N/m^2, \; \rho = 7400 Kg/m^3.$

(for half-space, M'-Lithium neobate)

$c'_{24} = -0.09 \times 10^{11} N/m^2$, $c'_{23} = 0.75 \times 10^{11} N/m^2$, $c'_{34} = 0$, $c'_{44} = 1.06 \times 10^{11} N/m^2$, $c'_{33} = 2.45 \times 10^{11} N/m^2$, $c'_{22} = 2.03 \times 10^{11} N/m^2$, $\rho' = 4700 Kg/m^3$, with corrugation parameter, $cor(pd) = 0.0001$ and frequency parameter, $fr(\omega/pc_0) = 100$ are taken unless and otherwise mentioned.

We developed a program on MATLAB for the computation of amplitude and energy ratios of reflected and transmitted waves due to incident qSV-waves. Figures 2.4-2.11 represent the variation of reflection and transmission coefficients with the angle of incidence for different values of corrugation and frequency parameters. Figures 2.12-2.14 represent the variation of reflection and transmission coefficients with corrugation parameter and Figures 2.15-2.17 represent the variation of reflection and transmission coefficients with frequency parameter at $\theta_0 = 20^0$.

In Fig. 2.2, all angles $(\theta, \phi, \alpha, \beta)$ of the regularly reflected and transmitted waves increase with the increase of angle of incidence (θ_0). It is observed that the angles of reflection and transmission for qSV-waves are less than that of the qP-waves.
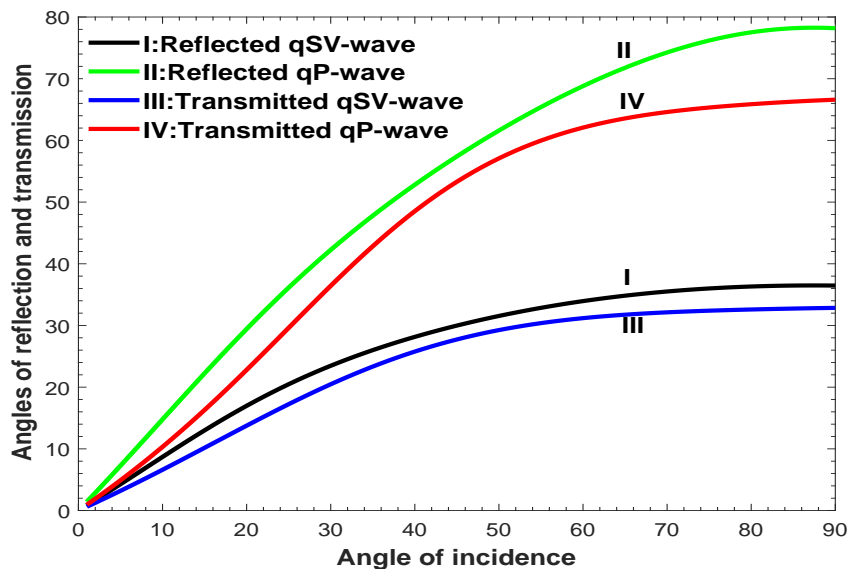
Figure 2.2: Variation of the angle of reflection and transmission with angle of incidence.

Curve I in Fig. 2.3 shows that r_{sv} starts from certain value which decreases to

zero at $\theta_0 = 15^0$ and then increases up to $\theta_0 = 51^0$ with the increase of θ_0. Thereafter, it decreases, touching zero value at $\theta_0 = 87^0$.
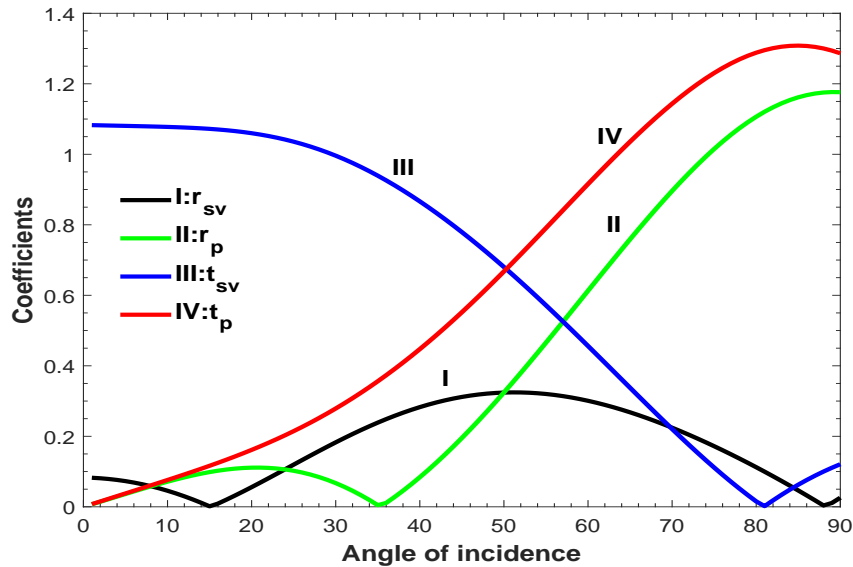
Figure 2.3: Variation of reflection and transmission coefficients with angle of incidence.

In the same figure, Curve II shows that r_p is parabolic in the region $0 \leq \theta_0 \leq 35^0$ and then, it increases with the increase of θ_0. Curve III shows the decreasing nature of t_{sv} up to $\theta_0 = 81^0$ and then increases with the increase of θ_0, while Curve IV shows that t_p increases with the increase of the angle of incidence θ_0.

2.8.1 Effect of corrugation and frequency parameters

We are interested to see the effect of corrugation and frequency parameters on the reflection and transmission coefficients. In Fig. 2.4, the reflection coefficient, $r_{sv^+}^1$ corresponding to the irregularly reflected qSV-wave starts from certain value and decreases to zero at $\theta_0 = 14^0$ making a parabolic region in $14^0 \leq \theta_0 \leq 81^0$, which then increases with the increase of θ_0. It is observed that $r_{sv^+}^1$ increases with the increase of corrugation (cor) and frequency (fr) parameters.
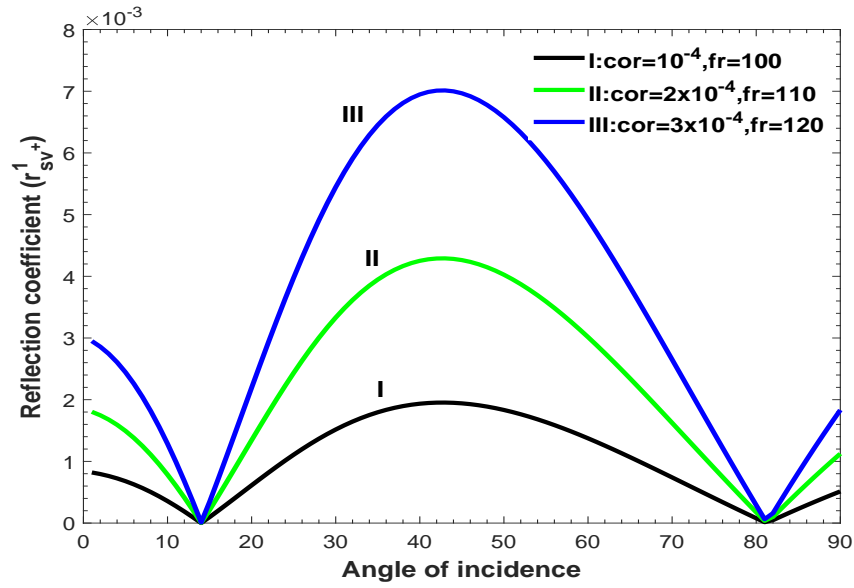
Figure 2.4: Variation of r^1_{sv+} with θ_0 for different values of pd and ω/pc_0.
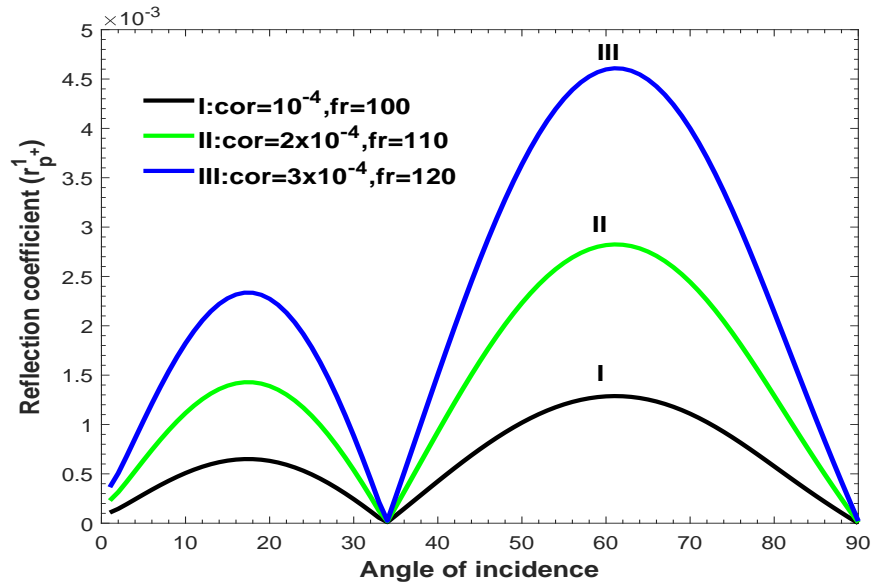
Figure 2.5: Variation of r^1_{p+} with θ_0 for different values of pd and ω/pc_0.

In Figure 2.5, r^1_{p+} makes two parabolic regions in $0^0 \leq \theta_0 \leq 34^0$ and $34^0 \leq \theta_0 \leq 90^0$ with the increase of θ_0. The values of this coefficient also increase with the increase of cor and fr. We have observed similar nature of r^1_{sv-} and r^1_{p-} with r^1_{sv+} and r^1_{p+} respectively in Figures 2.6 and 2.7.
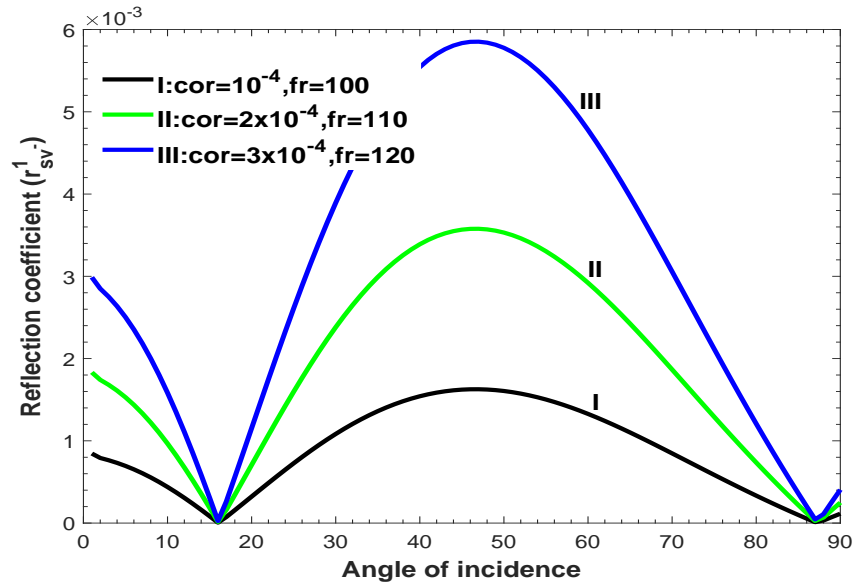
Figure 2.6: Variation of $r^1_{sv^-}$ with θ_0 for different values of pd and ω/pc_0.
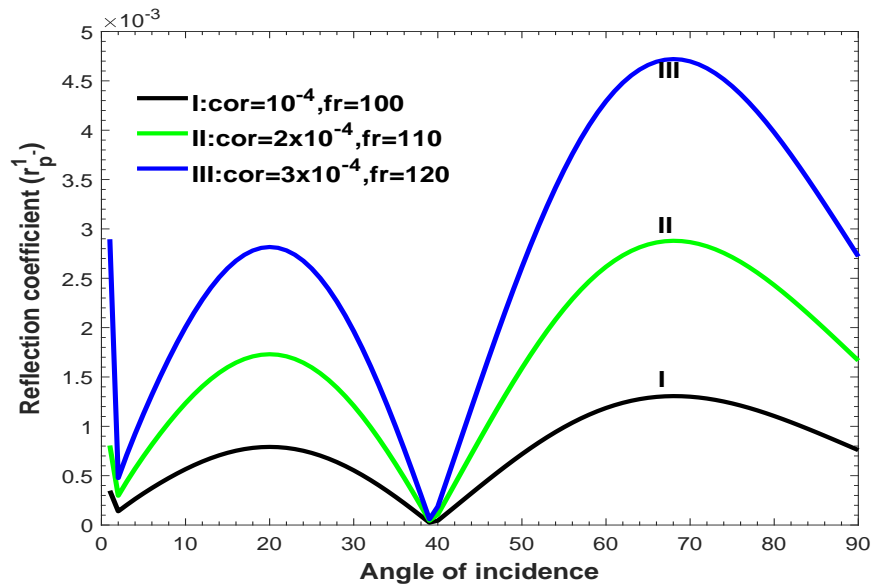
Figure 2.7: Variation of $r^1_{p^-}$ with θ_0 for different values of pd and ω/pc_0.
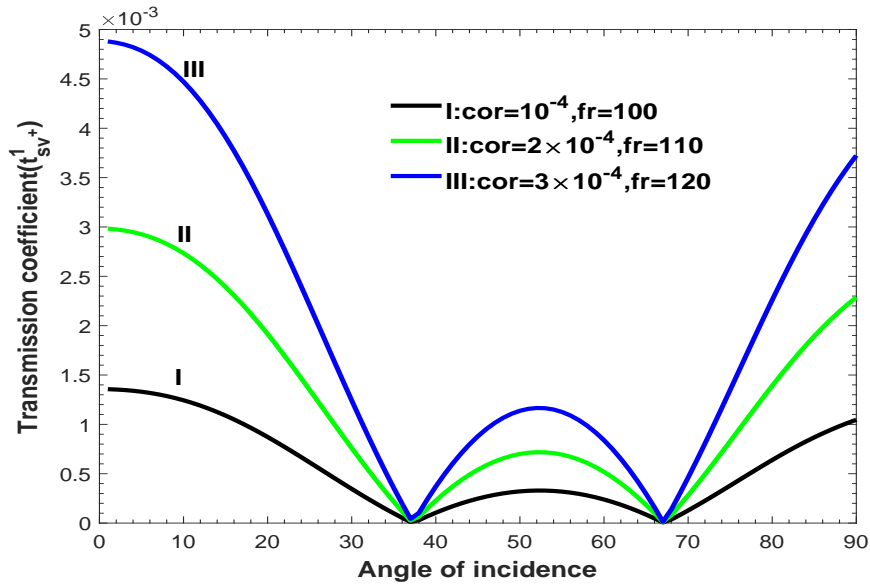
Figure 2.8: Variation of $t^1_{sv^+}$ with θ_0 for different values of pd and ω/pc_0.

The coefficient, $t^1_{sv^+}$ in Figure 2.8 decreases initially making a parabolic region in $37^0 \leq \theta_0 \leq 67^0$ and then increases with the increase of θ_0. It is observed that the values of $t^1_{sv^+}$ increase with the increase of cor and fr.
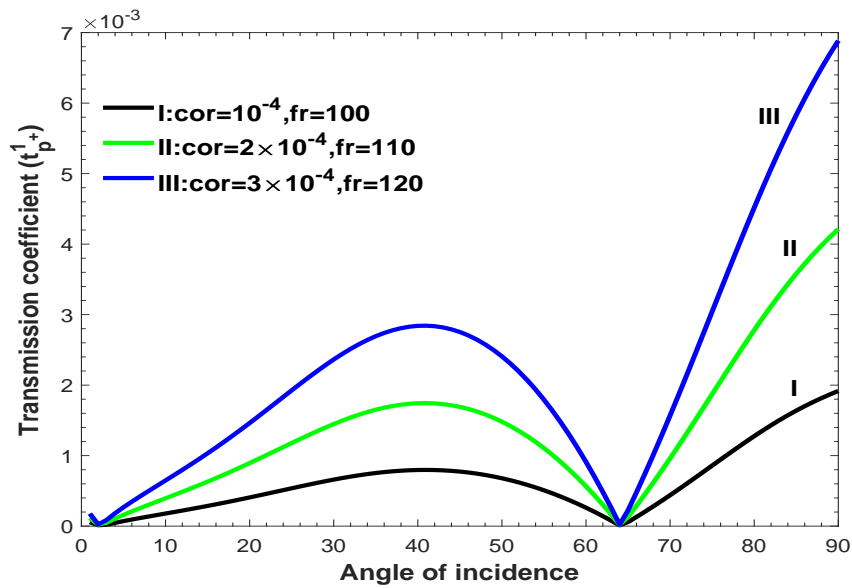
Figure 2.9: Variation of $t^1_{p^+}$ with θ_0 for different values of pd and ω/pc_0.

We see in Figure 2.9 that t_{p+}^1 makes a parabolic region in $2^0 \leq \theta_0 \leq 64^0$ and then increases with the increase of θ_0. The value of this coefficient increase with the increase of cor and fr. Similar natures of t_{sv-}^1 and t_{p-}^1 with t_{sv+}^1 and t_{p+}^1 respectively are observed in Figures 2.10 and 2.11.
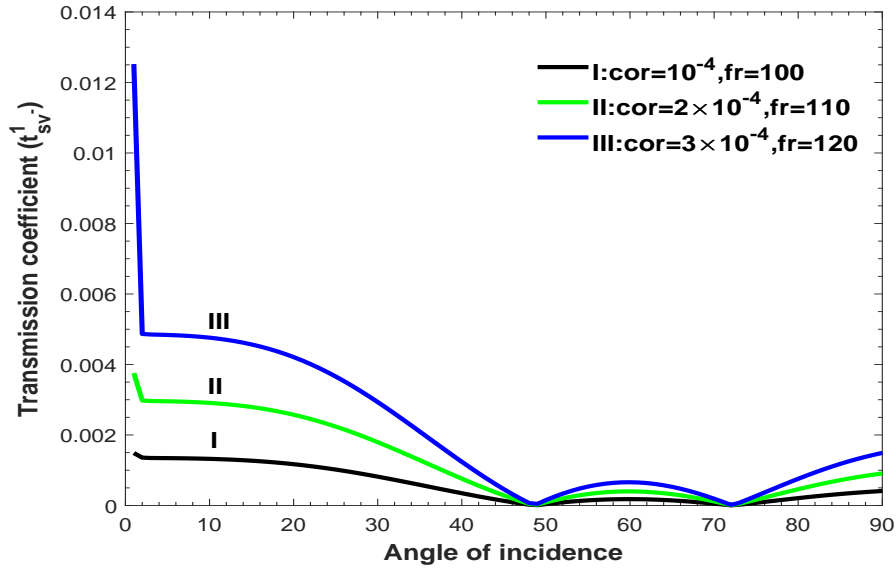
Figure 2.10: Variation of t_{sv-}^1 with θ_0 for different values of pd and ω/pc_0.
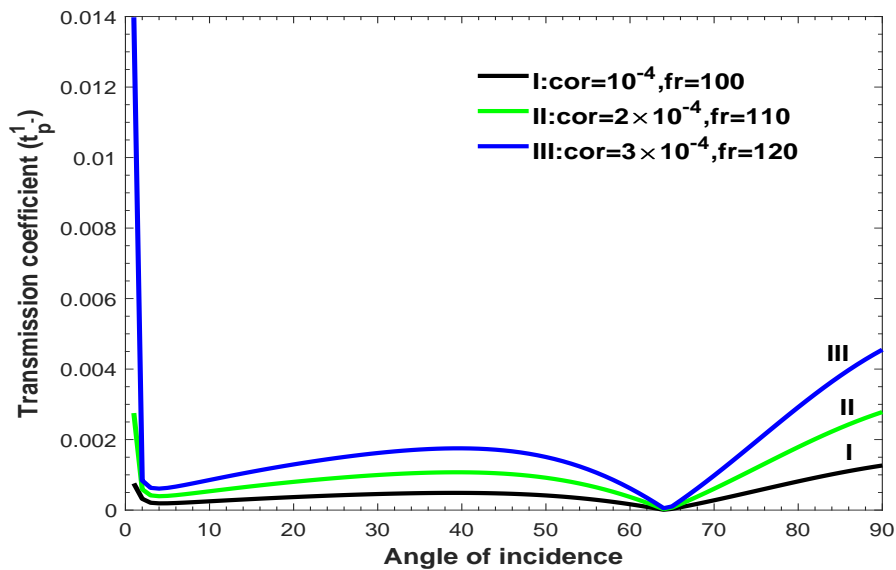
Figure 2.11: Variation of t_{p-}^1 with θ_0 for different values of pd and ω/pc_0.

We have seen from Figures 2.12 and 2.15 that the coefficients corresponding to the regularly reflected and transmitted waves are independent of cor and fr.
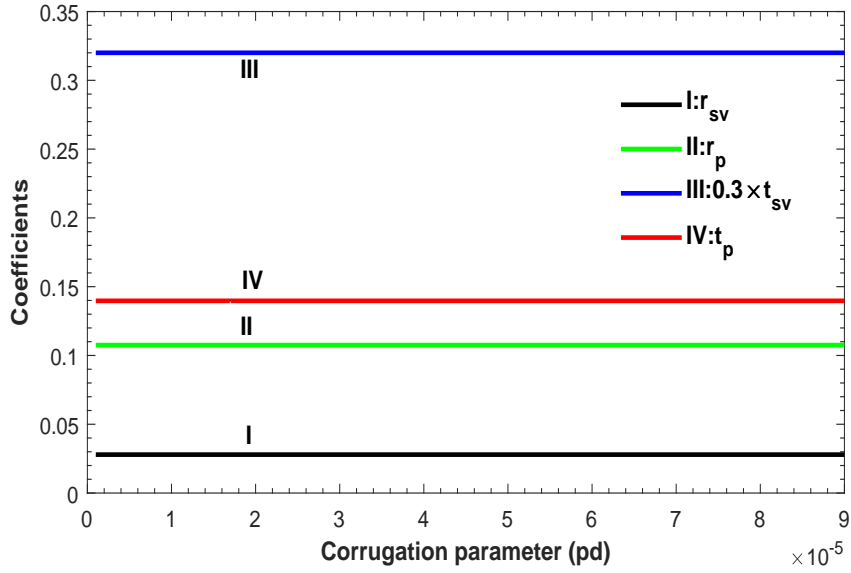
Figure 2.12: Variation of reflection and transmission coefficients of the regular qSV and qP-waves with pd.
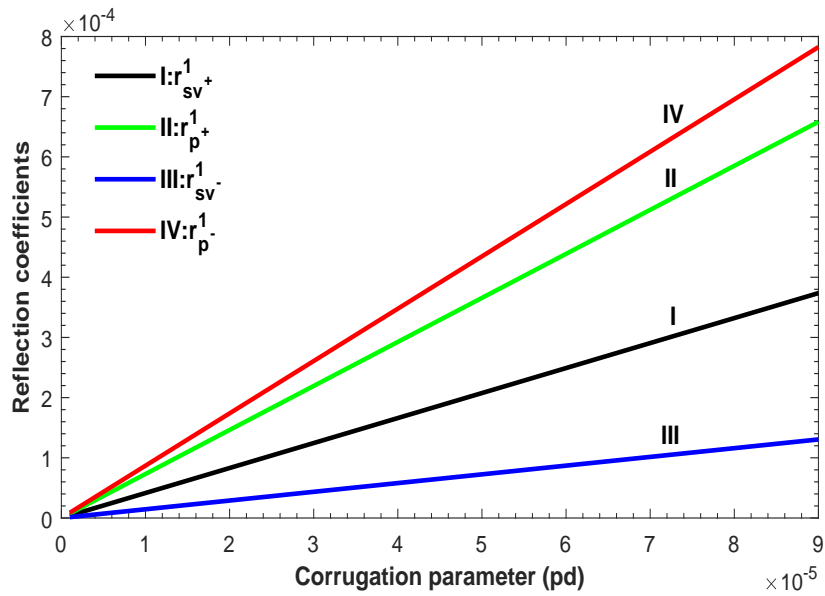
Figure 2.13: Variation of reflection coefficients of the irregularly reflected qSV and qP-waves with pd.

In Figures 2.13, 2.14, 2.16 and 2.17, the coefficients corresponding to the irregularly reflected and transmitted waves are linearly proportional to corrugation and frequency parameters, but at different rates.
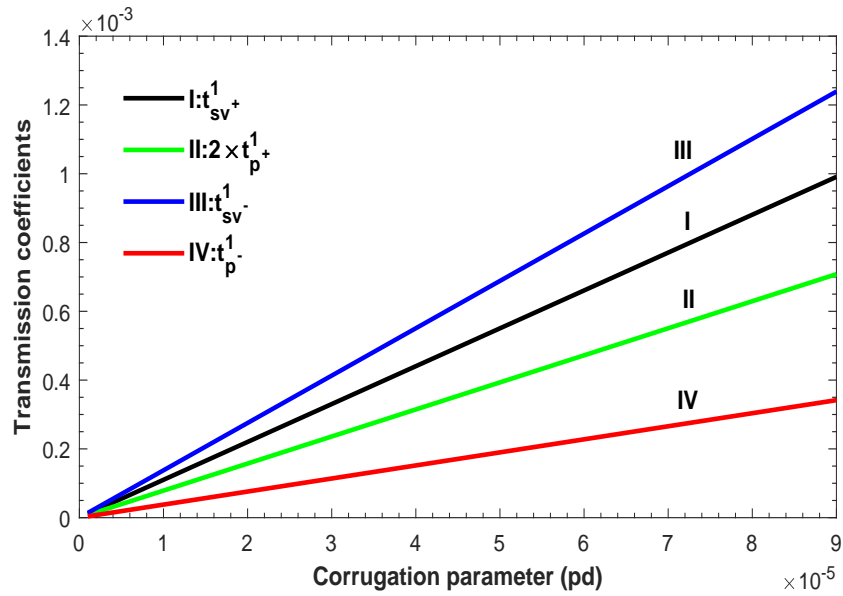
Figure 2.14: Variation of transmission coefficients of the irregularly transmitted qSV and qP-waves with pd.
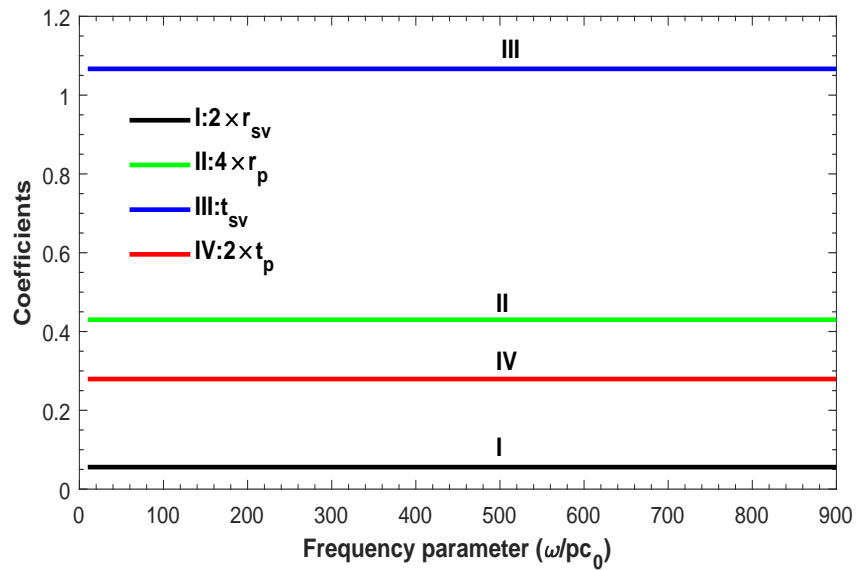
Figure 2.15: Variation of reflection and transmission coefficients of the regular qSV and qP-waves with ω/pc_0.
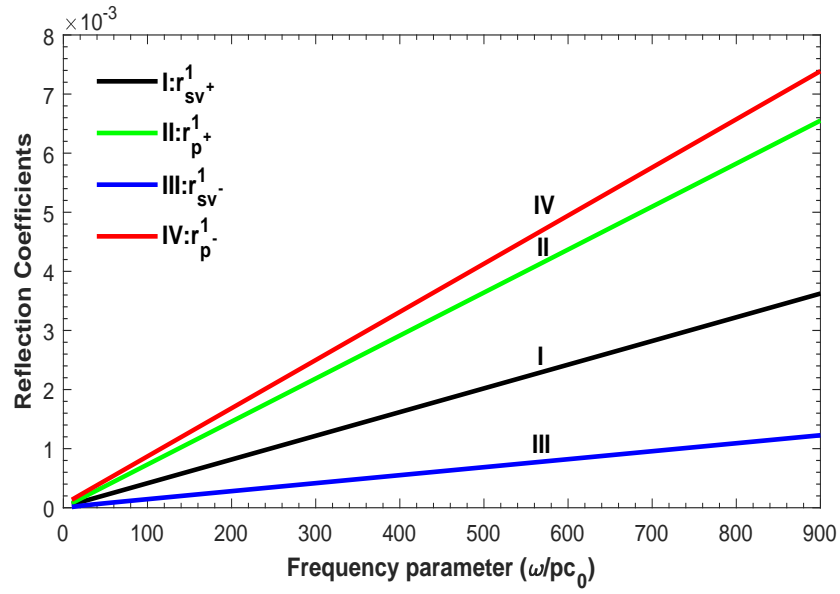
Figure 2.16: Variation of reflection and transmission coefficients of the irregular qSV and qP-waves with ω/pc_0.
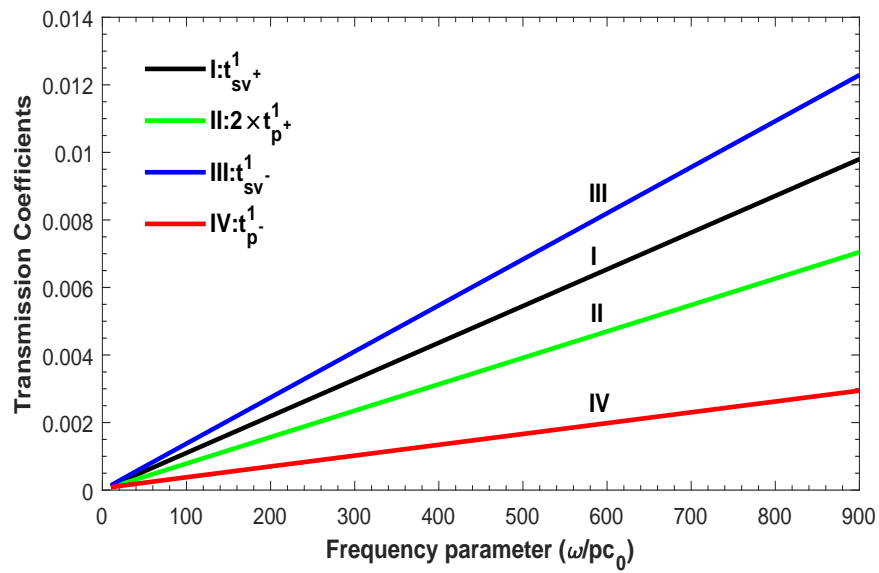
Figure 2.17: Variation of transmission coefficients of the irregularly transmitted qSV and qP-waves with ω/pc_0.

2.9   Conclusions

The problem of incident qSV-wave at a corrugated interface between two dissimilar monoclinic elastic half-spaces has been investigated. We have obtained the reflection and transmission coefficients for the first order of approximation corresponding to regularly and irregularly reflected and transmitted qSV and qP-waves with the help of Rayleigh's method of approximation. These coefficients are computed numerically for a specific model and the effect of corrugation and frequency parameters on these coefficients are discussed. We may conclude with the following remarks:

(i) All coefficients corresponding to regular waves are functions of angle of incidence and elastic constants, while those of irregular waves are found to be functions of angle of incidence, elastic constants, corrugation and frequency parameters.

(ii) Theoretically and numerically, the reflection and transmission coefficients of the regular waves are independent of corrugation and frequency parameters.

(iii) The coefficients corresponding to irregular waves are found to be linearly proportional to corrugation and frequency parameters.

(iv) It is found that the values of coefficients corresponding to irregular waves increase with increase of pd and ω/pc_0.

(v) The values of coefficients corresponding to irregular waves are found to be small.

Chapter 3

Effect of corrugation on incident qP/qSV-waves between two dissimilar nematic elastomers[2]

3.1 Introduction

Nematic elastomers (NEs) are soft materials that combine the hyper-elasticity of elastomers with anisotropy of liquid crystals, and they are synthesized by cross-linking of liquid crystal polymers. Such materials have the properties of elastic degrees of freedom of ordinary rubber and orientational degree of freedom of liquid crystals. Terentjev *et al.* (2002) developed a theory of elastic waves in oriented monodomain nematic elastomers and discussed the effect of soft elasticity combined with the Leslie-Ericksen version of dissipation function. Singh (2007a) discussed the problem of elastic waves propagation in the linear viscoelastic theory of nematic elastomer and obtained the reflection coefficients of the reflected waves. Singh (2015) investigated the problem of reflection and refraction of elastic waves due to an incident quasi-primary (qP)-wave at a plane interface between two dissimilar nematic elastomer half-spaces.

In this chapter, the problem of reflection and transmission of elastic waves at a corrugated interface between two dissimilar nematic elastomer half-spaces has been

---

investigated separately for the incident qP and qSV-waves. The expressions of the phase velocities corresponding to qP and qSV-waves are obtained. The closed form expression of the amplitude ratios corresponding to the reflected and transmitted waves for the incident qP and qSV-waves are derived by using appropriate boundary conditions. The energy partitions due to the corrugated interface are also obtained. The amplitude and energy ratios of the regular and irregular waves are computed numerically for a particular model, $d\cos px_1$ at different values of corrugation parameter. The results of Singh (2007a), Singh (2015) and similar results of Asano (1961) for the relevant problems are recovered from the present work.

3.2   Basic equation

The elastic potential energy density in nematic solid is (de Gennes 1980; Warner and Terentjev, 1996)

$$F = C_1(\mathbf{n} \cdot \epsilon \cdot \mathbf{n})^2 + 2C_2 tr[\mathbf{e}](\mathbf{n} \cdot \epsilon \cdot \mathbf{n}) + C_3(tr[\mathbf{e}])^2 + 2C_4(\mathbf{n} \times \epsilon \times \mathbf{n})^2$$
$$+ 4C_5(\mathbf{n} \times (\epsilon \cdot \mathbf{n}))^2 + \frac{1}{2}D_1(\mathbf{n} \times \mathbf{\Theta})^2 + D_2\mathbf{n} \cdot \epsilon \cdot (\mathbf{n} \times \mathbf{\Theta}), \tag{3.1}$$

Here, the Frank elastic energy is restricted only for uniform director rotations of the NEs. The director rotations are represented by $(\mathbf{n} \times \delta\mathbf{n})$, $\delta\mathbf{n}$ is small variation in the undistorted nematic director, $\mathbf{n} \cdot \mathbf{\Omega} = (curl\ \mathbf{u})/2$ is the local rotation vector, $\mathbf{\Theta} = \mathbf{\Omega} - (\mathbf{n} \times \delta\mathbf{n})$ is an independent rotational variable, $\epsilon_{ij} = e_{ij} - tr[\mathbf{e}]\delta_{ij}/3$ is the traceless part of linear symmetric strain, $e_{ij} = (u_{i,j} + u_{j,i})/2$ and C_i are elastic constants with D_1 and D_2 are coupling constants.

The Rayleigh dissipation function in the quadratic form can be written as (Ericksen, 1960; Leslie, 1966)

$$T\dot{s} = A_1(\mathbf{n} \cdot \dot{\epsilon} \cdot \mathbf{n})^2 + 2A_2 tr[\dot{\mathbf{e}}](\mathbf{n} \cdot \dot{\epsilon} \cdot \mathbf{n}) + A_3(tr[\dot{\mathbf{e}}])^2 + 2A_4(\mathbf{n} \times \dot{\epsilon} \times \mathbf{n})^2$$
$$+ 4A_5(\mathbf{n} \times (\dot{\epsilon} \cdot \mathbf{n}))^2 + \frac{1}{2}\gamma_1(\mathbf{n} \times \dot{\mathbf{\Theta}})^2 + \gamma_2\mathbf{n} \cdot \dot{\epsilon} \cdot (\mathbf{n} \times \dot{\mathbf{\Theta}}), \tag{3.2}$$

where A_i are viscous coefficients and superimposed dots denote derivative with respect to time. This equation describes two types of dissipation - by shear flow and by rotation of the director.

Neglecting the effects due to Frank elasticity on the director gradient, the equations of motion of viscous nematic solid are represented by (Fradkin et al., 2003)

$$\nabla \cdot \tau = \rho \ddot{\mathbf{u}},$$

$$\mathbf{n} \times [(D_1 + \gamma_1 \partial_t)\mathbf{n} \times \boldsymbol{\Theta} + (D_2 + \gamma_2 \partial_t)\mathbf{n} \cdot \boldsymbol{\epsilon}] = 0. \tag{3.3}$$

The viscoelastic symmetric stress tensors of NEs with the choice of the co-ordinate axis x_3 lies in the direction of the undistorted director $\mathbf{n}$ are

$$\tau_{11} = (1 + \tau_R \partial_t)(c_{11}\epsilon_{11} + c_{12}\epsilon_{22} + c_{13}\epsilon_{33}), \quad \tau_{22} = (1 + \tau_R \partial_t)(c_{12}\epsilon_{11} + c_{11}\epsilon_{22} + c_{13}\epsilon_{33}),$$

$$\tau_{33} = (1 + \tau_R \partial_t)(c_{13}\epsilon_{11} + c_{13}\epsilon_{22} + c_{33}\epsilon_{33}), \quad \tau_{12} = \tau_{21} = 2(1 + \tau_R \partial_t)c_{66}\epsilon_{12},$$

$$\tau_{13} = 2(1 + \tau_R \partial_t)c_{44}\epsilon_{13} - \frac{1}{2}D_2(1 + \tau_2 \partial_t)\Theta_2,$$

$$\tau_{23} = 2(1 + \tau_R \partial_t)c_{44}\epsilon_{23} + \frac{1}{2}D_2(1 + \tau_2 \partial_t)\Theta_1, \tag{3.4}$$

where τ_R is the characteristic time of rubber relaxation with τ_1 and τ_2 as director rotation times. The director rotation time has been experimentally measured as $10^{-1} - 10^{-2}s$ (Schmidtke et al., 2000; Schonstein et al., 2001). On the other hand τ_R is expected to be much shorter, which can be as low as $10^{-5} - 10^{-6}s$. The relations among the viscous coefficients, elastic constants and relaxation times satisfy (Terentjev et al., 2002)

$$A_i = C_i \tau_R, \quad \gamma_1 = D_1 \tau_1, \quad \tau_2 = D_2 \tau_2. \tag{3.5}$$

It may be noted that the Rayleigh dissipation function is positive for

$$\tau_2^2 \leq \frac{8C_5 D_1}{D_2^2}\tau_R \tau_1,$$

where C_5 is the shear modulus.

Using Equations (3.3) and (3.4), we get the components of rotational variable Θ as

$$
\begin{pmatrix} \Theta_1 \\ \Theta_2 \end{pmatrix} = \frac{D_2}{D_1} \frac{1+\iota\omega\tau_2}{1+\iota\omega\tau_1} \begin{pmatrix} -\epsilon_{23} \\ \epsilon_{13} \end{pmatrix},
$$

where ω is angular frequency.

3.3 Problem formulation

Let us consider two-dimensional wave propagation in x_1x_3-plane with x_1 and x_2-axis lying horizontally and x_3-axis vertically downward. Suppose two dissimilar anisotropic nematic elastomer half-spaces, $M : \zeta(x_1) \le x_3 < \infty$ and $M' : -\infty < x_3 \le \zeta(x_1)$, are separated by $x_3 = \zeta(x_1)$, which is a periodic function of x_1 independent of x_2 whose mean value is zero. It may be noted that all parameters in M will be denoted without prime, while those of M' with prime to the corresponding parameters of M. The Fourier series expansion of $\zeta(x_1)$ is given by (Asano, 1961)

$$
\zeta(x_1) = \sum_{n=1}^{\infty} \left(\zeta_{+n} e^{\iota npx_1} + \zeta_{-n} e^{-\iota npx_1} \right), \tag{3.6}
$$

where $\zeta_{\pm n}$ are the coefficients of series expansion of order n, p is the wavenumber and $\iota = \sqrt{-1}$.

We introduce constants d, c_n and s_n as

$$
\zeta_{\pm 1} = \frac{d}{2}, \qquad \zeta_{\pm n} = \frac{c_n \mp \iota s_n}{2}, \quad (n=2,3,4,....)
$$

so that

$$
\zeta(x_1) = d\cos(px_1) + \sum_{n=2}^{\infty} \{c_n \cos(npx_1) + s_n \sin(npx_1)\}. \tag{3.7}
$$

If the interface is $\zeta(x_1) = d\cos(px_1)$, then $2\pi/p$ is the wavelength of corrugation and d is the amplitude of corrugation.

The general equations of motion in the nematic elastomer half-spaces, M and M' are

respectively given by

$$\rho \ddot{u}_1 = (1 + \imath \omega \tau_R)\{c_{11} u_{1,11} + (c_{13} + c_{44}^R) u_{3,13} + c_{44}^R u_{1,33}\}, \tag{3.8}$$

$$\rho \ddot{u}_3 = (1 + \imath \omega \tau_R)\{c_{33} u_{3,33} + (c_{13} + c_{44}^R) u_{1,13} + c_{44}^R u_{3,11}\}, \tag{3.9}$$

and

$$\rho \ddot{u}_1' = (1 + \imath \omega \tau_R')\{c_{11}' u_{1,11}' + (c_{13}' + c_{44}'^R) u_{3,13}' + c_{44}'^R u_{1,33}'\}, \tag{3.10}$$

$$\rho \ddot{u}_3' = (1 + \imath \omega \tau_R')\{c_{33}' u_{3,33}' + (c_{13}' + c_{44}'^R) u_{1,13}' + c_{44}'^R u_{3,11}'\}, \tag{3.11}$$

where

$$c_{44}^R = 2C_5 - \frac{D_2^2(1 + \imath \omega \tau_2)^2}{4D_1(1 + \imath \omega \tau_1)(1 + \imath \omega \tau_R)}, \quad c_{44}'^R = 2C_5' - \frac{D_2'^2(1 + \imath \omega \tau_2')^2}{4D_1'(1 + \imath \omega \tau_1')(1 + \imath \omega \tau_R')}.$$

Suppose a plane wave (P/SV) propagating in the half-space, M be incident obliquely with an angle α_0 at the corrugated interface $x_3 = \zeta(x_1)$. Due to undulated nature of the interface, there are regularly and irregularly reflected and transmitted waves (Asano, 1961). The geometry of the problem is given in Figure 3.1.
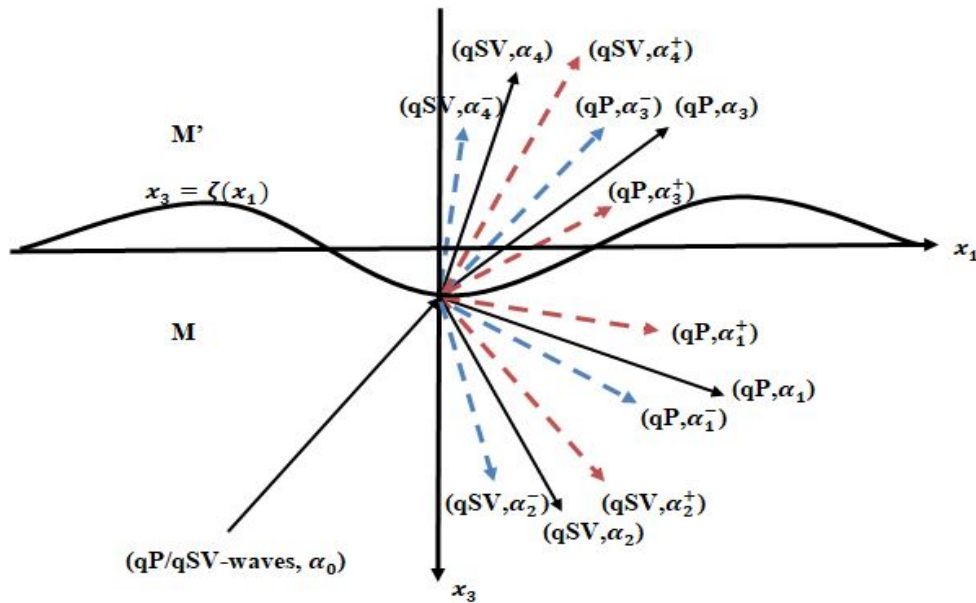
Figure 3.1: Geometry of the problem

The total displacement in the half-space, M is the sum of displacement components due to incident, regularly and irregularly reflected waves as

$$u_1 = \sum_{m=0}^{2} A_m d_1^{(m)} \exp(P_m) + \sum_{m=1}^{2} \sum_{n=1}^{\infty} A_{mn}^{\pm} d_{1\pm}^{(mn)} \exp(Q_m), \qquad (3.12)$$

$$u_3 = \sum_{m=0}^{2} A_m d_3^{(m)} \exp(P_m) + \sum_{m=1}^{2} \sum_{n=1}^{\infty} A_{mn}^{\pm} d_{3\pm}^{(mn)} \exp(Q_m), \qquad (3.13)$$

where $P_m = \imath(\omega t - k_1^{(m)} x_1 - k_3^{(m)} x_3)$, $Q_m = \imath(\omega t - k_{1\pm}^{(mn)} x_1 - k_{3\pm}^{(mn)} x_3)$, A_0 is the amplitude constant for the incident wave, A_m and $A_{mn}^{\pm}$ denotes amplitude constants, $(d_1^{(m)}, d_3^{(m)})$ and $(d_{1\pm}^{(mn)}, d_{3\pm}^{(mn)})$ are unit displacement vectors, $(k_1^{(m)}, k_3^{(m)})$ and $(k_{1\pm}^{(mn)}, k_{3\pm}^{(mn)})$ are propagation factors corresponding to regularly and irregularly reflected waves respectively.

Similarly, the total displacement in half-space, M' is the sum of the displacement components due to regularly and irregularly transmitted waves

$$u_1' = \sum_{m=3}^{4} \sum_{n=1}^{\infty} \left(A_m d_1^{(m)} \exp(P_m) + A_{mn}^{\pm} d_{1\pm}^{(mn)} \exp(Q_m) \right), \qquad (3.14)$$

$$u_3' = \sum_{m=3}^{4} \sum_{n=1}^{\infty} \left(A_m d_3^{(m)} \exp(P_m) + A_{mn}^{\pm} d_{3\pm}^{(mn)} \exp(Q_m) \right). \qquad (3.15)$$

It may be noted that $m = 1$ and $mn = 1n$ correspond to regularly and irregularly reflected qP-waves at angles α_1 and $\alpha_{1n}^{\pm}$, $m = 2$ and $mn = 2n$ correspond for the regularly and irregularly reflected qSV-waves at angles α_2 and $\alpha_{2n}^{\pm}$, $m = 3$ and $mn = 3n$ for regularly and irregularly transmitted qP-waves at angles α_3 and $\alpha_{3n}^{\pm}$ and $m = 4$ and $mn = 4n$ correspond for regularly and irregularly transmitted qSV-waves at angles α_4 and $\alpha_{4n}^{\pm}$ respectively.

The Snell's law for this problem is (Singh, 2015)

$$k_0 \sin \alpha_0 = k_1 \sin \alpha_1 = k_2 \sin \alpha_2 = k_3 \sin \alpha_3 = k_4 \sin \alpha_4. \qquad (3.16)$$

The angles of irregular waves are related with those of regular waves through the

Spectrum theorem (Abubakar, 1962b)

$$\sin \alpha_{mn}^{\pm} = \sin \alpha_m \pm \frac{np}{k_m}, \quad m = 1, 2, 3, 4 \quad \text{and} \quad n = 1, 2, 3, 4, ... \tag{3.17}$$

where k_m are the wavenumbers. The phase velocity (Singh, 2017) of the incident waves, regularly reflected and transmitted waves are given by (plus for qP-waves and minus for qSV-waves)

$$c_i^2(\alpha_i) = \begin{cases} \frac{B(\alpha_i)+E(\alpha_i)\pm\sqrt{\{B(\alpha_i)-E(\alpha_i)\}^2+4D^2(\alpha_i)}}{2\rho}, & i = 0, 1, 2 \\ \frac{B(\alpha_i)+E(\alpha_i)\pm\sqrt{\{B(\alpha_i)-E(\alpha_i)\}^2+4D^2(\alpha_i)}}{2\rho'}, & i = 3, 4 \end{cases} \tag{3.18}$$

where

$$B(\alpha_i) = (1 + \imath\omega\tau_R)\{c_{11}p_1^{(i),2} + c_{44}^R p_3^{(i),2}\}, \quad E(\alpha_i) = (1 + \imath\omega\tau_R)\{c_{44}^R p_1^{(i),2} + c_{33}p_3^{(i),2}\},$$

$$D(\alpha_i) = (1 + \imath\omega\tau_R)(c_{13} + c_{44}^R)p_1^{(i)}p_3^{(i)}, \quad \text{for i =0, 1, 2,}$$

$$B(\alpha_i) = (1 + \imath\omega\tau_R')\{c_{11}'p_1^{(i),2} + c_{44}'^R p_3^{(i),2}\}, \quad E(\alpha_i) = (1 + \imath\omega\tau_R')\{c_{44}'^R p_1^{(i),2} + c_{33}'p_3^{(i),2}\},$$

$$D(\alpha_i) = (1 + \imath\omega\tau_R')(c_{13}' + c_{44}'^R)p_1^{(i)}p_3^{(i)}, \quad \text{for i = 3, 4.}$$

It may be noted that c_0 is the phase velocity of the incident qP or qSV-wave, c_1 is the phase velocity of regularly reflected qP-wave, c_2 is the phase velocity of regularly reflected qSV-wave, c_3 is the phase velocity of regularly transmitted qP-wave and c_4 is the phase velocity of regularly transmitted qSV-wave.

3.4 Boundary conditions

The component of displacements and traction (normal and shear) are continuous at the corrugated interface, $x_3 = \zeta(x_1)$ (Asano, 1961). Mathematically, these conditions can be written as

(i) Continuity of displacements

$$u_1 = u_1', \quad u_3 = u_3', \tag{3.19}$$

(ii) Continuity of shear traction

$$\tau_{13} + (\tau_{33} - \tau_{11})\zeta' - \tau_{13}\zeta'^2 = \tau'_{13} + (\tau'_{33} - \tau'_{11})\zeta' - \tau'_{13}\zeta'^2, \tag{3.20}$$

(iii) Continuity of normal traction

$$\tau_{33} - 2\tau_{13}\zeta' + \tau_{11}\zeta'^2 = \tau'_{33} - 2\tau'_{13}\zeta' + \tau'_{11}\zeta'^2. \tag{3.21}$$

Using Eq. (3.4) into (3.20) and (3.21), we have

$$(1 - \zeta'^2)c_{44}^R(u_{1,3} + u_{3,1}) + \zeta'(\tau_3 u_{1,1} + \tau_4 u_{3,3})$$
$$= \tau_0(1 - \zeta'^2)c_{44}^{'R}(u'_{1,3} + u'_{3,1}) + \zeta'(\tau'_3 u'_{1,1} + \tau'_4 u'_{3,3}), \tag{3.22}$$

$$(c_{13} + \zeta'^2 c_{11})u_{1,1} + (c_{33} + \zeta'^2 c_{13})u_{3,3} - 2\zeta' c_{44}^R(u_{1,3} + u_{3,1})$$
$$= \tau_0\{(c'_{13} + \zeta'^2 c'_{11})u'_{1,1} + (c'_{33} + \zeta'^2 c'_{13})u'_{3,3} - 2\zeta' c_{44}^{'R}(u'_{1,3} + u'_{3,1})\}. \tag{3.23}$$

where

$$\tau_3 = c_{13} - c_{11}, \quad \tau_4 = c_{33} - c_{13}, \quad \tau'_3 = \tau_0(c'_{13} - c'_{11}), \quad \tau'_4 = \tau_0(c'_{33} - c'_{13}),$$

$$\tau_0 = (1 + \iota\omega\tau'_R)/(1 + \iota\omega\tau_R), \quad \zeta' = \sum_{n=1}^{\infty} \iota np \left(\zeta_{+n}e^{\iota npx_1} - \zeta_{-n}e^{-\iota npx_1}\right).$$

Using Eqs.(3.12)-(3.17) into (3.19), Eqs.(3.22) and (3.23), we get

$$\sum_{m=0}^{2} A_m d_1^{(m)} e^{\iota\zeta k_3^{(m)}} + \sum_{m=1}^{2}\sum_{n=1}^{\infty} A_{mn}^{\pm} d_{1\pm}^{(mn)} e^{\mp\iota npx_1} e^{\iota\zeta k_{3\pm}^{(mn)}}$$
$$= \sum_{m=3}^{4}\sum_{n=1}^{\infty} \left(A_m d_1^{(m)} e^{\iota\zeta k_3^{(m)}} + A_{mn}^{\pm} d_{1\pm}^{(mn)} e^{\mp\iota npx_1} e^{\iota\zeta k_{3\pm}^{(mn)}}\right), \tag{3.24}$$

$$\sum_{m=0}^{2} A_m d_3^{(m)} e^{\iota\zeta k_3^{(m)}} + \sum_{m=1}^{2}\sum_{n=1}^{\infty} A_{mn}^{\pm} d_{3\pm}^{(mn)} e^{\mp\iota npx_1} e^{\iota\zeta k_{3\pm}^{(mn)}}$$
$$= \sum_{m=3}^{4}\sum_{n=1}^{\infty} \left(A_m d_3^{(m)} e^{\iota\zeta k_3^{(m)}}\zeta + A_{mn}^{\pm} d_{3\pm}^{(mn)} e^{\mp\iota npx_1} e^{\iota\zeta k_{3\pm}^{(mn)}}\right), \tag{3.25}$$

$$\sum_{m=0}^{2} A_m \left((1 - \zeta'^2)\mu_m c_{44}^R + \zeta'(\tau_3 d_1^{(m)} k_1^{(m)} + \tau_4 d_3^{(m)} k_3^{(m)})\right) e^{\iota\zeta k_3^{(m)}} +$$

$$\sum_{m=1}^{2}\sum_{n=1}^{\infty} A_{mn}^{\pm}\left((1-\zeta'^2)\lambda_{mn}c_{44}^R + \zeta'(\tau_3 d_{1\pm}^{(mn)}k_{1\pm}^{mn} + \tau_4 d_{3\pm}^{(mn)}k_{3\pm}^{mn})\right)e^{\mp \imath n p x_1}e^{\imath \zeta k_{3\pm}^{(mn)}}$$

$$= \sum_{m=3}^{4} A_m\left((1-\zeta'^2)\tau_0'\mu_m + \zeta'(\tau_3' d_1^{(m)}k_1^{(m)} + \tau_4' d_3^{(m)}k_3^{(m)})\right)e^{\imath \zeta k_3^{(m)}} +$$

$$\sum_{m=3}^{4}\sum_{n=1}^{\infty} A_{mn}^{\pm}\left((1-\zeta'^2)\tau_0'\lambda_{mn} + \zeta'(\tau_3' d_{1\pm}^{(mn)}k_{1\pm}^{mn} + \tau_4' d_{3\pm}^{(mn)}k_{3\pm}^{mn})\right)e^{\mp \imath n p x_1}e^{\imath \zeta k_{3\pm}^{(mn)}}, \quad (3.26)$$

$$\sum_{m=0}^{2} A_m\left((c_{13}+c_{11}\zeta'^2)d_1^{(m)}k_1^{(m)} + (c_{33}+c_{13}\zeta'^2)d_3^{(m)}k_3^{(m)} - 2c_{44}^R\zeta'\mu_m\right)e^{\imath \zeta k_3^{(m)}}$$

$$+ \sum_{m=1}^{2}\sum_{n=1}^{\infty} A_{mn}^{\pm}\left((c_{13}+c_{11}\zeta'^2)d_{1\pm}^{(mn)}k_{1\pm}^{(mn)} + (c_{33}+c_{13}\zeta'^2)d_{3\pm}^{(mn)}k_{3\pm}^{(mn)} - 2c_{44}^R\zeta'\lambda_{mn}\right)$$

$$\times e^{\mp \imath n p x_1}e^{\imath \zeta k_{3\pm}^{(mn)}} = \sum_{m=3}^{4} A_m\{\tau_0(c_{13}'+c_{11}'\zeta'^2)(d_1^{(m)}k_1^{(m)} + \tau_0(c_{33}'+c_{13}'\zeta'^2)d_3^{(m)}k_3^{(m)}$$

$$- 2\tau_0'\zeta'\mu_m\}e^{\imath \zeta k_3^{(m)}} + \sum_{m=3}^{4}\sum_{n=1}^{\infty} A_{mn}^{\pm} \times \{\tau_0(c_{13}'+c_{11}'\zeta'^2)d_{1\pm}^{(mn)}k_{1\pm}^{(mn)}$$

$$+ \tau_0(c_{33}'+c_{13}'\zeta'^2)d_{3\pm}^{(mn)}k_{3\pm}^{(mn)} - 2\tau_0'\zeta'\lambda_{mn}\}e^{\mp \imath n p x_1}e^{\imath \zeta k_{3\pm}^{(mn)}}, \quad (3.27)$$

where

$$\tau_0' = \tau_0 c_{44}'^R, \quad \mu_m = d_1^{(m)}k_3^{(m)} + d_3^{(m)}k_1^{(m)}, \quad \lambda_{mn} = d_{1\pm}^{(mn)}k_{3\pm}^{(mn)} + d_{3\pm}^{(mn)}k_{1\pm}^{(mn)}.$$

These equations will help to find out the amplitude ratios corresponding to the regularly and irregularly reflected and transmitted waves.

3.5 Solution of first order approximation

If we assume that slope and amplitude of the corrugated interface are small enough to neglect the higher powers of ζ, then

$$e^{\mp \imath \zeta k_3^{(0)}} = 1 \mp \imath \zeta k_3^{(0)}, \quad e^{\mp \imath \zeta k_3^{(1)}} = 1 \mp \imath \zeta k_3^{(1)}, \quad \text{etc.} \quad (3.28)$$

Using Eqs.(3.6) and (3.28) into Eqs.(3.24)-(3.27) and collecting terms independent of ζ and x_1, we get a system of simultaneous equations as

$$[a_{ij}]x = b, \quad i,j = 1,2,3,4 \tag{3.29}$$

where

$$[a_{ij}] = \begin{bmatrix} d_1^{(1)} & d_1^{(2)} & -d_1^{(3)} & -d_1^{(4)} \\ d_3^{(1)} & d_3^{(2)} & -d_3^{(3)} & -d_3^{(4)} \\ l_1 & l_2 & -l_3 & -l_4 \\ m_1 & m_2 & -m_3 & -m_4 \end{bmatrix}, \quad x = \begin{bmatrix} A_1/A_0 \\ A_2/A_0 \\ A_3/A_0 \\ A_4/A_0 \end{bmatrix}, \quad b = \begin{bmatrix} b_1 \\ b_2 \\ b_3 \\ b_4 \end{bmatrix}$$

$b_1 = -d_1^{(0)}, \quad b_2 = -d_3^{(0)}, \quad b_3 = -\{d_1^{(0)}k_3^{(0)} + d_3^{(0)}k_1^{(0)}\},$

$b_4 = -\{c_{13}d_1^{(0)}k_1^{(0)} + c_{33}d_3^{(0)}k_3^{(0)}\}, \quad l_1 = d_1^{(1)}k_3^{(1)} + d_3^{(1)}k_1^{(1)},$

$l_2 = d_1^{(2)}k_3^{(2)} + d_3^{(2)}k_1^{(2)}, \quad l_3 = \tau_0'(d_1^{(3)}k_3^{(3)} + d_3^{(3)}k_1^{(3)}), \quad l_4 = \tau_0'(d_1^{(4)}k_3^{(4)} + d_3^{(4)}k_1^{(4)}),$

$m_1 = c_{13}d_1^{(1)}k_1^{(1)} + c_{33}d_3^{(1)}k_3^{(1)}, \quad m_2 = c_{13}d_1^{(2)}k_1^{(2)} + c_{33}d_3^{(2)}k_3^{(2)},$

$m_3 = \tau_0(c_{13}'d_1^{(3)}k_1^{(3)} + c_{33}'d_3^{(3)}k_3^{(3)}), \quad m_4 = \tau_0(c_{13}'d_1^{(4)}k_1^{(4)} + c_{33}'d_3^{(4)}k_3^{(4)}).$

It may be noted that $d_1^{(0)} = \sin\alpha_0$ and $d_3^{(0)} = -\cos\alpha_0$ for the case of incident qP-wave, while $d_1^{(0)} = \cos\alpha_0$ and $d_3^{(0)} = \sin\alpha_0$ for the incident qSV-wave.

On solving Eq.(3.29), we get the amplitude ratios of the regularly reflected and transmitted qP and qSV-waves as

$$r^{pp} \text{ or } r^{svp} = \frac{|a_{ij}|_1}{|a_{ij}|}, \qquad r^{psv} \text{ or } r^{svsv} = \frac{|a_{ij}|_2}{|a_{ij}|}, \tag{3.30}$$

$$t^{pp} \text{ or } t^{svp} = \frac{|a_{ij}|_3}{|a_{ij}|}, \qquad t^{psv} \text{ or } t^{svsv} = \frac{|a_{ij}|_4}{|a_{ij}|}, \tag{3.31}$$

where r^{pp} and r^{psv} are the amplitude ratios of the regularly reflected waves due to incident qP-wave, while r^{svp} and r^{svsv} are the amplitude ratios of the regularly reflected waves due to incident qSV-wave. Similarly t^{pp} and t^{psv} are the amplitude ratios of the regularly transmitted waves due to incident P-waves, while t^{svp} and t^{svsv} are the amplitude ratios of the regularly transmitted waves due to incident qSV-wave.

The values of $|a_{ij}|_1$, $|a_{ij}|_2$, $|a_{ij}|_3$ and $|a_{ij}|_4$ are obtained by replacing first, second, third and fourth column of $|a_{ij}|$ with column matrix, b respectively.

Next, comparing coefficients of $e^{\pm \imath n p x_1}$ on both sides of these equations, we get

$$[a_{ij}^{\mp}]x^{\mp} = b^{\pm}, \quad i, j = 1, 2, 3, 4 \tag{3.32}$$

where

$$[a_{ij}^{\mp}]_n = \begin{bmatrix} d_{1\mp}^{(1n)} & d_{1\mp}^{(2n)} & -d_{1\mp}^{(3n)} & -d_{1\mp}^{(4n)} \\ d_{3\mp}^{(1n)} & d_{3\mp}^{(2n)} & -d_{3\mp}^{(3n)} & -d_{3\mp}^{(4n)} \\ l_1^{\mp} & l_2^{\mp} & -l_3^{\mp} & -l_4^{\mp} \\ m_1^{\mp} & m_2^{\mp} & -m_3^{\mp} & -m_4^{\mp} \end{bmatrix}, \quad x^{\mp} = \begin{bmatrix} A_{1n}^{\mp}/A_0 \\ A_{2n}^{\mp}/A_0 \\ A_{3n}^{\mp}/A_0 \\ A_{4n}^{\mp}/A_0 \end{bmatrix}, \quad b^{\pm} = \begin{bmatrix} b_1^{\pm} \\ b_2^{\pm} \\ b_3^{\pm} \\ b_4^{\pm} \end{bmatrix},$$

$$l_1^{\mp} = d_{1\mp}^{(1n)} k_{3\mp}^{(1n)} + d_{3\mp}^{(1n)} k_{1\mp}^{(1n)}, \quad l_2^{\mp} = d_{1\mp}^{(2n)} k_{3\mp}^{(2n)} + d_{3\mp}^{(2n)} k_{1\mp}^{(2n)},$$

$$l_3^{\mp} = \tau_0'(d_{1\mp}^{(3n)} k_{3\mp}^{(3n)} + d_{3\mp}^{(3n)} k_{1\mp}^{(3)}), \quad l_4^{\mp} = \tau_0'(d_{1\mp}^{(4n)} k_{3\mp}^{(4n)} + d_{3\mp}^{(4n)} k_{1\mp}^{(4n)}),$$

$$m_1^{\mp} = c_{13} d_{1\mp}^{(1n)} k_{1\mp}^{(1n)} + c_{33} d_{3\mp}^{(1n)} k_{3\mp}^{(1n)}, \quad m_2^{\mp} = c_{13} d_{1\mp}^{(2n)} k_{1\mp}^{(2n)} + c_{33} d_{3\mp}^{(2n)} k_{3\mp}^{(2)},$$

$$m_3^{\mp} = \tau_0(c_{13}' d_{1\mp}^{(3n)} k_{1\mp}^{(3n)} + c_{33}' d_{3\mp}^{(3n)} k_{3\mp}^{(3n)}), \quad m_4^{\mp} = \tau_0(c_{13}' d_{1\mp}^{(4n)} k_{1\mp}^{(4n)} + c_{33}' d_3^{(4n)} k_{3\mp}^{(4n)}),$$

$$b_1^{\pm} = \imath \zeta_{\pm n}[-d_1^{(0)} k_3^{(0)} - \frac{A_1}{A_0} d_1^{(1)} k_3^{(1)} - \frac{A_2}{A_0} d_1^{(2)} k_3^{(2)} + \frac{A_3}{A_0} d_1^{(3)} k_3^{(3)} + \frac{A_4}{A_0} d_1^{(4)} k_3^{(4)}],$$

$$b_2^{\pm} = \imath \zeta_{\pm n}[-d_3^{(0)} k_3^{(0)} - \frac{A_1}{A_0} d_3^{(1)} k_3^{(1)} - \frac{A_2}{A_0} d_3^{(2)} k_3^{(2)} + \frac{A_3}{A_0} d_3^{(3)} k_3^{(3)} + \frac{A_4}{A_0} d_3^{(4)} k_3^{(4)}],$$

$$b_3^{\pm} = \imath \zeta_{\pm n}[-g_0^{\pm} - \frac{A_1}{A_0} g_1^{\pm} - \frac{A_2}{A_0} g_2^{\pm} + \frac{A_3}{A_0} g_3^{\pm} + \frac{A_4}{A_0} g_4^{\pm}],$$

$$b_4^{\pm} = \imath \zeta_{\pm n}[-h_0^{\pm} - \frac{A_1}{A_0} h_1^{\pm} - \frac{A_2}{A_0} h_2^{\pm} + \frac{A_3}{A_0} h_3^{\pm} + \frac{A_4}{A_0} h_4^{\pm}],$$

$$g_0^{\pm} = d_1^{(0)} k_3^{(0)} k_3^{(0)} + d_3^{(0)} k_1^{(0)} k_3^{(0)} \pm np(\tau_3 d_1^{(0)} k_1^{(0)} + \tau_4 d_3^{(0)} k_3^{(0)}),$$

$$g_1^{\pm} = d_1^{(1)} k_3^{(1)} k_3^{(1)} + d_3^{(1)} k_1^{(1)} k_3^{(1)} \pm np(\tau_3 d_1^{(1)} k_1^{(1)} + \tau_4 d_3^{(1)} k_3^{(1)}),$$

$$g_2^{\pm} = d_1^{(2)} k_3^{(2)} k_3^{(2)} + d_3^{(2)} k_1^{(2)} k_3^{(2)} \pm np(\tau_3 d_1^{(2)} k_1^{(2)} + \tau_4 d_3^{(2)} k_3^{(2)}),$$

$$g_3^{\pm} = \tau_0'(d_1^{(3)} k_3^{(3)} k_3^{(3)} + d_3^{(3)} k_1^{(3)} k_3^{(3)}) \pm np(\tau_3' d_1^{(3)} k_1^{(3)} + \tau_4' d_3^{(3)} k_3^{(3)}),$$

$$g_4^{\pm} = \tau_0'(d_1^{(4)} k_3^{(4)} k_3^{(4)} + d_3^{(4)} k_1^{(4)} k_3^{(4)}) \pm np(\tau_3' d_1^{(4)} k_1^{(4)} + \tau_4' d_3^{(4)} k_3^{(4)}),$$

$$h_0^{\pm} = c_{13} d_1^{(0)} k_1^{(0)} k_3^{(0)} + c_{33} d_3^{(0)} k_3^{(0)} k_3^{(0)} \mp 2 c_{44}^R np(d_1^{(0)} k_3^{(0)} + d_3^{(0)} k_1^{(0)}),$$

$$h_1^{\pm} = c_{13}d_1^{(1)}k_1^{(1)}k_3^{(1)} + c_{33}d_3^{(1)}k_3^{(1)}k_3^{(1)} \mp 2c_{44}^R np(d_1^{(1)}k_3^{(1)} + d_3^{(1)}k_1^{(1)}),$$

$$h_2^{\pm} = c_{13}d_1^{(2)}k_1^{(2)}k_3^{(2)} + c_{33}d_3^{(2)}k_3^{(2)}k_3^{(2)} \mp 2c_{44}np(d_1^{(2)}k_3^{(2)} + d_3^{(2)}k_1^{(2)}),$$

$$h_3^{\pm} = \tau_0\{c'_{13}d_1^{(3)}k_1^{(3)}k_3^{(3)} + c'_{33}d_3^{(3)}k_3^{(3)}k_3^{(3)} \mp 2c_{44}'^R np(d_1^{(3)}k_3^{(3)} + d_3^{(3)}k_1^{(3)})\},$$

$$h_4^{\pm} = \tau_0\{c'_{13}d_1^{(4)}k_1^{(4)}k_3^{(4)} + c'_{33}d_3^{(4)}k_3^{(4)}k_3^{(4)} \mp 2c_{44}'^R np(d_1^{(4)}k_3^{(4)} + d_3^{(4)}k_1^{(4)})\}.$$

On solving Eq.(3.32), we get the amplitude ratios corresponding to the irregularly reflected and transmitted qP and qSV-waves as

$$r_n^{pp\mp} \text{ or } r_n^{svp\mp} = \frac{|a_{ij}^{\mp}|_{1n}}{|a_{ij}^{\mp}|_n}, \qquad r_n^{psv\mp} \text{ or } r_n^{svsv\mp} = \frac{|a_{ij}^{\mp}|_{2n}}{|a_{ij}^{\mp}|_n},$$

$$t_n^{pp\mp} \text{ or } t_n^{svp\mp} = \frac{|a_{ij}^{\mp}|_{3n}}{|a_{ij}^{\mp}|_n}, \qquad t_n^{psv\mp} \text{ or } t_n^{svsv\mp} = \frac{|a_{ij}^{\mp}|_{4n}}{|a_{ij}^{\mp}|_n}, \qquad (3.33)$$

and the values of $|a_{ij}^{\mp}|_{1n}$, $|a_{ij}^{\mp}|_{2n}$, $|a_{ij}^{\mp}|_{3n}$ and $|a_{ij}^{\mp}|_{4n}$ are obtained by replacing first, second, third and fourth column of $|a_{ij}^{\mp}|_n$ with column matrix, $b^{\pm}$ respectively. We come to know that the amplitude ratios corresponding to the irregularly reflected and transmitted qP and qSV-waves are functions of characteristic time of rubber relaxation, director rotation times, the elastic constants, angle of incidence, corrugation and frequency parameters.

3.6 Energy partition

The energy due to the incident qP and qSV-waves are distributed to regularly and irregularly reflected and transmitted waves. The rate of transmission of energy per unit area is given by Achenbach (1976)

$$\wp^* = <\tau_{3i} \cdot \dot{u}_i> . \qquad (3.34)$$

The energy of the incident wave, qP/qSV-wave is given by

$$E = e_0\omega A_0^2 \exp\left[2\imath\{\omega t + k_1^{(0)}x_1 + k_3^{(0)}x_3\}\right], \qquad (3.35)$$

where

$$e_0 = (1 + \imath\omega\tau_R)\{(c_{13}d_1^{(0)}k_1^{(0)} + c_{33}d_3^{(0)}k_3^{(0)})d_3^{(0)} + c_{44}^R(d_1^{(0)}k_3^{(0)} + d_3^{(0)}k_1^{(0)})d_1^{(0)}\}.$$

Similarly, the energy due to reflected and transmitted qP and qSV-waves are given by

$$E_m = e_m\omega A_m^2 \exp\{2\imath(\omega t + k_1^{(m)}x_1 + k_3^{(m)}x_3)\}+$$

$$\sum_{n=1}^{\infty} e_{mn}^{\pm}\omega(A_{mn}^{\pm})^2 \exp\{2\imath(\omega t + k_{1\pm}^{(mn)}x_1 + k_{3\pm}^{(mn)}x_3)\}, \quad m = 1,2,3,4. \tag{3.36}$$

The expressions of e_m and $e_{mn}^{\pm}$ are given by

(for m=1, 2)

$$e_m = (1 + \imath\omega\tau_R)\{(c_{13}d_1^{(m)}k_1^{(m)} + c_{33}d_3^{(m)}k_3^{(m)})d_3^{(m)} + c_{44}^R(d_1^{(m)}k_3^{(m)} + d_3^{(m)}k_1^{(m)})d_1^{(m)}\},$$

$$e_{mn}^{\pm} = (1 + \imath\omega\tau_R)\{(c_{13}d_{1\pm}^{(mn)}k_{1\pm}^{(mn)} + c_{33}d_{3\pm}^{(mn)}k_{3\pm}^{(mn)})d_{3\pm}^{(mn)} + c_{44}^R(d_{1\pm}^{(mn)}k_{3\pm}^{(mn)}$$

$$+ d_{3\pm}^{(mn)}k_{1\pm}^{(mn)})d_{1\pm}^{(mn)}\},$$

(for m=3, 4)

$$e_m = (1 + \imath\omega\tau_R')\{(c_{13}'d_1^{(m)}k_1^{(m)} + c_{33}'d_3^{(m)}k_3^{(m)})d_3^{(m)} + c_{44}'^R(d_1^{(m)}k_3^{(m)} + d_3^{(m)}k_1^{(m)})d_1^{(m)}\},$$

$$e_{mn}^{\pm} = (1 + \imath\omega\tau_R')\{(c_{13}'d_{1\pm}^{(mn)}k_{1\pm}^{(mn)} + c_{33}'d_{3\pm}^{(mn)}k_{3\pm}^{(mn)})d_{3\pm}^{(mn)} + c_{44}'^R(d_{1\pm}^{(mn)}k_{3\pm}^{(mn)}$$

$$+ d_{3\pm}^{(mn)}k_{1\pm}^{(mn)})d_{1\pm}^{(mn)}\}.$$

Energy ratios are defined as the ratios of the energy corresponding to the reflected and transmitted waves to that of the incident wave. These ratios of the regularly and irregularly reflected and transmitted waves for incident qP/qSV-wave are given as

$$E_m^{pp} \text{ or } E_m^{svp} = \Big|\frac{e_m}{e_0}\Big|\Big|\frac{A_m}{A_0}\Big|^2, \tag{3.37}$$

$$E_{mn}^{pp\pm} \text{ or } E_{mn}^{svp\pm} = \Big|\frac{e_{mn}^{\pm}}{e_0}\Big|\Big|\frac{A_{mn}^{\pm}}{A_0}\Big|^2, \tag{3.38}$$

where (E_1^{pp}, E_2^{psv}) and $(E_{1n}^{pp\pm}, E_{2n}^{psv\pm})$ are the energy ratios corresponding to the regularly and irregularly reflected waves respectively due to incident qP-wave, while (E_1^{svp}, E_2^{svsv}) and $(E_{1n}^{svp\pm}, E_{2n}^{svsv\pm})$ correspond to the energy ratios for regularly and ir-

regularly reflected waves respectively due to incident qSV-wave. Similarly, (E_3^{pp}, E_4^{psv}) and $(E_{3n}^{pp\pm}, E_{4n}^{psv\pm})$ are energy ratios of the transmitted waves for incident qP-wave and (E_3^{svp}, E_4^{svsv}) and $(E_{3n}^{svp\pm}, E_{4n}^{svsv\pm})$ correspond to the energy ratios of transmitted waves for incident qSV-wave. These energy ratios depend on elastic constants, coupling constants, characteristic time of rubber relaxation, director rotation times, angle of incidence, corrugation and frequency parameters.

3.7 Special case: $\zeta = d\cos px_1$

If the corrugated interface is represented by only $\zeta(x_1) = d\cos px_1$ with d as the amplitude of corrugation, then the coefficient of Fourier series are given by

$$\zeta_{\pm n} = \begin{cases} 0 & \text{if } n \neq 1, \\ \dfrac{d}{2} & \text{if } n = 1. \end{cases} \tag{3.39}$$

Using these values into Eq.(3.33), the amplitude ratios of the reflected and transmitted waves for the first order approximation of corrugation are given by

$$r_1^{pp\mp} \text{ or } r_1^{svp\mp} = \frac{|a_{ij}^{\mp}|_{11}}{|a_{ij}^{\mp}|_1}, \qquad r_1^{psv\mp} \text{ or } r_1^{svsv\mp} = \frac{|a_{ij}^{\mp}|_{21}}{|a_{ij}^{\mp}|_1},$$

$$t_1^{pp\mp} \text{ or } t_1^{svp\mp} = \frac{|a_{ij}^{\mp}|_{31}}{|a_{ij}^{\mp}|_1}, \qquad t_1^{psv\mp} \text{ or } t_1^{svsv\mp} = \frac{|a_{ij}^{\mp}|_{41}}{|a_{ij}^{\mp}|_1}. \tag{3.40}$$

The energy ratios, in this case, are obtained from Eq.(3.38) by putting $n = 1$. The amplitude and energy ratios of the regularly and irregularly reflected and transmitted waves obtained in this section will be computed for a particular model.

3.8 Particular case

(a) When the two nematic elastomers, M and M' reduce to isotropic half-spaces, we have

$$D_1 = D_2 = 0, \quad c_{11} = c_{33} = \lambda + 2\mu, \quad c_{13} = \lambda, \quad c_{44} = c_{44}^R = \mu, \quad C_5 = \frac{1}{2}\mu,$$

$$D_1' = D_2' = 0, \quad c_{11}' = c_{33}' = \lambda' + 2\mu', \quad c_{13}' = \lambda', \quad c_{44}' = c_{44}'^R = \mu', \quad C_5' = \frac{1}{2}\mu'.$$

In this case, the phase velocity corresponding to the longitudinal and transverse waves are given by $c_0^2 = c_1^2 = \frac{\lambda + 2\mu}{\rho}$, $c_2^2 = \frac{\mu}{\rho}$, $c_3^2 = \frac{\lambda' + 2\mu'}{\rho'}$ and $c_4^2 = \frac{\mu'}{\rho'}$. This is the result of classical elasticity (Achenbach, 1976).

The amplitude ratios of the reflected and transmitted waves are given by Eqs. (3.30), (3.31) and (3.33) with the following modified values

$$m_1 = \lambda d_1^{(1)} k_1^{(1)} + (\lambda + 2\mu) d_3^{(1)} k_3^{(1)}, \quad m_2 = \lambda d_1^{(2)} k_1^{(2)} + (\lambda + 2\mu) d_3^{(2)} k_3^{(2)},$$

$$m_3 = \tau_0 \{\lambda' d_1^{(3)} k_1^{(3)} + (\lambda' + 2\mu') d_3^{(3)} k_3^{(3)}\}, \quad m_4 = \tau_0 \{\lambda' d_1^{(4)} k_1^{(4)} + (\lambda' + 2\mu') d_3^{(4)} k_3^{(4)}\},$$

$$b_4 = \lambda d_1^{(0)} k_1^{(0)} + (\lambda + 2\mu) d_3^{(0)} k_3^{(0)}, \quad m_1^{\mp} = \lambda d_{1\mp}^{(1n)} k_{1\mp}^{(1n)} + (\lambda + 2\mu) d_{3\mp}^{(1n)} k_{3\mp}^{(1n)},$$

$$m_2^{\mp} = \lambda d_{1\mp}^{(2n)} k_{1\mp}^{(2n)} + (\lambda + 2\mu) d_{3\mp}^{(2n)} k_{3\mp}^{(2)}, \quad m_3^{\mp} = \tau_0 \{\lambda' d_{1\mp}^{(3n)} k_{1\mp}^{(3n)} + (\lambda' + 2\mu') d_{3\mp}^{(3n)} k_{3\mp}^{(3n)}\},$$

$$m_4^{\mp} = \tau_0 \{\lambda' d_{1\mp}^{(4n)} k_{1\mp}^{(4n)} + (\lambda' + 2\mu') d_3^{(4n)} k_{3\mp}^{(4n)}\}$$

$$g_0^{\pm} = d_1^{(0)} k_3^{(0)} k_3^{(0)} + d_3^{(0)} k_1^{(0)} k_3^{(0)} \mp 2\mu np (d_1^{(0)} k_1^{(0)} - d_3^{(0)} k_3^{(0)}),$$

$$g_1^{\pm} = d_1^{(1)} k_3^{(1)} k_3^{(1)} + d_3^{(1)} k_1^{(1)} k_3^{(1)} \mp 2\mu np (d_1^{(1)} k_1^{(1)} - d_3^{(1)} k_3^{(1)}),$$

$$g_2^{\pm} = d_1^{(2)} k_3^{(2)} k_3^{(2)} + d_3^{(2)} k_1^{(2)} k_3^{(2)} \mp 2\mu np (d_1^{(2)} k_1^{(2)} - d_3^{(2)} k_3^{(2)}),$$

$$g_3^{\pm} = \tau_0' (d_1^{(3)} k_3^{(3)} k_3^{(3)} + d_3^{(3)} k_1^{(3)} k_3^{(3)}) \mp 2\mu' np (d_1^{(3)} k_1^{(3)} - d_3^{(3)} k_3^{(3)}),$$

$$g_4^{\pm} = \tau_0' (d_1^{(4)} k_3^{(4)} k_3^{(4)} + d_3^{(4)} k_1^{(4)} k_3^{(4)}) \mp 2\mu' np (d_1^{(4)} k_1^{(4)} - d_3^{(4)} k_3^{(4)}),$$

$$h_0^{\pm} = \lambda d_1^{(0)} k_1^{(0)} k_3^{(0)} + (\lambda + 2\mu) d_3^{(0)} k_3^{(0)} k_3^{(0)} \mp 2\mu np (d_1^{(0)} k_3^{(0)} + d_3^{(0)} k_1^{(0)}),$$

$$h_1^{\pm} = \lambda d_1^{(1)} k_1^{(1)} k_3^{(1)} + (\lambda + 2\mu) d_3^{(1)} k_3^{(1)} k_3^{(1)} \mp 2\mu np (d_1^{(1)} k_3^{(1)} + d_3^{(1)} k_1^{(1)}),$$

$$h_2^{\pm} = \lambda d_1^{(2)} k_1^{(2)} k_3^{(2)} + (\lambda + 2\mu) d_3^{(2)} k_3^{(2)} k_3^{(2)} \mp 2\mu np (d_1^{(2)} k_3^{(2)} + d_3^{(2)} k_1^{(2)}),$$

$$h_3^{\pm} = \tau_0 \{\lambda' d_1^{(3)} k_1^{(3)} k_3^{(3)} + (\lambda' + 2\mu') d_3^{(3)} k_3^{(3)} k_3^{(3)} \mp 2\mu' np (d_1^{(3)} k_3^{(3)} + d_3^{(3)} k_1^{(3)})\},$$

3.9   Numerical results and discussion

We will compute the angles of reflected and transmitted waves by introducing an apparent velocity, c_a so that $\bar{c} = \frac{c_a}{\beta} = \frac{c}{p_1 \beta}$, where $\bar{c}$ is non-dimensional velocity. Equation (3.18) can be written as

$$\bar{c}^4 - (\bar{B} + \bar{E})\bar{c}^2 + (\bar{B}\bar{E} - \bar{D}^2) = 0, \qquad (3.41)$$

where

$$\bar{B} = \frac{B}{p_1^2 c_{44}}, \quad \bar{E} = \frac{E}{p_1^2 c_{44}}, \quad \bar{D} = \frac{D}{p_1^2 c_{44}}, \quad \beta = \sqrt{\frac{c_{44}}{\rho}}, \quad \bar{c}_{ij} = \frac{c_{ij}}{c_{44}}.$$

There are two roots of $\bar{c}^2$ corresponding to qP and qSV-waves for a given $p = p_3/p_1$, and for a given value of $\bar{c}$, there are two roots of p corresponding to the angles of reflected qP and qSV-waves. Substituting the values of $\bar{B}, \bar{E}$, and $\bar{D}$ into Eq.(3.41), we get

$$t_0 p^4 + t_1 p^2 + t_2 = 0, \qquad (3.42)$$

where

$$t_0 = (1 + \imath\omega\tau_R)^2 \bar{c}_{33}\bar{c}_{44}^R, \quad t_1 = (1 + \imath\omega\tau_R)\{(\bar{c}_{11}\bar{c}_{33} - \bar{c}_{13}^2 - 2\bar{c}_{13}\bar{c}_{44}^R)(1 + \imath\omega\tau_R)$$

$$- (\bar{c}_{33} + \bar{c}_{44}^R)\bar{c}^2\}, \quad t_2 = \bar{c}^4 + (1 + \imath\omega\tau_R)\{(\bar{c}_{11}\bar{c}_{44}^R(1 + \imath\omega\tau_R) - (\bar{c}_{11} + \bar{c}_{44}^R)\bar{c}^2\}.$$

Transforming this equation with $q = \dfrac{1}{p} = \dfrac{p_1}{p_3}$, we have

$$t_2 q^4 + t_1 q^2 + t_0 = 0. \qquad (3.43)$$

For a given angle of incidence, there are two positive roots of q. The larger root say $\alpha_1 = \tan^{-1}(q_1)$ corresponds to reflected qP-wave, while the smaller root, $\alpha_2 = \tan^{-1}(q_2)$ corresponds to reflected qSV-waves. Similarly, we can set up for the transmitted qP and qSV-waves and obtained $\alpha_3 = \tan^{-1}(q_3)$ for qP-wave and $\alpha_4 = \tan^{-1}(q_4)$ for qSV-wave.

For the numerical computation, the following relevant values are taken (Singh, 2015):

(for half-space, M)

$$C_1 = 1.42 \times 10^5 N/m^2, \quad C_2 = 2.25 \times 10^5 N/m^2, \quad C_3 = 4.88 \times 10^5 N/m^2,$$

$$C_4 = 2.15 \times 10^5 N/m^2, \quad C_5 = 1.06 \times 10^5 N/m^2, \quad D_1 = 0.12, \quad D_2 = 0.05,$$

$$\rho = 1.66 \times 10^3 Kg/m^3, \quad \tau_1 = 0.02, \quad \tau_2 = 0.05, \quad \tau_R = 0.000002$$

(for half-space, M')

$$C_1' = 3.52 \times 10^5 N/m^2, \quad C_2' = 2.28 \times 10^5 N/m^2, \quad C_3' = 1.65 \times 10^5 N/m^2,$$

$$C_4' = 1.60 \times 10^5 N/m^2, \quad C_5' = 4.34 \times 10^5 N/m^2, \quad D_1' = 0.15, \quad D_2' = 0.17,$$

$$\rho' = 1.26 \times 10^3 Kg/m^3, \quad \tau_1' = 0.04, \quad \tau_2' = 0.06, \quad \tau_R' = 0.000003$$

with $pd = 0.000001$ and $\omega/pc_0 = 80$ are taken whenever not mentioned.
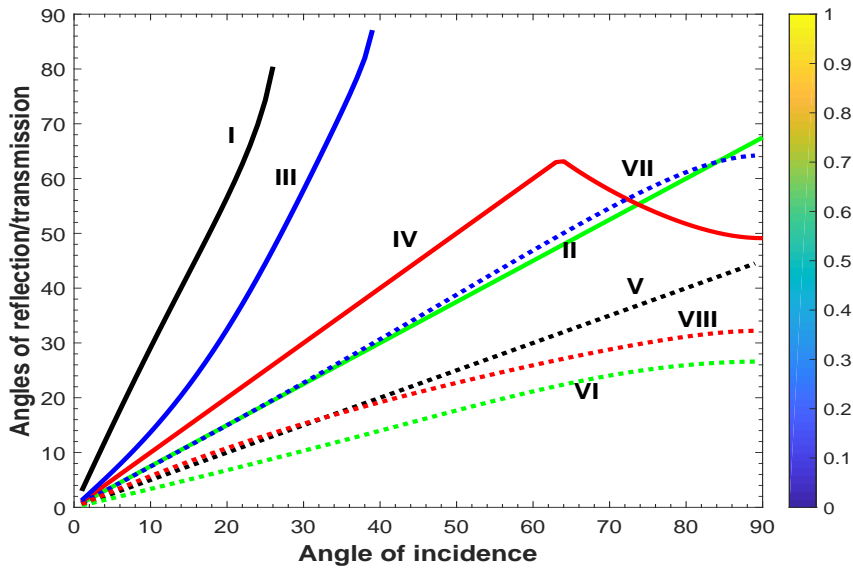
Figure 3.2: Variation of angles of reflection/transmission with angle of incidence. (Curves I-IV for incident qSV-wave and Curves V-VIII for incident qP-wave).

It is Figure 3.2 which shows the increase of the angles of reflected and transmitted qP and qSV-waves with the increase of angle of incidence α_0 except the angle of transmitted qSV-wave for the incident qSV-wave. In this figure, Curves I-IV correspond for the incident qSV-wave and Curves V-VIII correspond for the incident

qP-wave. Only Curve II is magnified by multiplying with 0.75. Furthermore, we have seen that there are critical angles for the reflected and transmitted qP-waves at $\alpha_1 = 26^0$ and $\alpha_3 = 39^0$ respectively, in the case of incident qSV-wave. It may be noted that Figures 3.3-3.12 correspond for the incident qP-waves, while Figures 3.13-3.22 correspond for the incident qSV-waves.

3.9.1   For the incident qP-wave

In Figure 3.3, r^{pp} corresponding to regularly reflected qP-wave starts from certain value which increases with the increase of α_0. In the same figure, r^{psv} and t^{psv} corresponding to regularly reflected and transmitted qSV-wave are parabolic in the region $0 \leq \theta_0 \leq 90^0$, while t^{pp} corresponding to regularly transmitted qP-wave starts from a certain value and then decreases with the increase of α_0 touching zero at grazing angle of incidence.
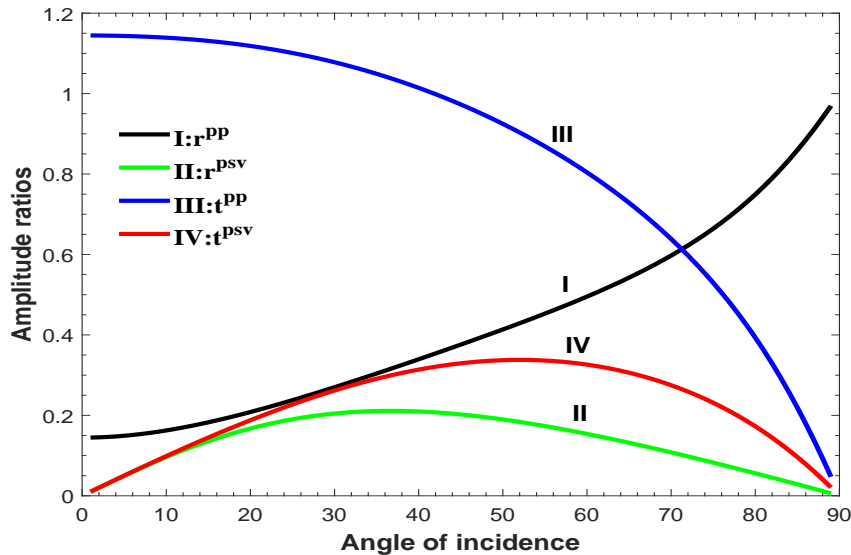
Figure 3.3: Variation of amplitude ratios for regular waves with α_0.

In Figures 3.4 and 3.5, the amplitude ratios r_1^{pp+} and r_1^{pp-} corresponding to irregularly reflected qP-waves increase from certain value which then decrease to zero at $\alpha_0 = 85^0$ and $\alpha_0 = 79^0$ respectively and thereafter they increases with the increase of

α_0. While r_1^{psv+} and r_1^{psv-} corresponding to irregularly reflected qSV-wave increase to the maximum value at $\alpha_0 = 23^0$ and $\alpha_0 = 24^0$ respectively and then they decrease to the minimum value at the grazing angle of incidence. The amplitude ratios corresponding to irregularly transmitted qP-wave, t_1^{pp+} and t_1^{pp-} start from a certain value which decrease with the increase of α_0 touching zero at $\alpha_0 = 49^0$ and $\alpha_0 = 44^0$ res-

Figure 3.4: Variation of amplitude ratios for irregular waves at α_{11}^+ with α_0.
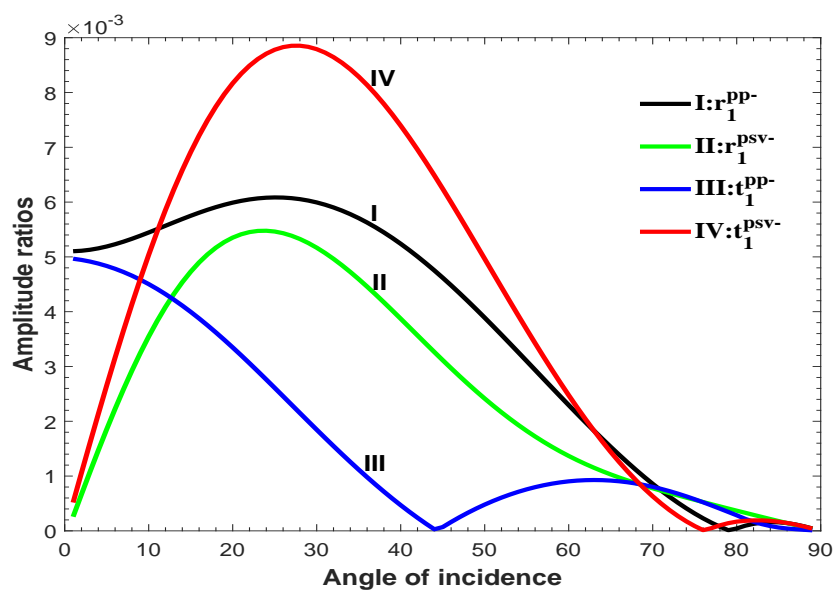
Figure 3.5: Variation of amplitude ratios for irregular waves at α_{11}^- with α_0.

pectively and then they make a parabolic region. Amplitude ratios t_1^{psv+} and t_1^{psv-} corresponding to irregularly transmitted qSV-wave increase and decrease with the increase α_0 thereby making parabolic regions at $81^0 \leq \theta_0 \leq 90^0$ and $76^0 \leq \theta_0 \leq 90^0$ respectively.
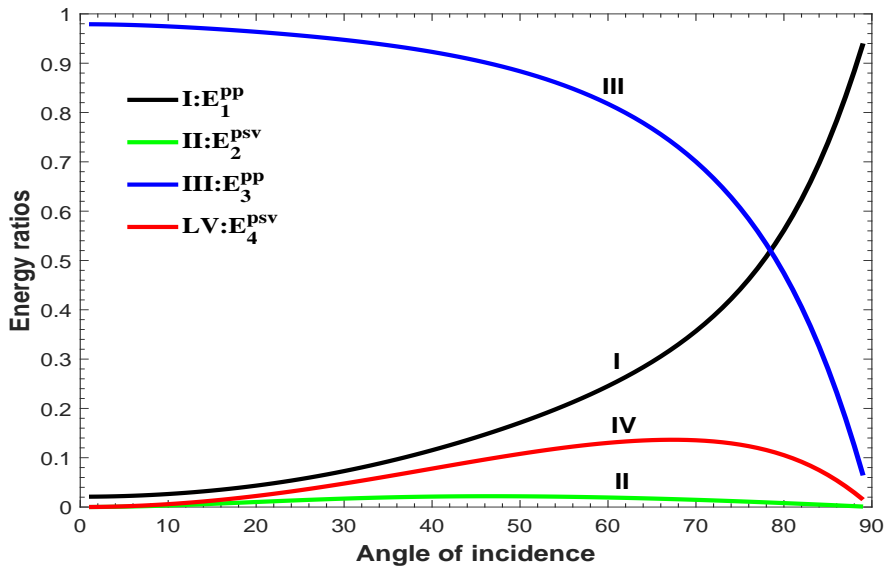
Figure 3.6: Variation of energy ratios for regular waves with α_0.
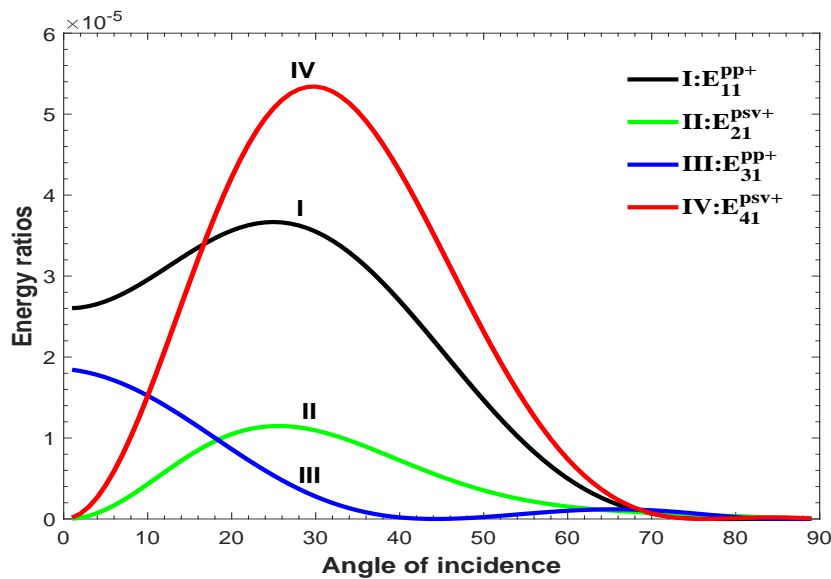
Figure 3.7: Variation of energy ratio for irregular waves at α_{11}^+ with α_0.

In Figure 3.6, energy ratios E_1^{pp} and E_3^{pp} corresponding to regularly reflected and transmitted qP-waves increase and decrease respectively with the increase of α_0. In the same figure, E_2^{psv} corresponding to regularly reflected qSV-wave shows a very small rate of increase and decrease with the increase of α_0 and E_4^{psv} corresponding to regularly transmitted qSV-wave increases and decreases with the minimum values at normal and grazing angle of incidence.

The energy ratios $(E_{11}^{pp+}, E_{11}^{pp-})$ in Figures 3.7 and 3.8 corresponding to irregularly reflected qP-waves start from a certain point which increase up to some extents and then decrease with the increase of α_0 touching zero at $\alpha_0 = 75^0$ and $\alpha_0 = 79^0$ respectively. In the same figures, $(E_{21}^{psv+}, E_{21}^{psv-})$ corresponding to irregularly reflected qSV-waves increase to maximum values at $\alpha_0 = 25^0$ which then decrease to the minimum value with the increase of α_0.
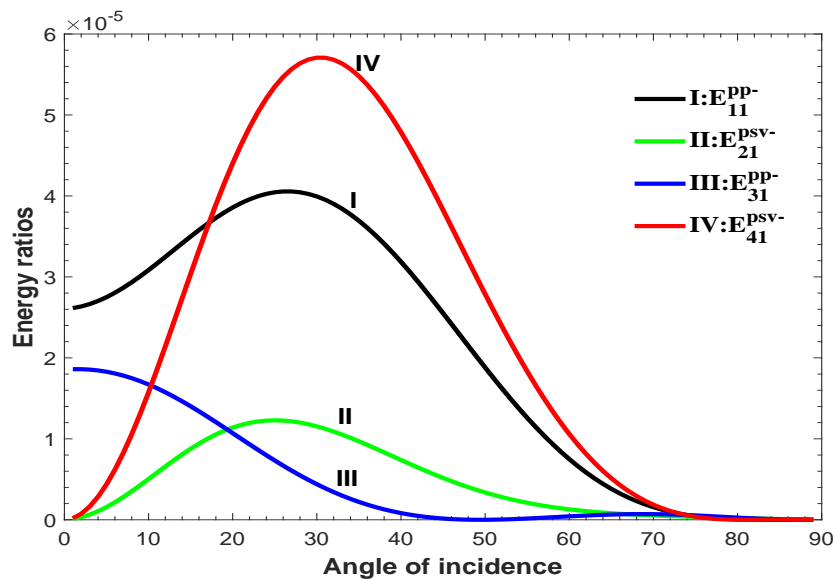
Figure 3.8: Variation of energy ratio for irregular waves at α_{11}^- with α_0.

The energy ratios $(E_{31}^{pp+}, E_{31}^{pp-})$ corresponding to irregularly transmitted qP-waves start from a certain point which decrease to the minimum value at $\alpha_0 = 42^0$ and $\alpha_0 = 47^0$ respectively, while $(E_{41}^{psv+}, E_{41}^{psv-})$ corresponding to irregularly transmitted qSV-waves make parabolic regions at $0^0 \leq \theta_0 \leq 73^0$ and $0^0 \leq \theta_0 \leq 75^0$ respectively.
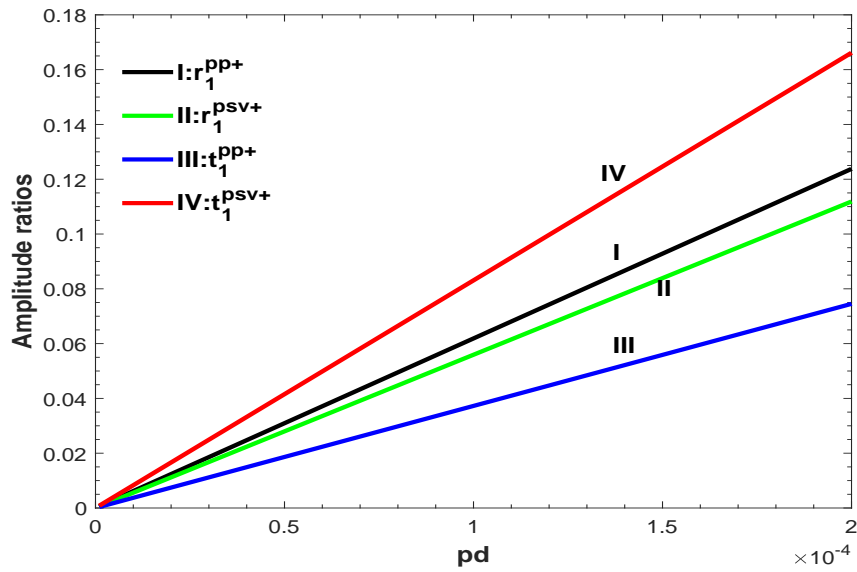
Figure 3.9: Variation of amplitude ratios of irregular waves at α_{11}^+ with corrugation parameter (pd).

Figures 3.9-3.12 show the variation of amplitude and energy ratios corresponding to irregularly reflected and transmitted waves with the corrugation parameter (pd).
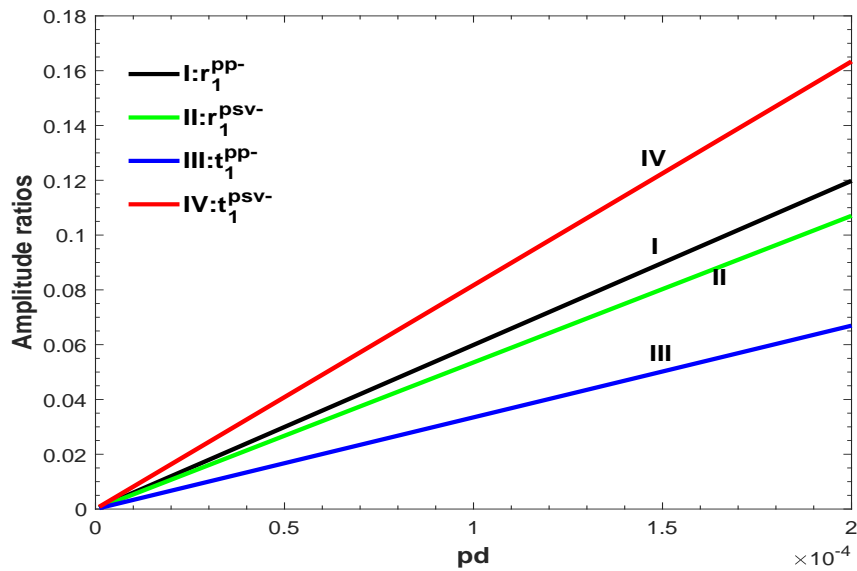
Figure 3.10: Variation of amplitude ratios of irregular waves at α_{11}^- with corrugation parameter (pd).

All the amplitude ratios, r_1^{pp+}, r_1^{pp-}, r_1^{psv+}, r_1^{psv-}, t_1^{pp+}, t_1^{pp-}, t_1^{psv+} and t_1^{psv-} in Figures 3.9 and 3.10 are linearly increasing with the increase of corrugation parameter but at different rates.
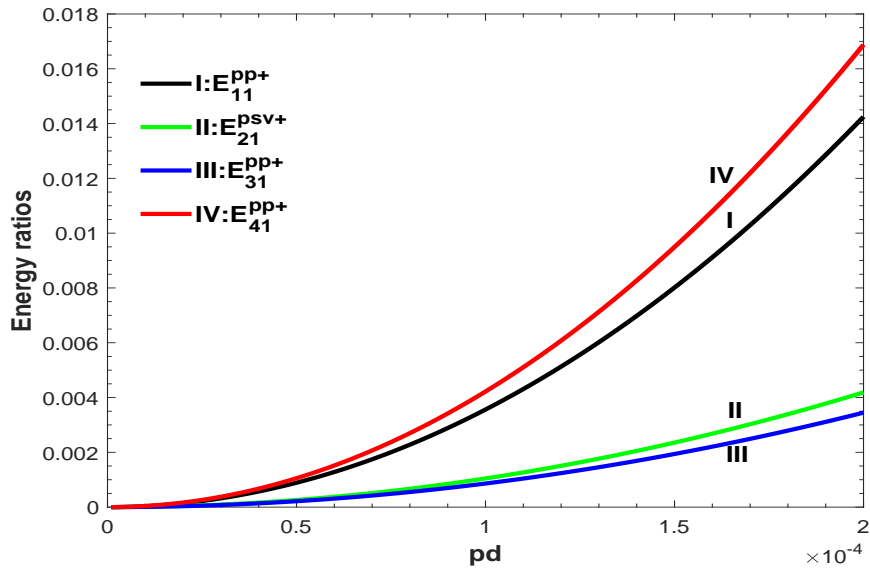
Figure 3.11: Variation of energy ratios of irregular waves at α_{11}^+ with corrugation parameter (pd).
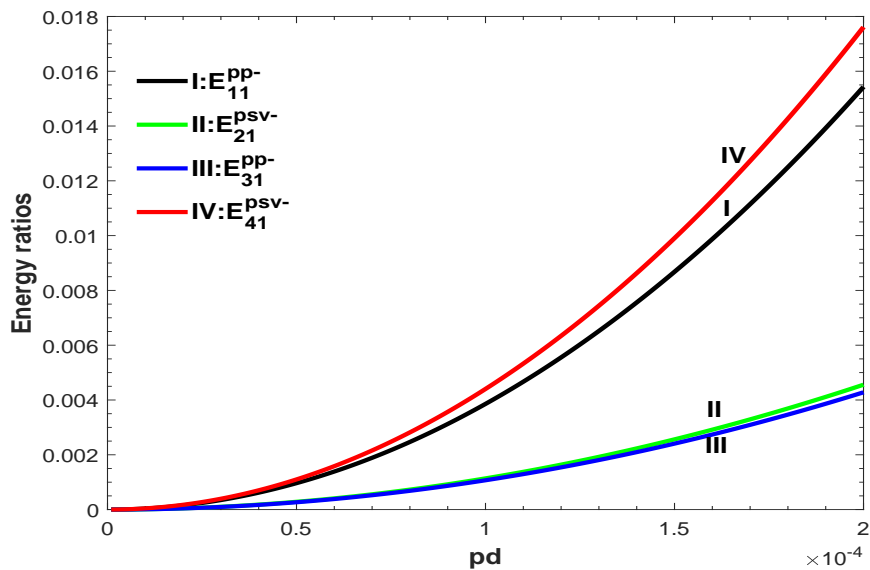
Figure 3.12: Variation of energy ratios at α_{11}^- with corrugation parameter (pd).

In Figures 3.11 and 3.12, we have noted that E_{11}^{pp+}, E_{11}^{pp-}, E_{21}^{psv+}, E_{21}^{psv-}, E_{31}^{pp+}, E_{31}^{pp-}, E_{41}^{psv+} and E_{41}^{psv-} increase with the increase of pd, but the modes are non-linear. Thus, the amplitude and energy ratios corresponding to irregular waves depend on the corrugation parameters.

3.9.2   For the incident qSV-wave

In Figure 3.13, the amplitude ratios r^{svp}, t^{svp} and t^{svsv} corresponding to regular waves increase with the increase of α_0, while r^{svsv} corresponding to regularly reflected qSV-wave is decreasing at very small rate with the increase of angle of incidence.
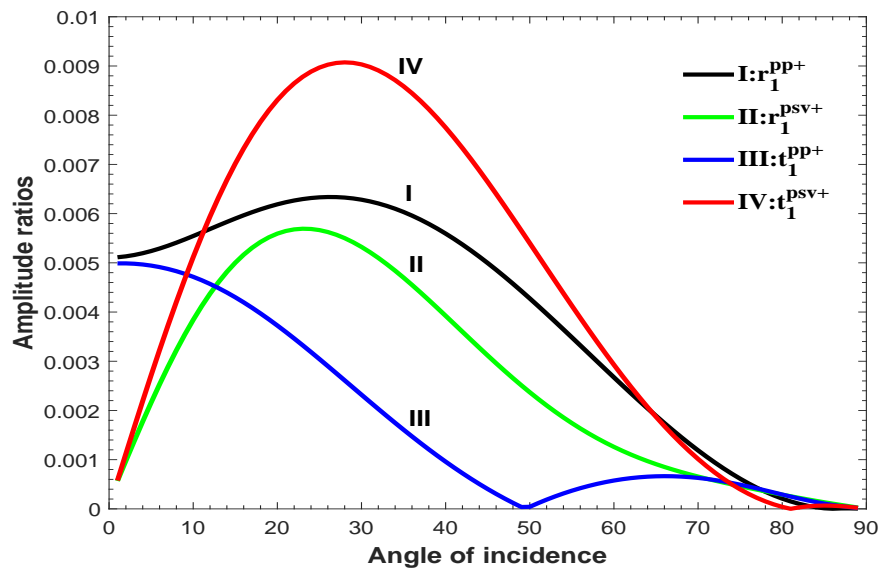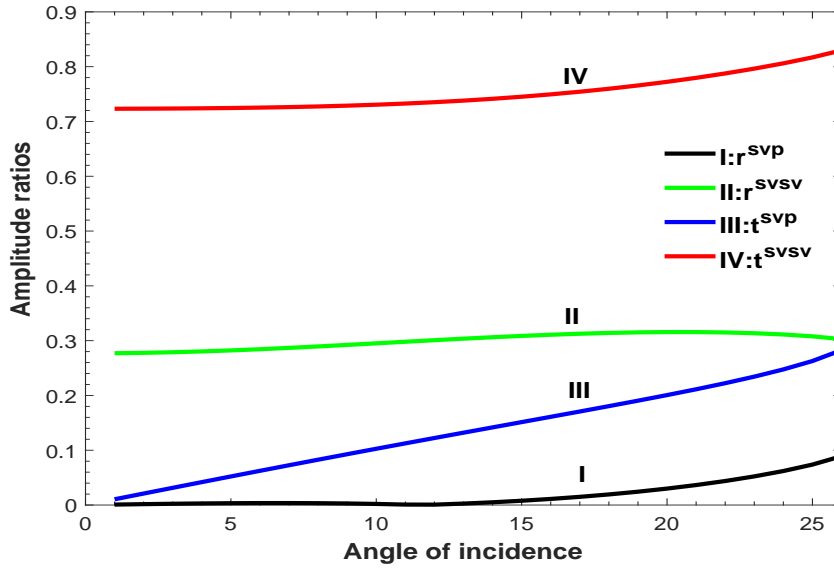

Figure 3.13: Variation of amplitude ratios of regular waves with α_0.
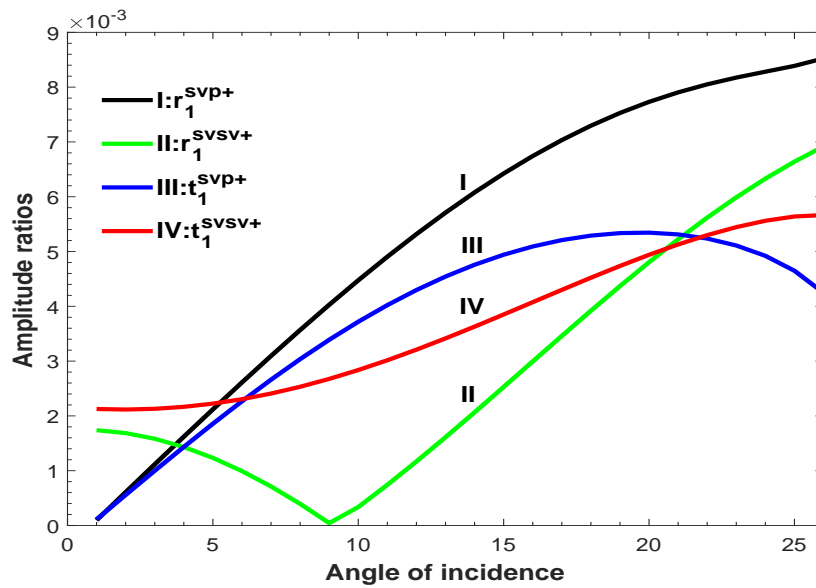
Figure 3.14: Variation of amplitude ratios of irregular waves at α_{11}^{+} with α_0.

The amplitude ratios r_1^{svp+}, t_1^{svp+} and t_1^{svsv+} in Figure 3.14 increase with the increase

of α_0, while r_1^{svsv+} corresponding to the irregularly reflected qSV-wave decreases to zero at $\alpha_0 = 9^0$ which then increases with the increase of α_0.
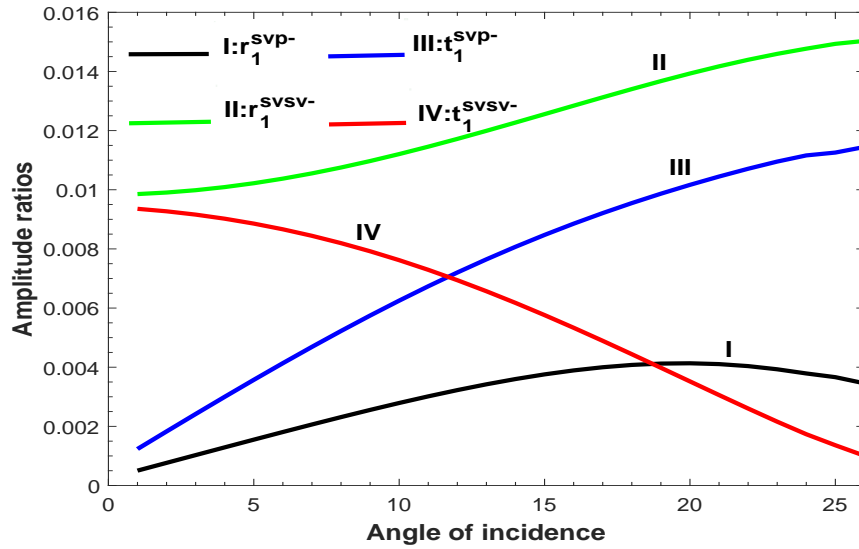
Figure 3.15: Variation of amplitude ratios of irregular waves at α_{11}^- with α_0.

The amplitude ratios r_1^{svsv-} and t_1^{svp-} in Figure 3.15 increase, while t_1^{svsv-} decreases with the increase of α_0. But the amplitude ratio r_1^{svp-} corresponding to irregularly reflected qP-wave increases and decreases with the increase of α_0.
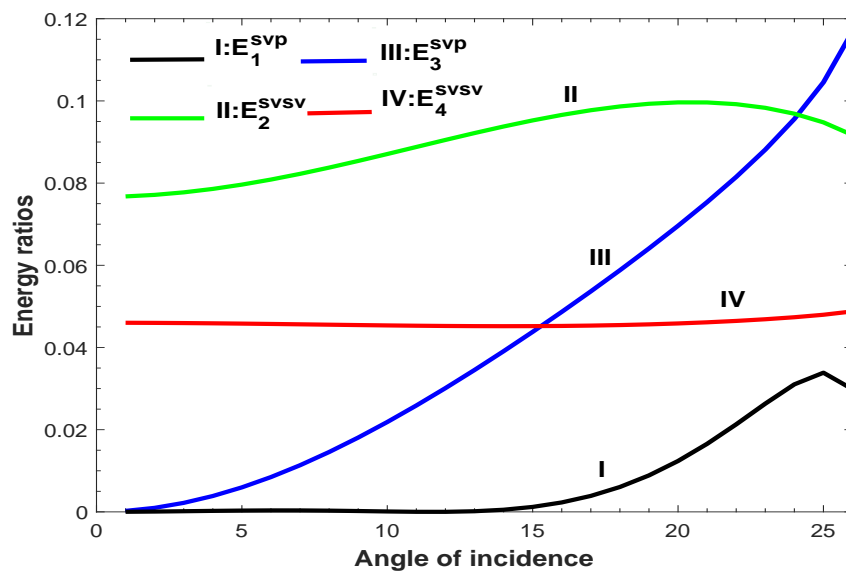
Figure 3.16: Variation of energy ratios for regular waves with α_0.

In Figure 3.16, the energy ratios, E_1^{svp} and E_2^{svsv} corresponding to regularly reflected waves for the incident qSV increase initially and then decrease with the increase of α_0. In the same figure, E_3^{svp} increases with the increase of α_0, while E_4^{svsv} decreases and increases at a very small rate.
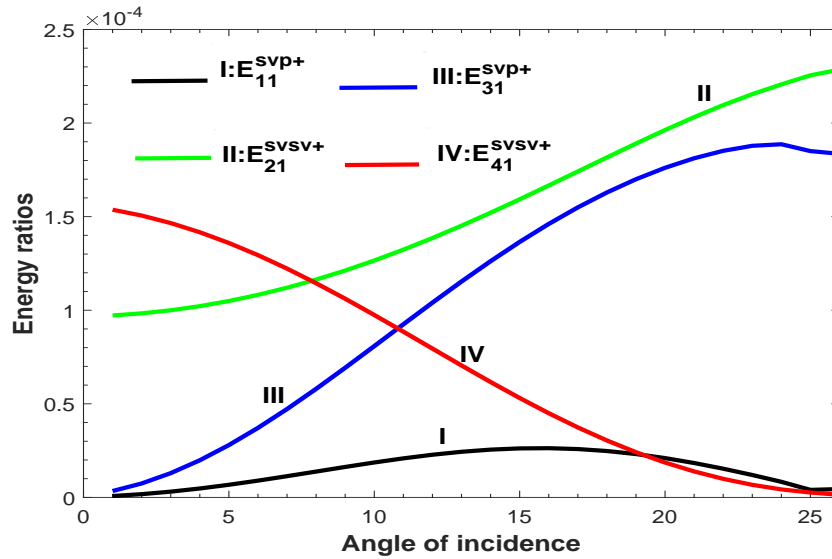
Figure 3.17: Variation of energy ratio for irregular waves at α_{11}^+ with α_0.

In Figures 3.17 and 3.18, the energy ratios, namely E_{11}^{svp+}, E_{11}^{svp-}, E_{31}^{svp+}, and E_{31}^{svp-} corresponding to irregular qP-waves increase to the maximum value at $\alpha_0 = 16^0$, $\alpha_0 = 18^0$, $\alpha_0 = 24^0$ and $\alpha_0 = 18^0$ respectively and then they decrease. In these figures, E_{21}^{svsv+} increases with the increase of α_0, while E_{21}^{svsv-} decreases to zero at $\alpha_0 = 9^0$ which then increases with the increase of α_0. But E_{41}^{svsv+} and E_{41}^{svsv-} corresponding to irregularly transmitted qSV-waves decreases and increases respectively with the increase of α_0.
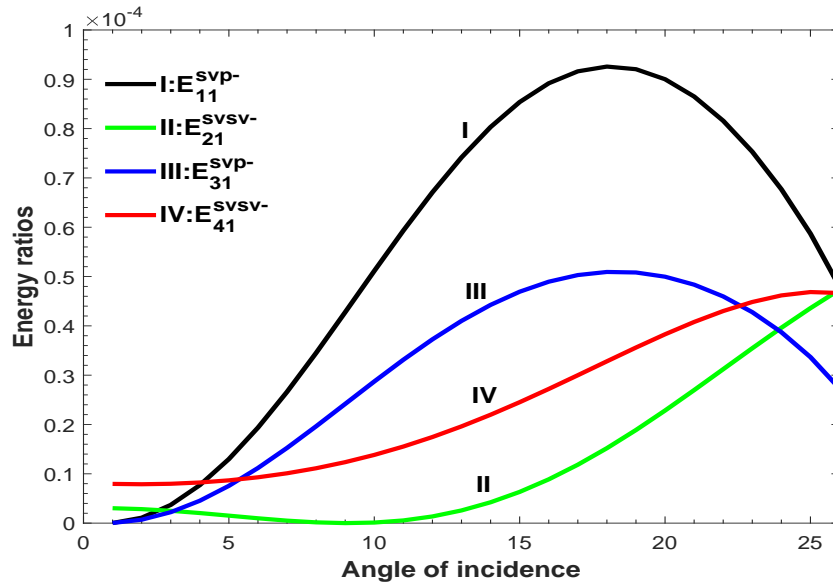
Figure 3.18: Variation of energy ratio for irregular waves at α_{11}^- with α_0.
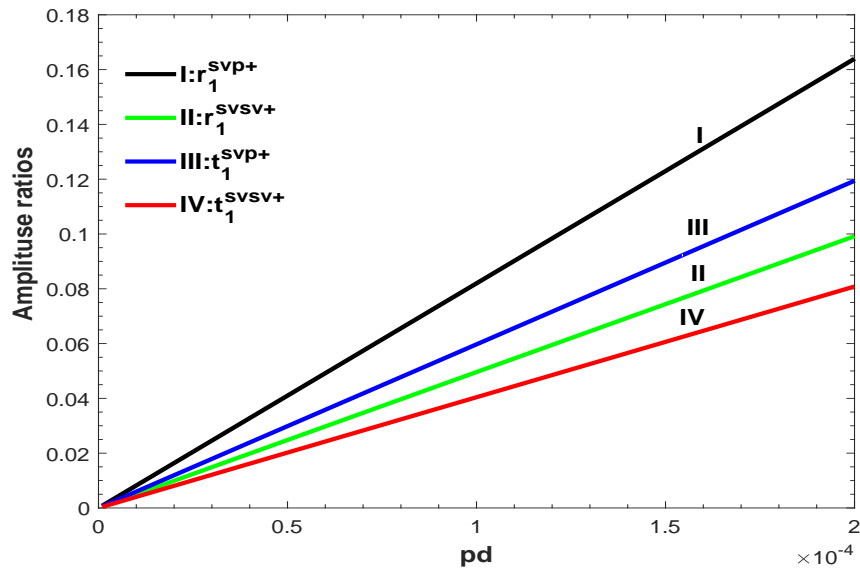
Figure 3.19: Variation of amplitude ratio of irregular waves at α_{11}^+ with corrugation parameter (pd).

All the amplitude ratios $(r_1^{svp+}, r_1^{svp-}, r_1^{svsv+}, r_1^{svsv-}, t_1^{svp+}, t_1^{svp-}, t_1^{svsv+}, t_1^{svsv-})$ in Figures 3.19 and 3.20 are linearly increasing with the increase of pd but at different rates.
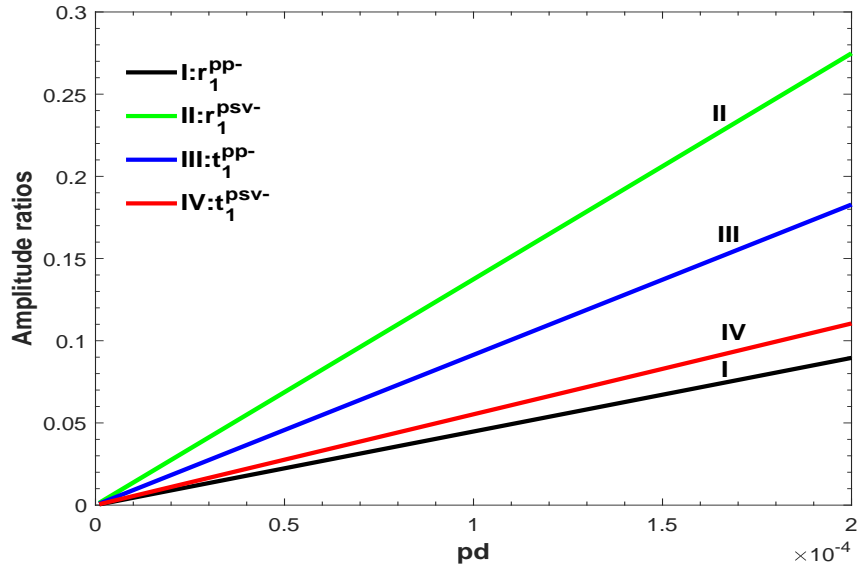
Figure 3.20: Variation of amplitude ratio of irregular waves at α_{11}^{-} with corrugation parameter (pd).
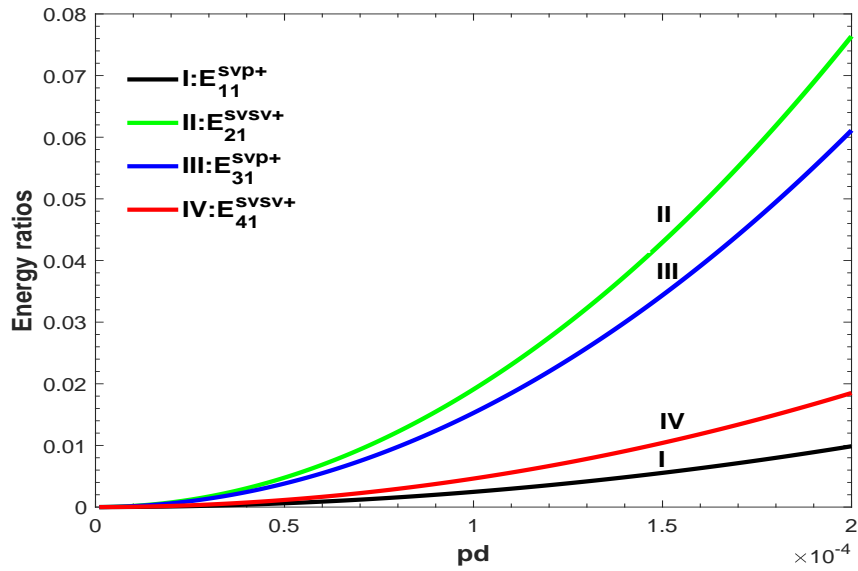
Figure 3.21: Variation of energy ratios at α_{11}^{+} with corrugation parameter (pd).

In Figures 3.21 and 3.22, we have observed that the energy ratios (E_{11}^{svp+}, E_{11}^{svp-}, E_{21}^{svsv+}, E_{21}^{svsv-}, E_{31}^{svp+}, E_{31}^{svp-}, E_{41}^{svsv+}, E_{41}^{svsv-}) are non-linearly increasing with the increase of pd.
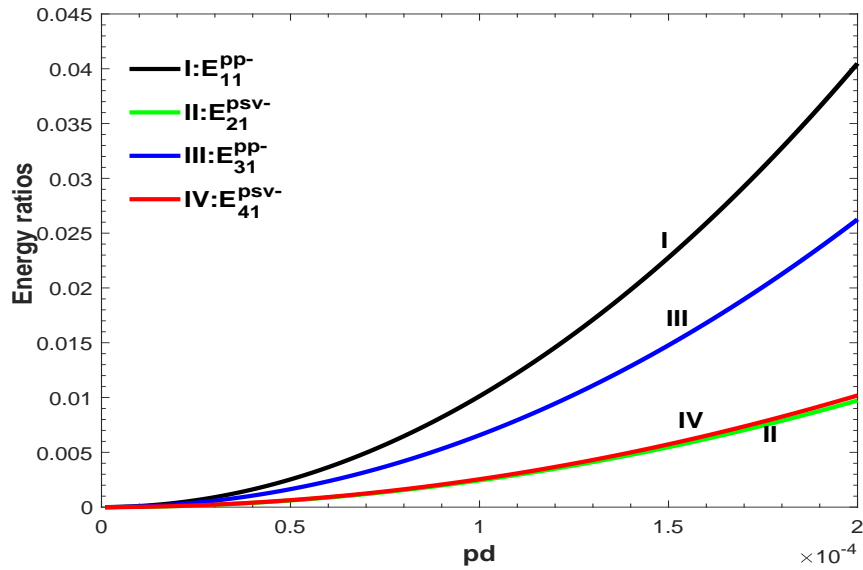
Figure 3.22: Variation of energy ratios at α_{11}^{-} with corrugation parameter (pd).

3.10   Conclusions

The problem of incident qP and qSV-waves at a corrugated interface between two dissimilar nematic elastomer half-spaces have been investigated separately. We have obtained the amplitude and energy ratios corresponding to regularly and irregularly reflected and transmitted qP and qSV-waves with the help of Rayleigh's method of approximation. These amplitude and energy ratios are computed numerically for a specific model, $\zeta = d \cos px_1$ and the effect of corrugation parameters on these amplitude and energy ratios are discussed. We may conclude with the following remarks:

(i) All amplitude ratios corresponding to irregular waves are functions of the angle of incidence, elastic constants, coupling constants, characteristic time of rubber relaxation, director rotation times, frequency and corrugation parameter.

(ii) The amplitude and the energy ratios corresponding to the regular waves are independent of pd and ω/pc_0.

(iii) The amplitude and energy ratios corresponding to the regular qP-waves are greater than those ratios corresponding to regular qSV-waves for the incident qP-

wave, but it is reversed in the case of incident qSV-wave.

(iv) The amplitude and energy ratios corresponding to the regularly reflected and transmitted waves are greater in magnitude than those of irregular waves. Those ratios corresponding to irregular waves are very small.

(v) The ratios r^{pp}, r^{svp}, t^{svp}, t^{svsv}, r_1^{svp+}, t_1^{svsv+}, r_1^{svsv-}, t_1^{svp-}, E_1^{pp}, E_3^{svp}, E_{21}^{svsv+}, E_{21}^{svsv-} and E_{41}^{svsv-} increase with the increase of α_0, while t^{pp}, t_1^{svsv-}, E_3^{pp} and E_{41}^{svsv+} decrease with the increase of α_0.

(vi) The amplitude ratios corresponding to irregular waves increase linearly with the increase of pd, but at different rates.

(vii) The energy ratios corresponding to irregular waves increase non-linearly with the increase of pd.

(viii) The sum of the energy ratio is close to unity at each angle of incidence at the corrugated boundary.

Chapter 4

Scattering of qSH-waves from a corrugated interface between two dissimilar nematic elastomers[3]

4.1 Introduction

Nematic elastomers(NEs) have many mechanical properties including the formation of fine-scale microstructures and fine-scale wrinkles due to the presence of considerable long macromolecules with rare intermolecular transversal bonds. An internal relaxation of the nematic director is responsible for its dynamic soft elasticity (de Gennes, 1980). The soft matter property makes a subject of numerous studies in the fields such as microelectronics, biomechanics, nanomechanics and device applicable in mechanical damping, optics or acoustics. Chattopadhyay (2004) obtained the expressions for reflection and refraction coefficients of qP, qSV and qSH-waves at an interface of two triclinic crystalline half-spaces and presented numerical results for different types of anisotropic media. Zhao and Liu (2018) studied the transverse wave dispersion in a nematic elastomer beam by considering anisotropy and viscoelasticity of NEs in the low frequency limit.

This chapter aims to investigate the reflection and transmission phenomena of elastic waves due to incident qSH-wave at a corrugated interface between two dif-

---

[3]***Waves in Random and Complex Media (2020)***

ferent nematic elastomer half-spaces. The expression of the phase velocity for shear harmonic wave is derived and observed that this phase velocity depends on the angle of propagation of the elastic waves. The amplitude ratios for various reflected and transmitted waves are derived using boundary conditions. The energy distribution, and hence the energy ratios due to various reflected and transmitted waves are also obtained. A particular case, $z = d \cos px$ has been performed to validate the present study for the amplitude and energy ratios.

4.2 Problem formulation

Consider the cartesian co-ordinates in which y and x-axis lying horizontal and z-axis vertical with positive direction pointing downward. Suppose two dissimilar anisotropic nematic elastomer half-spaces, $M = \{(x, z) : x \in \mathbb{R}, z \in [\zeta, \infty)\}$ and $M' = \{(x, z) : x \in \mathbb{R}, z \in (-\infty, \zeta)\}$, are separated by $z = \zeta(x)$ which is a periodic function of x independent of y whose mean value is zero. The geometry of the problem is given by Figure 4.1.
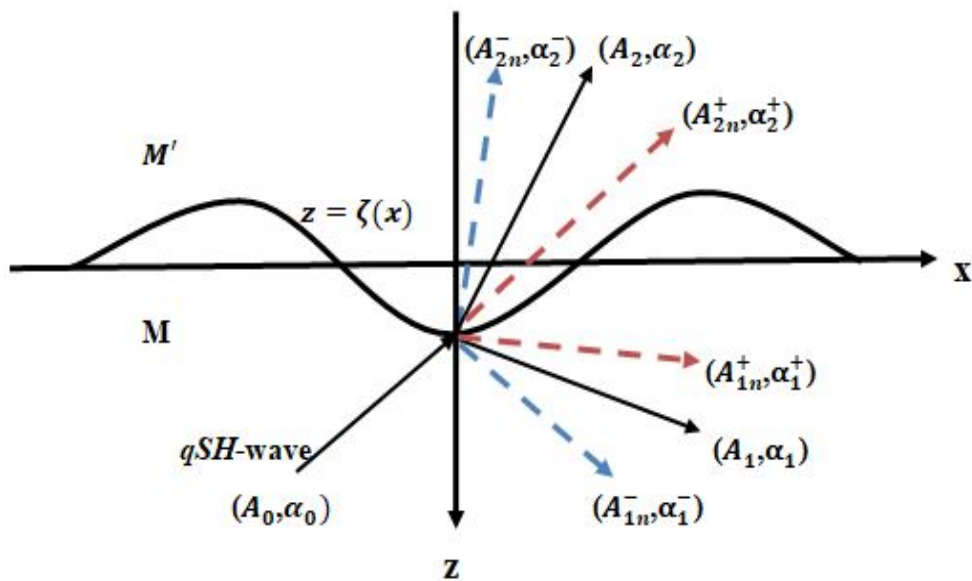
Figure 4.1: Geometry of the problem.

The Fourier series expansion of $\zeta(x)$ is given by

$$\zeta(x) = \sum_{n=1}^{\infty}(\zeta_{+n}e^{\imath npx} + \zeta_{-n}e^{-\imath npx}),\tag{4.1}$$

where $\zeta_{\pm n}$ are the coefficients of series expansion of order n, p is the wavenumber and $\imath = \sqrt{-1}$. We introduce constants d, c_n and s_n as

$$\zeta_{\pm 1} = \frac{d}{2}, \qquad \zeta_{\pm n} = \frac{c_n \mp \imath s_n}{2}, \quad (n = 2,3,4,....)$$

so that

$$\zeta(x) = d\cos(px) + \sum_{n=2}^{\infty}\{c_n\cos(npx) + s_n\sin(npx)\}.\tag{4.2}$$

If the interface is $\zeta(x) = d\cos(px)$, then $2\pi/p$ is the wavelength of corrugation and d is the amplitude of corrugation.

Consider two-dimensional problem of wave propagation in xz-plane. The equations of motion for qSH-waves for the half-spaces, M and M' are respectively given by

$$\rho\frac{\partial^2 u_2}{\partial t^2} = (1 + \imath\omega\tau_R)(c_{66}\frac{\partial^2 u_2}{\partial x^2} + c_{44}^R\frac{\partial^2 u_2}{\partial z^2})\tag{4.3}$$

and

$$\rho'\frac{\partial^2 u_2'}{\partial t^2} = (1 + \imath\omega\tau_R')(c_{66}'\frac{\partial^2 u_2'}{\partial x^2} + c_{44}'^R\frac{\partial^2 u_2'}{\partial z^2})\tag{4.4}$$

where

$$c_{44}^R = 2C_5 - \frac{D_2^2(1+\imath\omega\tau_2)^2}{4D_1(1+\imath\omega\tau_1)(1+\imath\omega\tau_R)}, \quad c_{44}'^R = 2C_5' - \frac{D_2'^2(1+\imath\omega\tau_2')^2}{4D_1'(1+\imath\omega\tau_1')(1+\imath\omega\tau_R')}$$

ρ being the density of the medium, $\mathbf{u} = (u_1, u_2, u_3)$ is the displacement potential, ω is angular frequency, c_i are elastic constants with D_1 and D_2 are coupling constants, C_5 is the shear modulus, τ_R is the characteristic time of rubber relaxation and τ_1 and τ_2 are director rotation times. Note that all parameters in M will be denoted without prime, while those of M' with prime to the corresponding parameters of M.

Suppose a plane qSH-wave propagating in the half-space M with angle α_0 and amplitude constant A_0 be incident at the corrugated interface $z = \zeta(x)$, then the phenomena of reflection of qSH-waves in the half-space, M and transmission of qSH-waves in the half-space, M' take place. Due to undulated nature of the interface, this incident wave give rise to regularly and irregularly reflected and transmitted qSH-waves (Asano, 1960). These irregular waves propagate with the same speed as the regular waves and appear on both sides of the regular waves. The full structures of wave field in the half spaces, M and M' are given by

$$u = \sum_{m=0}^{1} A_m \exp(P_m) + \sum_{n=1}^{\infty} A_{1n}^{\pm} \exp(P_{1n}^{\pm}), \tag{4.5}$$

$$u' = A_2 \exp(P_2) + \sum_{n=1}^{\infty} A_{2n}^{\pm} \exp(P_{2n}^{\pm}), \tag{4.6}$$

where $P_m = \imath(\omega t + xk_1^{(m)} + zk_3^{(m)})$, $P_{mn}^{\pm} = \imath(\omega t + xk_{1\pm}^{(mn)} + zk_{3\pm}^{(mn)})$, $(A_m, A_{mn}^{\pm})$ are the amplitude constants at angles $(\alpha_m, \alpha_{mn}^{\pm})$, $(k_1^{(m)}, k_3^{(m)})$ and $(k_{1\pm}^{(mn)}, k_{3\pm}^{(mn)})$ are the propagation factors. The phase velocity of the incident, reflected and transmitted qSH-waves are given by (Singh, 2017)

$$c_i^2 = \frac{(1 + \imath\omega\tau_R)(c_{66}p_1^2 + c_{44}^R p_3^2)}{\rho}, \; i = 0, 2; \quad c_2'^2 = \frac{(1 + \imath\omega\tau_R')(c_{66}'p_1'^2 + c_{44}'^R p_3'^2)}{\rho'}. \tag{4.7}$$

Note that the angles of propagation $(p_1, 0, p_3)$ for the incident, regularly reflected and transmitted waves are respectively $(-\sin\alpha_0, 0, \cos\alpha_0)$, $(-\sin\alpha_1, 0, -\cos\alpha_1)$ and $(-\sin\alpha_2, 0, \cos\alpha_2)$.

The Snell's law, for this problem, is

$$k_0 \sin\alpha_0 = k_2 \sin\alpha_1 = k_2' \sin\alpha_2, \tag{4.8}$$

The relations between the angles of irregular waves to those of regular waves are given through the Spectrum theorem (Abubakar, 1962c)

$$\sin\alpha_{1n}^{\pm} = \sin\alpha_1 \pm \frac{np}{k_2}, \quad \sin\alpha_{2n}^{\pm} = \sin\alpha_2 \pm \frac{np}{k_2'}, \quad n = 1, 2, ... \tag{4.9}$$

4.3   Boundary conditions

The component of displacement and traction are continuous at $z = \zeta(x)$. These conditions are

$$u = u', \tag{4.10}$$

$$\tau_{23} - \tau_{21}\zeta' = \tau'_{23} - \tau'_{21}\zeta', \tag{4.11}$$

which can be written as

$$(1 + \iota\omega\tau_R)(c_{44}^R\frac{\partial u}{\partial z} - \zeta'c_{66}\frac{\partial u}{\partial x}) = (1 + \iota\omega\tau'_R)(c_{44}'^R\frac{\partial u'}{\partial z} - \zeta'c_{66}'\frac{\partial u'}{\partial x}), \tag{4.12}$$

where

$$\zeta' = \sum_{n=1}^{\infty} \iota np(\zeta_{+n}e^{\iota npx} - \zeta_{-n}e^{-\iota npx}).$$

Using Eqs.(4.5), (4.6), (4.8) and (4.9) into Eqs.(4.10) and (4.12), we get

$$\sum_{m=0}^{1} A_m e^{\iota\zeta k_3^{(m)}} + \sum_{n=1}^{\infty} A_{1n}^{\pm} e^{\mp\iota npx} e^{\iota\zeta k_{3\pm}^{(1n)}} = A_2 e^{\iota\zeta k_3^{(2)}} + \sum_{n=1}^{\infty} A_{2n}^{\pm} e^{\mp\iota npx} e^{\iota\zeta k_{3\pm}^{(2n)}}, \tag{4.13}$$

$$\sum_{m=0}^{1} A_m(c_{44}^R k_3^{(m)} - c_{66}k_1^{(m)}\zeta')e^{\iota\zeta k_3^{(m)}} + \sum_{n=1}^{\infty} A_{1n}^{\pm}(c_{44}^R k_{3\pm}^{(1n)} - c_{66}k_{1\pm}^{(1n)}\zeta')e^{\mp\iota npx} e^{\iota\zeta k_{3\pm}^{(1n)}}$$

$$= \tau_0\{A_2(c_{44}'^R k_3^{(2)} - c_{66}'k_1^{(2)}\zeta')e^{\iota\zeta k_3^{(2)}} + \sum_{n=1}^{\infty} A_{2n}^{\pm}(c_{44}'^R k_{3\pm}^{(2n)} - c_{66}'k_{1\pm}^{(2n)}\zeta')e^{\mp\iota npx} e^{\iota\zeta k_{3\pm}^{(2n)}}\}, \tag{4.14}$$

where

$$\tau_0 = (1 + \iota\omega\tau'_R)/(1 + \iota\omega\tau_R).$$

These equations will help to find out the amplitude ratios corresponding to the regularly and irregularly reflected and transmitted waves.

4.4 Solution of first order approximation

We assume that the slope and amplitude of the corrugated interface are very small so that higher powers of ζ are neglected, then

$$e^{\pm i\zeta k_1^{(0)}} = 1 \pm i\zeta k_1^{(0)}, \quad e^{\pm i\zeta k_3^{(0)}} = 1 \pm i\zeta k_3^{(0)}, \quad \text{etc.} \tag{4.15}$$

Using Eqs.(4.1) and (4.15) into Eqs.(4.13) and (4.14) and collecting the terms independent of ζ and x, we obtain

$$\frac{A_1}{A_0} - \frac{A_2}{A_0} = -1,$$
$$k_3^{(1)}\frac{A_1}{A_0} - \tau_0' k_3^{(2)}\frac{A_2}{A_0} = -k_3^{(0)}, \tag{4.16}$$

where

$$\tau_0' = \tau_0 c_{44}'^R / c_{44}^R.$$

Solving the above equations, we get the amplitude ratios corresponding to regularly reflected and transmitted qSH-waves as

$$r = \frac{\tau_0' k_3^{(2)} - k_3^{(0)}}{k_3^{(1)} - \tau_0' k_3^{(2)}}, \tag{4.17}$$

$$t = \frac{k_3^{(1)} - k_3^{(0)}}{k_3^{(1)} - \tau_0' k_3^{(2)}}. \tag{4.18}$$

Next, comparing the coefficients of $e^{\pm inpx}$ on both sides of the equations, we get

$$\frac{A_{1n}^{\mp}}{A_0} - \frac{A_{2n}^{\mp}}{A_0} = b_1^{\pm},$$
$$c_{44}^R k_{3\mp}^{(1n)}\frac{A_{1n}^{\mp}}{A_0} - \tau_0 c_{44}'^R k_{3\mp}^{(2n)}\frac{A_{2n}^{\mp}}{A_0} = b_2^{\pm}, \tag{4.19}$$

with

$$b_1^{\pm} = i\zeta_{\pm n}[-k_3^{(0)} - \frac{A_1}{A_0}k_3^{(1)} + \frac{A_2}{A_0}k_3^{(2)}], \quad b_2^{\pm} = i\zeta_{\pm n}[-g_0^{\pm} - \frac{A_1}{A_0}g_1^{\pm} + \frac{A_2}{A_0}g_2^{\pm}],$$

$$g_0^{\pm} = c_{44}^R k_3^{(0)} k_3^{(0)} \mp c_{66}npk_1^{(0)}, \quad g_1^{\pm} = c_{44}^R k_3^{(1)} k_3^{(1)} \mp c_{66}npk_1^{(1)},$$

$$g_2^{\pm} = \tau_0(c_{44}'^R k_3^{(2)} k_3^{(2)} \mp c_{66}'npk_1^{(2)}).$$

We get the amplitude ratios corresponding to irregularly reflected and transmitted waves by solving Equation (4.19) as

$$r_n^{\pm} = \frac{b_2^{\pm} - \tau_0 c_{44}'^R k_{3\mp}^{(2n)} b_1^{\pm}}{c_{44}^R k_{3\mp}^{(1n)} - \tau_0 c_{44}'^R k_{3\mp}^{(2n)}}, \qquad t_n^{\pm} = \frac{b_2^{\pm} - c_{44}^R k_{3\mp}^{(1n)} b_1^{\pm}}{c_{44}^R k_{3\mp}^{(1n)} - \tau_0 c_{44}'^R k_{3\mp}^{(2n)}}. \qquad (4.20)$$

Here, the sign $(+ve)$ to the amplitude ratio represents for the irregular waves lying on the right side of the regular waves and $(-ve)$ sign represents for the irregular waves lying on the left side of the regular waves. It is clearly observed that these ratios are functions of the elastic parameters, angle of incidence, characteristic time of rubber relaxation, director rotation times, corrugation parameter and frequency of incident qSH-wave.

4.5 Energy partition

The energy due to the incident qSH-wave is distributed to regularly and irregularly reflected and transmitted waves. The rate of transmission of energy per unit area is given by Achenbach (1976)

$$\wp^* = < \tau_{23} \cdot \dot{u} > . \qquad (4.21)$$

The energy of the incident qSH-wave is given by

$$E_{inc} = f_0 \omega A_0^2 \exp\{2\imath(\omega t + k_1^{(0)} x + k_3^{(0)} z)\}, \qquad (4.22)$$

where $f_0 = (1 + \imath\omega\tau_R)c_{44}^R k_3^{(0)}$.

Similarly, the energy due to reflected and transmitted qSH-waves are given by

$$E_m = f_m \omega A_m^2 \exp\{2\imath(\omega t + k_1^{(m)} x + k_3^{(m)} z)\}$$
$$+ \sum_{n=1}^{\infty} f_{mn}^{\pm} \omega (A_{mn}^{\pm})^2 \exp\{2\imath(\omega t + k_{1\pm}^{(mn)} x + k_{3\pm}^{(mn)} z)\}, \quad m = 1, 2. \qquad (4.23)$$

The expressions of f_m and $f_{mn}^{\pm}$ are given by

$$f_m = (1 + \imath\omega\tau_R)c_{44}^R k_3^{(m)}, \quad f_{mn}^{\pm} = (1 + \imath\omega\tau_R)c_{44}^R k_{3\pm}^{(mn)}.$$

The energy ratios of the regularly and irregularly reflected and transmitted qSH-waves are given as

$$E_m = \left|\frac{f_m}{f_0}\right|\left|\frac{A_m}{A_0}\right|^2, \tag{4.24}$$

$$E_{mn}^{\pm} = \sum_{n=1}^{\infty} \left|\frac{f_{mn}^{\pm}}{f_0}\right|\left|\frac{A_{mn}^{\pm}}{A_0}\right|^2, \tag{4.25}$$

where E_1 and E_2 are the energy ratios of the regularly reflected and transmitted waves, $E_{1n}^{\pm}$ and $E_{2n}^{\pm}$ are the energy ratios of the irregularly reflected and transmitted waves for n^{th} spectrum. These ratios depend on elastic constants, the coupling constants, the characteristics time of rubber relaxation, director rotation times, angle of incidence, corrugation and frequency parameters. It may be noted that sum of energy ratios is equal to one.

4.6   Special case

If the corrugated interface is represented by only one cosine term, i.e., $\zeta(x) = d\cos px$, then

$$\zeta_{\pm n} = \begin{cases} 0 & \text{if } n \neq 1, \\ \frac{d}{2} & \text{if } n = 1. \end{cases} \tag{4.26}$$

Then, the amplitude ratios corresponding to the irregularly reflected and transmitted waves for the first order of approximation are given by

$$r_1^{\pm} = \frac{b_2^{\pm} - \tau_0 c_{44}'^R k_{3\mp}^{(21)} b_1^{\pm}}{c_{44}^R k_{3\mp}^{(11)} - \tau_0 c_{44}'^R k_{3\mp}^{(21)}}, \qquad t_1^{\pm} = \frac{b_2^{\pm} - c_{44}^R k_{3\mp}^{(11)} b_1^{\pm}}{c_{44}^R k_{3\mp}^{(11)} - \tau_0 c_{44}'^R k_{3\mp}^{(21)}}, \tag{4.27}$$

where

$$b_1^{\pm} = \imath\frac{d}{2}\{-k_3^{(0)} - \frac{A_1}{A_0}k_3^{(1)} + \frac{A_2}{A_0}k_3^{(2)}\}, \quad b_2^{\pm} = \imath\frac{d}{2}\{-g_0^{\pm} - \frac{A_1}{A_0}g_1^{\pm} + \frac{A_2}{A_0}g_2^{\pm}\},$$

$$g_0^{\pm} = c_{44}^R k_3^{(0)}k_3^{(0)} \mp c_{66}pk_1^{(0)}, \quad g_1^{\pm} = c_{44}^R k_3^{(1)}k_3^{(1)} \mp c_{66}pk_1^{(1)}, \quad g_2^{\pm} = \tau_0(c_{44}'^R k_3^{(2)}k_3^{(2)} \mp c_{66}'pk_1^{(2)}).$$

In the normal incidence, $\alpha_0 = 0^o$, we obtain that $\cos \alpha_{11}^+ = \cos \alpha_{11}^-$ and $\cos \alpha_{21}^+ = \cos \alpha_{21}^-$ due to Equations (4.8) and (4.9). Hence the amplitude ratios of the irregular waves are related as $r_1^+ = r_1^-$, $t_1^+ = t_1^-$. These are the result of Asano (1960) for the relevant problem.

In the grazing angle of incidence, $\alpha_0 = \frac{\pi}{2}$, the amplitude ratios are given by Eq.(4.27) with the following modifications

$$b_1^\pm = \frac{\imath d}{2} \{ \frac{A_1}{A_0} \sqrt{k_2^2 - k_0^2} + \frac{A_2}{A_0} \sqrt{k_2'^2 - k_0^2} \}, \qquad g_0^\pm = \pm c_{66} p k_0,$$

$$g_1^\pm = c_{44}^R (k_2^2 - k_0^2) \pm c_{66} p k_0, \quad g_2^\pm = \tau_0 \{ c_{44}'^R (k_2'^2 - k_0^2) \pm c_{66}' p k_0 \}.$$

The energy ratios are obtained from Eq.(4.25) by inserting $n = 1$.

4.7 Particular case

(a) When the two nematic half-spaces, M and M' reduce to isotropic half-spaces, we have

$$D_1 = D_2 = 0, \; c_{11} = c_{33} = \lambda + 2\mu, \; c_{13} = \lambda, \; c_{44} = c_{44}^R = c_{66} = \mu, \; C_1 = C_4 = C_5 = \frac{1}{2}\mu,$$

$$D_1' = D_2' = 0, \; c_{11}' = c_{33}' = \lambda' + 2\mu', \; c_{13}' = \lambda', \; c_{44}' = c_{44}'^R = c_{66}' = \mu', \; C_1' = C_4' = C_5' = \frac{1}{2}\mu'.$$

The phase velocity corresponding to the SH-waves become $c_2^2 = \frac{\mu}{\rho}$ and $c_2'^2 = \frac{\mu'}{\rho'}$ which are the results of classical elasticity (Achenbach, 1976).

The amplitude ratios of the reflected and transmitted waves are given by Eqs. (4.17), (4.18) and (4.20) with the following modified values

$$\tau_0' = \mu'/\mu, \; g_0^\pm = k_3^{(0)} k_3^{(0)} \mp n p k_1^{(0)}, \; g_1^\pm = k_3^{(1)} k_3^{(1)} \mp n p k_1^{(1)}, \; g_2^\pm = \mu' (k_3^{(2)} k_3^{(2)} \mp n p k_1^{(2)})/\mu.$$

These results are similar with those of Asano (1960) for the relevant problem. The energy ratios corresponding to the regularly and irregularly reflected and transmitted waves are given by Eqs. (4.24) and (4.25) with the following modified values

$$f_0 = k_3^{(0)}, \; f_1 = k_3^{(1)}, \; f_2 = \mu' k_3^{(2)}/\mu, \; f_{1n}^\pm = k_{3\pm}^{(1n)}, \; f_{2n}^\pm = \mu' k_{3\pm}^{(2n)}/\mu.$$

(b) If the amplitude of corrugated interface is neglected, i.e., $d = 0$, the problem reduces to the reflection/transmission of elastic waves at a plane interface between two dissimilar nematic half-spaces. The amplitude and energy ratios corresponding to the regularly reflected and transmitted qSH-waves are given by Eqs. (4.17), (4.18) and (4.24). These results exactly match with those of Singh (2015).

(c) If the half-space M' is absent, then the problem reduces to the reflection of elastic waves at the plane free surface. The amplitude ratio given by Eq. (4.17) will be modified as

$$r = -k_3^{(0)}/k_3^{(1)}.$$

This is the result of Kielczynski and Pajewski (1987) for the relevant problem.

4.8 Numerical results and discussion

We will compute the angles of reflected and transmitted waves through Snell's law. Introducing dimensionless velocity $\bar{c}$ such that $\bar{c} = \frac{c_a}{\beta} = \frac{c}{p_1 \beta}$ into Equation (4.7), we have

$$\bar{c}^2 = (1 + \imath\omega\tau_R)(\bar{c}_{66} + \bar{c}_{44}^R p^2), \tag{4.28}$$

where c_a is an apparent velocity and

$$p = \frac{p_3}{p_1}, \quad \beta = \sqrt{\frac{c_{44}}{\rho}}, \quad \bar{c}_{ij} = \frac{c_{ij}}{c_{44}}.$$

Transforming this equation with $q = \frac{1}{p} = \frac{p_1}{p_3}$, we have

$$q^2 = \frac{(1 + i\omega\tau_R)\bar{c}_{44}^R}{\bar{c}^2 - (1 + i\omega\tau_R)\bar{c}_{66}} \tag{4.29}$$

The Eq. (4.29) give rise to the reflected angle $\alpha_1 = \tan^{-1}(q)$ for a given α_0. Similarly, we obtained the angle of transmitted qSH-wave, $\alpha_2 = \tan^{-1}(q')$ in the half-space M'.

For the numerical computation, the following relevant values are considered (Singh, 2015)

Half-space, M	Value	Half-space, M'	Value	Units
C_1	1.42×10^5	C'_1	3.52×10^5	Nm^{-2}
C_2	2.25×10^5	C'_2	2.28×10^5	Nm^{-2}
C_3	4.88×10^5	C'_3	1.65×10^5	Nm^{-2}
C_4	2.15×10^5	C'_4	1.60×10^5	Nm^{-2}
C_5	1.06×10^5	$C'5$	3.34×10^5	Nm^{-2}
ρ	1.66×10^3	ρ'	1.26×10^3	kgm^{-3}
D_1	0.12	D'_1	0.15×10^6	
D_2	0.05	D'_2	0.17×10^6	
τ_1	0.02	τ'_1	0.04	
τ_2	0.05	τ'_2	0.06	
τ_R	0.000002	τ'_R	0.000003	

Table 1: Values of the parameters

and $(pd, \omega/pc_0) = (0.00001, 60)$ are taken whenever not mentioned.
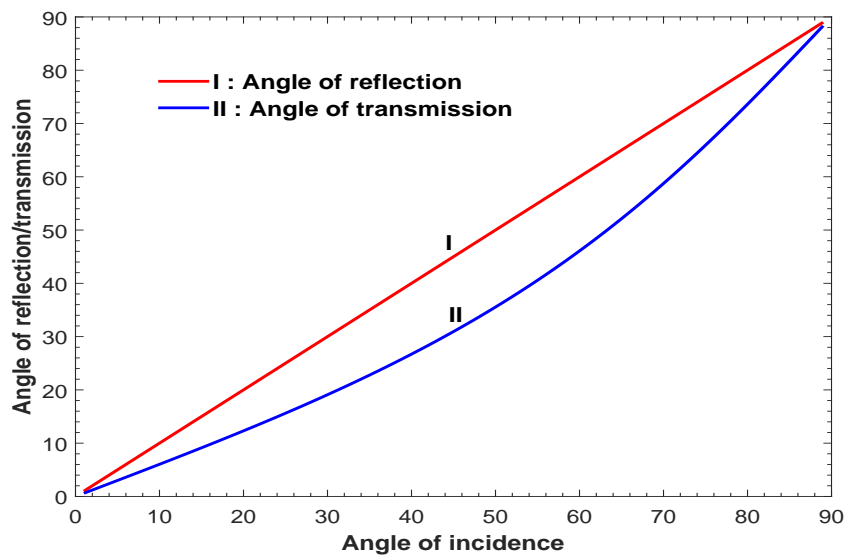
Figure 4.2: Variation of angles of regularly reflected and transmitted waves with α_0.

We notice in Figure 4.2 that angles of reflected and transmitted qSH-waves are increasing with the increase of angle of incidence, α_0. In Figure 4.3, amplitude ratios corresponding to the reflected and transmitted qSH-waves meet at $\alpha_0 = 63^0$, while E_1 increases and E_2 decreases with the increase of α_0.
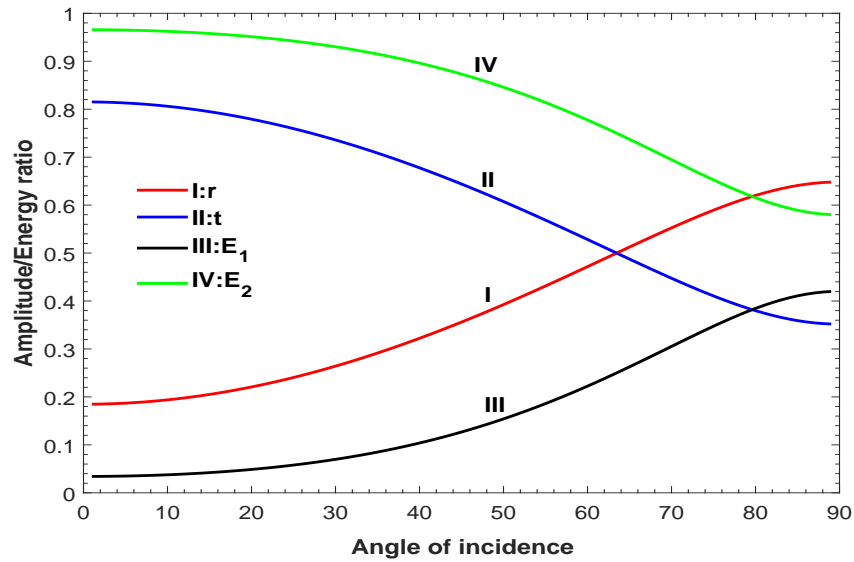
Figure 4.3: Variation of amplitude and energy ratios of the regular waves with α_0.
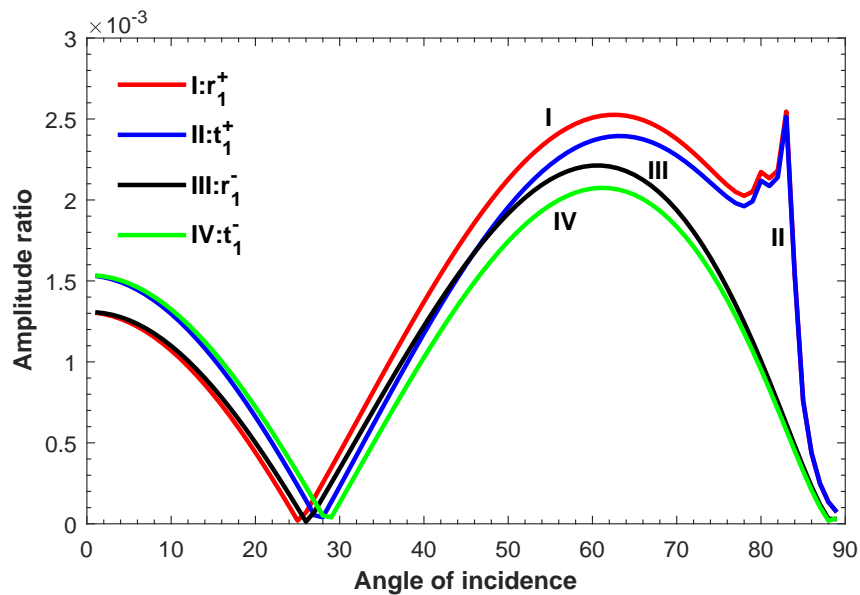
Figure 4.4: Variation of amplitude ratios of the irregular waves with α_0.

In Figure 4.4, the amplitude ratios (r_1^-, t_1^-) corresponding to irregularly reflected and transmitted waves decrease to zero at $(\alpha_0 = 26^0, \alpha_0 = 29^0)$ and then increase with the increase of α_0 attaining maximum values at $(\alpha_0 = 60^0, \alpha_0 = 62^0)$ respectively. Thereafter, they decrease with the increase of α_0. In the same figure, the amplitude ratios (r_1^+, t_1^+) decrease to zero at $(\alpha_0 = 25^0, \alpha_0 = 28^0)$ and then increase with the increase of α_0 attaining maximum values at $(\alpha_0 = 62^0, \alpha_0 = 64^0)$ respectively. They show irregular patterns making a peak at $\alpha_0 = 83^0$ and then decrease with the increase of α_0.
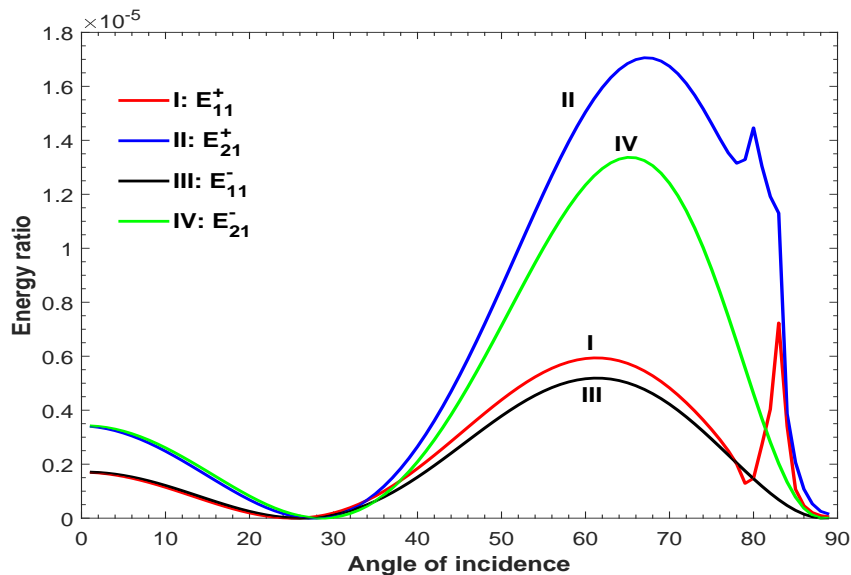
Figure 4.5: Variation of energy ratios of irregular waves with α_0.

The variation of energy ratios of the irregular waves with angle of incidence are shown in Figure 4.5. In this figure, E_{11}^-, E_{21}^-, E_{11}^+ and E_{21}^+ start from certain values which decrease to zero at $\alpha_0 = 26^0$, $\alpha_0 = 28^0$, $\alpha_0 = 25^0$ and $\alpha_0 = 27^0$ respectively which increase with α_0 attaining maximum values at $\alpha_0 = 61^0$, $\alpha_0 = 65^0$, $\alpha_0 = 61^0$ and $\alpha_0 = 67^0$ respectively. Then, Curves I and II show decreasing and increasing natures with peaks at $\alpha_0 = 83^0$ and $\alpha_0 = 80^0$ respectively, while Curves III and IV show the decreasing natures of E_{11}^- and E_{21}^- respectively.

The irregularities in the Curves I and II in the Figures 4.4 and 4.5 for $(r_1^+, \ t_1^+)$ and $(E_{11}^+, \ E_{21}^+)$ respectively in between the angles 75^0 and 85^0 are due to existence of critical angles for $\alpha_{11}^+ = \sin^{-1}(\sin\alpha_1 + p/k_2)$ and $\alpha_{21}^+ = \sin^{-1}(\sin\alpha_2 + p/k_2')$ at $\alpha_0 = 83^0$. The sum of energy ratios is very close to unity.

4.8.1   Effect of corrugation and frequency parameters

We are interested to see the effect of corrugation and frequency parameters on the amplitude and energy ratios. Figures 4.6 and 4.7 show the variation of amplitude and energy ratios with corrugation parameter pd. It is seen that amplitude and energy ratios increase with the increase of pd. We noted that these increases are linear at different rates for amplitude ratios and non-linear in the case of energy ratios.
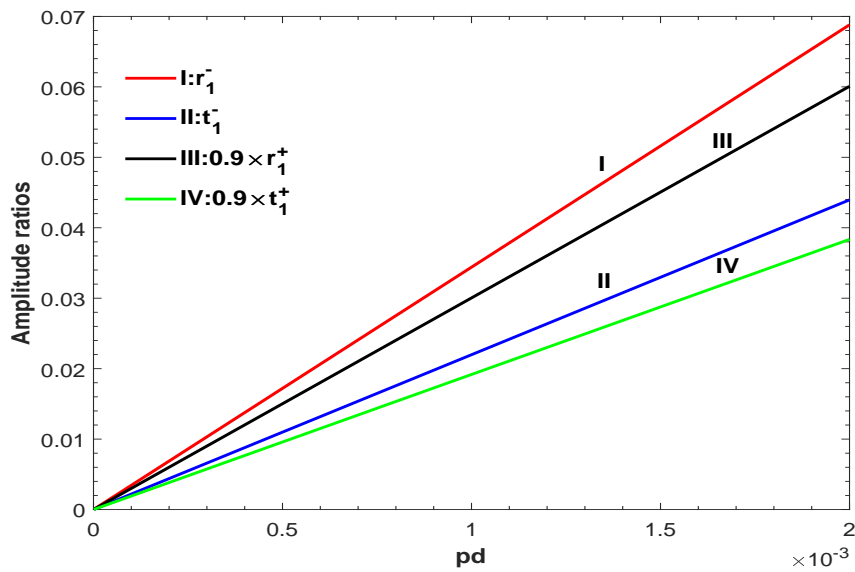
Figure 4.6: Variation of amplitude ratios of the irregular waves with corrugation parameter.
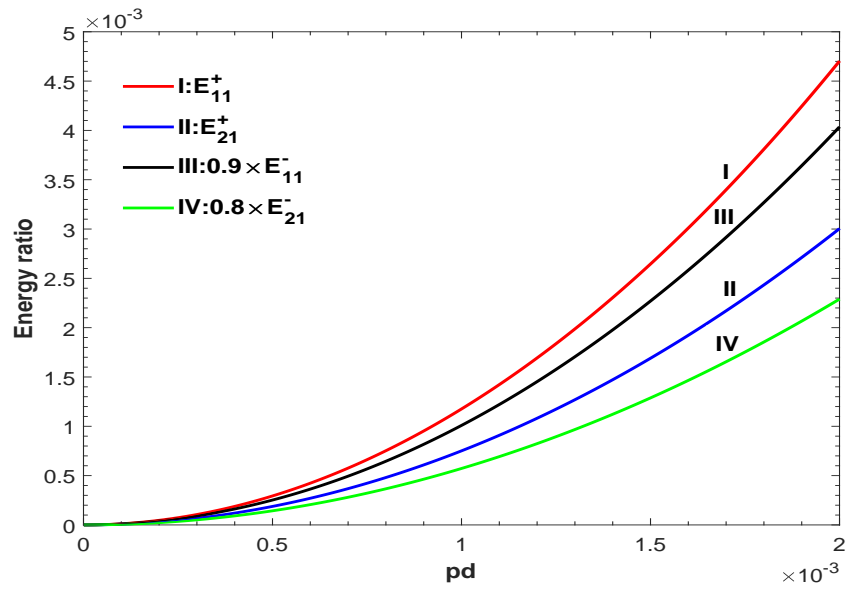
Figure 4.7: Variation of energy ratios of the irregular waves with corrugation parameter.

The variation of amplitude and energy ratios with angle of incidence, α_0 at different values of pd and ω/pc_0 are depicted through Figures 4.8-4.11 and Figures 4.12-4.15 respectively.
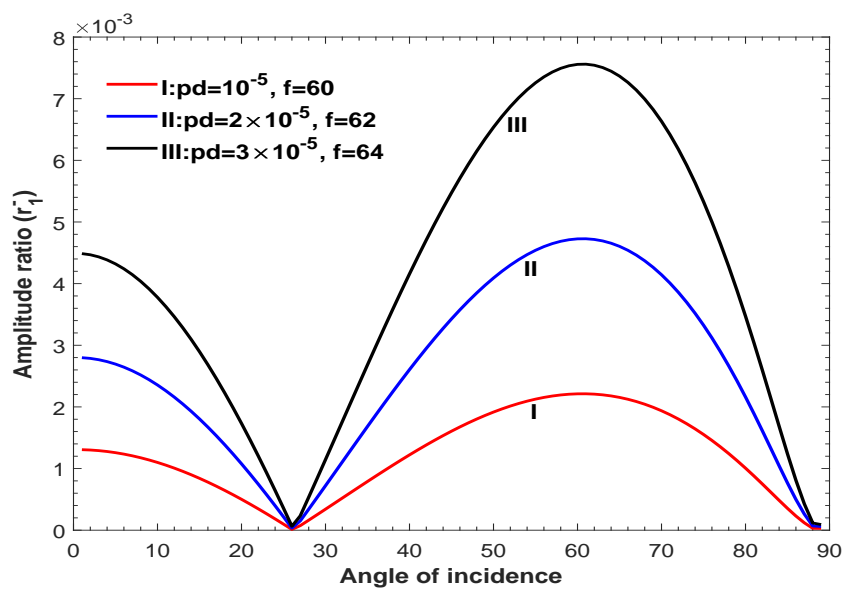
Figure 4.8: Variation of r_1^- with α_0 for different values of pd and ω/pc_0.

In Figures 4.8 and 4.9, r_1^- and t_1^- start from certain value and decrease to zero at $\alpha_0 = 26^0$ and $\alpha_0 = 29^0$ which then increase with the increase of α_0 attaining maximum values at $\alpha_0 = 60^0$ and $\alpha_0 = 62^0$ respectively. They decrease again with the increase of α_0.
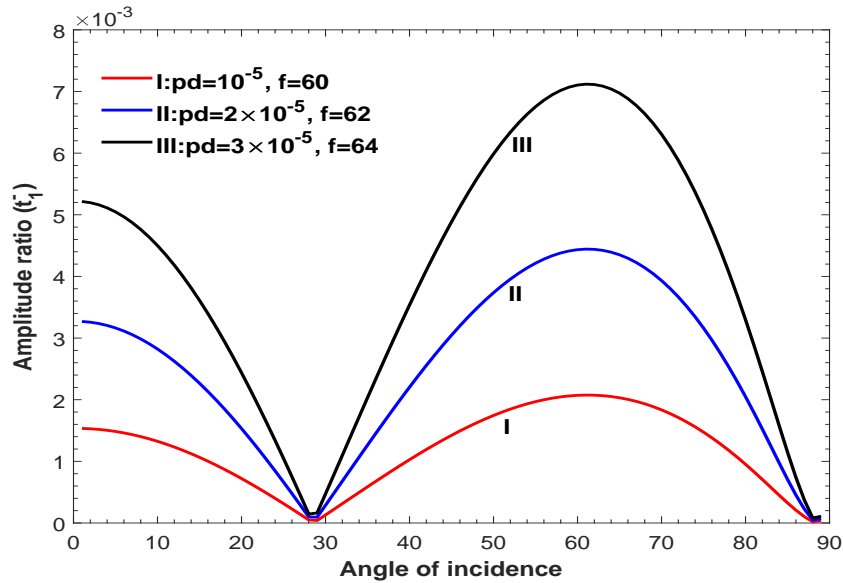
Figure 4.9: Variation of t_1^- with α_0 for different values of pd and ω/pc_0.
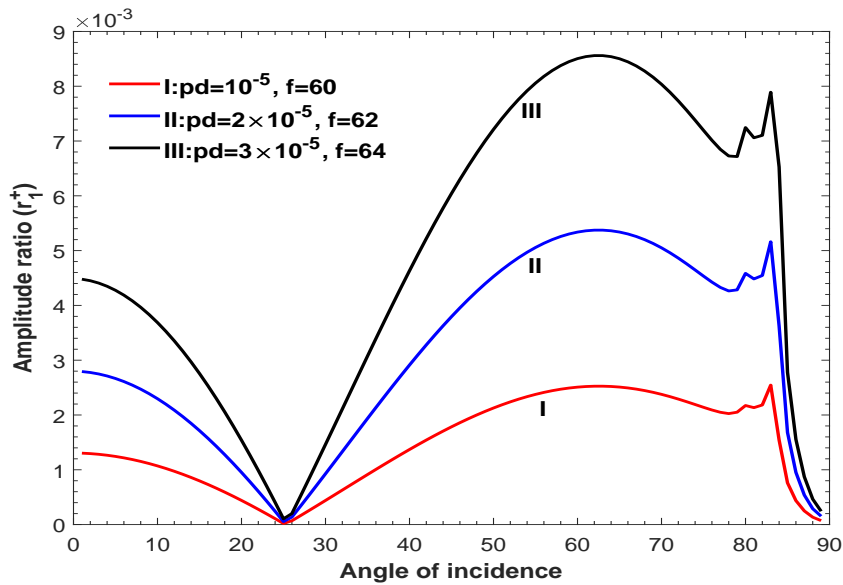
Figure 4.10: Variation of r_1^+ with α_0 for different values of pd and ω/pc_0.

The amplitude ratios, r_1^+ and t_1^+ in Figures 4.10 and 4.11 start from certain value

which decrease to zero at $\alpha_0 = 25^0$ and $\alpha_0 = 28^0$ which then increase with the increase of α_0 attaining maximum values at $\alpha_0 = 63^0$ and $\alpha_0 = 64^0$ respectively. Thereafter, they show irregular natures with α_0.
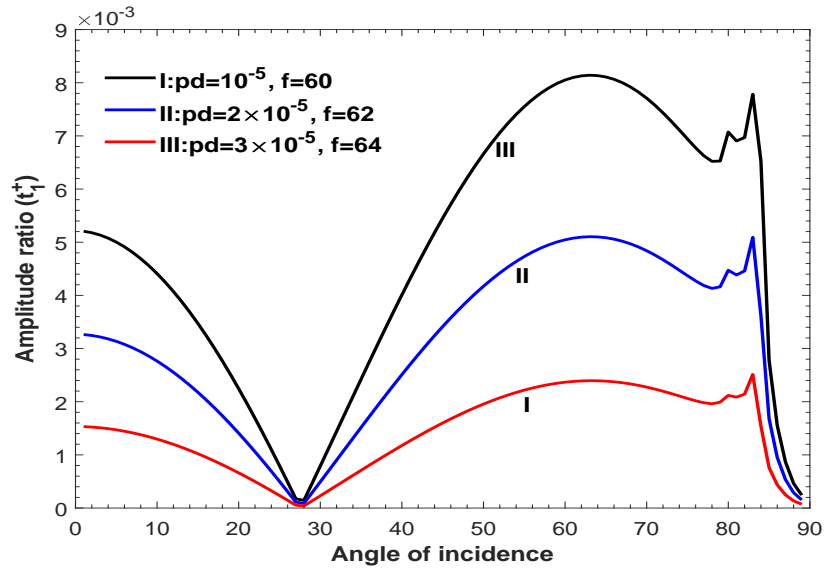
Figure 4.11: Variation of t_1^+ with α_0 for different values of pd and ω/pc_0.
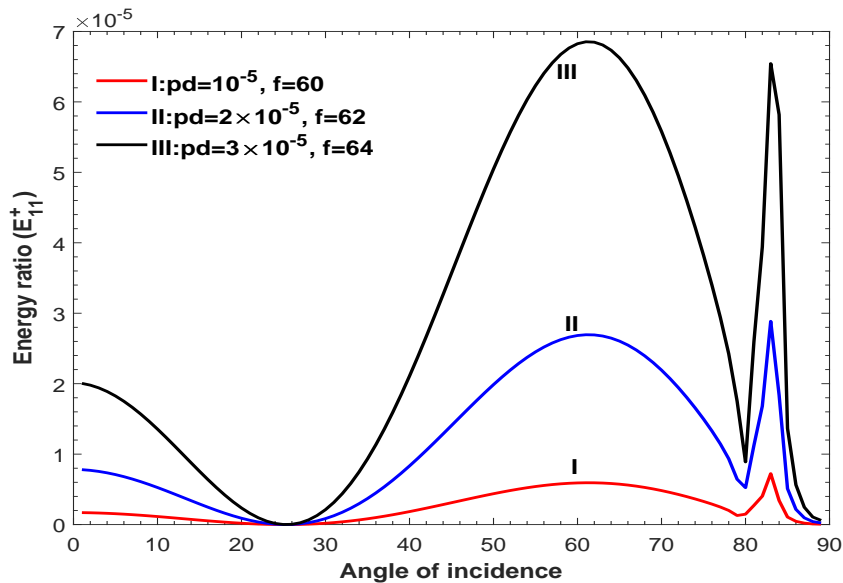
Figure 4.12: Variation of E_{11}^+ with α_0 for different values of pd and ω/pc_0.

Similar natures of (E_{11}^+, E_{21}^+) with (r_1^+, t_1^+) and (E_{11}^-, E_{21}^-) with (r_1^-, t_1^-) are observed in Figures 4.12-4.15. We come to know that the values of amplitude and energy ratios

increase upto certain extend with the increase of pd and ω/pc_0. It has been observed that there are irregularities in the figures corresponding to r_1^+, t_1^+, E_{11}^+, E_{21}^+ between the angles 75^0 and 85^0, while regular for r_1^-, t_1^-, E_{11}^-, E_{21}^-.
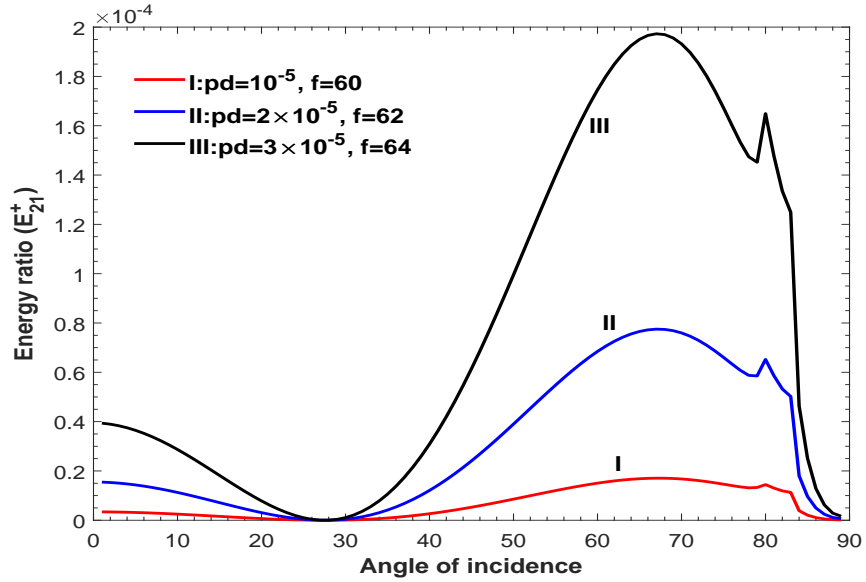
Figure 4.13: Variation of E_{21}^+ with α_0 for different values of pd and ω/pc_0.
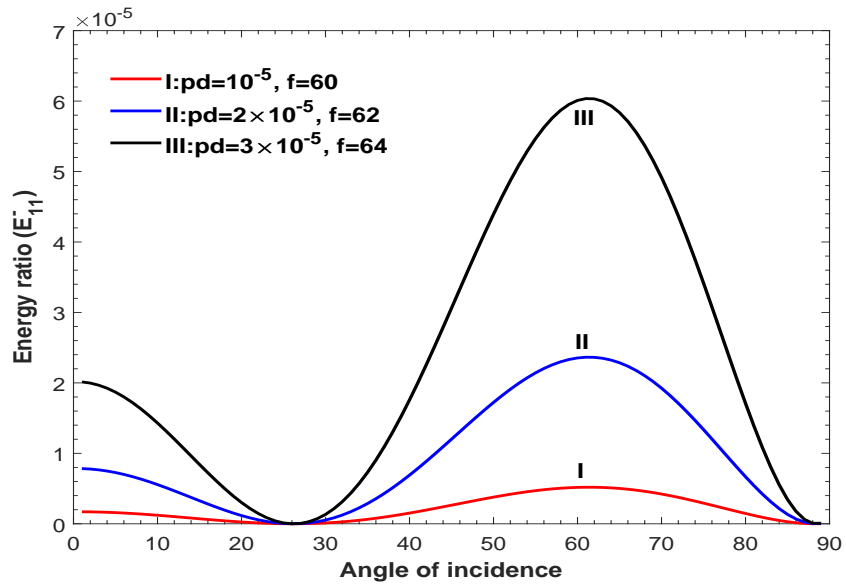
Figure 4.14: Variation of E_{11}^- with α_0 for different values of pd and ω/pc_0.

The existence of critical angles for $(\alpha_{11}^+, \alpha_{21}^+)$ and no critical angles for $(\alpha_{11}^-, \alpha_{21}^-)$ through the Spectrum theorem make these differences. These irregularities and critical angles depend on the corrugation and frequency parameter. No irregularities and no irregular waves exist if the corrugation parameter is equal to zero. With the increase of ω/pc_0, the critical angles also increase. We also see that the amplitude and energy ratios corresponding to the regularly reflected and transmitted waves are independent of corrugation and frequency parameters.
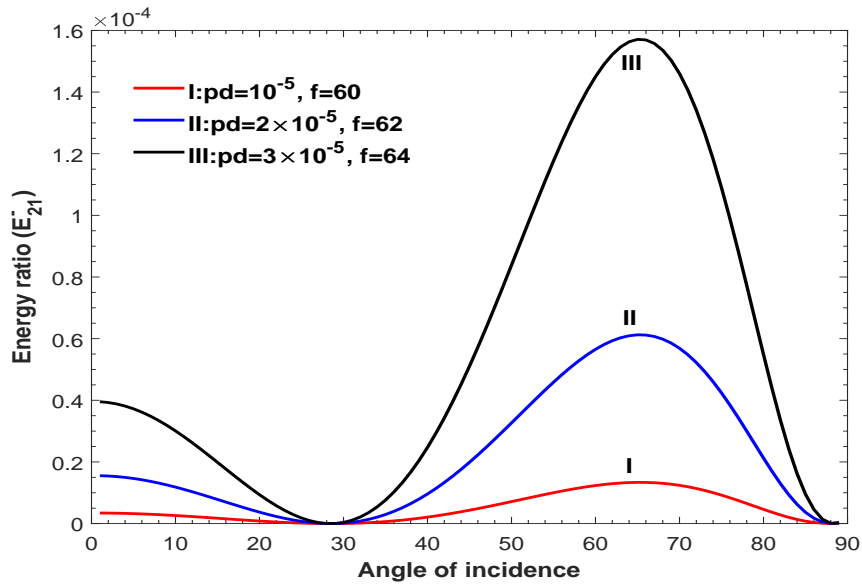
Figure 4.15: Variation of E_{21}^- with α_0 for different values of pd and ω/pc_0.

4.8.2   Effect of relaxation parameters

We have seen the effects of the characteristic time of rubber relaxation (τ_R, τ_R') on the amplitude and energy ratios through the Figures 4.16-4.21. The minimum effect of (τ_R, τ_R') on reflection and transmission coefficients $(r,\ t)$ as well as energy ratios E_1 and E_2 due to regular waves have been observed near $\alpha_0 = 60^0$.
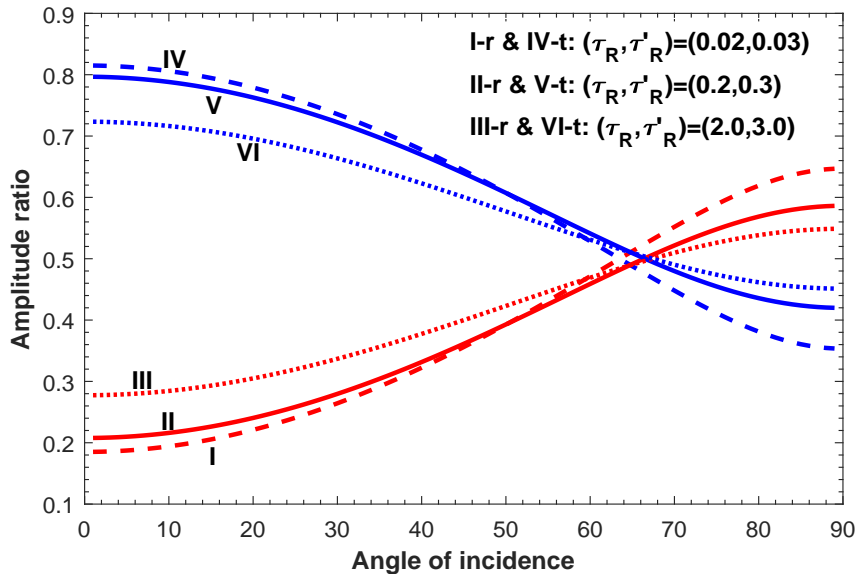
Figure 4.16: Variation of r and t with α_0 for different values of (τ_R, τ'_R).
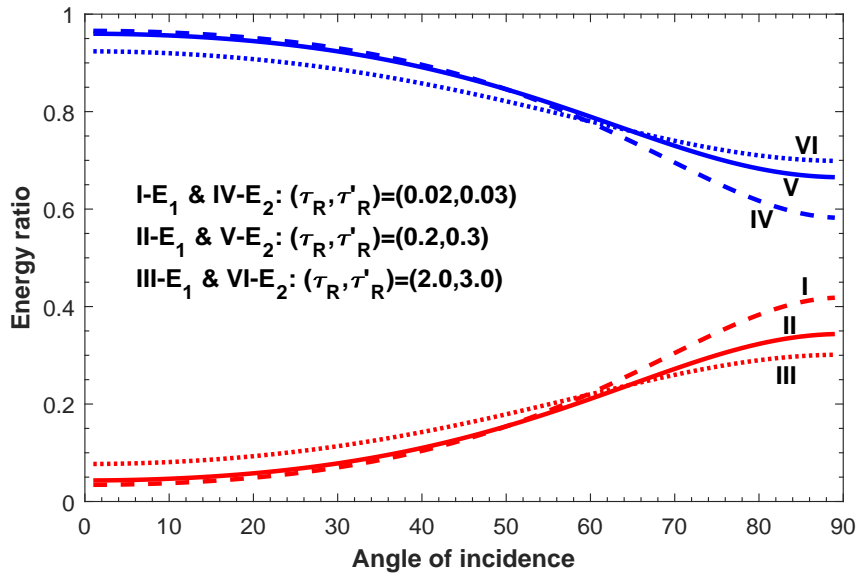
Figure 4.17: Variation of E_1 and E_2 with α_0 for different values of (τ_R, τ'_R).
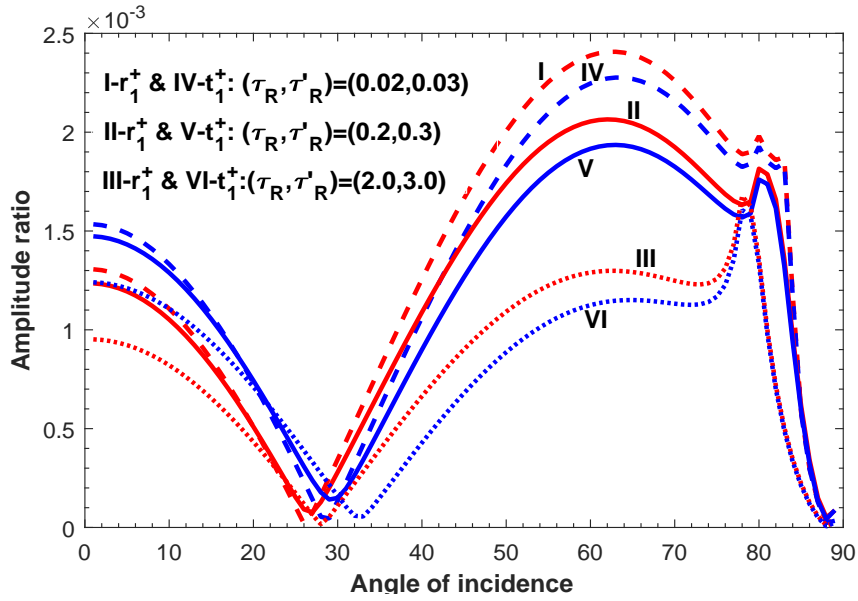
Figure 4.18: Variation of r_1^+ and t_1^+ with α_0 for different values of (τ_R, τ_R').
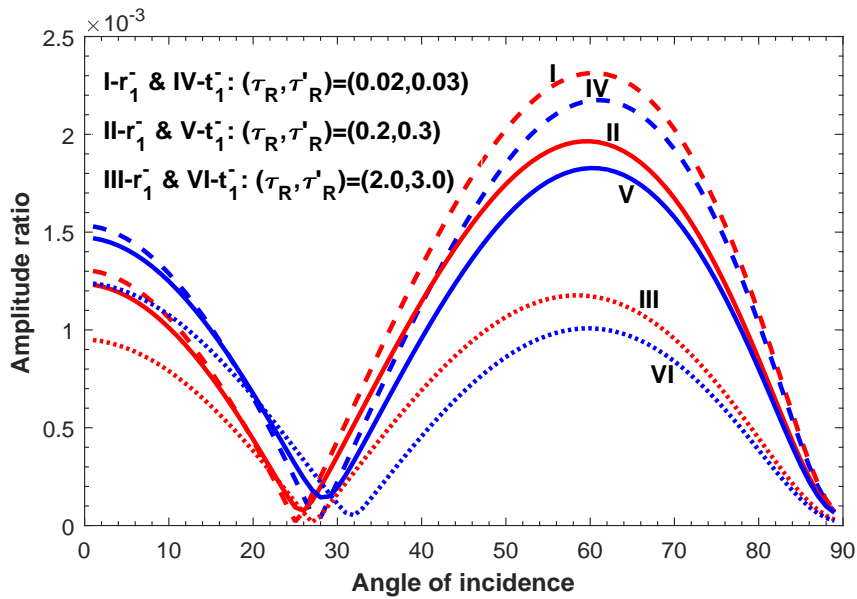
Figure 4.19: Variation of r_1^- and t_1^- with α_0 for different values of (τ_R, τ_R').

The relaxation times (τ_R, τ_R') on E_{11}^+, E_{21}^+, r_1^+ and t_1^+ has minimum and maximum effects near 30^0 and 64^0 respectively. It is also noticed that the minimum effect of (τ_R, τ_R') on E_{11}^-, E_{21}^-, r_1^- and t_1^- is observed near $\alpha_0 = 30^0$ and grazing angle of incidence.
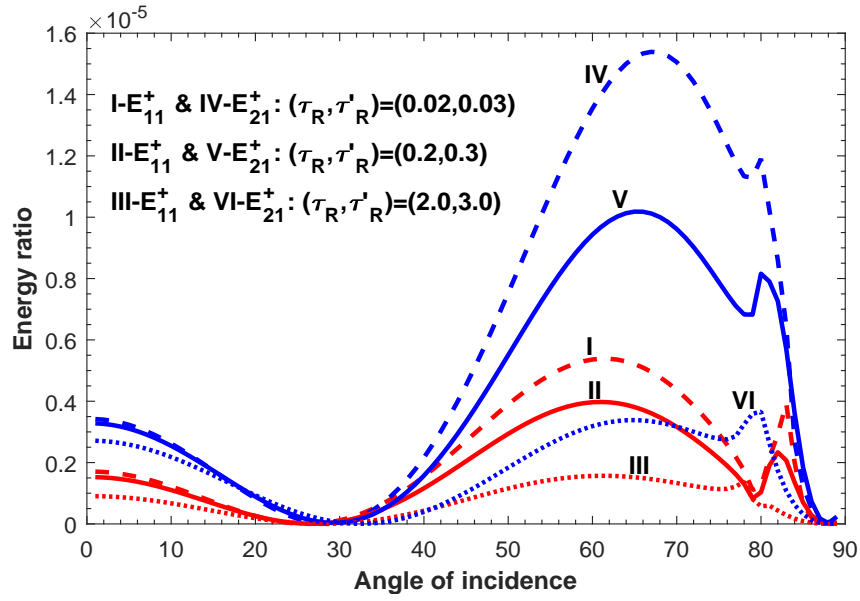
Figure 4.20: Variation of E_{11}^{+} and E_{21}^{+} with α_0 for different values of (τ_R, τ_R').
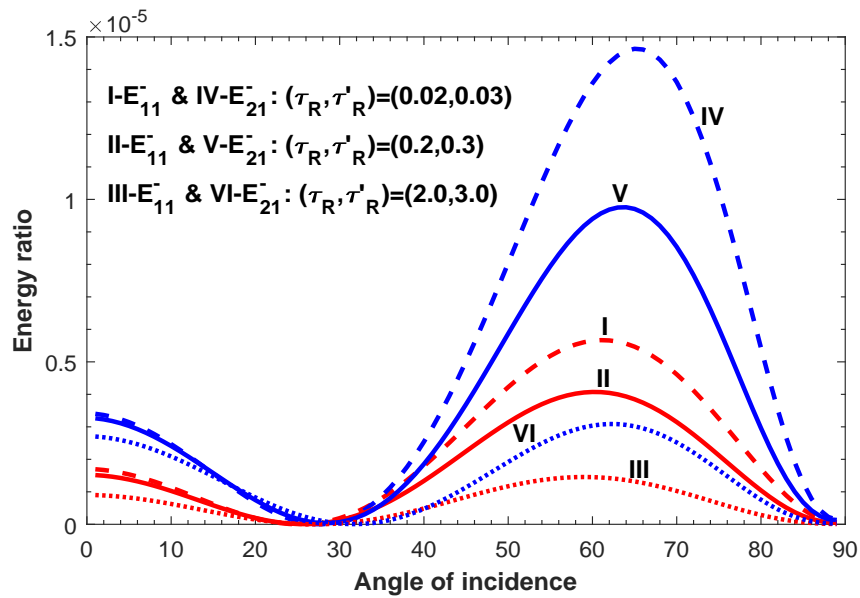
Figure 4.21: Variation of E_{11}^{-} and E_{21}^{-} with α_0 for different values of (τ_R, τ_R').

4.9   Conclusions

The problem of incident qSH-wave at a corrugated interface between two different nematic elastomer half-spaces has been investigated. We have obtained the amplitude and energy ratios corresponding to regularly and irregularly reflected and transmitted waves with the help of Rayleigh's method of approximation. These amplitude and energy ratios are computed numerically for a specific model, $z = d \cos px$ and the effect of corrugation and frequency parameters on these amplitude and energy ratios are discussed. We may conclude with the following remarks:

(i) The angles corresponding to the reflected and transmitted waves increase with the increase of the angle of incidence.

(ii) All amplitude and energy ratios corresponding to irregular waves are functions of the angle of incidence, elastic constants, coupling constants, the characteristic time of rubber relaxation, the director rotation-times, frequency and corrugation parameters.

(iii) The amplitude ratios corresponding to the regularly reflected and transmitted waves are greater in magnitude than those due to irregular waves.

(iv) The values of energy ratio corresponding to irregular waves are found to be significantly small in comparison to those due to regular waves.

(v) Theoretically and numerically, the amplitude and the energy ratios corresponding to the regular waves are independent of corrugation and frequency parameters.

(vi) The values of amplitude and energy ratios corresponding to irregular waves show linearly and non-linearly increase, respectively, with the increase of corrugation parameters.

(vii) The sum of all energy ratio is approximately unity at each value of incident angle which ensures the law of conservation of energy.

(viii) The results of Ben-Menahem and Singh (1981), Singh (2015) and Asano (1960) of the relevant problems are recovered from the present work.

Chapter 5

Waves due to corrugated interface between two dissimilar incompressible transversely isotropic fibre-reinforced elastic half-spaces[4]

5.1   Introduction

A composite material is a material made from two or more constituent materials with significantly different physical or chemical properties but when combined produce a material with characteristics different from the individual components. The constituent materials are of two main categories - matrix and reinforcement. The matrix material surrounds and supports the reinforcement materials by maintaining their relative positions. The reinforcements impart their special mechanical and physical properties to enhance the matrix properties. Reinforcement usually adds rigidity and greatly impedes crack propagation. Fibre-reinforced composites are materials in which a fibre made of one material is embedded in another material. They are widely used in many structural engineering for they possess high stiffness, strength and toughness often comparable with structural metal alloys. The strength and the

---

[4]*Mechanics of Advanced Materials and Structures (2020)*

unbendingness of the material rely on the mechanical properties of the constituents and the process of stress transfer occurring at the fibre/matrix interface. In nature, composite materials are not generally isotropic rather anisotropic and hence the rigidness of the materials largely depend on the direction of the forces and moments applied (Spencer, 1984).

A transversely isotropic material is one with physical properties which are symmetric about an axis that is normal to a plane of isotropy. This transverse plane has infinite planes of symmetry and thus within this plane the material properties are the same in all directions. This type of material exhibits hexagonal symmetry, so the number of independent constants in the linear constitutive relations reduced to 5. Further the presence of incompressibility constraint on the transversely isotropic theory results in the stress-strain relationship having only three material constants. Transverse isotropy is observed in sedimentary rocks at long wavelengths. Each layer has approximately the same properties in-plane but different properties through the thickness. The plane of each layer is the plane of isotropy and the vertical axis is the axis of symmetry. At present, despite their high cost, these materials are more and more popular in high-performance material products owing to its superiority in strength and durability, lightweight yet strong enough to take harsh loading conditions such as aerospace components, boat and scull hulls, bicycle frames and racing car bodies. Its applicability increased in the realm of orthopaedic surgery as well (Reid, 2018).

In this chapter, we have attempted the problem of elastic wave incident at an irregular interface between two different incompressible transversely isotropic fibre-reinforced medium using Rayleigh method. There can exist two reflected and transmitted quasi shear waves in certain limit of propagation, the existence of which depends on the formation of the associated slowness and in such angular range, the outer slowness is re-entrant. The usual stress-strain relations are modified to take into account the incompressibility constraint with pressure (Singh *et al.*, 2014). The

closed form expressions for modulus of coefficients due to reflection and transmission as well as the energy distribution to various waves at the irregular interface are obtained. Numerically, these energy ratios and coefficients are computed and are plotted in the form of graphs using MATLAB programming. The results of Singh (2007b) and Singh *et al.* (2014) are obtained from this work.

5.2 Governing equation

The constitutive equation showing stress-strain relationship which is appropriate for small deformation of an incompressible transversely isotropic elastic material has been derived by Baylis and Green (1986)

$$\sigma = -p^*I + 2\mu_T\epsilon + 2(\mu_L - \mu_T)\{\mathbf{e} \otimes (\epsilon\mathbf{e}) + (\epsilon\mathbf{e}) \otimes \mathbf{e}\} + 4(\mu_\mathbf{E} - \mu_\mathbf{L})\{\mathbf{e}(\epsilon\mathbf{e})\}\mathbf{e} \otimes \mathbf{e}, \quad (5.1)$$

where p^* is the pressure such that $tr\ \epsilon = 0$, ϵ is an infinitesimal strain tensor, σ is the stress tensor, $\mathbf{e}$ is an unit vector for the transversely isotropic axis, μ_L, μ_T and μ_E are longitudinal, transverse and weighted shear moduli respectively related by

$$\mu_E = \frac{E_L}{E_T}\mu_T, \quad (5.2)$$

where the longitudinal and transverse Young's muduli are represented by E_L and E_T respectively. If the material is highly anisotropic, it is observed that $E_L \gg E_T$ so that Eq. (5.2) implied that the order of magnitude of μ_E would be larger than μ_T.

Consider a cartesian system $Ox_1x_2x_3$ in which Ox_1 is parallel to the fibre direction of the transverse isotropy. The stress-strain relationships given by Eq.(5.1) reduces to the form

$$\sigma_{ij} = -p^*\delta_{ij} + 2\mu_T\epsilon_{ij} + 2(\mu_L - \mu_T)(\delta_{i1}\epsilon_{j1} + \epsilon_{i1}\delta_{j1}) + 4(\mu_E - \mu_L)\epsilon_{11}\delta_{i1}\delta_{j1} \quad (5.3)$$

The stress tensor in terms of displacement component (u_1, u_2, u_3) can be written as

$$\sigma_{11} = 2(2\mu_E - \mu_T)u_{1,1} - p^*, \quad \sigma_{22} = 2\mu_Tu_{2,2} - p^*, \quad \sigma_{33} = 2\mu_Tu_{3,3} - p^*,$$

$$\sigma_{12} = \mu_L(u_{1,2} + u_{2,1}), \quad \sigma_{13} = \mu_L(u_{1,3} + u_{3,1}), \quad \sigma_{23} = \mu_T(u_{2,3} + u_{3,2}). \qquad (5.4)$$

The general equation of motion for the elastic waves in an incompressible elastic medium without the body force is

$$\sigma_{ij,j} = \rho \ddot{u}_i, \quad (i, j = 1, 2, 3) \qquad (5.5)$$

where ρ is the density of the medium and superimposed dot is derivative with respect to time.

Inserting Equation (5.4) into (5.5), we get

$$2(2\mu_E - \mu_T)u_{1,11} + \mu_L(u_{1,22} + u_{2,12}) + \mu_L(u_{1,33} + u_{3,13}) - p_{,1}^* = \rho \ddot{u}_1, \qquad (5.6)$$

$$\mu_L(u_{1,12} + u_{2,11}) + 2\mu_T u_{2,22} + \mu_T(u_{2,33} + u_{3,23}) - p_{,2}^* = \rho \ddot{u}_2, \qquad (5.7)$$

$$\mu_L(u_{1,13} + u_{3,11}) + \mu_T(u_{2,23} + u_{3,22}) + 2\mu_T u_{3,33} - p_{,3}^* = \rho \ddot{u}_3. \qquad (5.8)$$

The incompressibility condition in the linearized form may be represented by the relation

$$u_{1,1} + u_{2,2} + u_{3,3} = 0 \qquad (5.9)$$

5.3 Wave propagation

Consider wave propagation in $x_1 x_2$-plane such that the x_1 and x_3-axis lies horizontal while the x_2-axis is vertical. Suppose two different half-spaces, $\Omega = \{(x_1, x_2) : x_1 \in \mathbb{R}, x_2 \in [\zeta, \infty)\}$ and $\Omega' = \{(x_1, x_2) : x_1 \in \mathbb{R}, x_2 \in (-\infty, \zeta)\}$, are separated by $x_2 = \zeta(x_1)$ which is periodic in x_1 and does not dependent on x_3 whose mean value being zero. The parameters in Ω are labelled without dashes, while the parameters in Ω' are labelled with dashes. The function $\zeta(x_1)$ is expanded by using Fourier series as

$$\zeta(x_1) = \sum_{n=1}^{\infty} \left(\zeta_{+n} e^{inpx_1} + \zeta_{-n} e^{-inpx_1} \right), \qquad (5.10)$$

where the coefficients of Fourier series expansion $\zeta_{\pm n}$ is of order n, the wavenumber is represented by p and $\imath = \sqrt{-1}$.

If we insert d, c_n and s_n such that

$$\zeta_{\pm 1} = \frac{d}{2}, \qquad \zeta_{\pm n} = \frac{c_n \mp \imath s_n}{2}, \quad (n = 2, 3, 4, ...)$$

then

$$\zeta(x_1) = d\cos(px_1) + \sum_{n=2}^{\infty}\{c_n\cos(npx_1) + s_n\sin(npx_1)\}. \tag{5.11}$$

If the interface of the wave takes only one term $\zeta(x_1) = d\cos(px_1)$, then the wavelength and amplitude of corrugation will be $2\pi/p$ and d respectively.

The equations of motion in an incompressible transversely isotropic fibre-reinforced elastic half-space Ω in the absence of body force reduces to

$$2(2\mu_E - \mu_T)u_{1,11} + \mu_L(u_{1,22} + u_{2,12}) - p^*_{,1} = \rho\ddot{u}_1, \tag{5.12}$$

$$\mu_L(u_{1,12} + u_{2,11}) + 2\mu_T u_{2,22} - p^*_{,2} = \rho\ddot{u}_2, \tag{5.13}$$

Similarly, in half-space Ω' we have

$$2(2\mu'_E - \mu'_T)u'_{1,11} + \mu'_L(u'_{1,22} + u'_{2,12}) - p'^*_{,1} = \rho\ddot{u}'_1, \tag{5.14}$$

$$\mu'_L(u'_{1,12} + u'_{2,11}) + 2\mu'_T u'_{2,22} - p'^*_{,2} = \rho\ddot{u}'_2. \tag{5.15}$$

Suppose an elastic wave be incident with an angle α at $x_2 = \zeta(x_1)$. There exists regular and irregular waves due to undulated nature of the interface (Asano, 1961). The total displacement components in the half-spaces $\{\Omega, \Omega'\}$ with pressure fields are given by

$$<u_1, u_2, p^*> = \sum_{m=0}^{2} <A_m d_1^{(m)}, A_m d_2^{(m)}, k_m B_m> \exp(iP_m)$$

$$+ \sum_{m=1}^{2}\sum_{n=1}^{\infty} <A_{mn}^{\pm}d_{1\pm}^{(mn)}, A_{mn}^{\pm}d_{2\pm}^{(mn)}, k_m B_{mn}^{\pm}> \exp(iP_{mn}^{\pm}), \tag{5.16}$$

$$< u_1', u_2', p'^* > = \sum_{m=3}^{4} < A_m d_1^{(m)}, A_m d_2^{(m)}, k_m B_m' > \exp(iP_m)$$

$$+ \sum_{m=3}^{4} \sum_{n=1}^{\infty} < A_{mn}^{\pm} d_{1\pm}^{(mn)}, A_{mn}^{\pm} d_{2\pm}^{(mn)}, k_m B_{mn}'^{\pm} > \exp(iP_{mn}^{\pm}), \qquad (5.17)$$

where $P_m = k_m(x_1 p_1^{(m)} + x_2 p_2^{(m)} - c_m t)$, $P_{mn}^{\pm} = k_m(x_1 p_{1\pm}^{(mn)} + x_2 p_{2\pm}^{(mn)} - c_m t)$, A_m and $A_{mn}^{\pm}$ denote amplitude constants with phase speed c_m, k_m denotes the wavenumber, $(d_1^{(m)}, d_2^{(m)})$ and $(d_{1\pm}^{(mn)}, d_{2\pm}^{(mn)})$ are unit displacement vectors, $(p_1^{(m)}, p_2^{(m)})$ and $(p_{1\pm}^{(mn)}, p_{2\pm}^{(mn)})$ are unit propagation vectors. Noted that $m = 0$, $m = 1, 2$ and $m = 3, 4$ denote for the wave incidence, regularly reflected and transmitted waves respectively, while $mn = 1n, 2n$ and $mn = 3n, 4n$ denote for the irregularly reflected and transmitted waves respectively.

The Snell's law (Singh, 2007b) may be represented by

$$k_0 p_1^{(0)} = k_q p_1^{(q)}, \quad q = 1(1)4. \qquad (5.18)$$

The angles of irregular waves and those of regular ones are related through spectrum theorem given by Abubakar (1962c)

$$\sin \alpha_{mn}^{\pm} = \sin \alpha_m \pm \frac{np}{k_m}, \quad m = 1(1)4 \quad \text{and} \quad n = 1, 2, 3, ... \qquad (5.19)$$

Using Eqs. (5.16) and (5.17) into Eqs. (5.12)-(5.15), the expressions of propagation velocity due to the incident wave, regularly reflected and transmitted waves at $\mathbf{p} = (p_1^{(m)}, 0, p_3^{(m)})$ and $\mathbf{p}' = (p_1'^{(m)}, 0, p_3'^{(m)})$ are obtained as

$$c_m^2 = \begin{cases} \frac{\mu_L - 4(\mu_L - \mu_E)(p_1^{(m)})^2 (p_2^{(m)})^2}{\rho}, & m = 0, 1, 2 \\ \frac{\mu_L' - 4(\mu_L' - \mu_E')(p_1'^{(m)})^2 (p_2'^{(m)})^2}{\rho'}, & m = 3, 4. \end{cases} \qquad (5.20)$$

Notice that these velocities depend on the angle of propagation and hence, these waves are quasi-nature.

5.4 Boundary conditions

The suitable boundary conditions for this problem at $x_2 = \zeta(x_1)$ are

(i) the displacements components are continuous,

(ii) the shear tractions are continuous,

(iii) the normal tractions are continuous.

These boundary conditions can be written as

$$u_1 = u_1', \quad u_2 = u_2', \tag{5.21}$$

$$\sigma_{12}(1 - \zeta'^2) + (\sigma_{22} - \sigma_{11})\zeta' = \sigma_{12}'(1 - \zeta'^2) + (\sigma_{22}' - \sigma_{11}')\zeta', \tag{5.22}$$

$$\sigma_{22} - 2\sigma_{12}\zeta' + \sigma_{11}\zeta'^2 = \sigma_{22}' - 2\sigma_{12}'\zeta' + \sigma_{11}'\zeta'^2. \tag{5.23}$$

Using Eq. (5.4) into Eqs.(5.22) and (5.23), we have

$$\mu_L(u_{1,2} + u_{2,1})(1 - \zeta'^2) + \{2\mu_T(u_{1,1} + u_{2,2}) - 4\mu_E u_{1,1}\}\zeta'$$

$$= \mu_L'(u_{1,2}' + u_{2,1}')(1 - \zeta'^2) + \{2\mu_T'(u_{1,1}' + u_{2,2}') - 4\mu_E' u_{1,1}'\}\zeta', \tag{5.24}$$

$$2\mu_T u_{2,2} - p^* - 2\mu_L(u_{1,2} + u_{2,1})\zeta' + \{2(2\mu_E - \mu_T)u_{1,1} - p^*)\}\zeta'^2$$

$$= 2\mu_T' u_{2,2}' - p^* - 2\mu_L'(u_{1,2}' + u_{2,1}')\zeta' + \{2(2\mu_E' - \mu_T')u_{1,1}' - p^*)\}\zeta'^2. \tag{5.25}$$

where

$$\zeta' = \pm \sum_{n=1}^{\infty} \imath np \zeta_{\pm n} e^{\pm \imath npx_1}.$$

Using Eqs.(5.16)-(5.19) into (5.21), (5.24) and (5.25), we get

$$\sum_{m=0}^{2} A_m d_1^{(m)} e^{\imath \zeta k_m p_2^{(m)}} + \sum_{m=1}^{2} \sum_{n=1}^{\infty} A_{mn}^{\pm} d_{1\pm}^{(mn)} e^{\pm \imath npx_1} e^{\imath \zeta k_m p_{2\pm}^{(mn)}}$$

$$= \sum_{m=3}^{4} \sum_{n=1}^{\infty} \left(A_m d_1^{(m)} e^{\imath \zeta k_m p_2^{(m)}} + A_{mn}^{\pm} d_{1\pm}^{(mn)} e^{\pm \imath npx_1} e^{\imath \zeta k_m p_{2\pm}^{(mn)}} \right), \tag{5.26}$$

$$\sum_{m=0}^{2} A_m d_2^{(m)} e^{\imath \zeta k_m p_2^{(m)}} + \sum_{m=1}^{2} \sum_{n=1}^{\infty} A_{mn}^{\pm} d_{2\pm}^{(mn)} e^{\pm \imath npx_1} e^{\imath \zeta k_m p_{2\pm}^{(mn)}}$$

$$= \sum_{m=3}^{4} \sum_{n=1}^{\infty} \left(A_m d_2^{(m)} e^{\imath \zeta k_m p_2^{(m)}} + A_{mn}^{\pm} d_{2\pm}^{(mn)} e^{\pm \imath npx_1} e^{\imath \zeta k_m p_{2\pm}^{(mn)}} \right), \tag{5.27}$$

$$\sum_{m=0}^{2} A_m \{(1-\zeta'^2)\mu_L\lambda_m + \zeta'\gamma_m\}k_m e^{\iota\zeta k_m p_2^{(m)}} + \sum_{m=1}^{2}\sum_{n=1}^{\infty} A_{mn}^{\pm}\{(1-\zeta'^2)\mu_L\lambda_{mn}$$

$$+ \zeta'\gamma_{mn}\}k_m e^{\pm \iota n p x_1} e^{\iota\zeta k_m p_{2\pm}^{(mn)}} = \sum_{m=3}^{4} A_m \{(1-\zeta'^2)\mu_L'\lambda_m + \zeta'\gamma_m'\}k_m e^{\iota\zeta k_m p_2^{(m)}}$$

$$+ \sum_{m=3}^{4}\sum_{n=1}^{\infty} A_{mn}^{\pm}\{(1-\zeta'^2)\mu_L'\lambda_{mn} + \zeta'\gamma_{mn}'\}k_m e^{\pm \iota n p x_1} e^{\iota\zeta k_m p_{2\pm}^{(mn)}}, \qquad (5.28)$$

$$\sum_{m=0}^{2} A_m [2\mu_T d_2^{(m)}p_2^{(m)} - F^{(m)} - 2\mu_L\lambda_m\zeta' + \{(4\mu_E - 2\mu_T)d_1^{(m)}p_1^{(m)} - F^{(m)}\}\zeta'^2]k_m$$

$$\times e^{\iota\zeta k_m p_2^{(m)}} + \sum_{m=1}^{2}\sum_{n=1}^{\infty} A_{mn}^{\pm}[2\mu_T d_{2\pm}^{(mn)}p_{2\pm}^{(mn)} - F^{(mn)} - 2\mu_L\lambda_{mn}\zeta' + \{(4\mu_E - 2\mu_T)d_{1\pm}^{(mn)}$$

$$\times p_{1\pm}^{(mn)} - F^{(mn)})\zeta'^2]k_m e^{\pm \iota n p x_1} e^{\iota\zeta k_m p_{2\pm}^{(mn)}} = \sum_{m=3}^{4} A_m [2\mu_T' d_2^{(m)}p_2^{(m)} - F'^{(m)} - 2\mu_L'\lambda_m\zeta'$$

$$+ \{(4\mu_E' - 2\mu_T')d_1^{(m)}p_1^{(m)} - F'^{(m)}\}\zeta'^2\}k_m e^{\iota\zeta k_m p_2^{(m)}} + \sum_{m=3}^{4}\sum_{n=1}^{\infty} A_{mn}^{\pm}[2\mu_T' d_{2\pm}^{(mn)}p_{2\pm}^{(mn)}$$

$$- F'^{(mn)} - 2\mu_L'\lambda_{mn}\zeta' + \{(4\mu_E' - 2\mu_T')d_{1\pm}^{(mn)}p_{1\pm}^{(mn)} - F'^{(mn)}\}\zeta'^2]k_m e^{\pm \iota n p x_1} e^{\iota\zeta k_m p_{2\pm}^{(mn)}},$$

$$(5.29)$$

where

$$\lambda_m = d_1^{(m)}p_2^{(m)} + d_2^{(m)}p_1^{(m)}, \quad \lambda_{mn} = d_{1\pm}^{(mn)}p_{2\pm}^{(mn)} + d_{2\pm}^{(mn)}p_{1\pm}^{(mn)}, \quad \gamma_m = -4\mu_E d_2^{(m)}p_2^{(m)},$$

$$\gamma_m' = -4\mu_E' d_2^{(m)}p_2^{(m)}, \quad \gamma_{mn} = -4\mu_E d_{2\pm}^{(mn)}p_{2\pm}^{(mn)}, \quad \gamma_{mn}' = -4\mu_E' d_{2\pm}^{(mn)}p_{2\pm}^{(mn)},$$

$$F^{(m)} = 2(2\mu_E - \mu_T)d_1^{(m)}p_1^{(m)3} + 2\mu_L p_1^{(m)}p_2^{(m)}(d_1^{(m)}p_2^{(m)} + d_2^{(m)}p_1^{(m)}) + 2\mu_T d_2^{(m)}p_2^{(m)3},$$

$$F^{(mn)} = 2(2\mu_E - \mu_T)d_{1\pm}^{(mn)}p_{1\pm}^{(mn)3} + 2\mu_L p_{1\pm}^{(mn)}p_{2\pm}^{(mn)}(d_{1\pm}^{(mn)}p_{2\pm}^{(mn)} + d_{2\pm}^{(mn)}p_{1\pm}^{(mn)}) + 2\mu_T d_{2\pm}^{(mn)}p_{2\pm}^{(mn)3},$$

$$F'^{(m)} = 2(2\mu_E' - \mu_T')d_1^{(m)}p_1^{(m)3} + 2\mu_L' p_1^{(m)}p_2^{(m)}(d_1^{(m)}p_2^{(m)} + d_2^{(m)}p_1^{(m)}) + 2\mu_T' d_2^{(m)}p_2^{(m)3},$$

$$F'^{(mn)} = 2(2\mu_E' - \mu_T')d_{1\pm}^{(mn)}p_{1\pm}^{(mn)3} + 2\mu_L' p_{1\pm}^{(mn)}p_{2\pm}^{(mn)}(d_{1\pm}^{(mn)}p_{2\pm}^{(mn)} + d_{2\pm}^{(mn)}p_{1\pm}^{(mn)}) + 2\mu_T' d_{2\pm}^{(mn)}p_{2\pm}^{(mn)3},$$

The reflection and transmission coefficients corresponding to the regular and irregular waves will be obtained using these equations.

5.5 Reflection and transmission coefficients

Following Rayleigh's method of approximation, we assume that the amplitude
and slope of the irregular interfaces are small enough such that

$$e^{\pm \imath \zeta p_2^{(0)}} = 1 \pm \imath \zeta p_2^{(0)}, \quad e^{\pm \imath \zeta p_{2\pm}^{(1n)}} = 1 \pm \imath \zeta p_{2\pm}^{(1n)}, \quad \text{etc.} \tag{5.30}$$

5.5.1 For regular waves

Using the Fourier series expansion given by Eq.(5.10) and Eq.(5.30) into Eqs.(5.26)-
(5.29) and picking the terms not containing ζ and x_1, we get a system of four non-
homogeneous equations as

$$[A_{dp}]X = F, \quad d,p = 1,2,3,4 \tag{5.31}$$

where

$$[A_{dp}] = \begin{bmatrix} d_1^{(1)} & d_1^{(2)} & -d_1^{(3)} & -d_1^{(4)} \\ d_2^{(1)} & d_2^{(2)} & -d_2^{(3)} & -d_2^{(4)} \\ l_1 & l_2 & -l_3 & -l_4 \\ m_1 & m_2 & -m_3 & -m_4 \end{bmatrix}, \quad X = \begin{bmatrix} X_1/X_0 \\ X_2/X_0 \\ X_3/X_0 \\ X_4/X_0 \end{bmatrix}, \quad F = \begin{bmatrix} f_1 \\ f_2 \\ f_3 \\ f_4 \end{bmatrix},$$

$$f_1 = -d_1^{(0)}, \; f_2 = -d_2^{(0)}, \; f_3 = -\mu_L(d_1^{(0)}p_2^{(0)} + d_2^{(0)}p_1^{(0)}), \; f_4 = -(2\mu_T d_2^{(0)}p_2^{(0)} - F^{(0)}),$$

$$l_1 = \frac{k_1}{k_0}\mu_L(d_1^{(1)}p_2^{(1)} + d_2^{(1)}p_1^{(1)}), \quad l_2 = \frac{k_2}{k_0}\mu_L(d_1^{(2)}p_2^{(2)} + d_2^{(2)}p_1^{(2)}),$$

$$l_3 = -\frac{k_3}{k_0}\mu_L'(d_1^{(3)}p_2^{(3)} + d_2^{(3)}p_1^{(3)}), \quad l_4 = -\frac{k_4}{k_0}\mu_L'(d_1^{(4)}p_2^{(4)} + d_2^{(4)}p_1^{(4)}),$$

$$m_1 = \frac{k_1}{k_0}(2\mu_T d_2^{(1)}p_2^{(1)} - F^{(1)}), \quad m_2 = \frac{k_2}{k_0}(2\mu_T d_2^{(2)}p_2^{(2)} - F^{(2)}),$$

$$m_3 = -\frac{k_3}{k_0}(2\mu_T'd_2^{(3)}p_2^{(3)} - F'^{(3)}), \quad m_4 = -\frac{k_4}{k_0}(2\mu_T'd_2^{(4)}p_2^{(4)} - F'^{(4)}).$$

It may be noted that,

$$d_1^{(0)} = p_2^{(0)} = \cos\alpha, \; d_2^{(0)} = -p_1^{(0)} = \sin\alpha; \quad d_1^{(1)} = p_2^{(1)}, \; d_2^{(1)} = -p_1^{(1)}; \; d_1^{(2)} = p_2^{(2)},$$

$$d_2^{(2)} = -p_1^{(2)}; \; d_1^{(3)} = p_2^{(3)}, \; d_2^{(3)} = -p_1^{(3)}; \; d_1^{(4)} = p_2^{(4)}, \; d_2^{(4)} = -p_1^{(4)}. \tag{5.32}$$

On solving Eq.(5.31), we get the reflection and transmission coefficients for the regular shear-waves as

$$r_1 = \frac{|A_{dp}|_1}{|A_{dp}|}, \qquad r_2 = \frac{|A_{dp}|_2}{|A_{dp}|}, \tag{5.33}$$

$$t_3 = \frac{|A_{dp}|_3}{|A_{dp}|}, \qquad t_4 = \frac{|A_{dp}|_4}{|A_{dp}|}. \tag{5.34}$$

The values of the determinant $|A_{dp}|_1$, $|A_{dp}|_2$, $|A_{dp}|_3$, $|A_{dp}|_4$ respectively are obtained from $|A_{dp}|$ by replacement of its 1st, 2nd, 3rd, 4th column with F.

5.5.2   For irregular waves

Comparing the coefficients of $e^{\pm \imath n p x_1}$, we have a system of four non-homogeneous equations as

$$[A_{dp}^{\pm}]X^{\pm} = F^{\pm}, \qquad d, p = 1, 2, 3, 4 \tag{5.35}$$

where

$$[A_{dp}^{\pm}]_n = \begin{bmatrix} d_{1\pm}^{(1n)} & d_{1\pm}^{(2n)} & -d_{1\pm}^{(3n)} & -d_{1\pm}^{(4n)} \\ d_{2\pm}^{(1n)} & d_{2\pm}^{(2n)} & -d_{2\pm}^{(3n)} & -d_{2\pm}^{(4n)} \\ l_1^{\pm} & l_2^{\pm} & -l_3^{\pm} & -l_4^{\pm} \\ m_1^{\pm} & m_2^{\pm} & -m_3^{\pm} & -m_4^{\pm} \end{bmatrix}, \qquad X^{\pm} = \begin{bmatrix} X_{1n}^{\pm}/X_0 \\ X_{2n}^{\pm}/X_0 \\ X_{3n}^{\pm}/X_0 \\ X_{4n}^{\pm}/X_0 \end{bmatrix}, \qquad F^{\pm} = \begin{bmatrix} f_1^{\pm} \\ f_2^{\pm} \\ f_3^{\pm} \\ f_4^{\pm} \end{bmatrix},$$

$$l_1^{\pm} = \frac{k_1}{k_0}\mu_L(d_{1\pm}^{(1n)}p_{2\pm}^{(1n)} + d_{2\pm}^{(1n)}p_{1\pm}^{(1n)}), \quad l_2^{\pm} = \frac{k_2}{k_0}\mu_L(d_{1\pm}^{(2n)}p_{2\pm}^{(2n)} + d_{2\pm}^{(2n)}p_{1\pm}^{(2n)}),$$

$$l_3^{\pm} = -\frac{k_3}{k_0}\mu_L'(d_{1\pm}^{(3n)}p_{2\pm}^{(3n)} + d_{2\pm}^{(3n)}p_{1\pm}^{(3n)}), \quad l_4^{\pm} = -\frac{k_4}{k_0}\mu_L'(d_{1\pm}^{(4n)}p_{2\pm}^{(4n)} + d_{2\pm}^{(4n)}p_{1\pm}^{(4n)}),$$

$$m_1^{\pm} = \frac{k_1}{k_0}(2\mu_T d_{2\pm}^{(1n)}p_{2\pm}^{(1n)} - F^{(1n)}), \quad m_2^{\pm} = \frac{k_2}{k_0}(2\mu_T d_{2\pm}^{(2n)}p_{2\pm}^{(2n)} - F^{(2n)}),$$

$$m_3^{\pm} = -\frac{k_3}{k_0}(2\mu_T' d_{2\pm}^{(3n)}p_{2\pm}^{(3n)} - F'^{(3n)}), \quad m_4^{\pm} = -\frac{k_4}{k_0}(2\mu_T' d_{2\pm}^{(4n)}p_{2\pm}^{(4n)} - F'^{(4n)}),$$

$$f_1^{\pm} = \imath\zeta_{\pm n}\{-d_1^{(0)}p_2^{(0)} - \frac{k_1}{k_0}d_1^{(1)}p_2^{(1)}\frac{X_1}{X_0} - \frac{k_2}{k_0}d_1^{(2)}p_2^{(2)}\frac{X_2}{X_0} + \frac{k_3}{k_0}d_1^{(3)}p_2^{(3)}\frac{X_3}{X_0} + \frac{k_4}{k_0}d_1^{(4)}p_2^{(4)}\frac{X_4}{X_0}\},$$

$$f_2^{\pm} = \imath \zeta_{\pm n}\{-d_2^{(0)}p_2^{(0)} - \frac{k_1}{k_0}d_2^{(1)}p_2^{(1)}\frac{X_1}{X_0} - \frac{k_2}{k_0}d_2^{(2)}p_2^{(2)}\frac{X_2}{X_0} + \frac{k_3}{k_0}d_2^{(3)}p_2^{(3)}\frac{X_3}{X_0} + \frac{k_4}{k_0}d_2^{(4)}p_2^{(4)}\frac{X_4}{X_0}\},$$

$$f_3^{\pm} = \imath \zeta_{\pm n}\{-g_0^{\pm} - g_1^{\pm}\frac{X_1}{X_0} - g_2^{\pm}\frac{X_2}{X_0} + g_3^{\pm}\frac{X_3}{X_0} + g_4^{\pm}\frac{X_4}{X_0}\},$$

$$f_4^{\pm} = \imath \zeta_{\pm n}\{-h_0^{\pm} - h_1^{\pm}\frac{X_1}{X_0} - h_2^{\pm}\frac{X_2}{X_0} + h_3^{\pm}\frac{X_3}{X_0} + h_4^{\pm}\frac{X_4}{X_0}\},$$

$$g_0^{\pm} = \mu_L(d_1^{(0)}p_2^{(0)} + d_2^{(0)}p_1^{(0)})p_2^{(0)}k_0^2 \mp npk_04\mu_E d_1^{(0)}p_1^{(0)},$$

$$g_1^{\pm} = \mu_L(d_1^{(1)}p_2^{(1)} + d_2^{(1)}p_1^{(1)})p_2^{(1)}k_1^2 \mp npk_14\mu_E d_1^{(1)}p_1^{(1)},$$

$$g_2^{\pm} = \mu_L(d_1^{(2)}p_2^{(2)} + d_2^{(2)}p_1^{(2)})p_2^{(2)}k_2^2 \mp npk_24\mu_E d_1^{(2)}p_1^{(2)},$$

$$g_3^{\pm} = \mu_L'(d_1^{(3)}p_2^{(3)} + d_2^{(3)}p_1^{(3)})p_2^{(3)}k_3^2 \mp npk_34\mu_E' d_1^{(3)}p_1^{(3)},$$

$$g_4^{\pm} = \mu_L'(d_1^{(4)}p_2^{(4)} + d_2^{(4)}p_1^{(4)})p_2^{(4)}k_4^2 \mp npk_44\mu_E' d_1^{(4)}p_1^{(4)},$$

$$h_0^{\pm} = (2\mu_T d_2^{(0)}p_2^{(0)} - F^{(0)})p_2^{(0)}k_0^2 \mp 2\mu_L npk_0(d_1^{(0)}p_2^{(0)} + d_2^{(0)}p_1^{(0)}),$$

$$h_1^{\pm} = (2\mu_T d_2^{(1)}p_2^{(1)} - F^{(1)})p_2^{(1)}k_1^2 \mp 2\mu_L npk_1(d_1^{(1)}p_2^{(1)} + d_2^{(1)}p_1^{(1)}),$$

$$h_2^{\pm} = (2\mu_T d_2^{(2)}p_2^{(2)} - F^{(2)})p_2^{(2)}k_2^2 \mp 2\mu_L npk_2(d_1^{(2)}p_2^{(2)} + d_2^{(2)}p_1^{(2)}),$$

$$h_3^{\pm} = (2\mu_T' d_2^{(3)}p_2^{(3)} - F'^{(3)})p_2^{(3)}k_3^2 \mp 2\mu_L' npk_3(d_1^{(3)}p_2^{(3)} + d_2^{(3)}p_1^{(3)}),$$

$$h_4^{\pm} = (2\mu_T' d_2^{(4)}p_2^{(4)} - F'^{(4)})p_2^{(4)}k_4^2 \mp 2\mu_L' npk_4(d_1^{(4)}p_2^{(4)} + d_2^{(4)}p_1^{(4)}).$$

On solving Eq.(5.35), we get the reflection and transmission coefficients for the irregular shear-waves as

$$r_{1n}^{\pm} = \frac{|A_{dp}^{\pm}|_{1n}}{|A_{dp}^{\pm}|_n}, \qquad r_{2n}^{\pm} = \frac{|A_{dp}^{\pm}|_{2n}}{|A_{dp}^{\pm}|_n}, \tag{5.36}$$

$$t_{3n}^{\pm} = \frac{|A_{dp}^{\pm}|_{3n}}{|A_{dp}^{\pm}|_n}, \qquad t_{4n}^{\pm} = \frac{|A_{dp}^{\pm}|_{4n}}{|A_{dp}^{\pm}|_n}, \tag{5.37}$$

where $|A_{dp}^{\pm}|_{mn}$ and $|A_{dp}^{\pm}|_n$ are similar representation as in Eq.(5.33) and Eq.(5.34). We have observed that these coefficients are functions of the corrugation parameters, frequency parameters, angles of propagation, unit displacement vectors, slowness vectors and elastic constants of the media.

5.6   Distribution of energy

Following Achenbach (1976), the energy due to incident wave is distributed to regular and irregular waves. The energy distribution rate can be written as

$$\wp^* = <\sigma_{2i} \cdot \dot{u}_i> + <\sigma'_{2i} \cdot \dot{u}'_i> . \tag{5.38}$$

The energy of incident wave is given by

$$E_0 = e_0 \omega X_0^2 e^{2\imath k_0 \{x_1 p_1^{(0)} + x_2 p_2^{(0)} - c_0 t\}}, \tag{5.39}$$

where $e_0 = \mu_L(d_1^{(0)} p_2^{(0)} + d_2^{(0)} p_1^{(0)}) d_1^{(0)} k_0 + 2\mu_T(d_2^{(0)} p_2^{(0)} - F^{(0)}) d_2^{(0)} k_0$.

The energy of the reflected and transmitted wave are given by

$$E = e_m \omega X_m^2 e^{2\imath k_m (x_1 p_1^{(m)} + x_2 p_2^{(m)} - c_m t)}$$
$$+ \sum_{n=1}^{\infty} e_{mn}^{\pm} \omega (X_{mn}^{\pm})^2 e^{2\imath k_m (x_1 p_{1\pm}^{(mn)} + x_2 p_{2\pm}^{(mn)} - c_m t)}, \ \ m = 1, 2, 3, 4 \tag{5.40}$$

where

(for m=1, 2) $e_m = \mu_L(d_1^{(m)} p_2^{(m)} + d_2^{(m)} p_1^{(m)}) d_1^{(m)} k_m + 2\mu_T(d_2^{(m)} p_2^{(m)} - F^{(m)}) d_2^{(m)} k_m,$

$e_{mn}^{\pm} = \mu_L(d_{1\pm}^{(mn)} p_{2\pm}^{(mn)} + d_{2\pm}^{(mn)} p_{1\pm}^{(mn)}) d_{1\pm}^{(mn)} k_m + 2\mu_T(d_{2\pm}^{(mn)} p_{2\pm}^{(mn)} - F^{(mn)}) d_{2\pm}^{(mn)} k_m,$

(for m=3, 4) $e_m = \mu'_L(d_1^{(m)} p_2^{(m)} + d_2^{(m)} p_1^{(m)}) d_1^{(m)} k_m + 2\mu'_T(d_2^{(m)} p_2^{(m)} - F'^{(m)}) d_2^{(m)} k_m,$

$e_{mn}^{\pm} = \mu'_L(d_{1\pm}^{(mn)} p_{2\pm}^{(mn)} + d_{2\pm}^{(mn)} p_{1\pm}^{(mn)}) d_{1\pm}^{(mn)} k_m + 2\mu'_T(d_{2\pm}^{(mn)} p_{2\pm}^{(mn)} - F'^{(mn)}) d_{2\pm}^{(mn)} k_m.$

When each corresponding energy is divided by the incident energy, we obtain the energy ratios for the regular and irregular waves given by

$$E_m = \Big|\frac{e_m}{e_0}\Big|\Big|\frac{X_m}{X_0}\Big|^2, \tag{5.41}$$

$$E_{mn}^{\pm} = \Big|\frac{e_{mn}^{\pm}}{e_0}\Big|\Big|\frac{X_{mn}^{\pm}}{X_0}\Big|^2. \tag{5.42}$$

These energy ratios depend on unit displacement components, elastic constants of the incompressible fibre-reinforced medium, angle of propagation, slowness vectors, corrugation and frequency parameters.

5.7 Special case, $\zeta = d\cos px_1$

If the corrugated interface is represented by $\zeta(x_1) = d\cos px_1$, d being the amplitude of corrugation. Then the coefficient $\zeta_{\pm n}$ become

$$\zeta_{\pm n} = \begin{cases} \dfrac{d}{2} & \text{if} \quad n = 1, \\ 0 & \text{if} \quad n \neq 1. \end{cases} \tag{5.43}$$

Using these values into Eqs.(5.36) and (5.37), the reflection and transmission coefficients become

$$r_{11}^{\pm} = \frac{|A_{pq}^{\pm}|_{11}}{|A_{pq}^{\pm}|_1}, \qquad r_{21}^{\pm} = \frac{|A_{pq}^{\pm}|_{21}}{|A_{pq}^{\pm}|_1}, \qquad t_{31}^{\pm} = \frac{|A_{pq}^{\pm}|_{31}}{|A_{pq}^{\pm}|_1}, \qquad t_{41}^{\pm} = \frac{|A_{pq}^{\pm}|_{41}}{|A_{pq}^{\pm}|_1}. \tag{5.44}$$

The energy ratios for this special case are obtained by assigning $n = 1$ in Eq.(5.42). These coefficients and the energy ratios obtained in this section will be calculated for a specific model and plotted in graphs.

5.8 Particular case

(a) If the corrugation of the interface is neglected, then $d = 0$. In this case, we now deal with the reflection and transmission at the plane interface of two different incompressible transversely isotropic fibre-reinforced medium. Here, the coefficients as well as the energy ratios exists only for the regular waves, which are given by Eqs.(5.33), (5.34) and (5.41) respectively. The results obtained, in this case, exactly match with the results of Singh *et al.* (2014) for the relevant problem.

(b) If the upper half-space Ω' is absent, then we are left with only the reflection from the plane free boundary. The reflection coefficients are given by Eq.(5.33) with the following modified values

$$|A_{dp}| = l_1 m_2 - l_2 m_1, \quad |A_{dp}|_1 = m_2 b_3 - l_2 b_4, \quad |A_{dp}|_2 = l_1 b_4 - m_1 b_3.$$

These are the same results as obtained by Singh (2007b) for the relevant problem.

5.9 Slowness section

To study the nature of reflected and transmitted wave, we consider the slowness section associated with the reflected and transmitted waves in the $x_1 x_2$-plane. For this, we seek the solution corresponding to equations of motion (5.12) and (5.13) in the form

$$< u_1, u_2 > = < U, V > \exp\{\iota\omega(x_1 s_1 + x_2 s_2 - t)\}, \tag{5.45}$$

where the slowness vector $\mathbf{s} = (s_1, s_2)$ is defined by $s_n = p_n/c, \quad n = 1, 2$. Inserting Eq.(5.45) into the Eqs.(5.12) and (5.13), the associated equation of slowness section is obtained as

$$a(s_1^4 + s_2^4) + c s_1^2 s_2^2 - (s_1^2 + s_2^2) = 0, \tag{5.46}$$

where

$$a = \frac{\mu_L}{\rho}, \qquad c = \frac{4\mu_E - 2\mu_L}{\rho}.$$

We differentiate Eq.(5.46) with respect to s_1 and take $\frac{ds_2}{ds_1} \to \infty$ provided $s_2 \neq 0$ for the outer section is re-entrant and obtain

$$s_2 = \sqrt{\frac{1 - c s_1^2}{2a}}. \tag{5.47}$$

With the help of Eq.(5.47), (5.46) can be expressed as a quadratic function in s_1^2 as

$$(4a^3 - ac^2)s_1^4 + (2ac - 4a^2)s_1^2 - a = 0 \tag{5.48}$$

which has a real root for

$$2a \geq c \tag{5.49}$$

Notice that when $s_2 = 0$, then Eq.(5.46) gives $s_1 = \frac{1}{\sqrt{a}}$. Thus Eq.(5.46) will have two real roots of s_2^2 provided $0 \leq s_1 \leq \frac{1}{\sqrt{a}}$.

Similarly, for the transmitted waves in the half-space Ω', we have

$$a'(s_1'^4 + s_2'^4) + c' s_1'^2 s_2'^2 - (s_1'^2 + s_2'^2) = 0, \qquad (5.50)$$

where $a' = \mu_L'/\rho'$, $c' = (4\mu_E' - 2\mu_L')/\rho'$.

The range of angle of incidence for two reflected and transmitted quasi-shear waves is

$$0 \le \alpha \le \tan^{-1}\left[\sqrt{\frac{\mu_T - \mu_L}{(2\mu_E - \mu_L - \mu_T)}}\right] \quad \text{or} \quad \tan^{-1}\left[\sqrt{\frac{\mu_T' - \mu_L'}{(2\mu_E' - \mu_L' - \mu_T')}}\right]. \qquad (5.51)$$

5.10 Numerical computations

In this section, numerical illustrations for coefficients and energy ratios are presented. We concentrate our analysis only to the possibility of having two quasi-shear waves. There are two choices for this and they are (Singh, 2007b)

$$s_1^{(0)} > 0, \ s_2^{(1)} < 0, \ s_2^{(2)} > 0 \quad \text{or} \quad s_1^{(0)} < 0, \ s_2^{(1)} > 0, \ s_2^{(2)} < 0$$

and

$$s_2'^{(3)} < 0, \ s_2'^{(4)} > 0 \quad \text{or} \quad s_2'^{(3)} > 0, \ s_2'^{(4)} < 0.$$

The following values of parameters are considered (Singh, 2007b):

(for lower half-space, Ω)

$$\mu_L = 1.05 GPa, \quad \mu_T = 0.84 GPa, \quad \mu_E = 0.63 GPa, \quad \rho = 2.1 gm/cm^3,$$

$$s_2^{(1)} = -0.36, \quad s_2^{(2)} = 0.05$$

(for upper half-space, Ω')

$$\mu_L' = 1.092 GPa, \quad \mu_T' = 0.882 GPa, \quad \mu_E' = 0.672 GPa, \quad \rho' = 7.80 gm/cm^3,$$

$$s_2'^{(3)} = -0.52, \quad s_2'^{(4)} = 0.60$$

with $pd = 0.000001$ and $\omega/pc_0 = 60$.
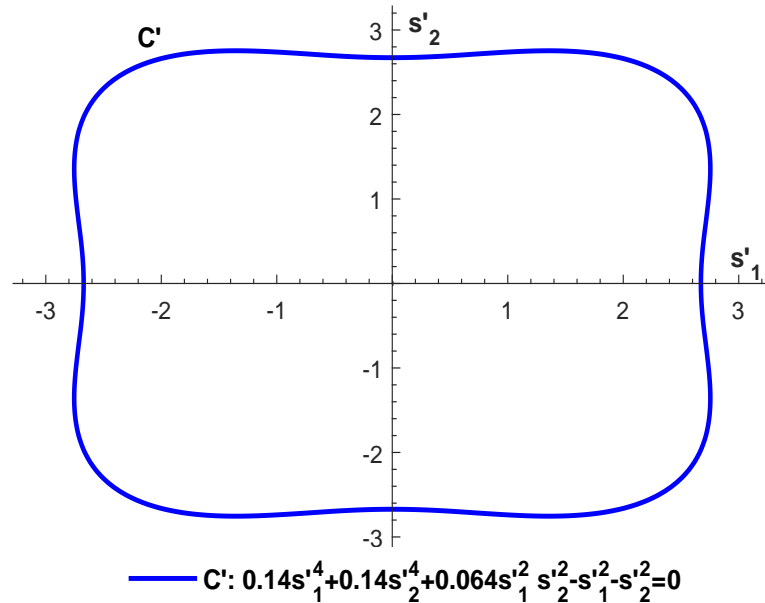
Figure 5.1: Slowness diagram for the half-space, Ω'.

The slowness diagram for the half-space Ω' is shown in Figure 5.1. There are two reflected and transmitted quasi shear waves within the range $0 \leq \alpha \leq 30^0$ due to Equation (5.51). The variation of the modulus of reflection and transmission coefficients are depicted in Figures 5.2-5.4, while Figures 5.5-5.7 depict the variation of energy ratios with incidence angle, α. Figures 5.8-5.11 show the variation of coefficients and energy ratios for irregular waves with the corrugation parameter, pd.

In Figure 5.2, the coefficient r_2 due to regularly reflected quasi-shear wave starts from a certain point at the normal angle of incidence which decreases to minimum value at $\alpha = 17.5^0$ and then increases with the increase of α. In the same figure, the coefficients r_1 and t_3 due to regularly reflected and transmitted quasi-shear waves start from certain point and then decrease with the increase of α while t_4 increases with the increase of α.

In Figure 5.3, the reflection coefficients r_{11}^+, r_{21}^+, r_{11}^- and r_{21}^- due to irregular waves start from certain value at the normal angle, increase initially and then decrease with the increase of the angle of incidence.
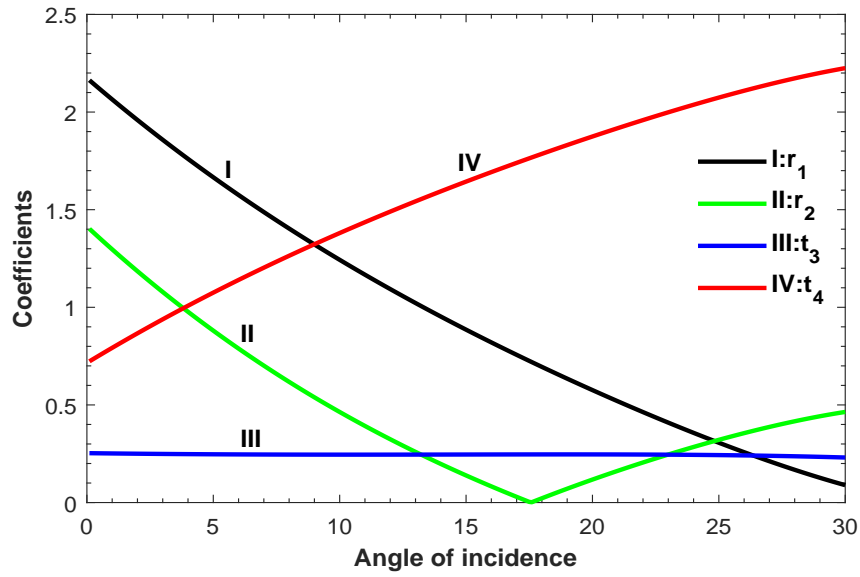
Figure 5.2: Variation of reflection and transmission coefficients for regular waves with α.
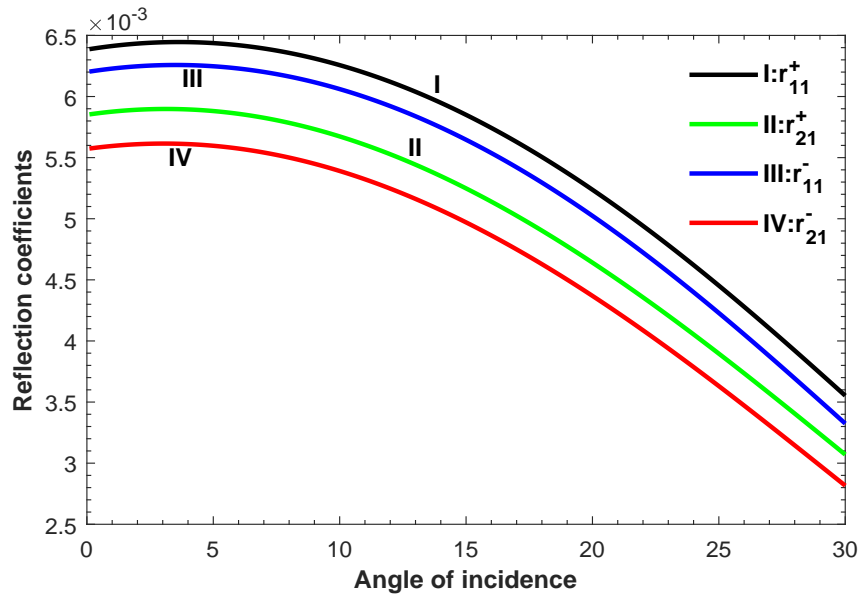
Figure 5.3: Variation of reflection coefficients for irregular waves with α.

In Figure 5.4, the transmitted coefficients t_{41}^{+} and t_{41}^{-} of the irregular waves decrease from certain point with the increase of angle of incidence, α. In the same figure, t_{31}^{+} and t_{31}^{-} increase at a slow rate with α, attaining their highest value at $\alpha = 19^{0}$ and $\alpha = 20^{0}$ respectively which then decrease with α.
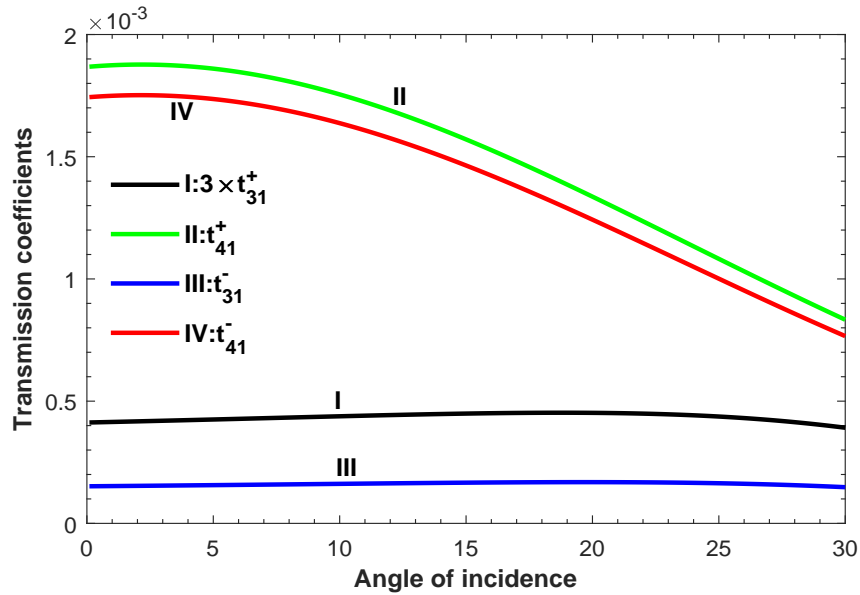
Figure 5.4: Variation of transmission coefficients for irregular waves with α.
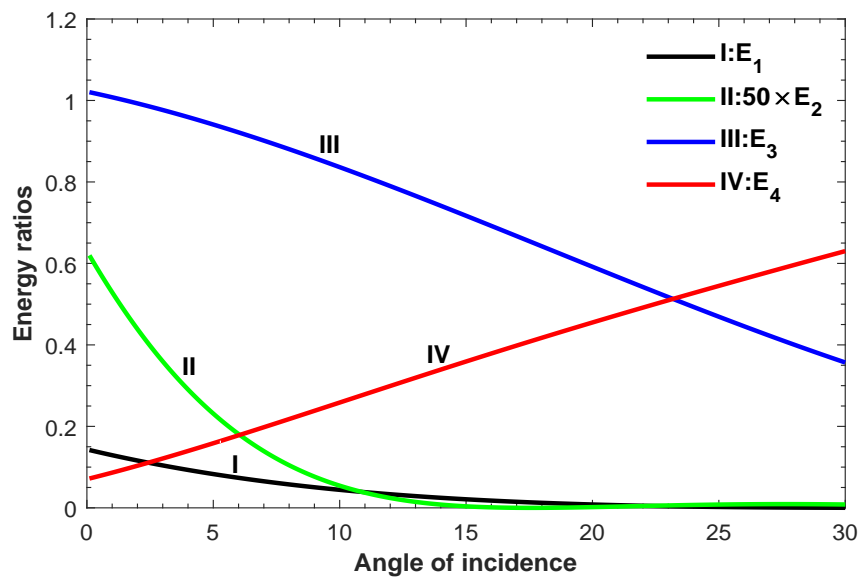
Figure 5.5: Variation of energy ratios for regular waves with α.

In Figure 5.5, the energy ratio E_3 of the regular wave starts from certain value at the normal angle of incidence and decreases while the energy ratio E_4 increases with the increase of angle of incidence, α. In the same figure, the energy ratios E_1 and E_2 decrease with the angle of incidence to zero at $\alpha = 20^0$ and $\alpha = 15^0$ respectively.
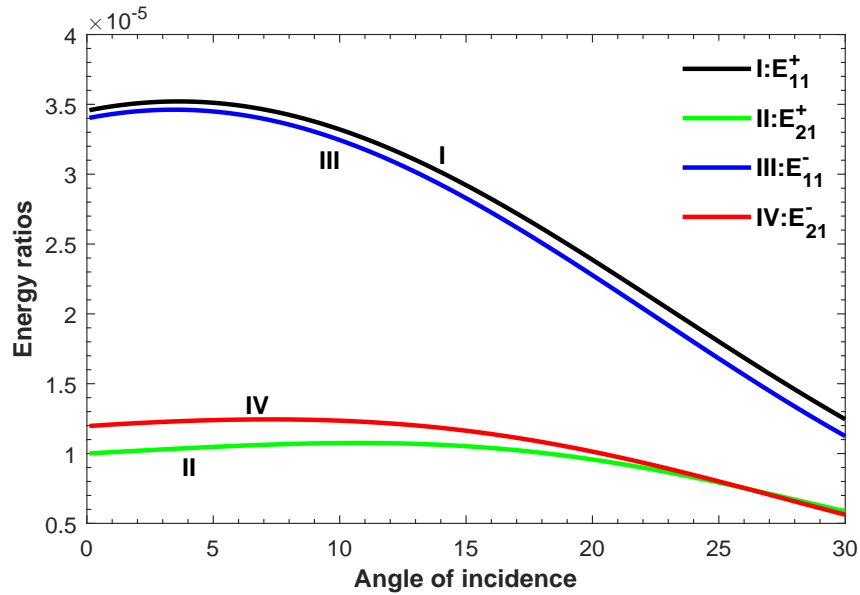
Figure 5.6: Variation of energy ratios $E_{11}^{\pm}$ and $E_{21}^{\pm}$ for irregular waves with α.

In Figure 5.6, the energy ratios E_{11}^{+}, E_{11}^{-} of the irregularly reflected waves decrease from certain point with the increase of α. The energy ratios E_{21}^{+} and E_{21}^{-} increase from a certain value attaining maximum value at $\alpha = 11^{0}$ and $\alpha = 8^{0}$ respectively and then decrease with α.
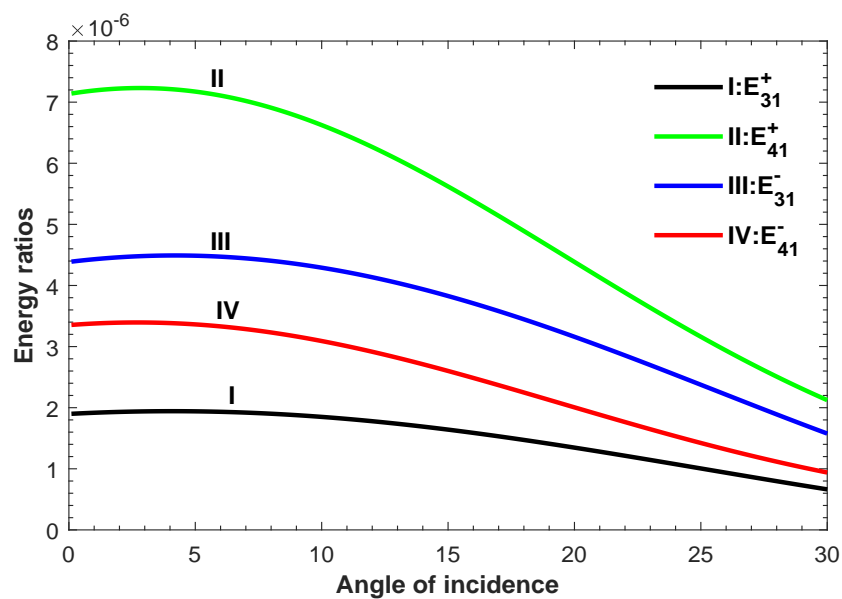
Figure 5.7: Variation of energy ratios $E_{31}^{\pm}$ and $E_{41}^{\pm}$ for irregular waves with α.

In Figure 5.7, the energy ratios E_{31}^-, E_{31}^+, E_{41}^- and E_{41}^+ of the irregularly transmitted quasi-shear waves decrease from a certain value at normal angle of incidence with the increase of α.
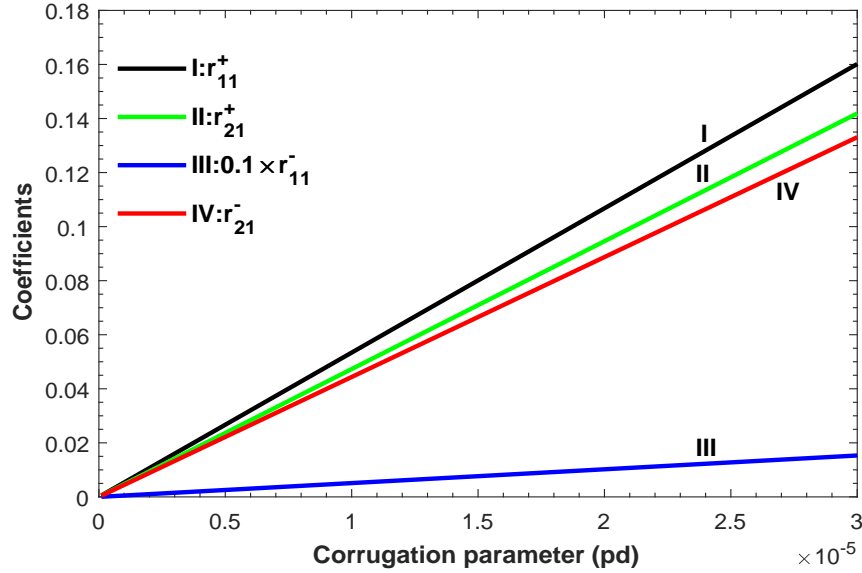
Figure 5.8: Variation of reflection coefficients $r_{11}^{\pm}$ and $r_{21}^{\pm}$ for irregular waves with pd.

All the reflection coefficients $(r_{11}^+, r_{21}^+, r_{11}^-, r_{21}^-)$ in Figure 5.8 and the transmission coefficients $(t_{31}^+, t_{41}^+, t_{31}^-, t_{41}^-)$ in Figure 5.9 are increasing linearly with the increase of pd.
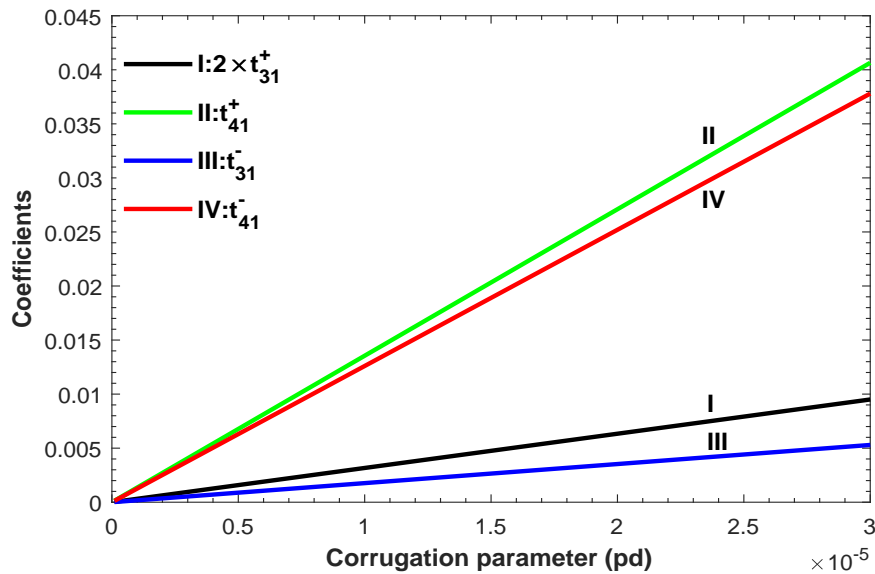
Figure 5.9: Variation of transmission coefficients $t_{31}^{\pm}$ and $t_{41}^{\pm}$ for irregular waves with pd.
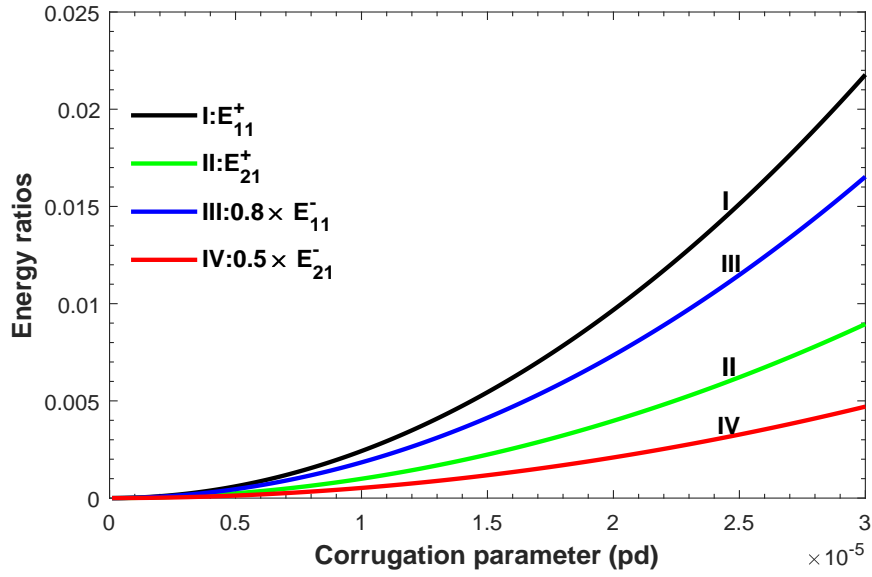
Figure 5.10: Variation of energy ratios $E_{11}^{\pm}$ and $E_{21}^{\pm}$ for irregular waves with pd.
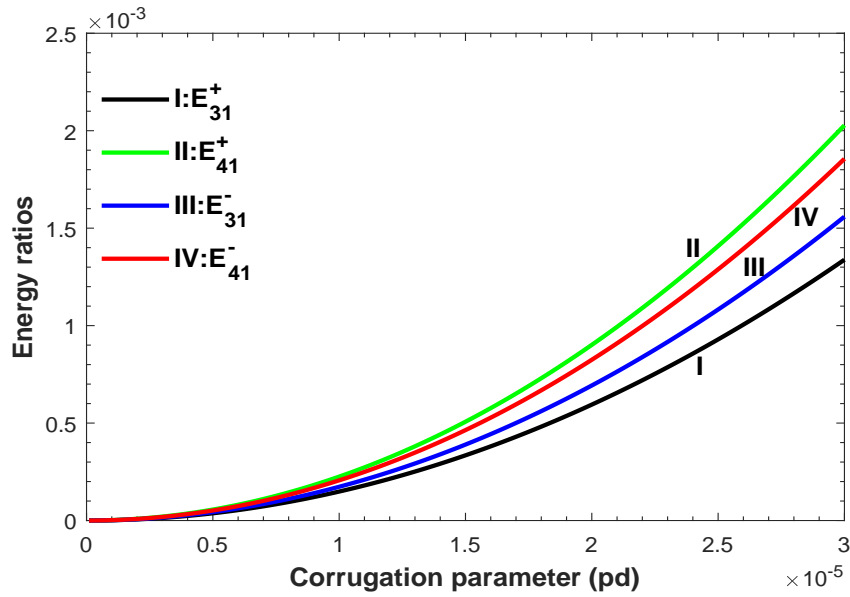
Figure 5.11: Variation of energy ratios $E_{31}^{\pm}$ and $E_{41}^{\pm}$ for irregular waves with pd.

In Figures 5.10 and 5.11, we observed that $E_{11}^{+}, E_{21}^{+}, E_{31}^{+}, E_{41}^{+}, E_{11}^{-}, E_{21}^{-}, E_{31}^{-}$ and E_{41}^{-} increase with the increase of pd, but the mode of increase are non-linear. Thus, we have noted that the coefficients as well as energy ratios due to irregular waves depend on the corrugation parameter, but they are independent of pd for regular waves.

5.11 Concluding remarks

The propagation of elastic wave at the corrugated interface between two dissimilar incompressible transversely isotropic fibre-reinforced half-spaces has been investigated. The reflection and transmission coefficients due to regular and irregular quasi-shear waves and their energy ratios are obtained. They are computed numerically for a specific model, $\zeta = d \cos p x_1$ and graphs are presented. We have following remark points:

(i) All the coefficients and energy ratios of the irregularly reflected and transmitted quasi-shear waves depend on the angle of propagation, unit displacement vectors, slowness vectors, elastic constants, corrugation and frequency parameters.

(ii) The modulus of coefficients and energy ratios of the regular waves do not depend on pd and ω/pc_0.

(iii) The values of the coefficients and energy ratios due to the irregular waves are very small in comparison to those of the regular waves.

(iv) The reflection and transmission coefficients of the irregular waves increase linearly but the energy ratios increase non-linearly with the increase of pd.

(v) The sum of energy ratios is close to one.

Chapter 6

Summary and Conclusions

In the present thesis, the problems of elastic wave propagation at a corrugated interface between two dissimilar elastic half-spaces have been investigated. The expression for phase velocities of the incident wave, reflected and transmitted waves are obtained which are dependent on the angle of propagation. The phenomena of reflection and transmission of longitudinal and shear waves are discussed with the help of appropriate boundary conditions using Rayleigh method of approximation. Amplitude and energy ratios of reflected and transmitted waves are obtained analytically and numerically for a particular model. We also discuss the effects of corrugation and frequency parameters on these ratios.

Chapter 1 is the general introduction. It includes basic definitions, different types of anisotropic symmetry, stress-strain relationship with generalized Hooke's law, conservation of linear momentum, Spectrum theorem, Rayleigh's method of approximation, importance of wave propagation and review of literature.

In Chapter 2, the problem of reflection and transmission phenomena of elastic qSV and qP-wave due to incident plane qSV-wave at a corrugated interface between two dissimilar monoclinic elastic half-spaces has been investigated. We have noticed that both qSV and qP-waves are reflected and transmitted for the incidence of qP/qSV-wave. We have obtained the reflection and transmission coefficients for the regularly and irregularly reflected and transmitted waves using Rayleigh's method

of approximation. These coefficients are computed numerically for a special type of interface, $z = d \cos py$ and discussed the effects of corrugation (pd) and frequency parameter (ω/pc_0). We have the following concluding remarks:

(i) All coefficients corresponding to regular waves are functions of angle of incidence and elastic constants, while those of irregular waves are found to be functions of angle of incidence, elastic constants, corrugation and frequency parameters.

(ii) Theoretically and numerically, those reflection and transmission coefficients corresponding to regular waves are independent of corrugation and frequency parameters.

(iii) The coefficients corresponding to irregular waves are found to be linearly proportional to corrugation and frequency parameters.

(iv) It is found that the values of coefficients corresponding to irregular waves increase with increase of pd and ω/pc_0.

(v) The values of coefficients corresponding to irregular waves are smaller than those of regular waves.

In Chapter 3, the problem of reflection and transmission of elastic waves at a corrugated interface between two dissimilar nematic elastomer half-spaces has been studied separately for the incident qP and qSV-waves. The expressions of the phase velocities corresponding to qP and qSV-waves are obtained. The closed form expression of the amplitude ratios corresponding to the reflected and transmitted waves for the incident qP and qSV-waves are derived by using appropriate boundary conditions. The energy partitions due to the corrugated interface are also discussed. The amplitude and energy ratios of the regular and irregular waves are computed numerically for a particular model, $x_3 = d \cos px_1$ for different values of corrugation parameter. We conclude the following points:

(i) All amplitude ratios corresponding to irregular waves are functions of the angle of incidence, elastic constants, coupling constants, characteristic time of rubber relaxation, director rotation times, frequency and corrugation parameter.

(ii) The amplitude and the energy ratios corresponding to the regular waves are independent of pd and ω/pc_0.

(iii) The amplitude and energy ratios corresponding to the regular qP-waves are greater than those ratios corresponding to regular qSV-waves for the incident qP-wave, but it is reversed in the case of incident qSV-wave.

(iv) The amplitude and energy ratios corresponding to the regularly reflected and transmitted waves are greater in magnitude than those of irregular waves. Those ratios corresponding to irregular waves are small.

(v) The ratios r^{pp}, r^{svp}, t^{svp}, t^{svsv}, r_1^{svp+}, t_1^{svsv+}, r_1^{svsv-}, t_1^{svp-}, E_1^{pp}, E_3^{svp}, E_{21}^{svsv+}, E_{21}^{svsv-} and E_{41}^{svsv-} increase with the increase of the angle of incidence (α_0), while t^{pp}, t_1^{svsv-}, E_3^{pp} and E_{41}^{svsv+} decrease with the increase of α_0.

(vi) The amplitude ratios corresponding to irregular waves increase linearly with the increase of pd, but at different rates.

(vii) The energy ratios corresponding to irregular waves increase non-linearly with the increase of pd.

(viii) The sum of the energy ratios is close to unity at each angle of incidence.

In Chapter 4, the reflection and refraction phenomena of elastic waves due to incident qSH-wave at a corrugated interface between two different nematic elastomer half-spaces have been studied. The expression of the phase velocity for shear harmonic wave is derived and observed that this phase velocity depends on the angle of propagation. The first order approximation of amplitude ratios corresponding to reflected and transmitted waves are obtained using Rayleigh's technique. There exists a critical angle at $\alpha_0 = 83^0$. The energy distribution, and hence the energy ratios due to various reflected and transmitted waves are also obtained. A particular case, $z = d\cos px$ has been performed to validate the present study for the amplitude and energy ratios. We conclude with the following points:

(i) The angles corresponding to the reflected and transmitted waves increase with the increase of the angle of incidence.

(ii) All amplitude and energy ratios corresponding to irregular waves are functions of the angle of incidence, elastic constants, coupling constants, the characteristic time of rubber relaxation, the director rotation-times, frequency and corrugation parameters.

(iii) The amplitude ratios corresponding to the regularly reflected and transmitted waves are greater in magnitude than those due to irregular waves.

(iv) The values of energy ratio corresponding to irregular waves are found to be significantly small in comparison to those due to regular waves.

(v) Theoretically and numerically, the amplitude and the energy ratios corresponding to the regular waves are independent of corrugation and frequency parameters.

(vi) The values of amplitude and energy ratios corresponding to irregular waves show a linear and non-linear increase respectively with increase of corrugation parameters.

(vii) The sum of all energy ratio is approximately unity at each value of incident angle which ensures the law of conservation of energy.

In Chapter 5, the reflection and transmission phenomena of elastic waves at an irregular interface between two dissimilar incompressible transversely isotropic fibre-reinforced half-spaces have been discussed. There exist two reflected and transmitted quasi-shear waves within the range $0 \leq \alpha \leq 30^0$ when the outer slowness is re-entrant. The expressions of propagation velocity are obtained for both the reflected and transmitted waves. The reflection and transmission coefficients due to regular and irregular quasi-shear waves and their energy ratios are obtained. They are computed numerically for a specific model, $\zeta = d \cos p x_1$ and graphs are presented. We have the following remarks:

(i) All the coefficients and energy ratios of the irregularly reflected and transmitted quasi-shear waves depend on the angle of propagation, unit displacement vectors, slowness vectors, elastic constants, corrugation and frequency parameters.

(ii) The coefficients and energy ratios of the regular waves do not depend on pd and ω/pc_0.

(iii) The values of the coefficients and energy ratios due to the irregular waves are small in comparison to those due to the regular waves.

(iv) The reflection and transmission coefficients of the irregular waves increase linearly but the energy ratios increase non-linearly with the increase of pd.

(v) The sum of energy ratios is close to one.

FUTURE SCOPE

We could suggest some interesting problems related with the works in this thesis.

1. Energy distribution at a corrugated interface between two dissimilar monoclinic elastic half-spaces.

2. Scattering of elastic waves at an irregular interface between two dissimilar incompressible transversely isotropic fibre-reinforced half-spaces due to incident qP/qSV-waves.

3. Scholars may also look for the extension of the present problems by finding the reflection and transmission coefficients for second order of approximation.

APPENDICES

(A) List of Research Publications

(1) Singh, S.S. and **J. Lalvohbika** (2018). Response of corrugated interface on incident qSV-wave in monoclinic elastic half-spaces, *International Journal of Applied Mechanics and Engineering*, **23(3)**: 727-750.

(2) **J. Lalvohbika** and Singh, S.S. (2019). Effect of corrugation on incident qP/qSV-waves between two dissimilar nematic elastomers, *Acta Mechanica*, **230(9)**: 3317-3338.

(3) **J. Lalvohbika** and Singh, S.S. (2020). Scattering of qSH-waves from a corrugated interface between two dissimilar nematic elastomers, *Waves in Random and Complex Media*, **2020**: doi:-10.1080/17455030.2020.1758359.

(4) **J. Lalvohbika** and Singh, S.S. (2020). Effect of corrugation and frequency parameters due to quasi-harmonic-waves on a corrugated interface of two different nematic elastomers, *Materials Today: Proceedings*, **2020**: doi:-10.1016/j.matpr.2020.04.055.

(5) **J. Lalvohbika** and Singh, S.S. (2020). Elastic waves at a corrugated interface between two dissimilar incompressible transversely isotropic fibre-reinforced elastic half-spaces, *Mechanics of Advanced Materials and Structures*, **2020**: doi:-10.1080/15376494.2020.1838005.

(B) Conferences/Seminars/Workshops

(1) Participated in *One day State Level Acquaintance Programme* organized by Department of Physics, School of Physical Sciences, Mizoram University and Inter University Accelerator Center, New Delhi on 28th March, 2014.

(2) Attended training programme on *Change Management, Leadership Skills & Personality Development* conducted by Administrative Training Institute, Aizawl, Mizoram during $8^{th} - 12^{th}$ December, 2014.

(3) Delivered a lecture on *Uses of Maths softwares - Mathstype, Algebrator, Bagatrix* in the *Two day workshop on Integration of Computer Software in Teaching Learning Mathematics for Higher Secondary School* organized by Science Promotion Wing, SCERT, Aizawl in collaboration with Department of Mathematics, Pachhunga University College, Aizawl - 796 001, Mizoram on $16^{th} - 17^{th}$ April, 2015.

(4) Delivered a lecture on *Question setting technique* in the *Workshop on Question setting technique for National Talent Search Examination (NTSE)* organized by State Council of Educational Research and Training, Mizoram on 22nd July, 2015.

(5) Presented a paper *A correlation study of students' scores in Mathematics and English in the HSLC examination under MBSE* in the *Second Mizoram Mathematics Society Congress* organized by Mizoram Mathematics Society, Aizawl on 22nd December, 2015.

(6) Participated in *One day Training-cum-sensitization Workshop* organized by AISHE, Mizoram Unit, sponsored by Ministry of Human Resource Development, Government of India on 14th January, 2016.

(7) Delivered a lecture on *Teacher Data-based Management of Pachhunga University College Faculty & Staffs* in the *Seminar on Data-based Management* organized by Department of Mathematics, Pachhunga University College, Aizawl - 796 001, Mizoram on 26th July, 2016.

(8) Presented a paper *Dynamical system -linear, non-linear system, chaos and some models of dynamical system* in the *Mizoram Science Congress 2016* organized

by NEC, DST(SERB) & MISTIC on 13th October, 2016.

(9) Participated in the 4th *Workshop on Official Statistics in North Eastern States* organized by ISI, Kolkata on $7^{th} - 13^{th}$ November, 2016.

(10) Presented a paper *Activity based Learning* in the *Seminar on "Learning Mathematics - Prospects and Challenges"* organized by State Council of Educational Research and Training, Mizoram on 14th November, 2016.

(11) Participated in *North-East ISI-MZU Winter School on 'Algorithms with special focus on Graphs'* organized by ISI, Kolkata and Department of Mathematics & Computer Science, Mizoram University, Aizawl during $6^{th} - 11^{th}$ March, 2017.

(12) Delivered a lecture on *Concept of Infinity* in the *Mathematics Summer Day Camp* organized by MMS & MISTIC, supported by NCSTC, DST, Government of India on 20th March, 2017.

(13) Presented a research paper *Effects of corrugation and frequency parameter due to incident qSV-wave in monoclinic elastic half-spaces* in the *Mizoram Science Congresss-2018* organized by MISTIC, MSS, MAS, STAM, GSM, BIOCONE, MMS & Pachhunga University College, Aizawl during $4^{th} - 5^{th}$ October, 2018.

(14) Presented a research paper *Problem of scattering of SH-waves from a corrugated interface between two dissimilar nematic elastomers* in the *Multidisciplinary International Seminar on 'A perspective Of Global Research Process': Present Scenario & Future Challenges* organized by Manipur University in Association with TOUCAN Research and Development, during $19^{th} - 20^{th}$ January, 2019.

(15) Participated in *The International Conference on Chemistry & Environmental Sustainability (ICCES-2019)* organized by Department of Chemistry, School of Physical Sciences, Mizoram University during $19^{th} - 22^{nd}$ February, 2019.

(16) Participated in *Instructional School for Teachers on "Mathematical Modelling in Continuum Mechanics and Ecology"* organized by National Centre for Mathematics, A joint centre of TIFR and IIT Bombay during $3^{rd} - 15^{th}$ June, 2019.

(17) Participated in *National Workshop on 'Ethics in Research and Preventing Plagiarism (ERPP-2019)'* organized by Department of Physics, School of Physical Sciences, Mizoram University on 3rd October, 2019.

(18) Participated in *"Workshop on Understanding Curriculum, Syllabus and Textbooks for developing Textbooks"* organized by State Council of Educational Research and Training, Mizoram in collaboration with Azim Premji University, Bangalore during $11^{th} - 22^{nd}$ November, 2019.

(19) Participated in the 39th *State Level Science, Mathematics and Environment Exhibition, 2019* organized by Science Promotion Wing, SCERT Mizoram in collaboration with NCERT, New Delhi during $18^{th} - 19^{th}$ December, 2019.

(20) Participated in *International Workshop on Tectonic and its implications with special reference to Indo-Burma Range* organized by Research and Seminar Committee and Department of Geology, Government Zirtiri Residential Science College, MISTIC, HTE, DM&R, Government of Mizoram during $17^{th} - 18^{th}$ January, 2020.

(21) Presented a research paper *Incident qSH-wave at a corrugated interface between two dissimilar Nematic Elastomers* in the *International Conference on Material Sciences (ICMS2020)* organized by Department of Physics, Tripura University during $4^{th} - 6^{th}$ March, 2020.

Bibliography

Abd-Alla A.M., Nofal, T.A., Abo-Dahab, S.M. and Al-Mullise, A. (2013). "Surface waves propagation in fibre-reinforced anisotropic elastic media subjected to gravity field" *Int. J. Phys. Sc.* **14(8)**, 574-584.

Abhemanyu, P.C., Prassanth, E., Kumar, T.N., Vidhyasagar, R., Marimuthu, K.P. and Pramod, R. (2019). "Characterization of natural fiber reinforced polymer composites", *AIP Conf. Proc.* **2080**, 020005-1−020005-7.

Abubakar, I. (1962a). "Scattering of plane elastic waves at rough surfaces I", *Math. Proc. Camb. Phil. Soc.* **58(1)**, 136-157.

Abubakar, I. (1962b). "Reflection and refraction of plane SH-waves at irregular interfaces - I", *J. Phys. Earth.* **10(1)**, 1-14.

Abubakar, I. (1962c). "Reflection and refraction of plane SH-waves at irregular interfaces - II", *J. Phys. Earth.* **10(1)**, 15-20.

Achenbach, J.D. (1976). *Wave Propagation in Elastic Solids*, North-Holland Publishing Company, New York.

Aki, K. and Richards P.G. (1930). *Quantitative Seismology, 2nd. Eds.*, University Science Books, California.

Alexe-ionescu, A.L., Barberi, R., Barbero, G. and Giocondo, M. (1994). "Anchoring energy for nematic liquid crystals: Contribution from the spacial variation of the elastic constants", *Phys. Rev. E* **49(6)**, 5378-5388.

Anderson, D.R., Carlson, D.E. and Fried, E. (1999). "A continuum-mechanical theory of nematic elastomers", *J. Elasticity* **56**, 33-58.

Asano, S. (1960). "Reflection and refraction of elastic waves at a corrugated boundary surface. Part I. The case of incidence of SH-wave", *Bull. Earthq. Res. Inst.* **38**, 177-197.

Asano, S. (1961). "Reflection and refraction of elastic waves at a corrugated boundary surface. Part II", *Bull. Earthq. Res. Inst.* **39(3)**, 367-466.

Asano, S. (1966). "Reflection and refraction of elastic waves at a corrugated interface", *Bull. Seismol. Soc. Am.* **56(1)**, 201-221.

Banerjee, S. and Kundu, T. (2006). "Elastic wave propagation in sinusoidally corrugated waveguides", *J. Acoust. Soc. Am.* **119(4)**, 2006-2017.

Baylis, E.R. and Green, W.A. (1986). "Flexural waves in fibre-reinforced laminated plates", *J. Sound Vib.* **110(1)**, 1-26.

Belfield, A.J., Rogers, T.G. and Spencer, A.J.M. (1983). "Stress in elastic plates reinforced by fibres lying in concentric circles", *J. Mech. Phys. Solids.* **31(1)**, 25-54.

Ben-Menahem, A. and Singh, S.J. (1981). *Seismic Waves and Sources*, Berlin, Springer-Verlag.

Bladon, P., Terentjev, E.M. and Warner, M. (1993). "Transitions and instability in liquid-crystal elastomers", *Rapid Commun. Phys. Rev. E* **46(6)**, 3838-3840.

Bladon, P., Warner, M. and Terentjev, E.M. (1994). "Orientational order in strained nematic networks", *Macromol.* **27**, 7067-7075.

Blake, L.V. (1950). "Reflection of radio waves from a rough sea", *Proc. Inst. Rad. Engs.* **38**, 301-304.

Blum, T.E., Snieder, R., Kasper van Wijk and Willis, M.E. (2011). "Theory and laboratory experiments of elastic wave scattering by dry planar fractures", *J. Geophys. Res.* **116**, 1-11.

Bowen, R.M. (1989). *Introduction to Continuum Mechanics*, Plenum Press, New York.

Brand, H.R. and Plenier, H. (1994). "Electrohydrodynamics of nematic liquid crystalline elastomers", *Physica. A* **(208)**, 359-372.

Brand, H.R., Pleiner, H. and Martinoty, P. (2006). "Selected macroscopic properties of liquid crystalline elastomers", *Soft Matter.* **2**, 182-189.

Brekhovskikh, L.M. (1952). "Wave diffraction on an uneven surface. I: General theory. II: Applications of general theory", *Zh. ksper. Teor. Fiz.* **23**, 275-288.

Brekhovskikh, L.M. (1960). *Waves in Layered Media*, Academic Press, New York.

Bullen, K.E. and Bolt, B.A. (1985). *Introduction to the Theory of Seismology*, Cambridge University Press, London.

Carlson, J.F. and Heins, I.E. (1946). "The reflection of an electromagnetic plane wave by an infnite set of plates", *Quart. Appl. Math.* **4(4)**, 313-329.

Cermelli, P., Fried, E. and Gurtin, M.E. (2004). "Sharp-interface nematic-isotropic phase transitions without flow", *Arch. Rat. Mech. Anal.* **174**, 151-178.

Chabaud, B.M., Brock, J.S., Williams, T.O. and Smith, B.M. (2013). "Benchmark analytic solution of the dynamic response of a spherical shell composed of a transverse isotropic elastic material", *Int. J. Solids Struct.* **50(24)**, 4089-4097.

Chadwick, P. (1985). "A general analysis of transonic states in anisotropic elastic body", *Proc. Roy. Soc. Lond. A* **401(1821)**, 203-223.

Chadwick, P. (1989a). "Wave propagation in transversely isotropic elastic media I. Homogeneous plane waves", *Proc. Roy. Soc. Lond. A* **(422)**, 23-66.

Chadwick, P. (1989b). "Wave propagation in transversely isotropic elastic media II. Surface Waves", *Proc. Roy. Soc. Lond. A* **422(1862)**, 67-101.

Chadwick, P. (1993). "Wave propagation in incompressible transversely isotropic elastic media I. Homogeneous plane waves", *Proc. Roy. Ir. Acad. A* **93(2)**, 231-253.

Chatterjee, M. and Chattopadhyay, A. (2015). "Propagation, reflection, and transmission of SH-waves in slightly compressible, finitely deformed elastic media", *Appl. Math. Mech. -Engl. Eds.* **36(8)**, 1045-1056.

Chattopadhyay, A. and Choudhury, S. (1990). "Propagation, reflection and transmission of magneto-elastic shear waves in a self-reinforced medium", *Int. J. Engng. Sc.* **28(6)**, 485-495.

Chattopadhyay, A. and Choudhury, S. (1995a). "The reflection phenomena of P-waves in a medium of monoclinic type", *Int. J. Engng. Sc.* **33(2)**, 195-207.

Chattopadhyay, A. and Choudhury, S. (1995b). "Magnetoelastic shear waves in an infinite self reinforced plate", *Int. J. Numer. Anal. Met. Geomech.* **19(4)**, 289-304.

Chattopadhyay, A. and Saha, S. (1996). "Reflection and refraction of P-waves at the interface of two monoclinic media", *Int. J. Engng. Sc.* **34(11)**, 1271-1284.

Chattopadhyay, A., Saha, S. and Chakraborty, M. (1996). "The reflection of SV-waves in monoclinic medium", *Indian J. Pure Appl. Math.* **27(10)**, 1029-1042.

Chattopadhyay, A. Saha, S. and Chakraborty, M. (1997). "Reflection and transmission of shear waves in monoclinic media", *Int. J. Numer. Anal. Met. Geomech.* **21(7)**, 495-504.

Chattopadhyay, A. and Saha, S. (1999). "Reflection and refraction of quasi-SV waves at the interface of the monoclinic media", *Acta Geophys. Pol.* **47(3)**, 307-322.

Chattopadhyay, A. and Rogerson, G.A. (2001). "Wave reflection in slightly compressible, finitely deformed elastic media", *Arch. Appl. Mech.* **71**, 307-316.

Chattopadhyay, A. (2004). "Wave reflection and refraction in triclinic crystalline media", *Arch. Appl. Mech.* **73**, 568-579.

Chattopadhyay, A. and Rajneesh, H. (2006). "Reflection and refraction of waves at the interface of an isotropic medium over a highly anisotropic medium", *Acta Geophys.* **54(3)**, 239-249.

Chattopadhyay, A. and Venkateswarlu, R.L.K. (2007). "Reflection and refraction of quasi P and SV waves at the interface of fibre-reinforced media", *Adv. Studies Theor. Phys.* **1(2)**, 57-73.

Chattopadhyay, A., Gupta, S., Sharma, V.K. and Kumari, P. (2009). "Reflection and refraction of plane quasi-P waves at a corrugated interface between distinct triclinic elastic half spaces", *Int. J. Solids Struct.* **46(17)**, 3241-3256.

Chattopadhyay, A., Kumari, P. and Sharma, V.K. (2013). "Reflection and refraction at the interface between distinct generally anisotropic half spaces for three-dimensional plane quasi-P waves", *J. Vib. Control.* **21(3)**, 493-508.

Chen, T.J., Chen, C.S. and Chen, C.W. (2011). "Dynamic response of fibre-reinforced composite plates", *Mech. Comp. Mater.* **47(5)**, 549-560.

Christie, D.G. (1955). "Reflection of elastic waves from a free boundary", *The London, Edinburgh, and Dublin Philosophical Magazine and Journal of Science, Series* **7**.

Clarke, S.M. and Terentjev, E.M (1998). "Slow stress relaxation in randomly disordered nematic elastomers and gels", *Phys. Rev. Lett.* **81(20)**, 4436-4439.

Clarke, S.M., Tajbakhsh, A.R., Terentjev, E.M. and Warner, M. (2001). "Anomalous viscoelastic response of nematic elastomers", *Phys. Rev. Lett.* **86(18)**, 4044-4047.

Clive, L.D. and Irving, H.S. (2013). *Solid Mechanics -A Variational Approach*, Springer, New York.

Conti, S., DeSimone, A. and Dolzmann, G. (2002). "Semi-soft elasticity and director reorientation in stretched sheets of nematic elastomers", *Phys. Rev. E* **66**, 61710-61718.

Cosserat, E. and Cosserat, F. (1909). *Theory of Deformable Bodies*, Scientific Library A. Hermann and Sons, Paris.

de Gennes, P.G. (1980). *Liquid crystals of one- and two-dimensional order, Edited by W. Helfrich and G. Heppke*, Springer-Verlag, Berlin.

de Gennes, P.G. and Prost, J. (1993). *The Physics of Liquid Crystals*, Oxford University Press, New York.

Deresiewicz, H. and Wolf, B. (1964). "The effect of boundaries on wave propagation in a liquid filled porous solid: IX: Reflection of plane waves at an irregular boundary", *Bull. Seismol. Soc. Am. A* **54(5)**, 1537-1561.

Destrade, M. (2001). "Surface waves in orthotropic incompressible materials", *J. Acoust. Soc. Am.* **110(2)**, 837-840.

DeSimone, A. and Dolzmann, G. (2000). "Material instabilities in nematic elastomers", *Physica D* **136**, 175-191.

DeSimone, A. and Teresi, L. (2009). "Elastic energies for nematic elastomers", *Eur. Phys. J. E* **29**, 191-204.

Ditter, D., Braun, L.B. and Zentel, R. (2020). "Influences of ortho-Fluoroazobenzenes on liquid crystalline phase stability and $2D$ (Planar) actuation properties of liquid crystalline elastomers", *Macromol. Chem. Phys.* **221**, 1900265-1−1900265-12.

Dowaikh, M.A. and Ogden, R.W. (1990). "On surface waves and deformations in a pre-stressed incompressible elastic solid", *IMA J. Appl. Math.* **44**, 261-284.

Dowaik, M.A. and Ogden, R.W. (1991). "Interfacial waves and deformations in pre-stressed elastic media", *Proc. Roy. Soc. Lond. A* **433**, 313-328.

Doyle, J.F. (1989). *Wave Propagation in Structures, An FFT-based Spectral Analysis Methodology*, Springer-Verlag, New York.

Doyle, J.F. (1997). *Wave Propagation in Structures, Spectral Analysis using Fast Discrete Fourier Transforms*, Springer Science & Business Media, New York.

Dravinsky, M. (2007). "Scattering of waves by a sedimentary basin with a corrugated interface", *Bull. Seismol. Soc. Am. B* **97(1)**, 256-264.

Dunkin, J.W. and Eringen, A.C. (1962). "Reflection of elastic waves from the wavy boundary of a half space", *Proc. 4th US Nat. Congr. Appl. Mech.* 143-160.

Dunkin, J.W. and Eringen, A.C. (1963). "On the propagation of waves in an electromagnetic elastic solid", *Int. J. Engng. Sci.* **1**, 461-495.

Elliott, R.S. (1954). "On the theory of corrugated plane surfaces", *I.R.E Trans.-Antennas and Propagation* **2(2)**, 71-81.

Ericksen, J.L. (1960). "Anisotropic fluids", *Arch. Rat. Mech. Anal.* **4**, 231-237.

Everaers, R. (1999). "Entanglement effects in defect-free model polymer networks", *New J. Phy.* **1**, 1-54.

Ewing, W.M., Jardetzky, W.S. and Press, F. (1957). *Elastic Waves in layered media*, McGraw-Hill Book Company Inc., London.

Fedorov, F.I. (1968). *Theory of Elastic Waves in Crystals*, Springer Science & Business Media, New York.

Feinberg, E. (1944). "On the propagation of radio waves along an imperfect surface", *J. Phys. USSR*, **8**, 317-330.

Finkelmann, H., Kock, H.J. and Rehage, H. (1981). "Liquid crystalline elastomers - a new type of liquid crystalline material", *Makromol. Chem. Rapid Commun.* **2**, 317-322.

Finkelmann, H., Kundler, I., Terentjev, E.M. and Warner, M. (1997). "Critical stripe-domain instability of nematic elastomers", *J. Phys. II France.* **7**, 1059-1069.

Finkelmann, H., Greve, A. and Warner, M. (2001). "The elastic anisotropy of nematic elastomers", *Eur. J. Phys. E* **5**, 281-293.

Fradkin, L.J., Kamotski, I.V., Terentjev, E.M. and Zakharov, D.D. (2003). "Low-frequency acoustic waves in nematic elastomers", *Proc. Roy. Soc. Lond. A* **459**, 2627-2642.

Fried, E. and Todres, R.E. (2002). "Disclinated states in nematic elastomers", *J. Mech. Phys. Solids.* **50**, 2691-2716.

Gattinger, J., Koppl, R. and Zeppenfeld, M. (2019). "Compounding and direct compounding of crimped fiber reinforced thermoplastic elastomers", *AIP Conf. Proc.* **2139**, 110001-1−110001-5.

Gebretsadkan, W.B. and Kalra, G.L. (2002). "Propagation of linear waves in relativistics anisotropic magneto-hydrodynamics", *Phys. Rev. E* **66**, 057401-057404.

Golubovic, L. and Lubensky, T.C. (1989). "Nonlinear elasticity of amorphous solids", *Phys. Rev. Lett.* **63(10)**, 1082-1085.

Graff, K.F. (1991). *Wave Motion in Elastic Solids*, Dover Publications, New York.

Green, W.A. (1982). "Bending waves in strongly anisotropic plates", *Q. J. Mech. Appl. Math.* **35(4)**, 485-507.

Guin, T., Settle, M.J., Kowalski, B.A., Auguste, A.D., Beblo, R.V., Reich, G.W. and White, T.J. (2018). "Layered liquid crystal elastomer actuators", *Nature Commun.* **9:2531**, 1-7.

Gupta, S.K. (1978). "Reflections and refractions from curved interfaces: model-study", *Geophys. Prospect.* **26(1)**, 82-96.

Gupta, S. (1987). "Reflection and transmission of SH-waves in a laterally and vertically heterogeneous media at an irregular boundary, *Geophys. Trans.* **33(2)**, 89-111.

Gurtin, M.E. (1981). *An Introduction to Continuum Mechanics*, Academic Press, New York.

Homma, T. (1940). "Terrain effects on the surface vibration value of Rayleigh wave characteristic equation delta", *Q. J. Seismol.* **11(4)**, 349-364.

Hosten, B. (1991). "Reflection and transmission of acoustic plane waves on an immersed orthotropic and viscoelastic solid layer", *J. Acoust. Soc. Am.* **89(6)**, 2745-2752.

Itskov, M. and Aksel, N. (2002). "Elastic constants and their admissible values for incompressible and slightly compressible anisotropic materials", *Acta Mech.* **157**, 81-96.

Kaur, J. and Tomar, S.K. (2004). "Reflection and refraction of SH-waves at a corrugated interface between two monoclinic elastic half-spaces", *Int. J. Numer. Anal. Met. Geomech.* **28(15)**, 1543-1575.

Kaur, J., Tomar, S.K. and Kaushik, V.P. (2005). "Reflection and refraction of SH-waves at a corrugated interface between two laterally and vertically heterogeneous viscoelastic solid half-spaces", *Int. J. Solids Struct.* **42(13)**, 3621-3643.

Kennett, B.L.N. (1972). "Seismic wave scattering by obstacles on interfaces", *Geophys. J. Int.* **28(3)**, 249-266.

Kielczynski, P. and Pajewski, W. (1987). "Reflection of an obliquely incident SH-plane wave at a plane interface between an elastic solid and a viscoelastic liquid", *J. Acoust. Soc. Am.* **81(3)**, 599-605.

Komijani, M., Mahbadi, H. and Eslami, M.R. (2013). "Thermal and mechanical cyclic loading of thick spherical vessels made of transversely isotropic materials", *Int. J. Press. Vess. Pip.* **107**, 1-11.

Koniuszewska, A.G. and Kaczmar, J.W. (2016). "Application of polymer based composite materials in transportation", *Prog. Rub. Plast. Recy. Tech.* **32(1)**, 1-24.

Korneev, V.A. and Johnson, L.R. (1993). "Scattering of elastic waves by a spherical inclusion-I. Theory and numerical results", *Geophys. J. lnt.* **115**, 230-250

Kossovich, L.Y., Moukhomodiarov, R.R. and Rogerson, G.A. (2002). "Analysis of the dispersion relation for an incompressible transversely isotropic elastic plate", *Acta Mech.* **153**, 89-111.

Kuo, J.T. and Nafe, J.E. (1962). "Period equation for Rayleigh waves in a layer overlying a half space with a sinusoidal interface", *Bull. Seismol. Soc. Am.* **52(4)**, 807-822.

Kumar, R., Tomar, S.K. and Chopra, A. (2003). "Reflection/refraction of SH-waves at a corrugated interface between two different anisotropic and vertically heterogeneous elastic solid half-spaces", *ANZIAM J.* **44**, 447-460.

Kumar, R. and Hundal, B.S. (2007). "Surface wave propagation in a fluid-saturated incompressible porous medium", *Sadhana* **32(3)**, 155-166.

Kumari, P., Sharma, V.K. and Modi, C. (2014). "Reflection/refraction pattern of quasi-(P/SV) waves in dissimilar monoclinic media separated with finite isotropic layer", *J. Vib. Control.* **22(11)**, 2745-2758.

Kumar, S., Pal, P.C. and Majhi, S. (2016). "Reflection and transmission of SH-waves at a corrugated interface between two semi-infinite anisotropic magnetoelastic half-spaces", *Waves Rand. Compl. Med.* **27(2)**, 339-358.

Kumhar, R., Kundu, S. and Kumari, C. (2019). "Propagation of torsional wave at a corrugated interface between viscoelastic sandy medium and inhomogeneous half-space", *AIP Conf. Proc.* **2061**, 020012-1−020012-8.

Kumari, C., Kundu, S. and Kumahar, R. (2019). "Dispersion characteristics of SH-wave propagation in a viscous fiber-reinforced stratified media", *AIP Conf. Proc.* **2061**, 020025-1−020025-9.

Kundler, I. and Finkelmann, H. (1995). "Strain-induced director reorientation in nematic liquid single crystal elastomers", *Macromol. Rapid Commun.* **16**, 679-686.

Kupfer, J. and Finkelmann, H. (1991). "Nematic liquid single crystal elastomers", *Makromol. Chem. Rapid Commun.* **12**, 717-726.

Kupfer, J., Nishikawa, E. and Finkelmann, H. (1993). "Densely crosslinked liquid single-crystal elastomers", *Polym. Adv. Tech.* **5**, 110-115.

Lai, W.M., Rubin, D. and Krempl, E. (1993). *Introduction to Continuum Mechanics*, Pergamon Press, Oxford.

Lakhtakia, A., Depine, R.A., Marina, E.I. and Brudny, V.L. (1993). "Scattering by a periodically corrugated interface between free space and a gyroelectromagnetic uniaxial medium", *Appl. Optics.* **32(15)**, 2765-2772.

Lamb, H. (1881). "On the vibrations of an elastic sphere", *Proc. Lond. Math. Soc.* 189-212.

Lamb, H. (1917a). "On waves in an elastic plate", *Proc. Roy. Soc. Lond. A* **93**, 114-128.

Lamb, H. (1917b). "On the deflection of the vertical by tidal loading of the earth's surface", *Proc. Roy. Soc. Lond. A* **93**, 293-312.

Lauke, B. and Schultrich, B. (1983). "Deformation behaviour of short fibre reinforced materials with de-bonding interfaces", *Fibre Sc. Tech.* **19**, 111-126.

Levy, A. and Deresiewicz, H. (1967). "Reflection and transmission of elastic waves in a system of corrugated layers", *Bull. Seismol. Soc. Am.* **57(3)**, 393-419.

Leslie, F.M. (1966). "Some constitutive equations for anisotropic fluids", *Q. J. Mech. Appl. Math.* **19(3)**, 357-370.

Long, D. and Morse, D.C. (2000). "Linear viscoelasticity and director dynamics of nematic liquid crystalline polymer melts", *Eur. Phys. Lett.* **49(2)**, 255-261.

Love, A.E.H. (1892). *A Treatise on the Mathematical Theory of Elasticity*, Cambridge University Press, London.

Love, A.E.H. (1911). *Some Problems of Geodynamics*, Cambridge University Press, London.

Mahanty, M., Kumar, P. and Singh, A.K. (2020). "Dynamic response of an irregular heterogeneous anisotropic poroelastic composite structure due to normal moving load", *Acta Mech.* **231**, 2303-2321.

Malla R.P., Sindhuja, A. and Rajitha, G. (2019). "Study of reflection and transmission of axially symmetric body waves incident on a base of semi-infinite poroelastic solid cylinder", *Arch. Appl. Mech.* **89(12)**, 2507-2517.

Matteis, G.D. (2012). "Acoustic torque acting upon nematic liquid crystals", *Acta Appl. Math.* **122**, 205-223.

Miles, J.W. (1954). "On non-specular reflection at a rough surface", *J. Acoust. Soc. Am.* **26(2)**, 191-199.

Mindlin, R.D. (1964). "Micro-structure in linear elasticity", *Arch. Rat. Mech. Anal.* **16(1)**, 51-78.

Mitchell, G.R., Davis, F.J. and Ashman, A. (1987). "Structural studies of side-chain liquid crystal polymers and elastomers", *POLYMER* **28(4)**, 639-647.

Mitchell, G.R., Davis, F.J. and Guo, W. (1993). "Strain-induced transitions in liquid-crystal elastomers", *Phys. Rev. Lett.* **71(18)**, 2947-2950.

Mohammed, L., Ansari, M.N.M., Pua, G., Jawaid, M. and Islam, M.S. (2015). "A review on natural fiber reinforced polymer composite and its applications", *Int. J. Polym. Sc.* 1-15.

Muller, G. (2007). *Theory of Elastic Waves*, Geo Forschungs Zentrum, Potsdam.

Munch, I., Neff, P. and Wagner, W. (2011). "Transversely isotropic material: non-linear Cosserat versus classical approach", *Continuum Mech. Thermodyn.* **23(1)**, 27-34.

Nair, S. (2009). *Introduction to Continuum Mechanics*, Cambridge University Press.

Nair, S. and Sotiropoulos, D.A. (1977). "Elastic waves in orthotropic incompressible materials and reflection from an interface", *J. Acoust. Soc. Am.* **102(1)**, 102-109.

Nayfeh, A.H. (1991). "Elastic wave reflection from liquid-anisotropic substrate interfaces", *Wave Motion* **14(1)**, 55-67.

Ogden, R.W. and Sotiropoulos, D.A. (1997). "The effect of pre-stress on the propagation and reflection of plane waves in incompressible elastic solids", *IMA J. Appl. Math.* **59**, 95-121.

Ogden, R.W. and Singh, B. (2011). "Propagation of waves in an incompressible transversely isotropic elastic solid with initial stress: Biot revisited", *J. Mech. Mater. Struct.* **6**, 1-4.

Ogden, R.W. and Vinh, P.C. (2004). "On Rayleigh waves in incompressible orthotropic elastic solids", *J. Acoust. Soc. Am.* **115(2)**, 530-533.

Ohm, C., Brehmer, M. and Zentel, R. (2012). "Applications of liquid crystalline elastomers", *Adv. Polym. Sci.* **250**, 49-94.

Ohm, C., Mory, M., Forst, F.R., Braun, L., Eremin, A., Serra, C., Stannarius, R. and Zentel, R. (2011). "Preparation of actuating fibres of oriented main-chain liquid crystalline elastomers by a wetspinning process", *Soft Matter* **7**, 3730-3734.

Ohzono, T., Saed, M.O. and Terentjev, E.M. (2019). "Enhanced dynamic adhesion in nematic liquid crystal elastomers", *Adv. Mater.* **1902642** (1-6).

Ohzono, T., Saed, M.O., Yue, Y., Norikane, Y. and Terentjev, E.M. (2020). "Dynamic manipulation of friction in smart textile composites of liquid-crystal elastomers", *Adv. Mater. Interfaces* **7**, 1901996 (1-7).

Othman, M.I.A. and Song, Y. (2008). "Reflection of magneto-thermoelastic waves with two relaxation times and temperature dependent elastic moduli", *Appl. Math. Model.* **32**, 483-500.

Ota, Y. (2009). "On the analysis of the scattering problem for the elastic wave in the case of the transverse incident wave", *Proc. Jpn. Acad. Math. Sci.* **85(A)**, 138-142.

Paul, A. and Campillo, M. (1988). "Diffraction and conversion of elastic waves at a corrugated interface", *Geophys.* **53(11)**, 1415-1424.

Payton, R.G. (1983). *Elastic Wave Propagation in Transversely Isotropic Media*, Boston/Lancaster, The Netherlands.

Payton, R.G. (1992). "Wave propagation in a restricted transversely isotropy solid whose slowness surface contains conical points", *Q. J. Mech. Appl. Math.* **45(2)**, 183-197.

Pike, E.R. and Sabatier, P.C. (2002). *Scattering and Inverse Scattering in Pure and Applied Science*, Academic Press, San Diego.

Pipkin, A.C. (1979). "Stress analysis for fibre-reinforced materials", *Adv. Appl. Mech.* **19**, 1-51.

Plucinsky, P. and Bhattacharya, K. (2017). "Microstructure-enabled control of wrinkling in nematic elastomer sheets", *J. Mech. Phys. Solids.* **102**, 125-150.

Prikazchikov, D.A. and Rogerson, G.A. (2004). "On surface wave propagation in incompressible, transversely isotropic, pre-stressed elastic half-spaces", *Int. J. Engng. Sci.* **42**, 967-986.

Pujol, J. (2003). *Elastic Wave Propagation and Generation in Seismology*, Cambridge University Press, UK.

Rayleigh, L. (1877). *The Theory of Sound*, Dover Publication, New York.

Rayleigh, L. (1885). "On waves propagated along the plane surface of an elastic solid", *Proc. Lond. Math. Soc.* **17(1)**, 4-11.

Rayleigh, L. (1893). "On the reflection of sound or light from a corrugated surface", *Brit. Assoc. Rep.* 690-691.

Rayleigh, L. (1907). "On the dynamical theory of gratings", *Proc. Roy. Soc. Lond. A* **79**, 399-416.

Reddy, J.N. (2008). *An Introduction to Continuum Mechanics*, Cambridge University Press, London.

Rice, O. (1951). "Reflection of electromagnetic waves from slightly rough surfaces", *Comm. Pure Appl. Math.* **4(2-3)**, 351-378.

Reid, R. (2018). *Inorganic Chemistry*, ED-TECH Press, UK.

Rose, J.L. (2014). *Ultrasonic Guided Waves in Solid Media*, Cambridge University Press, UK.

Rogerson, G.A. (1991). "Some dynamic properties of incompressible, transversely isotropic elastic media", *Acta Mech.* **89**, 179-186.

Rogerson, G.A. (1992). "Penetration of impact waves in a six-ply fibre composite laminate", *J. Sound Vib.* **158(1)**, 105-120.

Rogerson, G.A. and Sandiford, K.J. (2000). "Asymptotic representations of the dispersion relation for a two-ply, pre-stressed incompressible elastic laminate", *Acta Mech.* **143**, 179-201.

Rouison, D., Sain, M. and Couturier, M. (2004). "Resin transfer molding of natural fiber reinforced composites: cure simulation", *Comp. Sci. Tech.* **64**, 629-644.

Saed, M.O. and Terentjev, E.M. (2020). "Siloxane crosslinks with dynamic bond exchange enable shape programming in liquid-crystalline elastomers", *Scientific Reports* **10**, 1-10.

Sanjay, M.R., Arpitha, G.R., Naik, L.L., Gopalakrishna, K. and Yogesha, B. (2019). "Applications of natural fibers and its composites: An overview", *Natural Resources.* **7**, 108-114.

Sato, R. (1955). "The reflection of elastic waves on corrugated surfaces", *J. Seismol. Soc. Jpn.* **8**, 8-22.

Schmidtke, J., Stille, W. and Strobl, G. (2000). "Static and dynamic light scattering of a nematic sidegroup polysiloxane", *Macromol.* **33(8)**, 2922-2928.

Schonstein, M., Stille, W. and Strobl, G. (2001). "Effect of the network on the director fluctuations in a nematic side-group elastomer analysed by static and dynamic light scattering", *Eur. Phys. J. E* **5(5)**, 511-517.

Scott, N. (1975). "Acceleration waves in constrained elastic materials", *Arch. Rat. Mech. Anal.* **58(1)**, 57-75.

Selinger, J.V., Jeon, H.G. and Ratna, B.R. (2002). "Isotropic-nematic transition in liquid-crystalline elastomers", *Phys. Rev. Lett.* **89(22)**, 225701-225704.

Semenov, A.N. and Kokhlov, A.R. (1988). "Statistical physics of liquid-crystalline polymers", *Sov. Phy. Usp.* **31(11)**, 988-1014.

Selinger, J.V., Spector, M.S., Greanya, V.A., Weslowski, B.T., Shenoy, D.K. and Shashidhar, R. (2002a). "Acoustic realignment of nematic liquid crystal", *Phys. Rev. E* **66**, 51708-51715.

Selinger, J.V., Jeon, H.G., Ratna, B.R. (2002b). "Isotropic-nematic transition in liquid-crystalline elastomers", *Phys. Rev. Lett.* **89(22)**, 225701-225704.

Shearer, P.M. (2009). *Introduction to Seismology, Second Edition*, Cambridge University Press, UK.

Sheriff, R.E. and Geldart, P.L. (1995). *Exploration Seismology*. Cambridge University Press, Cambridge.

Singh, A.K., Mistri, K.C. and Das, A. (2016). "Propagation of SH-wave in a corrugated viscous sandy layer sandwiched between two elastic half-spaces", *Waves Rand. Compl. Med.* **27(2)**, 213-240.

Singh, A.K., Lakshman, A. and Chattopadhyay, A. (2015). "Influence of corrugated boundary surface and reinforcement of fibre-reinforced layer on propagation of torsional surface wave", *J. Vib. Control.* **23(9)**, 1-20.

Singh, B. (2007a). "Reflection of homogeneous elastic waves from free surface of nematic elastomer half-space", *J. Phys. D: Appl. Phys.* **40**, 584-592.

Singh, B. (2007b). "Wave propagation in an incompressible transversely isotropic fibre-reinforced elastic media", *Arch. Appl. Mech.* **77**, 253-258.

Singh, B. (2010). "Reflection of plane waves at the free surface of a monoclinic thermoelastic solid half-space", *Eur. J. Mech. A/Solids.* **29(5)**, 911-916.

Singh, B. (2013). "Reflection and transmission of plane waves at an imperfect interface between two dissimilar monoclinic elastic half-spaces", *Int. J. Appl. Math. Comp.* **5(1)**, 3843.

Singh, B. and Singh, S.J. (2004). "Reflection of plane waves at the free surface of a fibre-reinforced elastic half-space", *Sadhana* **29(3)**, 249-257.

Singh, S.S. (2011a). "Effect of initial stresses on incident qSV-waves in pre-stressed elastic half-spaces", *ANZIAM J.* **52**, 395-371.

Singh, S.S. (2011b). "Response of shear wave from a corrugated interface between elastic solid/ viscoelastic half-spaces", *Int. J. Numer. Anal. Meth. Geomech.* **35**, 529-543.

Singh, S.S. (2013). *Elastic Waves in Continuum Mechanics*, Lambert Academic Publishing, Germany.

Singh, S.S. (2015). "Transmission of elastic waves in anisotropic nematic elastomers", *ANZIAM J.* **56**, 381-396.

Singh, S.S. (2017). "Harmonic waves in anisotropic nematic elastomers", *Appl. Math. Comp.* **302**, 1-8.

Singh, S.J. (1999). "Comments on the reflection phenomena of P-waves in a medium of monoclinic type by Chattopadhyay and Choudhury", *Int. J. Engng. Sci.* **37(3)**, 407-410.

Singh, S.J. and Khurana, S. (2001). "Reflection and transmission of P- and SV-waves at the interface between two monoclinic elastic half-spaces", *Proc. Nat. Acad. Sci. India A* **71(4)**, 305-319.

Singh, S.J. and Khurana, S. (2002). "Reflection of P and SV-waves at the free surface of a monoclinic elastic half-space", *Proc. Indian Acad. Sci.* **111(4)**, 401-412.

Singh, S.J., Kumar, A. and Singh, J. (2003). "Deformation of a monoclinic elastic half-space by a long inclined strike-slip fault", *ISET J. Earthq. Tech.* **40(1)**, 51-59.

Singh, S.S. and Singh, J. (2013). "Effect of corrugation on incident qSV-waves in pre-stressed elastic half-space", *Int. J. Appl. Math. Mech.* **9(9)**, 92-106.

Singh, S.S. and Tomar, S.K. (2007a). "Quasi P-waves at a corrugated interface between two dissimilar monoclinic elastic half-spaces", *Int. J. Solids Struct.* **44(1)**, 197-228.

Singh, S.S. and Tomar, S.K. (2007b). "Elastic waves at a corrugated interface between two dissimilar fibre-reinforced elastic half-spaces", *Int. J. Numer. Anal. Meth. Geomech.* **31(9)**, 1085-1116.

Singh, S.S. and Tomar, S.K. (2007c). "Shear waves at a corrugated interface between two dissimilar fibre-reinforced elastic half-spaces", *J. Mech. Mater. Struct.* **2(1)**, 167-188.

Singh, S.S. and Tomar, S.K. (2008a). "Corrigendum to Quasi *P*-waves at a corrugated interface between two dissimilar monoclinic elastic half-spaces", *Int. J. Solids Struct.* **45(11)**, 3610-3621.

Singh, S.S. and Tomar, S.K. (2008b). "*qP*-wave at a corrugated interface between two dissimilar pre-stressed elastic half-spaces", *J. Sound Vib.* **317(3-5)**, 687-708.

Singh, S.S., Zorammuana, C. and Singh, B. (2014). "Elastic waves at a plane interface between two dissimilar incompressible transversely isotropic fibre-reinforced elastic half-spaces", *Int. J. Appl. Math. Sci.* **7(2)**, 131-146.

Singh, A.K., Mistri, K.C. and Das, A. (2016). "Propagation of *SH*-wave in a corrugated viscous sandy layer sandwiched between two elastic halfspaces", *Waves Rand. Compl. Med.* **27(2)**, 213-240.

Sokolnikof, I.S. (1956). *Mathematical Theory of Elasticity*, McGraw-Hill Book Company, Inc., New York.

Sobczyk, K. (1985). *Stochastic Wave Propagation, Fundamental Study in Engineering 6*, Institute of Fundamental Technological Research, Warsaw, Poland.

Sotiropoulos, D.A. and Nair, S. (1999). "Elastic waves in monoclinic incompressible materials and reflection from an interface", *J. Acoust. Soc. Am.* **105(5)**, 2981-2983.

Spencer, A.J.M. (1984). *Continuum Theory of the Mechanics of Fibre-Reinforced Composites*, New York, Springer.

Spencer, A.J.M. and Soldatos, K.P. (2007). "Finite deformations of fibre-reinforced elastic solids with fibre bending stiffness", *Int. J. Non-Lin. Mech.* **42**, 355-368.

Teixeira, P.I.C. and Warner, M. (1999). "Dynamics of soft and semisoft nematic elastomers", *Phys. Rev. E* **60(1)**, 603-609.

Terentjev, E.M. (1993). "Phenomenological theory of non-uniform nematic elastomers: Free energy of deformations and electric-field effects", *Eur. Phys. Lett.* **23(l)**, 27-32.

Terentjev, E.M. (1999). "Liquid-crystalline elastomers", *J. Phys.: Condens. Matt.* **11**, 239-257.

Terentjev, E.M. and Warner, M. (2001). "Linear hydrodynamics and viscoelasticity of nematic elastomers", *Eur. Phys. J. E* **4**, 343-353.

Terentjev, E.M., Kamotski, I.V., Zakharov, D.D. and Fradkin, L.J. (2002). "Propagation of acoustic waves in nematic elastomers", *Phys. Rev. E* **66**, 52701-52704.

Tomar, S.K. and Saini, S.L. (1997). "Reflection and refraction of SH-Waves at a corrugated interface between two-dimensional transversely isotropic half-spaces", *J. Phys. Earth.* **45**, 347-362.

Tomar, S.K., Kumar, R. and Chopra, A. (2002). "Reflection and refraction of SH-waves at a corrugated interface between transversely isotropic and visco-elastic solid half-spaces", *Acta Geophys. Pol.* **50(2)**, 231-249.

Tomar, S.K. and Kaur, J. (2003). "Reflection and transmission of SH-waves at a corrugated interface between two laterally and vertically heterogeneous anisotropic elastic solid half-spaces", *Earth Planets Space* **55**, 531-547.

Tomar, S.K. and Kaur, J. (2007a). "SH-waves at a corrugated interface between a dry sandy half-space and an anisotropic elastic half-space", *Acta Mech.* **190**, 1-28.

Tomar, S.K., Kaur, J. (2007b). "Shear waves at a corrugated interface between anisotropic elastic and visco-elastic solid half-spaces", *J. Seismol.* **11**, 235-258.

Tomar, S.K. and Singh, S.S. (2006). "Plane SH-waves at a corrugated interface between two dissimilar perfectly conducting self-reinforced elastic half-spaces", *Int. J. Numer. Anal. Meth. Geomech.* **30**, 455-487.

Tong, M.S. and Chew, W.C. (2009). "Multilevel fast multipole algorithm for elastic wave scattering by large three-dimensional objects", *J. Comp. Phys.* **228(3)**, 921-932.

Toupin, R.A. (1962). "Elastic materials with couple stresses", *Arch. Rat. Mech. Anal.* **11(1)**, 385-414.

Udias, A. (1999). *Principles of Seismology*, Cambridge University Press, UK.

Uchida, N. (2000). "Soft and non-soft structural transitions in disordered nematic networks", *Phys. Rev. E* **62(4)**, 5119-5136.

Urbanski, M., Reyes, C.G., Noh, J.H., Sharma, A., Geng, Y., Jampani, V.S.R. and Lagerwall, J.P.F. (2017). "Liquid crystals in micron-scale droplets, shells and fibers", *J. Phys.: Condens. Matt.* **29**, 1-53.

Verma, G., Thakur, P. and Rana, P. (2019). "Elastic-plastic analysis of transversely isotropic spherical shell under internal pressure", *AIP Conf. Proc.* **2061**, 020031-1−020031-7.

Verwey, G.C., Warner, M. and Terentjev, E.M. (1996). "Elastic instability and stripe domains in liquid crystalline elastomers", *J. Phys. II France.* **6**, 1273-1290.

Vinh, P.C. and P.T.H. Giang (2011). "On formulas for the velocity of Stoneley waves propagating along the loosely bonded interface of two elastic half-spaces", *Wave Motion* **48**, 647-657.

Voronovich, A.G. (1994). *Wave Scattering From Rough Surfaces*, Springer Series on Wave Phenomena 17, Springer-Verlag, Berlin.

Warner, M. and Terentjev, E.M. (1996). "Nematic elastomers: a new state of matter?", *Prog. Polym. Sci.* **21**, 853-891.

Warner, M. and Terentjev, E.M. (2003). *Liquid Crystal Elastomers*, Oxford University Press, Oxford.

Wilmanski, K. (2010). *Fundamentals of Solid Mechanics*, IUSS Press, Pavia, Italy.

Wim H. de Jeu (2012). *Liquid Crystal Elastomers: Materials and Applications* Springer-Verlag, Berlin.

Xia, J., Miller, R.D. and Park, C.B. (1999). "Estimation of near surface shear wave velocity by inversion of Rayleigh waves", *Geophys.* **64(3)**, 691-700.

Xie, P. and Zhang, R. (2005). "Liquid crystal elastomers, networks and gels: advanced smart materials", *J. Mater. Chem.* **15**, 2529-2550.

Yang, S., Liu, Y., Gu, Y. and Yang, Q. (2014). "Rayleigh wave propagation in nematic elastomer", *Roy. Soc. Chem.* **10**, 4110-4117.

Yu, C.W. and Dravinsky, M. (2009). "Scattering of plane harmonic P, SV or Rayleigh waves by a completely embedded corrugated cavity", *Geophys. J. Int.* **178**, 479-487.

Zarutskii, V.A. and Podilchuk, I.Y. (2006). "Propagation of harmonic waves in longitudinally reinforced cylindrical shells with low shear stiffness", *Int. Appl. Mech.* **42(5)**, 525-528.

Zak, A. and Krawczuk, M. (2018). "A higher order transversely deformable shell-type spectral finite element for dynamic analysis of isotropic structures", *Fin. Elt. Anal. Design,* **142**, 17-29.

Zakharov, D.D. (2011). "Surface and edge waves in solids with nematic coating", *Math. Mech. Solids.* **17(1)**, 67-80.

Zhao, D. and Liu, Y. (2018). "Effects of director rotation relaxation on viscoelastic wave dispersion in nematic elastomer beams", *Math. Mech. Solids.* **24(4)**, 1103-1115.

Zhang, R. and Shinozuka, M. (1996). "Effects of irregular boundaries in a layered half-space on seismic waves", *J. Sound Vib.* **195(1)**, 1-16.

Zhang, Y., Xuan, C., Jiang, Y. and Huo, Y. (2019). "Continuum mechanical modeling of liquid crystal elastomers as dissipative ordered solids", *J. Mech. Phys. Solids* **126**, 285-303.

Zhu, Y. and Tsvankin, I. (2006). "Plane-wave propagation in attenuative transversely isotropic media", *Geophys.* **71(2)**, 17-30.

BIO-DATA OF THE CANDIDATE

Personal Information:

Name : J. LALVOHBIKA

Father's name : J. ZATAWNA

Mother's name : F. REMTHANGI

Date of Birth : 06.12.1977

Nationality : Indian

Gender : Male

Marital Status : Married

Present Address : C-118, Zonuam -796009, Aizawl, Mizoram.

Email : vohbikajongte@gmail.com

Academic Records:

X^{th} : M.B.S.E., Mizoram (1993)

Pre-University : N.E.H.U. (1996)

B.Sc. (Hons - Mathematics) : N.E.H.U. (1999)

M.Sc. (Mathematics) : D.U. (2001)

N.E.T. : CSIR-UGC (2006)

I have been working as Assistant Professor in the Department of Mathematics in Pachhunga University College, Aizawl since 2007 till date. I have availed the Award of Teacher Fellowship under Faculty Development Programme during the 12th Plan Period from 2017-2019 under University Grants Commission, Ministry of Human Resource Development, Govt. of India.

PARTICULARS OF THE CANDIDATE

NAME OF CANDIDATE : J. LALVOHBIKA

DEGREE : DOCTOR OF PHILOSOPHY

DEPARTMENT : MATHEMATICS AND COMPUTER SCIENCE

TITLE OF THESIS : SCATTERING OF ELASTIC WAVES FROM A CORRUGATED INTERFACE

DATE OF ADMISSION : 13. 09. 2013

APPROVAL OF RESEARCH PROPOSAL :

  1. BOS : 12. 05. 2014

  2. SCHOOL BOARD : 16. 05. 2014

MZU REGISTRATION NO. : 5668 of 2013

Ph. D. REGISTRATION NO. AND DATE : MZU/Ph.D./687 of 16.05.2014

EXTENSION (IF ANY) : No. 16-2/MZU(Acad)/19/29-31 Dated 18th June 2019 upto 15.5.2021

Dr. Jay Prakash Singh
(Head of Department)
Dept. Maths. & Comp. Sc.
Mizoram University

Abstract of the thesis titled

SCATTERING OF ELASTIC WAVES FROM A CORRUGATED INTERFACE

A THESIS SUBMITTED IN PARTIAL FULFILMENT OF THE REQUIREMENTS FOR THE DEGREE OF DOCTOR OF PHILOSOPHY

J. LALVOHBIKA

Ph.D. REGN. No.: MZU/Ph.D./687 of 16.05.2014

MZU REGN. No.: 5668 of 2013

DEPARTMENT OF MATHEMATICS AND COMPUTER SCIENCE

SCHOOL OF PHYSICAL SCIENCES

MIZORAM UNIVERSITY

JULY, 2020

ABSTRACT

The subject of wave propagation is an interesting area of research that deals with numerous problems in the fields of Seismology, geophysics, Earthquake engineering, tele-communication, medicines (echography), metallurgy and signal processing. It is useful to detect the notches and faults in different types of materials such as in railway tracks, buried land-mines, etc. The technique of wave propagation is used in exploration of valuable materials such as minerals, crystals, hydrocarbons, fluids (oils, water) etc. beneath the earth surface. The following objectives are taken up in the thesis:

1. Elastic waves at a corrugated interface between two dissimilar monoclinic elastic half spaces.

2. Elastic waves at a corrugated interface in nematic elastomers half-spaces.

3. Elastic waves at a corrugated interface between two dissimilar incompressible transversely isotropic fibre-reinforced elastic half-spaces.

Chapter 1 is the general introduction which includes basic definitions, different types of anisotropic symmetry, stress-strain relationship with generalized Hooke's law, conservation of linear momentum, Spectrum theorem, Rayleigh's method of approximation, importance of wave propagation and review of literatures.

Chapter 2 discusses the problem of reflection and transmission phenomena of elastic qSV and qP-wave due to incident plane qSV-wave at a corrugated interface between two dissimilar monoclinic elastic half-spaces. We have obtained the reflection and transmission coefficients for those regularly and irregularly reflected and transmitted waves using Rayleigh's method of approximation. These coefficients are computed numerically for a special type of interface, $z = d \cos py$ and discussed the effects of corrugation (pd) and frequency parameter (ω/pc_0).

Chapter 3 investigates the problem of reflection and transmission of elastic waves at a corrugated interface between two dissimilar nematic elastomer half-spaces due

to incident qP and qSV-waves. The expressions of the phase velocities corresponding to qP and qSV-waves depend on the angle of propagation. The amplitude and energy ratios corresponding to the reflected and transmitted waves for the incident qP and qSV-waves are derived by using appropriate boundary conditions. These ratios of the regular and irregular waves are computed numerically for a particular model, $x_3 = d \cos p x_1$ for different values of corrugation and frequency parameters.

Chapter 4 studies the problem of scattering of elastic waves due to incident qSH-wave at a corrugated interface between two different nematic elastomer half-spaces. The phase velocity for shear harmonic wave is obtained and it is observed that this phase velocity depends on the angle of propagation. The first order approximation of amplitude ratios corresponding to reflected and transmitted qSH-waves are obtained using Rayleigh's technique. The energy ratios due to various reflected and transmitted waves are also presented. A particular case of the corrugated interface, i.e., $z = d \cos px$ has been investigated to validate the present study. The effects of corrugation, frequency and relaxation parameters on the amplitude and energy ratios have been discussed.

The problem of elastic waves at an irregular interface between two dissimilar incompressible transversely isotropic fibre-reinforced half-spaces has been discussed in Chapter 5. We come across the existence of two reflected and transmitted qSH-waves in an angular range, $0 \le \alpha \le 30^0$. The reflection and transmission coefficients due to regular and irregular qSH-waves are obtained using Rayleigh's method of approximation. Energy ratios at the corrugated interface are also presented. These coefficients and energy ratios are computed numerically for a specific model, $\zeta = d \cos p x_1$.

Chapter 6 is summary and conclusion.

Finally, a list of references is given at the end.